



**ROBERT GORDON
UNIVERSITY•ABERDEEN**

OpenAIR@RGU

The Open Access Institutional Repository at Robert Gordon University

<http://openair.rgu.ac.uk>

Citation Details

Citation for the version of the work held in 'OpenAIR@RGU':

MICHEL, L., 2012. Studies to determine the mechanisms of the anti-atherosclerotic effects of eicosapentaenoic acid – possible role for endocannabinoids? Available from *OpenAIR@RGU*. [online]. Available from: <http://openair.rgu.ac.uk>

Copyright

Items in 'OpenAIR@RGU', Robert Gordon University Open Access Institutional Repository, are protected by copyright and intellectual property law. If you believe that any material held in 'OpenAIR@RGU' infringes copyright, please contact openair-help@rgu.ac.uk with details. The item will be removed from the repository while the claim is investigated.

STUDIES TO DETERMINE THE MECHANISMS OF THE ANTI-
ATHEROSCLEROTIC EFFECTS OF EICOSAPENTAENOIC
ACID – POSSIBLE ROLE FOR ENDOCANNABINOIDS?

LISA MICHEL

PhD

2012

STUDIES TO DETERMINE THE MECHANISMS OF THE ANTI-
ATHEROSCLEROTIC EFFECTS OF EICOSAPENTAENOIC ACID –
POSSIBLE ROLE FOR ENDOCANNABINOIDS?

LISA MICHEL

A thesis submitted in partial fulfilment of the
requirements of
The Robert Gordon University
for the degree of Doctor of Philosophy

May 2012

Declaration

This thesis in candidature for the degree of Doctor of Philosophy has been composed entirely by myself. The work which is documented was carried out by myself. All sources of information contained within which have not arisen from the results generated have been specifically acknowledged.

Lisa Michel

“Things should be as simple as possible, but no simpler”

- **Albert Einstein**

Contents	Page
Acknowledgements	I
Publications	II
Abstract	III
Abbreviations	IV
Chapter 1: Introduction.	1
1.1. Vascular physiology	2
1.1.1. Blood vessel structure	2
<i>1.1.1.1. Tunica intima</i>	2
<i>1.1.1.2. Tunica media</i>	2
<i>1.1.1.3. Tunica adventitia</i>	3
1.1.2. Collagen in the vasculature	3
1.1.3. Collagen in the myocardium	4
<i>1.1.3.1. Collagen synthesis</i>	4
<i>1.1.3.2. Maturation</i>	5
1.2. Coronary heart disease	7
1.2.1. Aetiology	7
1.2.2. Development of early atherosclerotic lesions	7
<i>1.2.2.1. Lipoprotein accumulation</i>	8
<i>1.2.2.2. Lipoprotein modification</i>	9
<i>1.2.2.3. The early inflammatory response</i>	10
1.2.3. Fatty streak formation	10
1.2.4. Development of fibrofatty lesions	11
1.2.5. Progression to advanced, complicated lesion	11
<i>1.2.5.1. Macrophages: role in atherosclerosis</i>	13
1.2.6. Clinical outcome of atherosclerosis progression	14
1.2.7. Animal models of atherosclerosis	14
1.2.8. Pharmaceutical intervention	15
<i>1.2.8.1. Statins</i>	16
<i>1.2.8.2. Fibrates</i>	16
1.3. Diet and coronary heart disease	17
1.3.1. Dietary sources of ω -3 PUFAs	19
1.3.2. Endogenous biosynthesis of long chain ω -3 PUFAs	19

1.3.3. ω -3 PUFAs and cardiovascular function	22
1.3.4. ω -3 PUFAs and lipid metabolism	22
1.3.5. ω -3 PUFAs: Role in atherosclerosis	23
1.4. The endocannabinoid system	25
1.4.1. Cannabinoid receptors	26
1.4.2. Endogenous cannabinoids	26
<i>1.4.2.1. Anandamide: biosynthesis and metabolism</i>	27
<i>1.4.2.2. 2-arachidonoylglycerol: biosynthesis and metabolism</i>	28
1.4.3. Cardiovascular effects of the endocannabinoid system	28
1.4.4. The endocannabinoid system and atherosclerosis	32
1.5. Hypothesis	33
1.5.1. Objectives	33
Chapter 2: General Methods.	34
2.1. In Vitro techniques	35
2.1.1. Cell resuscitation	35
2.1.2. Cell freezing	35
2.1.3. THP-1 cell culture	35
2.1.5. Cell counting assays	36
<i>2.1.5.1. Trypan blue staining</i>	36
<i>2.1.5.2. Coomassie brilliant blue staining</i>	36
2.1.6. Cell fixation	38
2.1.7. Bradford dye-binding assay	38
2.1.8. Oil red O staining	38
2.1.9. ELISA assay	40
2.1.11. MTS assay	42
2.2. In Vivo techniques	42
2.2.1. Animal sourcing and housing	42
2.2.2. Dietary intervention	43
2.2.3. Surgical procedure for the measurement of haemodynamics	43
2.2.4. Tissue harvest	45
2.2.5. Blood sample analysis	45
2.2.6. Tissue lipid extraction	46
2.2.7. FAME analysis	46

2.2.8. Endocannabinoid measurement	47
2.2.8.1. <i>Extraction</i>	47
2.2.8.2. <i>LC-MS/MS conditions</i>	48
2.2.8.3. <i>Analysis</i>	48
2.2.9. Collagen and collagen cross-link measurement	49
2.2.9.1. <i>Preparation of standards and samples</i>	49
2.2.9.2. <i>LC-MS/MS procedure</i>	50
2.2.9.3. <i>Analysis</i>	50
2.2.10. Western blotting	50
2.2.10.1. <i>Protein extraction</i>	51
2.2.10.2. <i>Electrophoresis and immunoblotting</i>	51
2.3. Materials	53
2.3.1. Antibodies and reagents	53
Chapter 3: Modelling lipid accumulation in the activated THP-1 macrophage.	55
3.1. Introduction	56
3.1.1. Foam cell origin and development	56
3.1.2. Atherosclerosis and ω -3 PUFAs	57
3.1.3. <i>In vitro</i> models of foam cell activity	57
3.2. Aims	58
3.3. Methods	59
3.3.1. Optimisation of differentiation	59
3.3.2. Optimisation of lipid loading and quantification	59
3.3.2.1. <i>Linoleic acid loading</i>	59
3.3.2.2. <i>Oleic acid loading: comparison to linoleic acid</i>	60
3.3.2.3. <i>ω-3 PUFA loading</i>	60
3.4. Results	60
3.4.1. THP-1 monocyte differentiation	60
3.4.2. Optimisation of lipid loading: linoleic acid	62
3.4.3. Lipid loading: oleic acid	62
3.4.4. Lipid loading: ω -3 PUFAs	62
3.5. Discussion	67

Chapter 4: Role of the endocannabinoid system in lipid accumulation in the activated THP-1 macrophage.	70
4.1. Introduction	71
4.1.1. The endocannabinoid system: an overview	71
4.1.2. Endocannabinoids and disease pathology	71
4.1.3. Endocannabinoids and atherosclerosis	71
4.1.3.1. <i>CB₁ receptor mediated effects</i>	72
4.1.3.2. <i>CB₂ receptor mediated effects</i>	72
4.1.3.3. <i>Endocannabinoids and foam cell formation</i>	73
4.2. Aims	73
4.3. Methods	74
4.3.1. Optimisation of drug pre-incubation period	74
4.3.2. The effect of cannabinoid and endocannabinoid compounds on ω -3 PUFA accumulation	74
4.3.3. The effect of cannabinoid and endocannabinoid compounds on cell viability	74
4.3.4. The effect of AEA and JWH133 on MCP-1 production	75
4.3.5. Endocannabinoid production in lipid loaded THP-1 macrophages	75
4.3.5.1. <i>Endocannabinoid analysis: generation of the standard curve</i>	75
4.3.5.2. <i>Normalisation of endocannabinoid results</i>	76
4.4. Results	76
4.4.1. Optimisation of drug pre-incubation	76
4.4.2. The effect of endocannabinoid and cannabinoid compounds on OA accumulation in PMA-stimulated THP-1 macrophages	81
4.4.3. MCP-1 production in OA and CB agonist treated THP-1 macrophages	81
4.4.4. Endocannabinoid production in OA loaded THP-1 macrophages	81
4.4.5. The effect of endocannabinoid and cannabinoid compounds on EPA accumulation in PMA-stimulated THP-1 macrophages	87
4.4.6. MCP-1 production in EPA and CB agonist treated THP-1 macrophages	87
4.4.7. 2-AG production in EPA treated THP-1 macrophages	87
4.4.8. The effect of endocannabinoid and cannabinoid compounds on DHA accumulation in PMA-stimulated THP-1 macrophages	87
4.4.9. MCP-1 production in DHA and CB agonist treated THP-1 macrophages	95
4.4.10. 2-AG production in DHA treated THP-1 macrophages	95
4.5. Discussion	101

4.5.1. The effect of endocannabinoids and cannabinoids on FA accumulation in THP-1 macrophages	101
4.5.2. MCP-1 production in endocannabinoid and cannabinoid FA-loaded THP-1 macrophages	104
4.5.3. The effect of FA loading on endocannabinoid production	105
4.5.4. Conclusion	107
Chapter 5: The physiological impact of chronic EPA intervention in a murine model of atherosclerosis.	108
5.1. Introduction	109
5.1.1. ω -3 fatty acids: <i>in vitro</i> to <i>in vivo</i> investigations	109
5.1.2. ApoE ^{-/-} mice: a tool for atherosclerosis study	109
5.1.3. Aims	110
5.2. Methods	111
5.2.1. Study Design	111
5.2.2. Intervention diets	111
5.2.3. Endpoint Studies	112
5.2.3.1. <i>Vascular function studies</i>	112
5.2.3.2. <i>Lipid profiling</i>	112
5.2.3.3. <i>Endocannabinoid quantification</i>	113
5.2.3.4. <i>Collagen and collagen cross-link quantification</i>	113
5.3. Results	116
5.3.1. Baseline measurements	116
5.3.2. Hepatic lipid profiles	116
5.3.3. Blood plasma lipid profiles	121
5.3.4. Collagen and cross-link measurement	126
5.3.4.1. <i>Cardiac tissue</i>	126
5.3.4.2. <i>Vascular tissue</i>	134
5.3.5. Tissue endocannabinoid levels	134
5.3.5.1. <i>Thoracic aorta endocannabinoid levels</i>	134
5.3.5.2. <i>Brain endocannabinoid levels</i>	134
5.3.5.3. <i>Heart endocannabinoid levels</i>	139
5.3.6. Haemodynamic responses to bradykinin	139

5.3.7. Haemodynamic responses to sodium nitroprusside	148
5.4. Discussion	148
5.4.1. The impact of dietary intervention on baseline physiology in the ApoE ^{-/-} mouse	154
5.4.2. The impact of an atherogenic diet on lipid metabolism in the ApoE ^{-/-} mouse	155
5.4.2.1. EPA supplementation and lipid metabolism in the ApoE ^{-/-} mouse	156
5.4.2.2. Fenofibrate supplementation and lipid metabolism in the ApoE ^{-/-} mouse	157
5.4.3. The impact of an atherogenic diet on cardiac and vascular remodelling	158
5.4.3.1. EPA supplementation and cardiac and vascular remodelling	161
5.4.3.2. Fenofibrate supplementation and cardiac and vascular remodelling	162
5.4.4. The impact of an atherogenic diet on tissue endocannabinoid levels	163
5.4.4.1. EPA supplementation and tissue endocannabinoid levels	166
5.4.4.2. Fenofibrate supplementation and tissue endocannabinoid levels	167
5.4.5. The impact of an atherogenic diet on endothelial function	168
5.4.5.1. EPA/fenofibrate supplementation and endothelial function	169
5.4.6. Conclusion	171
 Chapter 6: General discussion.	 172
6.1. Key findings	173
6.1.1. Activated endocannabinoid system in stimulated THP-1 macrophages	173
6.1.2. Regulation of endocannabinoid synthesis	174
6.1.3. Activated endocannabinoid system and dysregulated FA uptake	174
6.1.4. Hypercholesterolaemia in a murine model of atherosclerosis	175
6.1.5. EPA supplementation in the hyperlipidaemic ApoE ^{-/-} mouse	176
6.1.6. Fenofibrate supplementation in the hyperlipidaemic ApoE ^{-/-} mouse	177
6.2. Future studies	178
6.2.1. Histological examination of atherosclerotic lesion development	178
6.2.2. Cannabinoid receptor antagonist studies	179
6.3. Conclusion	179

List of figures

Figure 1.1 Collagen cross-link formation.	6
Figure 1.2 Structures of EPA and DHA.	20
Figure 1.3 Biosynthesis of the ω -3 series of PUFAs.	21
Figure 1.4 Endocannabinoid structures.	29
Figure 1.5 Biosynthetic pathways of the endocannabinoids AEA and 2-AG.	30
Figure 3.1 Optimisation of THP-1 monocyte differentiation.	61
Figure 3.2 ORO staining of lipid accumulation in activated THP-1 cells.	63
Figure 3.3 Optimisation of lipid accumulation in THP-1 cells using linoleic acid.	64
Figure 3.4 Lipid loading with oleic acid.	65
Figure 3.5 Lipid loading with omega-3 fatty acids.	66
Figure 4.1 Original LC-MS/MS chromatograms of standards and internal standard.	77
Figure 4.2 Example standard curves for AEA and 2-AG.	78
Figure 4.3 Original LC-MS/MS chromatogram outlining sample peak.	79
Figure 4.4 The time dependent effects of ACEA pre-treatment on OA uptake in THP-1 macrophages stimulated with PMA.	80
Figure 4.5 OA accumulation in ACEA and 2-AG treated THP-1 macrophages stimulated with PMA.	82
Figure 4.6 OA accumulation in AEA and JWH133 treated THP-1 macrophages stimulated with PMA.	89
Figure 4.7 Baseline MCP-1 production in OA and drug treated THP-1 macrophages.	84
Figure 4.8 The effect of AEA/JWH133 on MCP-1 production in OA treated THP-1 macrophages.	85
Figure 4.9 The effect of OA and fenofibrate on 2-AG production in PMA stimulated THP-1 macrophages.	86
Figure 4.10 EPA accumulation in ACEA and 2-AG THP-1 macrophages stimulated with PMA.	88
Figure 4.11 EPA accumulation in AEA and JWH133 treated THP-1 macrophages stimulated with PMA.	89
Figure 4.12 Baseline MCP-1 production in EPA loaded THP-1 macrophages.	90
Figure 4.13 The effect of AEA/JWH133 pre-treatment on MCP-1 production in EPA loaded THP-1 macrophages.	91
Figure 4.14 The effect of EPA accumulation on 2-AG production in PMA	92

stimulated THP-1 macrophages.	
Figure 4.15 DHA accumulation in ACEA and 2-AG treated THP-1 macrophages stimulated with PMA.	93
Figure 4.16 DHA accumulation in AEA and JWH133 treated THP-1 macrophages stimulated with PMA.	94
Figure 4.17 The effect of AEA treatment on the viability of PMA stimulated THP-1 macrophages.	96
Figure 4.18 The effect of JWH133 treatment on the viability of PMA stimulated THP-1 macrophages.	97
Figure 4.19 Baseline MCP-1 production in DHA loaded THP-1 macrophages.	98
Figure 4.20 The effect of AEA/JWH133 on MCP-1 production in DHA loaded THP-1 macrophages.	99
Figure 4.21 The effect of DHA accumulation on 2-AG production in PMA stimulated THP-1 macrophages.	100
Figure 5.1 <i>In vivo</i> drug protocol.	115
Figure 5.2 Hepatic lipid profiles – total lipids.	118
Figure 5.3 Hepatic lipid profiles – triglycerides.	119
Figure 5.4 Hepatic lipid profiles – adipophilin expression.	120
Figure 5.5 Hepatic lipid profiles – fatty acid profiling.	122
Figure 5.6 Hepatic lipid profiles – EPA and DHA content of hepatic fatty acid profiles.	123
Figure 5.7 Plasma lipid profiles – total cholesterol.	124
Figure 5.8 Plasma lipid profiles – LDL cholesterol.	125
Figure 5.9 Plasma lipid profiles – HDL cholesterol.	127
Figure 5.10 Plasma lipid profiles – total cholesterol/HDL cholesterol ratio.	128
Figure 5.11 Plasma lipid profiles – triglycerides.	129
Figure 5.12 The total collagen content of C57 and ApoE ^{-/-} mouse heart tissue.	130
Figure 5.13 The DHLNL, HLNL and HHL content of C57 and ApoE ^{-/-} mouse heart tissue.	131
Figure 5.14 The PYD, DPD and total DES/IDE content of C57 and ApoE ^{-/-} mouse heart tissue.	132
Figure 5.15 Mature:immature cross-link ratio in cardiac tissue.	133
Figure 5.16 Endocannabinoid content of C57 and ApoE ^{-/-} mouse vascular tissue.	137
Figure 5.17 Endocannabinoid content of C57 and ApoE ^{-/-} mouse brain tissue.	138
Figure 5.18 Endocannabinoid content of C57 and ApoE ^{-/-} mouse cardiac tissue.	140

Figure 5.19 Original trace showing the haemodynamic response to heparinised saline.	142
Figure 5.20 Original trace showing the depressor response to bradykinin.	143
Figure 5.21 Original trace showing the depressor response to sodium nitroprusside.	144
Figure 5.22 Blood pressure responses to bradykinin ($3\mu\text{g kg}^{-1}$).	145
Figure 5.23 Blood pressure responses to bradykinin (30 and $300\mu\text{g kg}^{-1}$).	146
Figure 5.24 Area under the curve analysis of blood pressure responses to bradykinin.	147
Figure 5.25 Heart rate responses to bradykinin.	149
Figure 5.26 Blood pressure responses to sodium nitroprusside ($3\mu\text{g kg}^{-1}$).	150
Figure 5.27 Blood pressure responses to sodium nitroprusside (30 and $300\mu\text{g kg}^{-1}$).	151
Figure 5.28 Area under the curve analysis of blood pressure responses to sodium nitroprusside.	152
Figure 5.29 Heart rate responses to sodium nitroprusside.	153
Figure 5.30 Schematic representation of cardiac collagen cross-link formation.	160

List of Tables

Table 2.1 Coomassie Blue Stain: Preparation of staining solutions and fixative.	37
Table 2.2 Preparation of phosphate buffered saline.	39
Table 2.3 Bradford Assay: Preparation of standards.	39
Table 2.4 Oil red O: Preparation of ORO solutions.	39
Table 2.5 ELISA Assay: Solutions purchased from R&D systems.	41
Table 2.6 Surgical Procedure: Preparation of solutions used in surgery.	44
Table 2.7 Western Blot: Preparations of polyacrylamide gels.	52
Table 2.8 Western Blot: Preparation of solutions required for Western Blotting.	52
Table 5.1 Experimental group details.	114
Table 5.2 Tissue weights in C57 and ApoE ^{-/-} mice.	117
Table 5.3 Collagen content of ApoE ^{-/-} mouse thoracic aorta tissue.	135
Table 5.4 Collagen and elastin cross-link content of ApoE ^{-/-} mouse tissue.	136
Table 5.5 Resting blood pressure and heart rate.	141

Acknowledgements

I would like to thank the following people:

First and foremost, I'd like to extend my sincerest thanks to my director of studies Prof. Cherry Wainwright for her continuous guidance, support and encouragement throughout this process. I would also like to thank the other members of my supervisory team, Dr Baukje de Roos, Dr Marie Goua and Dr Helen Vosper who provided expert knowledge, help and guidance.

To my family, my mum and dad for their constant support, love and for listening. To my sister, Julie, for always knowing how to cheer me up, even if it did involve her 'wonderful' singing! To my brother Colin, for the constant distraction of youtube videos and movies...some better than others!

To the British Heart Foundation, for providing me with a BHF studentship which enabled me to conduct my studies.

To the Technical Staff at the School of Pharmacy for their practical support and guidance, particularly Dorothy Moir, for her assistance in the cell culture suite, for the many trips to and from the Rowett and for the daily gossips!

To the Lipids and Atherosclerosis group at the Rowett Research Institute, who were so welcoming of me, ensuring my time at the Rowett was all the more enjoyable. A special thanks to Sharon Wood, for her expert assistance in the lab, the 5.30am wake-up calls and constant laughs.

To the inhabitants of PC27 past and present, Karen, Barbara, Scott, Owen, Pramod, Bernie, Steven, Vicky and Claire for their support, encouragement and entertainment which made the last three years so enjoyable.

Finally, to Sarah, Karen, Emma and particularly my twinny Claire who deserve a special thanks, for the ridiculous lunchtime chat, wine fuelled trips to Club Tropicana, instigating my new addiction to tea and in general, making the last three years so much fun!

Publications

Michel L, Walsh S, Wood S, De Roos B, Vosper H, Goua M, Wainwright C.L. (2011). Fenofibrate, but not eicosapentanoic acid, attenuates hyperlipidaemia-induced endothelial dysfunction and elevated vascular endocannabinoid levels in ApoE^{-/-} mice. *Proceedings of the British Pharmacological Society (pA2 online)* (Abstracts, 2011 Winter Meeting of the BPS) *In Press*.

Michel L, Skene K, Teixeira S, Hector E, Vosper H, Wainwright C.L. (2010) Cannabinoid receptor activation inhibits smooth muscle cell proliferation and endothelial cytokine production. 16th IUPHAR World Congress of Basic and Clinical Pharmacology, Copenhagen, Denmark.

Michel L, Walsh S, Wood S, De Roos B, Vosper H, Goua M, Wainwright C.L. (2010) Eicosapentaenoic Acid as a Vasculoprotective Dietary Supplement: Involvement Of The Endocannabinoid System? Scottish Cardiovascular Forum, Scotland, UK.

Abstract

The ω -3 polyunsaturated fatty acids (ω -3 PUFAs), eicosapentaenoic acid (EPA) and docosahexaenoic acid (DHA), have been shown to have cardioprotective and anti-atherosclerotic actions. While it has been proposed that ω -3 PUFAs may structurally stabilise atherosclerotic lesions, the underlying mechanisms have yet to be fully elucidated. There is evidence that increased dietary intake of ω -3 PUFAs alters the concentration of endocannabinoids (ECs) in central and peripheral tissues and, since synthetic cannabinoid agonists have been shown to exert anti-atherosclerotic effects, this thesis explored whether a link exists between the endocannabinoid system and the beneficial effects of ω -3 PUFAs in the setting of experimental atherosclerosis. Therefore, the present studies were performed to (1) determine the impact of long-term intervention with ω -3 PUFAs on several physiological parameters, including the function of the endocannabinoid system, in an *in vivo* model of hypercholesterolaemia and (2) to examine the role, if any, of the activated endocannabinoid system in the activity of an *in vitro* model of macrophage lipid accumulation. At the cellular level, the present study demonstrated the interference of cannabinoid receptor signalling with intracellular uptake and accumulation of DHA, an effect which was demonstrated to be mediated, at least in part, via CB₂ receptor signalling. Moreover, the study provided the novel observation that DHA treatment of activated macrophages significantly inhibited 2-arachidonoylglycerol (2-AG) synthesis. This finding is strongly suggestive of an association between the effects of ω -3 PUFAs and regulation of the endocannabinoid system and its function. In the ApoE^{-/-} mouse model of experimental atherosclerosis, maintenance on an atherogenic diet induced significant hyperlipidaemia, an effect which was associated with endothelial dysfunction, cardiac remodelling, and significantly elevated anandamide (AEA) and 2-AG levels in brain, heart and aortic tissues. Supplementation of the atherogenic diet with the EPA, while having a negligible impact on endothelial dysfunction or cardiac remodelling, improved the hypercholesterolaemic profile and normalised the overproduction of ECs in both central (brain) and peripheral (heart and vascular) tissues. Fenofibrate, a lipid lowering control administered as a supplement to the atherogenic diet, was observed to significantly attenuate hypercholesterolaemia, endothelial dysfunction and elevated EC levels although no effect on cardiac remodelling was observed. In light of the observation that hypercholesterolaemia was associated with elevated tissue EC levels, together with the demonstration that EPA improved hypercholesterolaemia and attenuated EC levels suggests (1) a detrimental role of the endocannabinoid system in hypercholesterolaemia in the ApoE^{-/-} model and (2) regulation of this interaction by ω -3 PUFAs. Given the mounting evidence implicating the endocannabinoid system in various disease pathologies, the capacity of ω -3 PUFAs to influence the activation and function of this system may prove key to their beneficial effects.

Abbreviations

AA	Arachidonic acid
ABCA1	ATP-binding cassette reporter 1
ACEA	Arachidonyl-2'-chloroethylamide
ACS	Acyl-CoA synthetase
ADFP	Adipose differentiation-related protein
AEA	Anandamide
AHA	American Heart Association
ALA	α -linoleic acid
ANOVA	Analysis of variance
ApoA-I	Apolipoprotein-A I
ApoB	Apolipoprotein-B
ApoC-III	Apolipoprotein-C III
ApoE	Apolipoprotein-E
ApoE ^{-/-}	Apolipoprotein-E deficient mouse
AUTC	Area under the curve
2-AG	2-Arachidonoylglycerol
BK	Bradykinin
BP	Blood pressure
BPM	Beats per minute
BR	Bradykinin receptor
CAC	Coronary artery calcification
CAD	Coronary artery disease
cAMP	Cyclic adenosine monophosphate
CB ₁	Cannabinoid receptor 1
CB ₂	Cannabinoid receptor 2
CE	Cholesteryl ester
CETP	Cholesteryl ester transfer protein
CHF	Coronary heart disease
CRLP	Chylomicron remnant like particle
C57	C57BL/6J mice
DAG	Diacylglycerol
deH-HLNL	Dehydro-hydroxylysino-norleucine
deH-LNL	Dehydro-lysino-norleucine
DES	Desmosine
DHA	Docosahexaenoic acid

DHLNL	Dihydroxylysionorleucine
DIT	Diffuse intimal thickening
DMSO	Dimethyl sulfoxide
DOX	Doxorubicin
DPA	Docosapentaenoic acid
DPD	Deoxypyridinoline
EC	Endocannabinoids
ECM	Extracellular matrix
EDP	End diastolic pressure
EDPVR	End diastolic pressure volume relationship
EDV	End diastolic volume
EEL	External elastic lamina
EFA	Essential fatty acid
ELISA	Enzyme-linked immunosorbent assay
eNOS	Endothelial nitric oxide synthase
EPA	Eicosapentaenoic acid
ES	Endocannabinoid system
E3L	ApoE*3-Leiden transgenic mouse
FA	Fatty acid
FAAH	Fatty amide hydrolase
FACIT	Fibril-associated collagens with interrupted triple helices
FAME	Fatty acid methyl ester
FATP	Fatty acid transporter protein
FBS	Foetal bovine serum
FC	Free cholesterol
GM-CSF	Granulocyte colony-stimulating factor
GpAEA	Glycerophospho-arachidonoyl ethanolamide
GPCR	G protein coupled receptor
HCAEC	Human coronary artery endothelial cell
HDL	High density lipoprotein
H&E	Haematoxylin & eosin
HETE-EA	Hydroperoxyeicosatetraenoic acid ethanolamide
HHL	Histidinohydroxylysionorleucine
HLNL	Hydroxylysionorleucine
HMG-CoA	3-hydroxy-3-methylglutaryl CoA
9-HODE	9-Hydroxyoctadecadienoic acid
13-HODE	13-Hydroxyoctadecadienoic acid

HOSF	High oleic sunflower oil
HPLC	High performance liquid chromatography
HR	Heart rate
ICAM-1	Intercellular adhesion molecule-1
ICAM- 2	Intercellular adhesion molecule-2
IDE	Isodesmosine
IDL	Intermediate-density lipoprotein
IEL	Internal elastic lamina
IFN- γ	Interferon- γ
IL-1	Interleukin-1
IL-1 β	Interleukin-1 β
IL-6	Interleukin-6
IL-8	Interleukin-8
IMT	Intima-media thickness
I/R	Ischaemia/reperfusion
i.v.	Intravenous
JNK	p38/Jun N-terminal kinase
JWH133	CB ₂ agonist
LA	Linoleic acid
LC-MS/MS	Liquid chromatography mass spectrophotometry
LDL	Low density lipoprotein
LDL ^{r-/-}	LDL receptor deficient mouse
LHNL	Lysinohydroxynorleucine
LOX-1	Lectin-like oxLDL receptor
LPL	Lipoprotein lipase
LPS	Lipopolysaccharide
LV	Left ventricular
Lyso-PI	Lyso-phosphatidylinositol
MABP	Mean arterial blood pressure
MACIT	Membrane-associated collagens with interrupted triple helices
MAGL	Monoacylglycerol
MAPK	Mitogen activated protein kinase
MCP-1	Monocyte chemotactic protein-1
M-CSF	Macrophage colony-stimulating factor
MI	Myocardial infarction
MMP	Matrix metalloproteinase
MRM	Multiple reaction monitoring

MTS	3-(4, 5-dimethylthiazol-2-yl)-5-(3-carboxymethoxyphenyl)-2-(4-sulfophenyl)-2H-tetrazolium salt
MUFA	Monounsaturated fatty acid
MULTIPLEXIN	Multiple triple-helix domains and interruptions
n	Number of replicates
NADPH	Nicotinamide adenine dinucleotide phosphate dehydrogenase
NAPE	<i>N</i> -arachidonyl-phosphatidyl ethanolamine
NAPE-PLD	NAPE-selective phospholipase D
NF-κB	Nuclear factor-κB
NO	Nitric oxide
Nox2	NADPH oxidase 2
OA	Oleic acid
ORO	Oil red O
oxLDL	Oxidised low-density lipoprotein
pAEA	Phospho-anandamide
PAF	Platelet-activating factor
PBS	Phosphate buffered saline
PE	Phosphatidyl-ethanolamine
PFPA	Pentafluoropropionic acid
PG	Prostaglandin
PGDF	Platelet derived growth factor
PLC	Phospholipase C
PMA	Phorbol myristate acetate
PPAR	Peroxisome proliferator activated receptor
PPAR α	Peroxisome proliferator activated receptor alpha
PPAR δ	Peroxisome proliferator activated receptor delta
PPAR γ	Peroxisome proliferator activated receptor gamma
PPRE	Peroxisome proliferator response element
PUFA	Polyunsaturated fatty acid
PYD	Pyridinoline
RISK	Reperfusion injury salvage kinase
ROS	Reactive oxygen species
RXR	Retinoic X receptor
SDS-PAGE	Sodium dodecyl sulphate polyacrylamide gel electrophoresis
SEM	Standard error of the mean
SFA	Saturated fatty acid
SMC	Smooth muscle cell

SNP	Sodium nitroprusside
<i>sn</i> 1-DAGL	<i>sn</i> -1 specific diacylglycerol lipase
SR-A	Scavenger receptor A
SR-B1	Scavenger receptor B1
SREBP	Sterol regulatory element-binding protein
TEMED	Tetramethylethylenediamine
TGF- β 1	Transforming growth factor- β 1
Δ^9 -THC	Δ^9 -Tetrahydrocannabinol
THP-1	Human acute monocytic leukaemia cells
TNF- α	Tumor necrosis factor- α
TRPV1	Transient receptor potential vanilloid type-1
VCAM-1	Vascular adhesion molecule-1
VD3	1,25-dihydroxyvitamin D3
VLDL	Very low density lipoprotein
VSMC	Vascular smooth muscle cell

Chapter 1: Introduction

1.1 Vascular physiology

1.1.1 Blood vessel structure

The circulatory system is responsible for mediating the supply, exchange and removal of nutrients, vital gases and waste products at a cellular level. It is comprised of two independent structures: - the cardiovascular system which distributes blood and the lymphatic system which distributes lymph. Arteries underpin the main function of the cardiovascular system to supply nutrient rich, oxygenated blood to parenchymal organs and are functionally diverse from capillaries, which represent a gas exchange interface, and veins, which return deoxygenated blood to the heart and lungs. Three morphologically distinct layers comprise the normal arterial wall: the tunica intima, tunica media and tunica adventitia.

1.1.1.1 Tunica intima

The innermost layer of the arterial vascular wall, the tunica intima, constitutes a monolayer of endothelial cells exposed to the vessel lumen. The endothelium is supported by an underlying layer of connective tissue, containing collagen bundles and laminin interspersed with smooth muscle cells, which is bound to a fenestrated elastic lamellae boundary, the internal elastic lamina (IEL). The endothelium acts as an interface between circulating blood and vessel wall components, provides physical structure to the vessel and conducts a number of synthetic and metabolic functions. These functions include: (1) maintaining a non-thrombogenic luminal surface through regulation of thrombosis and platelet adherence; (2) modulating vascular tone; (3) preservation of the supporting basement collagen membrane; (4) production of growth factors and (5) regulation of inflammatory responses by controlling the interaction of white blood cells on the vessel wall (as reviewed by Sumpio, Riley and Dardik, 2002).

1.1.1.2 Tunica media

The middle layer of the vascular wall, the tunica media, is composed of concentric layers of smooth muscle cells embedded within an extracellular matrix (ECM) of fibril-forming collagens (type I, III and V), elastic fibres and dermatan and chondroitin sulphate proteoglycans. Viscoelasticity imparted by the presence of coiled elastic fibres in the ECM of the tunica media allows the vessel to expand or

rebound, buffering pressure variations that occur during the cardiac cycle to maintain a constant flow of blood (as reviewed by Arribas, Hinek and Gonzalez, 2006).

Under normal physiological conditions, the principal function of arterial smooth muscle cells is to contract. The cylindrical shape and circumferential orientation of smooth muscle cells in the tunica media enables modulation of arteriolar diameter. Vasoactive (constrictor and dilatory) substances derived from the endothelium (e.g. nitric oxide and endothelin) and the circulation (e.g. angiotensin II) contribute to arterial tone. However, smooth muscle cells may convert to a 'synthetic' state in response to alterations in local conditions (often mechanical or inflammatory changes) in which they can conduct a number of non-contractile functions including migration, proliferation, synthesis/degradation of ECM components, and release of inflammatory mediators such as interleukin-6 (IL-6) and tumor necrosis factor- α (TNF- α) (Loppnow and Libby, 1990; Li *et al.*, 1999).

1.1.1.3 Tunica adventitia

The exterior layer of the vascular wall, which is separated from the tunica media by the external elastic lamina (EEL), is known as the tunica adventitia. It is composed of vascular fibroblasts embedded within a collagen rich ECM. Vaso vasorum are present in larger arteries: networks of small blood vessels that penetrate the tunica media ensuring a continual supply of nutrients and oxygen to the endothelium. Perivascular innervation of this layer suggests the tunica adventitia may regulate vascular tone. Indeed, Laflamme *et al* (2006) demonstrated the ability of the adventitia (independent of the media and intima) to contract and relax in response to vasoactive substances.

1.1.2 Collagen in the vasculature

Collagen represents a principal component of the ECM of blood vessels. The majority of vascular collagen is derived from vascular smooth muscle cells; however endothelial cells, adventitial fibroblasts and macrophages have also been reported to produce collagen (Sage *et al.*, 1983; Shi *et al.*, 1997; Weitkamp *et al.*, 1999). In excess of 25 types of collagen have been identified to date, which are categorised into either: - (1) fibrillar and network forming collagens; (2) FACITs (fibril-associated collagens with interrupted triple helices); (3) MACITs (membrane-associated collagens with interrupted triple helices) or (4) MULTIPLEXINs (multiple triple-helix domains and interruptions) based on their supramolecular organisation (as reviewed by Shoulders and Raines, 2009). While several collagen types have been identified in the vasculature, the fibrillar collagens Types I and III, which confer tensile strength and elastic resilience respectively, represent the predominant collagen

fibrils present in blood vessels (Shekhonin *et al.*, 1985). Taken together, Type I and III collagen fibres provide structural stability and elasticity to the blood vessel enabling the structure to remain compliant but resist multi-directional stress.

1.1.3 Collagen in the myocardium

Cardiac fibroblasts, which constitute 60-70% of the cellular content of the human heart, represent the primary source of ECM component production in the myocardium. The ECM of the myocardium is composed mainly of the fibrillar collagens Type I (approximately 85%) and Type III and contains smaller amounts of fibronectin, laminin and elastin (Heeneman *et al.*, 2003). The foremost function of the cardiac ECM is to act as a scaffold for the transmission of mechanical, electrical and chemical signals between the various components of the myocardium enabling organised contraction and preventing myocardial movement (reviewed by Porter and Turner, 2009). Under physiological conditions, the synthesis and deposition of collagen is essential for normal cardiac function as it serves as the major stress-bearing element of the ECM, conferring tensile strength and structure to the myocardium. However, excessive collagen accumulation in the heart, known as cardiac fibrosis, can lead to tissue stiffening and cardiac dysfunction and has been implicated in the early stages of heart failure (Norton *et al.*, 1997; Kuwahara *et al.*, 2002; Gurtl *et al.*, 2009).

1.1.3.1 Collagen Synthesis

Transcriptional regulation of collagen synthesis is primarily dependent upon cell type but the process can be modulated by a number of growth factors and cytokines including transforming growth factor- β 1 (TGF- β 1), interleukin-1 (IL-1) and platelet derived growth factor (Amento *et al.*, 1991; Durante *et al.*, 2001). Collagens are synthesised from proto-collagen, precursor chains which contain additional end terminal propeptides (Bellamy and Bornstein, 1971). Newly synthesised procollagen strands undergo a degree of post-translational modification, primarily hydroxylation and glycosylation, and associate into procollagen trimers. Disulphide bonds at the COOH terminus stabilise the three procollagen chains and subsequent folding of the triple helix progresses to the NH₂ terminus. Following assembly, procollagen is secreted to the extracellular matrix where removal of terminal propeptides is facilitated by the action of the matrix metalloproteinases (MMPs) NH₂ proteinase and COOH proteinase (Kohn *et al.*, 1974; Hojima *et al.*, 1985). Processed procollagen strands are referred to as tropocollagen monomers.

1.1.3.2 Maturation

The process of collagen fibrillogenesis alters the molecular structure and stability of collagen triple helices and increases the tensile strength of collagen fibrils. Upon assembly, tropocollagen monomers spontaneously aggregate into intermediate collagen fibrils, named microfibrils. As demonstrated via electron density mapping by Orgel *et al.* (2001), microfibrils are comprised of five tropocollagen monomers organised in a quasi-hexagonal three-dimensional stack to form a right-handed, super twisted structure. Mature collagen fibrils are composed of interdigitated microfibrils.

The macromolecular structure of mature collagen is further strengthened by the formation of covalent bonds, known as collagen cross-links, between the protein sub-units. Immature (difunctional) cross-links stabilise collagen microfibrils by forming intermolecular bonds between the tropocollagen monomers of the microfibril unit (Kang, 1972; Nicholls and Bailey, 1980; see Figure 1.1). The mechanism of immature cross-link formation in fibrillar collagen is facilitated by the reactions of aldehydes derived from the telopeptide precursor's lysine or hydroxylysine, a process which is facilitated by the action of the copper dependent enzyme, lysyl oxidase (Williamson and Kagan, 1986). Lysine derived aldehydes follow the allysine cross-linking pathway in which the aldehydes condense with adjacent lysine residues on adjacent molecules to form the reducible aldimine base cross-links. Dehydro-hydroxylysinonorleucine (deH-HLNL) and dehydro-lysinonorleucine (deH-LNL) represent the most common lysine-aldehyde derived cross-links (as reviewed by Eyre and Wu, 2005). Hydroxylysine derived aldehydes follow the hydroxyallysine cross-linking pathway to generate the reducible keto-imine bases dihydroxy-lysinonorleucine (DHLNL) and to a lesser extent lysinohydroxynorleucine (LHNL) (as reviewed by Eyre and Wu, 2005).

The subsequent conversion of immature cross-links into mature (trifunctional) cross-links is spontaneous and governed by the structural organisation of the collagen fibril. Mature cross-links constitute covalent intermolecular bonds between individual microfibrils (see Figure 1.1) which are significantly more stable than the immature cross-links (Light and Bailey, 1985). The aldimine bases are converted to non-reducible histidin adducts (deH-LNL reacts with histidine to form histidino-hydroxylysinonorleucine [HHL]) (Yamauchi *et al.*, 1987). The keto-imine bases react with either hydroxylsine residues or another keto-imine base on adjacent collagen microfibrils to generate the pyridinium cross-links (Fujimoto *et al.*, 1978; Ogawa *et al.*, 1982) hydroxylysyl-pyridinoline (PYD) and deoxy-pyridinoline (DPD).

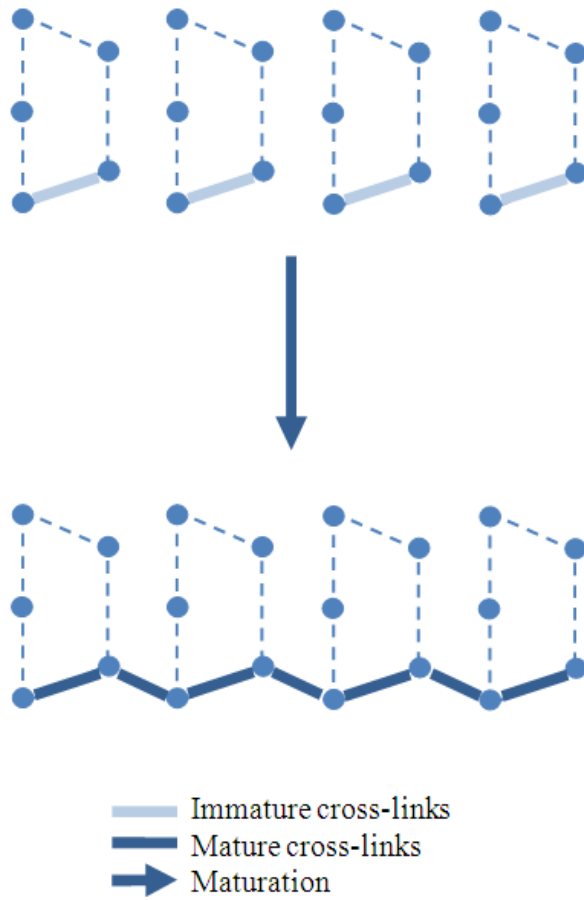


Figure 1.1 Collagen cross-link formation: Diagram illustrating the placement of immature and mature cross-links within, and between collagen microfibrils.

1.2 Coronary heart disease

1.2.1 Aetiology

Coronary heart disease (CHD) presents a major cause of death in the westernised world. Atherosclerosis, a manifestation of CHD, is a chronic inflammatory condition characterised by the accumulation of fatty material within the wall of arterial blood vessels. The progression of atherosclerosis is asymptomatic. However at the advanced stage, plaque complications can instigate potentially fatal clinical repercussions including myocardial infarction and stroke. Anitschkow and Chalutow (1913) reported the first evidence of a direct link between cholesterol and atherosclerosis development when it was observed that rabbits fed a cholesterol rich diet developed human-like atherosclerotic lesions (Anitschkow and Chalutow, 1913 as cited in Williams and Tabas, 1995). From these initial findings emerged the lipid infiltration hypothesis that high intake, and hence circulating levels, of cholesterol lead to the development of atherosclerosis. Other theories of disease origin have been proposed, including the monoclonal theory and infectious theory of atherosclerosis (Benditt and Benditt, 1973; Fabricant *et al.*, 1978). The response-to-injury hypothesis, initially proposed by Ross and Glomset (1973), suggests that endothelial injury induced by abnormal physiological conditions (e.g. hypercholesterolaemia, hypertension and hypoxia) precedes lesion development which is fuelled by an overactive immune response (Davis *et al.*, 2003). However, the alternate (although not entirely dissimilar) response-to-retention theory advocates that the key to atherosclerosis lesion development is the retention of atherogenic lipoproteins in the subendothelial space in association with ECM proteoglycans, which triggers subsequent inflammation (Williams and Tabas, 1995). While the causative ‘event’ initiating lesion formation may differ between the injury and retention theories, both support a role of inflammation in disease development.

1.2.2 Development of early atherosclerotic lesions

In humans, fibrocellular thickening of the tunica intima, referred to as diffuse intimal thickening (DIT), occurs in the aorta and coronary arteries in an age dependent manner, irrespective of race. DIT comprises primarily stable, non-proliferative smooth muscle cells, elastin, proteoglycans and a small macrophage population with no lipid pool present (Stary *et al.*, 1992). DIT has been reported in fetuses and infants, with thickening of the proximal left anterior descending artery evident three months after birth (Ikari *et al.*, 1999). Moreover, the intima:media ratio increases to >1.0 in young adults (Nakashima *et al.*, 2002). In human autopsy subjects (aged between 36 weeks gestation and 30 years old), the systemic distribution of DIT was consistently localised to the atherosclerosis-prone

(abdominal and descending aorta, coronary, carotid and iliac) arteries (Nakashima *et al.*, 2002), hence DIT is thought to be related to early atherosclerosis development.

Type I lesions, as defined by the American Heart Association (AHA) histological classification (Stary *et al.*, 1994), constitute focal accumulations of extracellular lipid in pre-existing DIT, preferentially in those located at vessel bifurcations and branches where blood flow is turbulent. While it is generally agreed that the large lipid core characteristic of advanced atherosclerotic lesions is derived from the apoptosis of foam cell (lipid laden) macrophages (see section 1.2.5), numerous studies indicate that accumulation of extracellular lipid precedes macrophage infiltration in the early Type I lesion. Indeed in humans, electron microscopy revealed evidence of an early lipid core in non-diseased aortic intima from young adults (Guyton and Klemp, 1993). Furthermore, the accumulation of apolipoprotein B (apoB)-containing lipids in the aortic intima of human fetuses, which was increased significantly by maternal hypercholesterolaemia, was reported in the absence of macrophage infiltration (Napoli *et al.*, 1997). While the formation of intimal extracellular lipid pools characterises Type I lesions, progression to more advanced stages involves macrophage infiltration. Indeed in human coronary arteries, the presence of CD68-positive macrophages in the deep intima was demonstrated to increase proportionately to increasing lipid accumulation (Nakashima *et al.*, 2007).

1.2.2.1 Lipoprotein accumulation

Lipoprotein particles are removed from the circulation and transported across the endothelium to the subendothelial space via transcytosis. *In vivo* and *in situ* experimental models of hypercholesterolemia, employing either low-density (LDL) or very-low-density lipoproteins (VLDL), have demonstrated a correlation between elevated plasma lipoproteins and increased transcytosis of lipoproteins across the endothelium (Schwenke and Carew, 1989; Nordestgaard, Tybjaerg-Hansen and Lewis, 1992; Fry *et al.*, 1993; Truskey *et al.*, 1993). Transcytosis is facilitated by caveolae, membrane invaginations present on the surface of endothelial cells. The importance of caveolae mediated lipoprotein transcytosis in atherosclerosis development was highlighted in a study by Frank *et al.* (2004) who observed a 70% reduction in aortic lesion formation in caveolin-1 (a major protein component of caveolae) deficient apolipoprotein E knockout (ApoE^{-/-}) mice compared to control ApoE^{-/-} mice, despite maintenance on an atherogenic diet. Although not fully understood, caveolae are thought to transport lipoproteins across the endothelium via either: - (1) receptor mediated transfer or (2) fluid phase transfer. Candidate receptors suggested for the former pathway include the scavenger receptor B1 (SR-B1) and the LDL receptor (as reviewed by Frank, Pavlides and Lisanti, 2009).

The retention of transcytosed lipoproteins in the sub-endothelial space of the blood vessel is thought to be facilitated, in part, by their association with various proteoglycan components of the ECM. Indeed, in comparison to mice expressing wild-type LDL, atherosclerosis development was markedly reduced in mice expressing LDL which could not bind proteoglycans (Skalen *et al.*, 2002). Biglycan, a chondroitin sulphate/dermatan sulphate containing proteoglycan, has a reported binding capacity for apoB-containing lipoproteins (Olin-Lewis *et al.*, 2002) and has been observed to co-localise with lipoproteins in DIT, early and advanced atherosclerotic lesions (O'Brien *et al.*, 1998; Nakashima *et al.*, 2007).

1.2.2.2 Lipoprotein modification

During transcytosis and/or following retention in the sub-endothelial space, lipoproteins are subject to chemical modification, a process that endows particles with a greater pro-inflammatory and pro-atherogenic profile than native lipoproteins. Proteolysis, lipolysis and most importantly oxidation appear key to this process. Endothelial cells, smooth muscle cells, monocytes and macrophages are capable of oxidising LDL particles (Morel *et al.*, 1984; Steinbrecher *et al.*, 1984; Parthasarathy *et al.*, 1986). The exact mechanism(s) of cell-mediated oxidation are not precisely understood. The identification of stable oxidation products in LDL particles extracted from atherosclerotic plaques however, indicate an involvement of reactive nitrogen species, myeloperoxidase, metal ion and lipoxygenase pathways (Folcik *et al.*, 1995; Hazen and Heinecke, 1997; Leeuwenburgh *et al.*, 1997a; Leeuwenburgh *et al.*, 1997b).

The oxidative damage incurred by lipoprotein particles retained in the vascular intima, particularly LDL, induces alterations to their biochemical properties. LDL in its oxidised form (oxLDL), but not its native form, propagates a number of pro-inflammatory actions that can activate and damage endothelial cells. Cellular internalisation of oxLDL induces apoptosis and necrosis via upregulation of reactive oxygen species (ROS) formation (superoxide anion and hydrogen peroxide) and activation of the nuclear factor- κ B (NF- κ B) pathway, an effect which has been demonstrated in bovine and human endothelial cells (Cominacini *et al.*, 2000; Chen *et al.*, 2007). OxLDL is also known to modulate monocyte recruitment to the endothelium. OxLDL was demonstrated to mediate a significant increase in the adhesion of monocytes to human coronary artery endothelial cells *in vitro* (Li and Mehta, 2000), an effect which was associated with a marked increase in the expression of the chemokine, monocyte chemoattractant protein-1 (MCP-1). The aforementioned effects of oxLDL were reported to be mediated by its binding to, and activation of lectin-like oxLDL (LOX-1) receptors (Cominacini *et al.*, 2000; Li and Mehta, 2000; Chen *et al.*, 2007), Class E scavenger receptors which are expressed primarily on endothelial cells (as reviewed by Twigg *et al.*, 2012).

1.2.2.3 The early inflammatory response

The damage incurred by endothelial cells following their exposure to, and uptake of, modified lipoproteins, induces cell activation and the upregulated expression of a number of pro-inflammatory genes. Upregulated expression of adhesion molecules (selectins, integrins and the immunoglobulin superfamily of cell adhesion molecules) triggers the well documented adhesion cascade in which circulating leukocytes transmigrate the activated endothelium to aggregate at the site of injury (Metsas and Ley, 2008). The expression of pro-inflammatory cytokines, particularly IL-1 and TNF- α further upregulates adhesion molecule expression, primarily intercellular adhesion molecule-1 (ICAM-1), ICAM-2 and vascular cell adhesion molecule-1 (VCAM-1) (reviewed by Fogel and Pober, 2012).

1.2.3 Fatty streak formation

Type II lesions (defined by the AHA classification; Stary *et al.*, 1994), often referred to as fatty streaks, are characterised by an accumulation of lipid-laden macrophages (stratified in adjacent layers) and smooth muscle cells (known as foam cells), T lymphocytes and a small number of mast cells. The majority of the lipid present in Type II lesions is sequestered within macrophage derived foam cells, while the extracellular space contains only dispersed, isolated lipid droplets.

Foam cell formation involves the unregulated internalisation of lipoprotein particles to generate a lipid engorged cell, a process which is primarily due to an imbalance between lipoprotein uptake and cholesterol efflux. Macrophage uptake of modified lipoproteins is enabled by both receptor dependent and independent mechanisms. Receptor mediated endocytosis of modified lipoproteins (acetylated and oxidised) is facilitated by several receptors, primarily those of the scavenger receptor family including the SR-A (I and II), CD36, SR-B1, CD68 and LOX-1 receptors (Smirnova *et al.*, 2004; Sun *et al.*, 2007; as reviewed by Greaves and Gordon, 2009). Studies suggest a major role of the CD36 and SR-A receptors in macrophage mediated oxLDL (modified by the myeloperoxidase/peroxynitrite pathways) clearance *in vitro*. Indeed, the CD36 and SR-A receptors have been reported to mediate 75-90% of cholesterol ester accumulation in mouse peritoneal macrophages (Podrez *et al.*, 2000; Kunjathoor *et al.*, 2002). A more recent study however, reported a significant attenuation of atherosclerotic lesion progression but no significant abrogation of foam cell formation in mice genetically deficient in SR-A/CD-36 receptors, suggesting the involvement of other receptors *in vivo* (Manning-Tobin *et al.*, 2009). Macrophages have also been reported to internalise lipoproteins via micro- and macropinocytosis of extracellular fluid (Zhao *et al.*, 2006; Yao *et al.*, 2009; Anzinger *et*

al., 2010). Unlike receptor mediated endocytosis which only permits uptake of modified lipoproteins, receptor independent mechanisms facilitate the internalisation of native lipoproteins and subsequent foam cell formation.

Intimal smooth muscle cells have also been demonstrated to express SR-A and CD36 scavenger receptors *in vitro* and *in vivo* (Mietus-Snyder *et al.*, 2000; Zingg *et al.*, 2002; Rong *et al.*, 2003). Foam cells derived from a smooth muscle cell lineage can be distinguished from macrophage derived foam cells due to expression of vimentin and S-100 proteins (Vukovic *et al.*, 2006). Both macrophage and smooth muscle foam cells exhibit upregulated gene expression of pro-inflammatory cytokines (MCP-1, IL-6) and MMPs (Klouche *et al.*, 2000; Shiffman *et al.*, 2000). Smooth muscle foam cells demonstrate impaired collagen and fibronectin assembly (Frontini *et al.*, 2009). Foam cell production of pro-inflammatory mediators promotes local inflammation which, in combination with persistent transcytosis of lipoprotein particles from the circulation, perpetuates monocyte recruitment, foam cell formation and ultimately, lesion progression.

1.2.4 Development of fibrofatty lesions

Gradually, fatty streaks develop into fibrofatty lesions (Type III lesions as defined by the AHA classification; Stary *et al.*, 1994). The fibrofatty lesion represents an intermediate morphological link between early lesion development and progression to the advanced atheroma. Early lesions (Type I to III) represent clinically silent manifestations of atherosclerosis. Type II lesions are histologically characterised by the presence of microscopically visible pools of extracellular lipid droplets dispersed throughout the lesion. Lipid pools develop among the layers of smooth muscle cells that constitute the location of the DIT and lie below the stratified layers of macrophages and foam cell macrophages. Lipid pools displace intercellular matrix proteoglycans and force smooth muscle cells apart. Extracellular droplet accumulation is most likely the result of: - (1) lipid entry into the vessel wall exceeding the phagocytic ability of macrophages (Libby *et al.*, 2000) and (2) the apoptosis (and subsequent expulsion of cell contents) of macrophages due to excessive accumulation of free cholesterol which is cytotoxic to these cells (Warner *et al.*, 1995).

1.2.5 Progression to advanced, complicated lesion

The prominent histological feature of Type IV lesions (as defined by the AHA classification; Stary *et al.*, 1995), also known as atheroma, is the presence of a dense core of extracellular lipid. It is believed that the lipid core originates from the amalgamation of smaller lipid pools which are known to be

dispersed throughout the preceding Type II lesion (Stary *et al.*, 1994). Furthermore, continued apoptosis of saturated macrophage foam cells is thought to contribute to the growing lipid core (Ball *et al.*, 1995). In the case of Type IV lesions, the presence of a lipid core results in thickening of the arterial wall, but does not compromise vascular lumen diameter due to the capacity of the vessel for outward remodelling. However, it is worthwhile to note that should the lipid core develop rapidly in size, this lesion may impinge on vessel diameter. A connective tissue layer, corresponding to the proteoglycan rich layer of the normal intima, separates the lipid core and the endothelial surface and is referred to as the fibrous cap. This region contains primarily proteoglycan-collagen matrix, smooth muscle cells and some macrophages and T lymphocytes (Virmani *et al.*, 2000). Concentrated pockets of macrophages, T lymphocytes and macrophage foam cells populate the lesion periphery. Type IV lesions are susceptible to physical disruption such as fissures and macroscopic ulceration due to flow induced stress and strain. Disturbances tend to occur in the shoulder regions of the lesion, where the cap is thinnest with little tensile strength. In response to the aforementioned physical disturbances, haemorrhage can occur within the vessel lumen or vaso vasorum of the adventitia, with accumulation of platelet and fibrin aggregates at lesion sites.

Type V lesions (as defined by the AHA classification; Stary *et al.*, 1995) are not dissimilar to type IV lesions and are characterised by thinning of the fibrous cap region. Morphology of type V lesions varies considerably, as does the potential for vascular remodelling and a reduction in lumen diameter. Nomenclature is based upon the composition of material underlying the thinned fibrous cap. Fibroatheromas (type Va lesions) comprise several lipid core layers segregated by thick layers of connective tissue. It has been suggested that such lesions may develop as a result of lesion surface disruption where subsequent haematomas and thrombotic deposition act as a structural framework for the accumulation of more macrophages and extracellular lipid droplets. Calcified lesions (type Vb lesions) are characterised by mineralisation of the lipid core due to calcification of extracellular lipid and smooth muscle organelle remnants (Stary *et al.*, 1995). Mineral deposits can often replace the entire lipid core. Fibrotic lesions (type Vc) contain a core rich in connective tissue which lacks substantial levels of extracellular lipid. In addition, it is found that connective tissue gradually replaces the normal intima.

Complications of Type IV and Type V lesions (surface disruptions, haematoma and/or haemorrhage, thrombotic deposition) are generally responsible for the morbidity and mortality associated with atherosclerosis. Type VI lesions constitute either a Type IV or Type V lesions exhibiting one or more of the aforementioned complications.

1.2.5.1 Macrophages: role in atherosclerosis

Macrophages represent a key cellular component of atherosclerotic lesions. Indeed, the importance of these cells in disease manifestation and progression was demonstrated *in vivo*, where mice deficient in macrophage colony-stimulating factor (M-CSF), a growth factor required for monocyte and macrophage maturation, exhibited markedly reduced atherosclerotic lesion development compared to wild-type controls (Smith *et al.*, 1995). Macrophages present within the atherosclerotic plaque exhibit phenotypic heterogeneity. During the process of transmigration, local levels of M-CSF and granulocyte colony-stimulating factor (GM-CSF), as well as the levels of pro- and anti-inflammatory mediators together determine the phenotypic outcome of monocyte maturation (reviewed by Newby *et al.*, 2009). Macrophages derived from an environment dominated by pro-inflammatory signalling (IL-1, TNF- α , interferon- γ (IFN- γ)) are termed 'classically activated' (M1) macrophages. M1 macrophages exhibit enhanced phagocytic and cytotoxic activity, upregulated scavenger receptor expression, and increased secretion of pro-inflammatory cytokines. Conversely, macrophages derived from an environment dominated by anti-inflammatory signalling (IL-4, IL-13) are termed 'alternatively activated' (M2) macrophages and promote resolution of inflammation and tissue repair. Atherosclerotic lesions are thought to contain primarily M1 macrophage derived foam cells, although foam cells carrying markers of both M1 and M2 phenotypes have been identified in mouse atherosclerotic lesions (Bouhlef *et al.*, 2007). Recently, *in vivo* studies in mice have identified another macrophage foam cell phenotype, the MOX foam cell, which demonstrates anti-inflammatory and anti-oxidant activity (Boyle *et al.*, 2009). The presence of this phenotype in human lesions has yet to be confirmed, therefore, the relevance of the MOX phenotype to human atherosclerosis progression remains to be determined.

In the atherosclerotic lesion, macrophages act as a potent source of pro-inflammatory cytokines and ROS, which serve to augment the local inflammatory response, maintaining endothelial activation and leukocyte recruitment. Furthermore, macrophages secrete a number of proteinases including, most notably, the matrix metalloproteinases (MMPs). MMPs constitute endopeptidases involved in the direct degradation of ECM components. In studies examining human atherosclerotic lesion composition, it has been demonstrated that the expression of MMPs, particularly MMPs-1, -2, -3, and -9, are significantly elevated in diseased vessels compared to control vessels (Orbe *et al.*, 2003; Higashikata *et al.*, 2006; Dollery and Libby, 2006). The excessive degradation of elastin and interstitial collagen (including the fibrillar collagens Type I and III) by activated MMPs is thought to play a role in vascular remodelling and plaque destabilisation. The importance of the macrophage foam cell in atherosclerosis pathology is emphasised by their capacity to propagate and maintain local

inflammation and to induce structural alterations within the developing lesion, effects which can influence the clinical outcome of lesion progression.

1.2.6 Clinical outcome of atherosclerosis progression

The clinical outcome of atherosclerotic lesion rupture is incredibly difficult to predict as the severity of the event is largely dependent upon the underlying composition of the lesion. Lesion rupture can manifest in one of two forms: - frank rupture or superficial erosion. Dependent on the form of rupture, there may or may not be significant clinical repercussions (as reviewed by Schoenhagen *et al.*, 2002). Myocardial infarction (MI), sudden death and stroke are potential complications of atherosclerotic lesions should they rupture and, through thrombus formation (and possibly, embolism), lead to vessel occlusion.

1.2.7 Animal models of atherosclerosis

A number of animal models are currently available to study atherosclerosis *in vivo*, and while advantages to using such systems exist, no model is without its drawbacks. Pigs, rabbits, dogs and to a lesser extent, non-human primates, represent large animal models currently in use. Such models exhibit similar physiology to humans including cardiovascular anatomy (pig) and thrombogenic profiles (non-human primates and dogs) however their use entails ethical, financial and logistical difficulties (reviewed by Vilahur *et al.*, 2011; Zaragoza *et al.*, 2011).

Of the small animal models available (mouse, rat, hamster and guinea pig), murine models are the most widely used. Wild-type mouse strains are generally resistant to spontaneous lesion development due to their lipid physiology which differs drastically from that of humans. The cholesterol of wild-type mice is transported largely in HDL particles, conferring a degree of protection against atherosclerosis. C57BL/6J represents the wild-type strain most sensitive to the development of mild lesions when maintained on a high fat diet (Paigen *et al.*, 1987). Genetic manipulation of C57BL/6J mice has enabled the generation of new strains which are susceptible to, and exhibit varying degrees of, atherosclerosis. The LDL receptor deficient ($LDLR^{-/-}$) mouse, apolipoprotein-E deficient ($ApoE^{-/-}$) mouse and ApoE*3-Leiden (E3L) transgenic mouse constitute three such models. Both $LDLR^{-/-}$ and E3L mice, which exhibit only mild hyperlipidemia and limited lesion development when maintained on regular chow (Ishibashi *et al.*, 1993; Sehayek *et al.*, 2001; Moore *et al.*, 2003), are considered moderate models of atherosclerosis due to their development of moderate hyperlipidemia and lesions following high fat feeding (Ishibashi *et al.*, 1993; van Vlijmen *et al.*, 1994).

ApoE^{-/-} mice are considered a severe model of atherosclerosis. Apolipoprotein E (apoE), a glycoprotein component of plasma lipoproteins, serves as a ligand for cell surface lipoprotein receptors (such as the LDL receptor) and facilitates the removal of lipoproteins from the circulation (Mahley, 1988). Homozygous deletion of the apoE gene, results in a marked increase of plasma LDL and VLDL even when animals are maintained on regular chow (Plump *et al.*, 1992). ApoE^{-/-} mice develop extensive lesions that mimic those of humans in terms of anatomical location and development. Early lesions, which resemble fatty streaks, can be detected in the aortic root and proximal aorta around 10 weeks of age and develop, over time, into fibrous, complicated plaques which are detected throughout the macrovasculature (Zhang *et al.*, 1994; Nakashima *et al.*, 1994; Reddick *et al.*, 1994). Maintenance on a high fat diet significantly accelerates this process and further elevates plasma cholesterol (Nakashima *et al.*, 1994). One shortcoming of the ApoE^{-/-} model is that the majority of plasma cholesterol is confined to the VLDL lipoprotein fraction as opposed to the LDL fraction in humans. In addition, evidence that ApoE has immunomodulatory actions (Tenger and Zhou, 2003) has raised questions regarding the effect of ApoE removal on the inflammatory component of atherosclerosis. However despite these limitations, the ApoE^{-/-} mouse is currently the most widely utilised murine model for the study of atherosclerosis progression.

1.2.8 Pharmaceutical intervention

Dyslipidaemia in the form of elevated plasma lipoproteins represents a major risk factor for the development of atherosclerosis. Lipoprotein metabolism has thus been identified as a target for pharmaceutical intervention in the prevention and/or treatment of atherosclerosis. Cholesterol represents a functional constituent of cell membranes and serves as an essential precursor in the biosynthesis of steroid hormones, bile acids and vitamin D. Cholesterol is obtained either exogenously, from dietary cholesterol, or endogenously through its synthesis, which occurs primarily in the liver. Due to its hydrophobic nature, the transport of cholesterol in the circulation requires its sequestration in lipoprotein particles: macromolecular complexes of triglycerides, cholesterol esters, non-esterified cholesterol, phospholipids and apolipoproteins. There are five major classes of lipoproteins: - (1) chylomicrons; (2) VLDL; (3) intermediate-density lipoproteins (IDL); (4) LDL and (5) high-density lipoproteins (HDL). Elevated plasma concentrations of apolipoprotein B (apoB) containing lipoproteins (chylomicron, IDL and LDL lipoprotein fractions) have been associated with elevated CHD risk, while HDL represents a strong inverse indicator of CHD risk (Walldius *et al.*, 2001; Luc *et al.*, 2002; Talmud *et al.*, 2002).

1.2.8.1 Statins

The statin class of drugs constitute powerful lipid lowering agents used in the primary and secondary prevention of primary hypercholesterolaemia and mixed dyslipidaemias. The key rate limiting step of endogenous cholesterol biosynthesis is the reduction of 3-hydroxy-3-methylglutaryl CoA (HMG-CoA) to mevalonic acid via the enzymatic action of HMG-CoA reductase. Statins represent potent inhibitors of HMG-CoA reductase and thus impair cholesterol synthesis. The net result of reduced cholesterol synthesis is reduced assembly and secretion of lipoproteins, upregulated hepatic LDL receptor expression and increased hepatic uptake of lipoproteins (Igel *et al.*, 2002). Two sub-classes of statins exist: - the fermentation derived statins (lovastatin, pravastatin, and simvastatin) and the synthetic statins (atorvastatin, cerivastatin, fluvastatin). Randomised trials have reported that lowering LDL lipoprotein cholesterol through statin treatment decreases the incidence of major cardiovascular events by 25-35% (Ridker *et al.*, 2008). The beneficial actions of statins extend beyond lipid-lowering to include anti-inflammatory, anti-oxidant and immunomodulatory effects however monotherapy has been associated with adverse side effects including myopathy, rhabdomyolysis, and elevated hepatic transaminases in some patients (Paoletti *et al.*, 2002; Heeba *et al.*, 2009).

1.2.8.2 Fibrates

The fibrate class of drugs constitute a group of fibric acid derivatives used in the treatment of hypoalphalipoproteinaemia (low plasma HDL) and hypertriglyceridaemia. Of the drug preparations currently available (including bezafibrate, clofibrate and gemfibrozil), fenofibrate represents the most widely clinically used fibrate. Fibrates are selective agonists of the peroxisome proliferator-activated receptor (PPAR) family of nuclear receptor proteins. As lipid sensitive nuclear transcription factors, PPARs regulate multiple cellular functions including fatty acid metabolism, cytokine production and glucose homeostasis (reviewed by Soskic *et al.*, 2011). Three ligand-specific isoforms of PPAR exist: - PPAR α , PPAR γ and PPAR δ . Upon activation, PPARs heterodimerise with the retinoic X receptor (RXR) to recognise and bind DNA sequences, termed the peroxisome proliferator response elements (PPREs), upstream of the target gene (Muerhoff *et al.*, 1992; Keller *et al.*, 1993). In addition to positively regulating gene expression, there is evidence to suggest that PPAR signalling can trans-repress the expression of non-target genes through physical interaction with other transcription factors including NF- κ B and Smad-3 (Delerive *et al.*, 1999; Fu *et al.*, 2001). PPAR α is highly expressed in the liver and is found in the heart, skeletal muscle and kidney, where its main function is to regulate fatty acid and lipoprotein metabolism (Braissant *et al.*, 1996; Soskic *et al.*, 2011). PPAR γ is involved in glucose homeostasis and insulin sensitivity, while the function of PPAR δ , which is not well understood, is thought to involve metabolism (Soskic *et al.*, 2011).

Fibrates bind to PPAR α , mimicking the endogenous lipid ligands which bind the receptor. The most pronounced effect of fibrate treatment, which underpins their clinical use in the management of dyslipidaemia, is a decrease in plasma triglycerides. Fibrate treatment has been reported to lower LDL-cholesterol and to elevate HDL-cholesterol (Caslake *et al.*, 1993; Guerin *et al.*, 2002); however these effects vary in magnitude depending on patient baseline plasma concentrations and the dose and potency of the fibrate used. Fibrates have been shown to alter the concentrations of LDL lipoprotein sub-fractions, lowering the plasma content of smaller, denser and more atherogenic LDL particles and increasing the plasma content of larger, buoyant, less atherogenic LDL particles (Caslake *et al.*, 1993; de Graaf *et al.*, 1993; Tokuno *et al.*, 2007; Soskic *et al.*, 2011). Furthermore, fibrates are reported to reduce the expression of apoC-III, an apolipoprotein which inhibits the activity of lipoprotein and hepatic lipases and represents a marker of atherogenesis (Chapman *et al.*, 2010). Fenofibrate-mediated activation of PPAR α has also been reported to reduce the cholesterol ester and triglyceride exchange between HDL and VLDL-lipoproteins, an activity which is mediated via the cholesteryl ester transfer protein (CETP) (Guerin *et al.*, 2002).

Experimental evidence of the triglyceride lowering action of fibrates has given insight into the major underlying mechanisms conferring these effects. Murine studies have reported an increase in hepatic free fatty acid uptake and conversion to acyl-coA due to upregulated expression of the fatty acid transporter protein (FATP) and acyl-CoA synthetase (ACS) activity following fibrate treatment (Schoonjans *et al.*, 1995; Martin *et al.*, 1997). This induction of the β -oxidation pathway may serve to sequester the pool of free fatty acids available for assembly and secretion of triglyceride-rich lipoproteins, thus lowering hepatic lipoprotein secretion. Another likely mechanism suggests increased lipoprotein lipolysis. This notion is supported by experimental evidence from murine and human studies where fibrate treatment was demonstrated to suppress hepatic gene expression and secretion of ApoC-III (Staels *et al.*, 1995; Staels *et al.*, 1998). The subsequent reduction in the ApoC-III content of lipoproteins would therefore increase their accessibility for triglyceride hydrolysis via the enzymatic action of lipases.

1.3 Diet and coronary heart disease

Saturated, monounsaturated and polyunsaturated fats constitute the three forms of naturally occurring fats. Until recently, consumption of fat in any of the aforementioned forms was considered detrimental to health. The key observation that Greenland Inuit populations exhibit low mortality rates from CHD despite consuming a diet rich in fat, led to the notion that reduced CHD mortality rate was due to the high percentage of polyunsaturated fats present in the diet (Dyerberg *et al.*, 1975).

Fatty acids constitute carboxylic acids with carbon chains which can vary in length between two and thirty-six carbons. Polyunsaturated fatty acids (PUFAs) are characterised by the presence of two or more double bonds in the carbon chain structure. PUFA nomenclature is derived from the location of the first double bond relative to the methyl terminus of the molecule. The PUFAs linoleic acid (LA; 18:2n-6) and α -linoleic acid (ALA; 18:3n-3) are denoted *essential fatty acids* (EFAs) as the human body lacks the required desaturase enzymes (Δ 12- and Δ 15-desaturase) to synthesise these fatty acids *de novo* (Nelson and Cox, 2005 cited in Tvrzicka *et al.*, 2011). LA and ALA serve as precursors to the ω -6 series of fatty acids, e.g. arachidonic acid (AA; 20:4n-6), and the ω -3 series of fatty acids, e.g. eicosapentaenoic acid (EPA; 20:5n-3) and docosahexaenoic acid (DHA; 22:6n-3), respectively. The production of these sub-families of PUFAs is therefore directly related to the availability of EFAs. The Westernised diet is rich in ω -6 PUFAs, largely due to intensive production of cultured meats and eggs through modern agricultural practice. Modern Western diets are generally deficient in ω -3 PUFAs compared to ancestral diets. Current estimates of an ω -6: ω -3 PUFA ratio of ~25:1 in modern Western diets as opposed to the likely <2:1 in ancestral diets supports this notion (Sayanova and Napier, 2004).

The ω -6: ω -3 PUFA ratio has significant implications in terms of cell signalling and function. The eicosanoids represent a family of bioactive lipid mediators derived from the oxidation (primarily via the activity of cyclooxygenase and lipoxygenase enzymes) of PUFAs which regulate the magnitude of inflammatory responses. Eicosanoids derived from the ω -6 PUFA AA, including thromboxanes, two-series prostaglandins (PGs) and four-series leukotrienes, tend to promote a physiological state that is pro-inflammatory, pro-thrombotic and induces vasospasm and vasoconstriction (reviewed by Harizi *et al.*, 2008). If formed in large quantities, such mediators can contribute to the pathophysiology of certain inflammatory conditions and therefore serve as a recognised target of anti-inflammatory therapeutics. However, it is worthwhile to note that ω -6 PUFA derived eicosanoids are not solely pro-inflammatory mediators as anti-inflammatory properties of the AA derived lipoxins have been described (Serhan *et al.*, 2003). The ω -3 PUFAs EPA and DHA are also precursors for the lipoxygenase and cyclooxygenase oxidative pathways; however the products of their oxidation differ from AA to include the three-series prostaglandins, five-series leukotrienes and the anti-inflammatory E- and D-series resolvins (Serhan *et al.*, 2000; Hong *et al.*, 2003). The generation of eicosanoids from ω -3 PUFAs, which are often, although not exclusively, of a lesser potency than ω -6 PUFA derived eicosanoids, is largely associated with an anti-inflammatory, anti-thrombotic and vasodilatory physiological profile (Russo, 2009). It is these properties of ω -3 PUFAs which have been studied extensively in relation to their therapeutic potential in various disease pathologies.

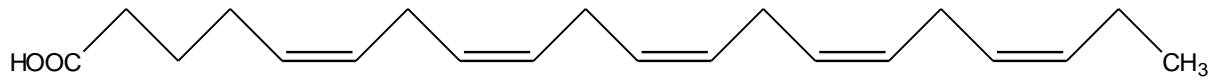
1.3.1 Dietary sources of ω -3 PUFAs

Botanical sources of ALA, the parent fatty acid of the ω -3 PUFAs, include soybeans, linseed, blackcurrant seeds and their oils. The ALA metabolites EPA and DHA can be directly sourced from cold water oily fish including salmon, sardines, mackerel and herring (Tvrzicka *et al.*, 2011). Fish oil supplements, which contain 30%-50% ω -3 PUFAs by weight, are an important source also. The majority of EPA and DHA present in humans is exogenously sourced from fish or fish oil supplements as human metabolism of ALA is relatively inefficient (Brenna *et al.*, 2009).

1.3.2 Endogenous biosynthesis of long chain ω -3 PUFAs

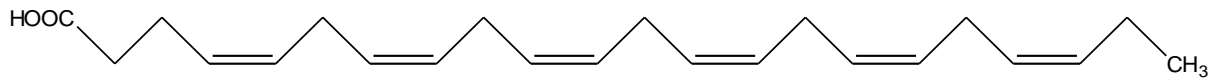
The long chain ω -3 PUFAs, EPA and DHA, are synthesised from the elongation and desaturation of ALA. The initial desaturation of ALA by the enzymatic action of Δ^6 -desaturase (D6D) constitutes the first and rate limiting step of long chain ω -3 PUFA synthesis. PPAR agonists and EFA deficiency have been demonstrated to influence D6D activity (Kawashima *et al.*, 1990; Cho *et al.*, 1999). Desaturation of ALA generates the transient production of octadecatetraenoic acid (OTA; 18:4n-3) which is further desaturated by Δ^5 -desaturase (D5D) to form EPA (see Figure 1.3 for structure). The subsequent biosynthesis of DHA is thought to occur via one of two main pathways. The first pathway, involves two consecutive elongations of EPA to yield tetracosapentaenoic acid, which is desaturated by D6D and undergoes a final C₂ shortening cycle via β -oxidation in the peroxisome to yield DHA. This pathway is largely considered the predominant route of DHA biosynthesis in mammals (reviewed by Sayanova and Napier, 2004). The alternate linear pathway involves the elongation of EPA to docosapentaenoic acid (DPA; 22:5n-3) which is then desaturated by Δ^4 -desaturase (D4D) to generate DHA (reviewed by Sayanova and Napier, 2004), the structure of which is illustrated in Figure 1.3. The presence of the linear pathway remained speculative until the isolation and purification of D4D from the marine protist *Thraustochytrium* spp. (Qiu *et al.*, 2001), confirmation of the pathways existence. The biosynthetic pathways of EPA and DHA are illustrated in Figure 1.4.

(A)



Eicosapentaenoic acid
(EPA)

(B)



Docosahexaenoic acid
(DHA)

Figure 1.2 Structures of EPA and DHA: The diagram illustrates the structure of (A) EPA and (B) DHA.

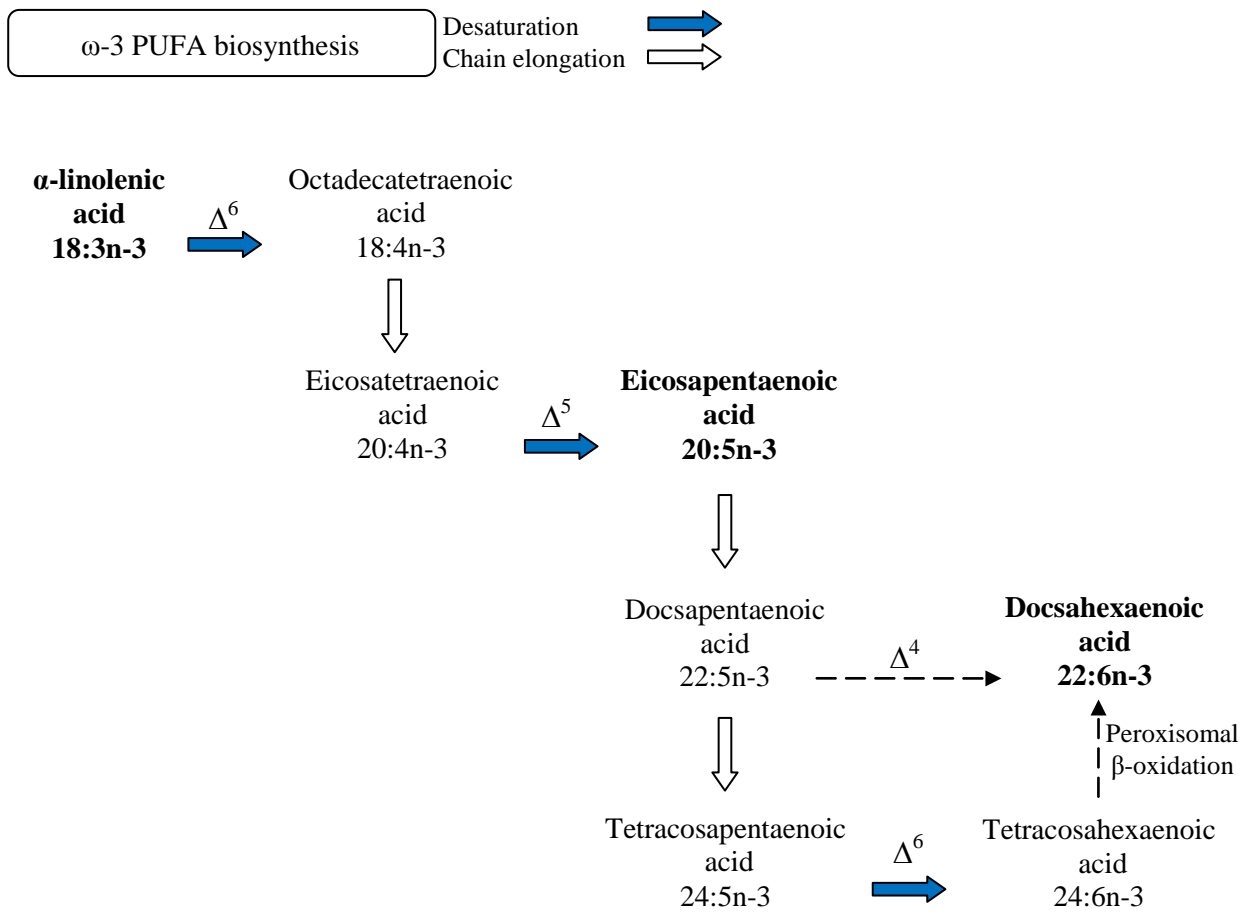


Figure 1.3 Biosynthesis of the ω-3 series of PUFAs: Diagram illustrating the endogenous biosynthesis of the ω-3 PUFAs EPA and DHA from the dietary precursor ALA.

1.3.3 ω -3 PUFAs and cardiovascular function

Experimental evidence suggests that ω -3 PUFAs have the capacity to influence cardiac function. Indeed a recent study reported an inverse correlation between the DHA content of serum phospholipids and resting and 24 hour ambulatory diastolic blood pressure (Liu *et al.*, 2011). A meta-analysis of 36 randomised trials reported an association between fish oil intake (median dose 3.7g/day EPA + DHA) and reduced systolic and diastolic blood pressure; effects which were most noticeable in elderly and hypertensive populations (Geleijnse *et al.*, 2002). Another meta-analysis of randomised trials, reported a reduced heart rate in individuals receiving fish oil (~3.5g/day EPA + DHA) compared to placebo (Mozzaffarian *et al.*, 2005). The study also revealed that a greater reduction in heart rate was reported in longer interventions (>12 weeks) and in patients with higher baseline heart rates (>69 beats per minute). While the aforementioned findings reflect the effects of higher ω -3 PUFA doses, studies employing low to moderate doses demonstrate equivocal results. It was recently reported that low dose DHA (700mg/day for 12 weeks) significantly lowered resting diastolic, but not systolic, blood pressure compared to placebo while in contrast, low dose EPA (480mg/day for 12 weeks) had no effect on BP (Dokholyan *et al.*, 2004; Theobald *et al.*, 2007).

The ω -3 PUFAs have also been implicated in the modulation of endothelial function, although there is a degree of ambiguity between experimental findings. *Ex vivo* studies conducted in bovine and ovine isolated vessel preparations (pulmonary and coronary arteries) have demonstrated the capacity of EPA to dose-dependently relax blood vessels; an effect which is associated with nitric oxide production (Omura *et al.*, 2001; Singh *et al.*, 2010). However, further investigation of the association between ω -3 PUFAs and endothelial function in humans has yielded findings inconsistent to those of animal experiments. Indeed, the majority of human studies have reported no effect of ω -3 PUFA supplementation (0.45-3.4g/day EPA + DHA) on flow mediated dilatation and/or arterial stiffness, markers of endothelial function (Anderson *et al.*, 2010; Sanders *et al.*, 2011; Skulas-ray *et al.*, 2011; Mackay *et al.*, 2012).

1.3.4 ω -3 PUFAs and lipid metabolism

The hypotriglyceridaemic effects of ω -3 PUFAs are well established. A meta-analysis of thirty-six cross-over and twenty-nine parallel-design studies collated the observed effects of ω -3 PUFA supplementation on serum lipids. The study reported a 25-30% reduction in serum triglycerides with intakes of approximately 4g/day of ω -3 PUFAs; effects which were dose-dependent and proportionate to baseline levels (Harris, 1997). Despite the well accepted capacity of ω -3 PUFAs to lower fasting

and postprandial serum triglycerides, the molecular mechanisms through which these effects are achieved are yet to be fully elucidated.

The bulk of experimental evidence derived from pre-clinical studies suggests two major routes of triglyceride reduction: - (1) a reduction in hepatic triglyceride synthesis (and assembly and secretion of triglyceride-rich VLDL) and (2) enhanced clearance of triglycerides from the circulation (reviewed by Harris *et al.*, 2008). The reduction in hepatic triglyceride reduction is thought to be the result of decreased hepatic lipogenesis. Indeed, fish oil feeding of mice was reported to decrease serum triglycerides and, concomitantly, to decrease hepatic mRNA expression of the sterol regulatory element-binding protein (SREBP) SREBP-1c, a transcription factor involved in the regulation of *de novo* lipogenesis (Kim *et al.*, 1999). This finding was supported by the observation that EPA mediated inhibition of SREBP-1c protein expression was associated with decreased triglyceride synthesis in human hepatoma cells (Zaima *et al.*, 2006). EPA and DHA represent ligands of PPAR receptors. In light of this, it has been postulated that EPA and DHA may modulate hepatic peroxisomal and/or mitochondrial fatty acid β -oxidation via interaction with PPAR α receptors (Harris *et al.*, 2008). Supplementation with both EPA and DHA (administered individually, 4g/day for 4 weeks) has been reported to significantly reduce chylomicron half-lives, to reduce chylomicron particle size and to significantly enhance pre-heparin lipoprotein lipase activity during the fed state (Park and Harris, 2003). As chylomicrons represent triglyceride rich lipoproteins, these data provide evidence to suggest enhanced triglyceride clearance from the circulation following regular intake of ω -3 PUFAs.

1.3.5 ω -3 PUFAs: Role in atherosclerosis

In a review of twenty-five studies that examined the association between ω -3 PUFA supplementation and CHD risk, Harris *et al.* (2007) highlighted the collective demonstration of an inverse correlation between tissue levels of EPA and DHA and the occurrence of major cardiovascular events. In support of this finding, several large-scale randomised trials (DART Trial, GISSI-Prevenzione Study, JELIS Study) have documented the effectiveness ω -3 PUFA supplementation in the primary and secondary prevention of CHD. Indeed consumption of ω -3 PUFAs, either in the form of oily fish or fish oil capsules, has been reported to significantly reduce all cause mortality (≥ 1 year follow up), major cardiac events (non-fatal myocardial infarction and stroke) and sudden cardiac death (Burr *et al.*, 1989; GISSI-Prevenzione Investigators, 1999; Yokoyama *et al.*, 2007).

Considering the acute, often fatal, clinical repercussions of atherosclerotic plaque rupture, the effects of ω -3 PUFAs may arise from modulation of processes key to atherosclerosis progression. Indeed,

several epidemiological studies have provided evidence to support this notion. In patients exhibiting angiographically evident coronary artery disease, supplementation with fish oil concentrate (EPA + DHA, approximately 1.5g/day for 24 months) was demonstrated to reduce coronary artery lesion progression and the occurrence of acute cardiovascular events in comparison to individuals receiving the placebo intervention (von Schacky *et al.*, 1999). A population based, cross-sectional study examined sub-clinical atherosclerosis in three cohorts: - (1) 360 Caucasian men residing in the U.S.; (2) 281 Japanese men residing in the U.S. and (3) 281 Japanese men residing in Japan, using intima-media thickness (IMT) and coronary artery calcification (CAC) as markers of disease. Although there were no difference in CAC burden between cohorts, serum ω -3 PUFA levels were found to inversely correlate with IMT in the Japanese men residing in Japan cohort, while no such correlation was demonstrated in the other cohorts (Sekikawa *et al.*, 2008). These findings support the proposed anti-atherosclerotic effects of ω -3 PUFAs; however the underlying mechanism(s) conferring these effects remain unclear.

One of the mechanisms postulated to confer the anti-atherosclerotic and cardioprotective benefits of ω -3 PUFAs is the stabilisation of atherosclerotic plaques – an effect which would slow disease progression to the advanced, complicated stages and therefore reduce the likelihood of an acute cardiovascular event. A number of direct and indirect mechanisms have been propounded to account for the potential plaque stabilising effects of ω -3 PUFAs. The aforementioned effects of ω -3 PUFAs on lipid metabolism may represent one such indirect mechanism. Indeed, hypertriglyceridaemia is a recognised risk factor for cardiovascular disease, therefore its attenuation by ω -3 PUFA supplementation most likely contributes to their overall effects. Furthermore, dietary supplementation with ω -3 PUFAs (1.24g/day for 12 weeks) has been reported to modify the phenotype of lipoproteins in patients exhibiting metabolic syndrome. Ω -3 PUFA enrichment of LDL lipoproteins was demonstrated to shift the phenotype of particles from the small, dense atherogenic LDL sub-class pattern B, to the larger, more buoyant, less atherogenic LDL sub-class pattern A (Hartwich *et al.*, 2009). The phenotype of the LDL particles infiltrating the developing lesion may influence lesion progression, as small dense LDL particles are known to promote inflammation and oxidative stress – key factors in disease development. The recruitment of leukocytes to the atherosclerotic vessel wall may also be influenced by the effects of ω -3 PUFAs. Indeed, dietary fish oil intake has been documented to lower chemoattractant production in mononuclear cell fractions, including platelet derived growth factor (PDGF) and MCP-1 (Baumann *et al.*, 1999). Moreover, *in vitro* studies have reported the capacity of ω -3 PUFAs to decrease surface expression of the adhesion molecules ICAM-1 and VCAM-1 by cultured human aortic endothelial cells (Wang *et al.*, 2011). Reduced leukocyte

infiltration into developing plaques could serve to contain, even mitigate, the inflammatory response which fuels plaque progression.

Other lines of evidence support a direct plaque stabilising property of ω -3 PUFAs. Thies et al. (2003) reported the key observation that dietary fish oil supplementation (1.4g/day EPA + DHA) directly altered plaque morphology inducing structural changes consistent with increased stability. Indeed, plaques obtained from fish oil supplemented individuals tended to be of the more stable Type IV phenotype (lipid core, thick fibrous cap) in contrast to plaques collected from placebo treated individuals, which tended to be of the less stable Type V phenotype (lipid core, thin fibrous cap). Furthermore, macrophage infiltration of plaques was found to be reduced in ω -3 PUFA supplemented individuals. Together, these findings were attributed to the effects of EPA, which was found to populate lesions in greater quantities than DHA. A more recent study in patients awaiting carotid endarterectomy revealed that in individuals randomly assigned to receive ω -3 PUFA ethyl ester capsules (providing 0.81g EPA and 0.675g DHA/day), the EPA content of plaque phospholipids inversely correlated with plaque instability and inflammation (Cawood *et al.*, 2010). Interestingly, the study reported a significant reduction in foam cell infiltration and mRNA expression of MMP-7, 9- and 12 in plaques from ω -3 PUFA supplemented individuals. Downregulation of MMP activity could serve to stabilise plaques through preservation of the collagen component of the plaque. Indeed this notion is supported by the findings of Matsumoto et al (2008), who reported a significant increase in the collagen content of aortic root plaques in high fat fed ApoE^{-/-} mice supplemented with 5% EPA (w/w) respective to high fat fed controls. It is worthwhile to note that the overall potential of ω -3 PUFAs to stabilise plaques may involve a combination of the aforementioned mechanisms, and perhaps, alternative effects which have yet to be determined.

1.4 The endocannabinoid system

The endocannabinoid system constitutes an endogenous signalling system which plays a pivotal role in a variety of centrally and peripherally regulated physiological processes. Pain sensation, appetite, memory and mood are influenced by the activity of the endocannabinoid system. Intense investigation of Δ^9 -tetrahydrocannabinol (Δ^9 -THC), the psychoactive component of *Cannabis sativa*, preceded the discovery and subsequent identification of the various components of the endocannabinoid system which comprises: (i) G-protein-coupled receptors (GPCRs); (ii) endogenous cannabinoid ligands, of which *N*-arachidonoyl-ethanolamine (anandamide; AEA) and 2-arachidonoylglycerol (2-AG) represent the most intensively studied, and (iii) the associated enzymatic apparatus which controls their synthesis and degradation (as reviewed by Montecucco and Di Marzo, In Press).

1.4.1 Cannabinoid receptors

Molecular cloning has permitted the identification of two cannabinoid (CB) receptors, the CB₁ receptor and the CB₂ receptor (Matsudo *et al.*, 1990; Munro *et al.*, 1993). The CB₁ receptor, which has been cloned in human and murine tissue, is a seven transmembrane, GPCR containing 472 (human) or 473 (rat) amino acids (as reviewed by Sugiura and Waku, 2002). CB₁ receptors are predominantly expressed in the central nervous system (e.g. the cortex, hippocampus, basal ganglia and hypothalamus), but are also located in numerous peripheral tissues including the heart, vasculature, adipose, liver and pancreas (reviewed by Vemuri *et al.*, 2008; Rajesh *et al.*, 2008). The CB₂ receptor is also a GPCR which, in humans, shares ~44% amino acid sequence homology with the CB₁ receptor. CB₂ receptors are expressed primarily in the periphery, particularly by immune cells, although there are reports of receptor expression by microglial cells and neurones (Van Sickle *et al.*, 2005). “Classical” CB receptor transmission is coupled through inhibitory G-proteins (G_{i/o}) linked either negatively, to adenylate cyclase, or positively, to mitogen-activated protein kinase, to downstream signals. However, CB₁ receptors, via G_{i/o}, are also coupled to certain ion channels (reviewed by Vemuri *et al.*, 2008). There is also experimental evidence that CB₁ receptor activation may stimulate adenylate cyclase via a G_s protein coupled mechanism (Glass and Felder, 1997).

Furthermore, evidence from functional studies has suggested the existence of non-CB receptor targets of the endocannabinoids. For example Δ⁹-THC, which is known to exert profound hypotension via CB₁ receptor activation *in vivo* (Lake *et al.*, 1997), did not induce vasodilation in the same rat mesenteric vascular bed preparations in which AEA induced sustained vasodilation (Wagner *et al.*, 1999). Indeed, several non-CB receptor targets of the endocannabinoids have since been identified including transient receptor potential vanilloid type-1 (TRPV1) channels (activated by AEA), PPARs and the speculated orphan receptor GPR55 and the vascular ‘anandamide’ receptor (Zygmunt *et al.*, 1999; reviewed by Montecucco and Di Marzo, In Press).

1.4.2 Endogenous cannabinoids

Endogenous cannabinoids (endocannabinoids) represent long-chain fatty acid derivatives that were discovered shortly after characterisation of the CB receptors to be natural ligands of the endocannabinoid system. The first endocannabinoid described, anandamide (AEA), was extracted from porcine brain in 1992, while a second endocannabinoid, 2-AG, was later isolated from canine gut (Devane *et al.*, 1992; Mechoulam *et al.*, 1995). AEA is a partial agonist of CB receptors, with a marginally higher affinity and markedly higher efficacy for the CB₁ receptor compared to the CB₂

receptor, while 2-AG, which has a similar affinity for both CB receptors as AEA, has a higher efficacy at the CB₂ receptor compared to AEA (reviewed by Pertwee and Ross, 2002). The endocannabinoids docosatetraenyl-ethanolamide, N-arachidonoyl dopamine, virodhamine and noladin ether have also been identified but not studied with the same intensity as AEA and 2-AG (Hanus *et al.*, 2001; Porter *et al.*, 2002; reviewed by Hiley, 2009). The endocannabinoids AEA and 2-AG, of which the structures are illustrated in Figure 1.4, are of relevance to the present study and will be discussed further below.

1.4.2.1 Anandamide: biosynthesis and metabolism

Anandamide is synthesised from the phospholipid precursor *N*-arachidonoyl-phosphatidyl ethanolamine (NAPE), an *N*-acylated derivative of phosphatidyl-ethanolamine (PE). The primary pathway of synthesis involves the hydrolysis of NAPE by a calcium (Ca²⁺) sensitive, NAPE-selective phospholipase D (NAPE-PLD) to yield AEA (Di Marzo *et al.*, 1994). Indeed, it was reported that stable overexpression of NAPE-PLD in mammalian cells led to a 50-90% reduction in NAPE levels, and a significant increase in AEA levels (Okamoto *et al.*, 2005). However, the finding that brain AEA levels were unaltered in NAPE-PLD knockout mice compared to wild-type mice and moreover, that AEA could be synthesised from NAPE in a Ca²⁺ independent manner (Leung *et al.*, 2006), suggested the presence of alternate routes of AEA biosynthesis. One such pathway has been identified, in which NAPE is converted to 2-lyso-NAPE via the enzymatic action of phospholipase A₂, and then to AEA through a Ca²⁺ independent mechanism (Sun *et al.*, 2004). The production of AEA via this pathway is thought to involve the enzyme α/β -hydrolase 4 (Abhd4), which was shown to generate glycerophospho-arachidonoyl ethanolamide (GpAEA) from lyso-NAPE, which in turn can be cleaved by a phosphodiesterase to yield AEA (Simon and Cravatt, 2006). A third pathway was also characterised in murine macrophages, whereby hydrolysis of NAPE by phospholipase C (PLC) yields the intermediate phospho-anandamide (pAEA), which is further hydrolysed by the activity of several phosphatases (notably PTPN22 and SHIP1) to produce AEA (Li *et al.*, 2006; Li *et al.*, 2008). The three main pathways of AEA synthesis are illustrated in Figure 1.5.

Inactivation of AEA mediated signalling is achieved by its degradation. AEA is hydrolysed to its components, AA and ethanolamide, primarily via the activity of fatty amide hydrolase (FAAH), a membrane bound enzyme expressed by several tissues including the brain, heart and bladder (Riley *et al.*, 2009; Strittmatter *et al.*, 2012). Confirmation of FAAH mediated degradation of AEA was provided by *in vivo* studies in FAAH knockout mice where brain AEA levels were elevated >10 fold compared to wild-type counter-parts (Cravatt *et al.*, 2001). In addition to the hydrolysis of AEA by FAAH, oxygenation pathways have been reported in the characterisation of AEA metabolism,

namely: (1) the lipoxygenase pathway, which metabolises AEA to hydroperoxyeicosatetraenoic acid ethanolamides (HETE-EAs); (2) the cyclooxygenase pathway, which metabolises AEA to prostamide products (PGE₂ and PGD₂) and (3) cytochromes P450, which metabolise AEA to epoxyeicosatrienoic acids (reviewed by Rouzer and Marnett, 2011).

1.4.2.2 2-arachidonoylglycerol: biosynthesis and metabolism

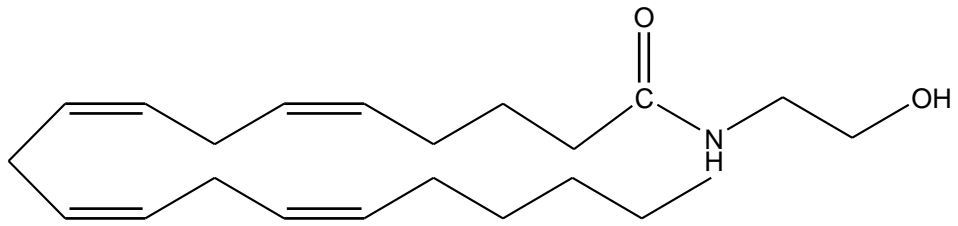
To date, two major pathways have been described for the synthesis of 2-AG, which is generated from arachidonic acid containing phospholipids. The first pathway involves the production of diacylglycerol from phosphatidylinositol via the activity of PLC β (Kondo *et al.*, 1998). Diacylglycerol is subsequently hydrolysed by an *sn*-1 specific diacylglycerol lipase (*sn*1-DAGL), evidence implicates *sn*1-DAGL α and *sn*1-DAGL β , to yield 2-AG (Bisogno *et al.*, 2003). The second pathway is typified by the generation of the intermediate lyso-phosphatidylinositol (lyso-PI) from phosphatidylinositol via the action of phospholipase A₁. Lyso-PI is hydrolysed by a lyso-PI selective PLC to yield 2-AG (Ueda *et al.*, 1993; reviewed in Muccioli, 2010). The biosynthetic pathways of 2-AG production are illustrated in Figure 1.5.

The metabolism of 2-AG to its constituent components, AA and glycerol, has been characterised to a lesser degree than that of AEA. The majority of experimental evidence implicates the activity of monoacylglycerol (MAGL), a serine hydrolase originally purified and cloned from adipose tissue (Tornqvist and Belfrage, 1976), although it is believed FAAH may also play a role in 2-AG metabolism. Indeed, convincing evidence of MAGL mediated 2-AG hydrolysis was provided by Dinh and colleagues, who demonstrated that overexpression of MAGL in rat neurones significantly depleted 2-AG concentrations, while in MAGL expressing HeLa cells, silencing of MAGL significantly elevated 2-AG concentrations (Dinh *et al.*, 2002; Dinh *et al.*, 2004). A more recent study confirmed that ~85% of 2-AG hydrolysis in the brain is mediated by MAGL activity. Furthermore, the same study reported the activity of two previously uncharacterised enzymes, ABHD12 and ABHD6, which were demonstrated to account for a further ~9% and ~4% of 2-AG hydrolysis respectively (Blankman *et al.*, 2007).

1.4.3 Cardiovascular effects of the endocannabinoid system

Under normal physiological conditions, the endocannabinoid system can regulate cardiovascular homeostasis. In humans, the acute effects of smoking marijuana have been documented to include peripheral vasodilation, increased heart rate, altered cardiac function and moderate changes in blood

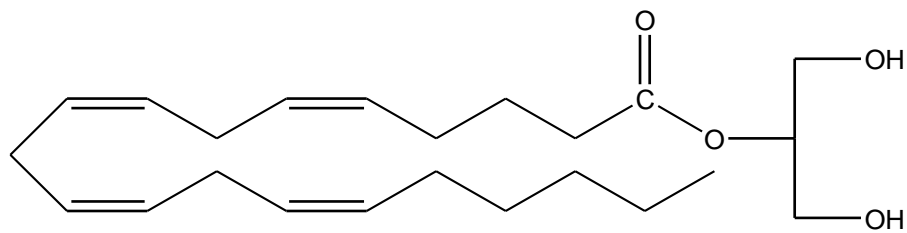
(A)



N-arachidonoyl-ethanolamine

(AEA)

(B)

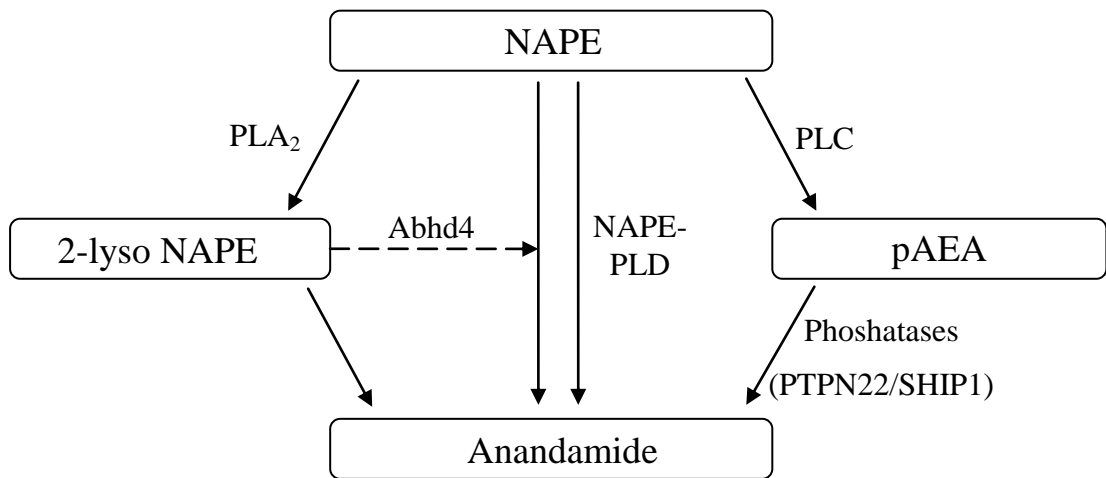


2-arachidonoyl-glycerol

(2-AG)

Figure 1.4 Endocannabinoid structures: Diagram illustrating the structure of (A) anandamide and (B) 2-AG.

(A)



(B)

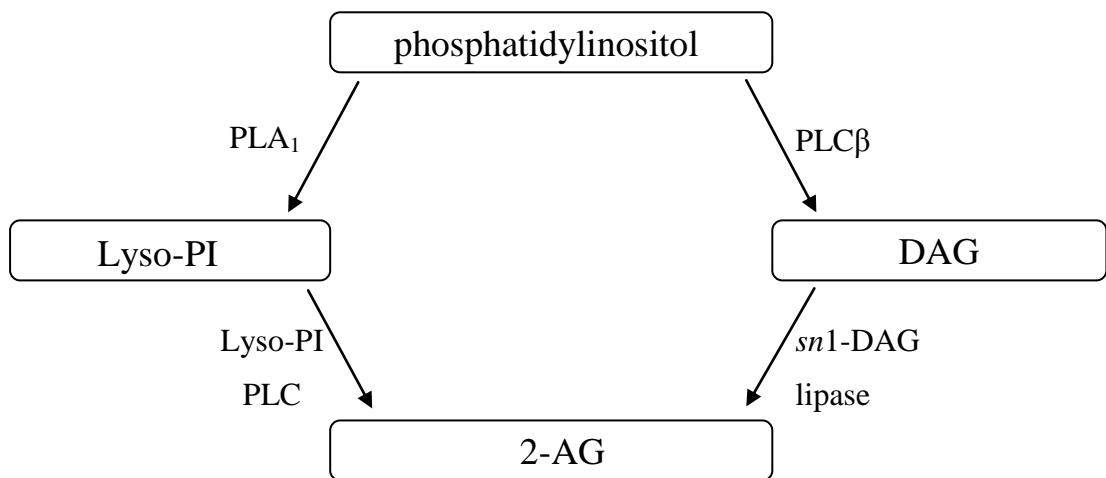


Figure 1.5 Biosynthetic pathways of the endocannabinoids AEA and 2-AG: Diagrams illustrating the various pathways in which (A) AEA and (B) 2-AG are synthesised.

pressure (reviewed by Montecucco and Di Marzo, In Press). In anaesthetised animals, administration of the phytocannabinoid Δ^9 -THC induces bradycardia and a prolonged hypotensive effect (Lake *et al.*, 1997). Similarly, the endocannabinoid AEA has been reported to exert vasodilatory and cardio-depressive actions compounded in a triphasic response involving: - (1) an initial vagally modulated period of bradycardia and hypotension; (2) a transient pressor stage and (3) a prolonged hypotensive effect (Varga *et al.*, 1995; Lake *et al.*, 1997; Pacher *et al.*, 2004). The third phase of the response to AEA, and the prolonged hypotension associated with Δ^9 -THC, was found to be sensitive to the effects of the cannabinoid SR-14176A, a CB₁ selective antagonist, strongly suggesting a role of the CB₁ receptor in this effect (Varga *et al.*, 1995; Pacher *et al.*, 2004). Similar to AEA, the endocannabinoid 2-AG has been reported to induce sustained hypotension in anaesthetised animals, however, in contrast to the actions of AEA, this effect was associated with tachycardia (Varga *et al.*, 1998; Járai *et al.*, 2000).

The endocannabinoid system and its components have also been implicated in cardiovascular pathophysiology. Ischaemia/reperfusion (I/R) injury represents the principle cause of tissue damage during incidences of stroke, myocardial infarction and circulatory shock. Multiple studies have reported elevated levels of tissue and circulating endocannabinoids following cerebral, hepatic and myocardial I/R injury (Wagner *et al.*, 2001; Berger *et al.*, 2004; Batkai *et al.*, 2007). The cellular source and exact role of the endocannabinoids remains a point of contention however receptor studies have provided some evidence of their potential function in this setting. In murine models of myocardial I/R injury, pre-conditioning was found to significantly reduce infarct size and the occurrence and duration of arrhythmias; an effect which was abrogated by antagonism of the CB₂ (AM630), but not the CB₁ (AM251), receptor (Hajrasouliha *et al.*, 2009; Montecucco *et al.*, 2009). Moreover selective agonism of the CB₂ receptor prior to reperfusion, using the synthetic cannabinoid JWH133, was associated with attenuation of oxidative stress and inflammation (Montecucco *et al.*, 2009). Taken together, these studies propose a cardioprotective effect of endocannabinoids in the setting of I/R injury, mediated via CB₂ receptor signalling.

In relation to other cardiac pathologies, evidence from experimental models of heart failure implicate a detrimental role of CB₁ receptor signalling in ventricular dysfunction, myocardial injury and oxidative/nitrative stress (Mukhopadhyay *et al.*, 2007; Rajesh *et al.*, 2012). Furthermore, plasma endocannabinoid levels were significantly elevated in patients with severe heart failure and in the myocardium of mice exhibiting type-1 diabetic cardiomyopathy (Weis *et al.*, 2010; Rajesh *et al.*, 2012).

1.4.4 The endocannabinoid system and atherosclerosis

In the vasculature, the endocannabinoid system has been demonstrated to influence atherosclerosis pathophysiology. Indeed Sugamura et al (2009) demonstrated activation of the endocannabinoid system in patients exhibiting advanced coronary artery disease, where patients displayed elevated levels of circulating endocannabinoids and increased CB₁ receptor expression in coronary plaques. In 2005, Steffens and colleagues reported the key observation that exogenous administration of the phytocannabinoid Δ^9 -THC dose dependently reduced the progression of atherosclerotic lesions in the aortic sinus of high fat fed ApoE^{-/-} mice. The reduction in lesion progression was associated with reduced leukocyte adhesion to the vascular wall; effects which were abolished by co-administration of Δ^9 -THC with SR144528, a CB₂ selective antagonist. More recently, Dol-Gleizes et al (2009) demonstrated a pro-atherogenic role of the CB₁ receptor in a murine model of atherosclerosis, where administration of a CB₁ selective antagonist (rimonabant) attenuated lesion development, suggesting a possible pro-atherogenic effect of endocannabinoid signalling at this receptor. Endocannabinoids may influence lesion progression through their effects on inflammatory cells. Indeed, AEA has been demonstrated to dose dependently attenuate TNF- α induced expression of ICAM-1 and VCAM-1 in human coronary artery endothelial cells (HCAECs) and moreover, to attenuate TNF- α stimulated THP-1 monocyte adhesion; both effects of which were sensitive to CB₁ and CB₂ receptor blockade (Batkai *et al.*, 2007). Furthermore, there is evidence to suggest a possible pro-thrombotic role of the endocannabinoids (AEA and 2-AG), which have been reported to activate platelets (Braud *et al.*, 2000; Maccarrone *et al.*, 2001). Taken together, it is evident from the literature that there is a functional involvement of components of the endocannabinoid system, in atherosclerosis development.

There is some preliminary evidence to suggest a potential interaction between the long chain ω -3 PUFAs and activation of the endocannabinoid system. Indeed, *in vivo* feeding studies have demonstrated the capacity of dietary intervention with ω -3 PUFAs to modulate the levels of endocannabinoids present in the brain (Berger *et al.*, 2001; Wood *et al.*, 2010), although it is currently unknown whether or not a similar effect would occur in the cardiovascular system. In animal models of experimental hyperlipidaemia, feeding of an atherogenic diet has been reported to influence endocannabinoid levels present in peripheral tissues (Matias *et al.*, 2008; Montecucco *et al.*, 2009). Given the association between hyperlipidaemia and CHD risk and, considering the previously discussed role(s) of ω -3 PUFAs and endocannabinoids in atherosclerosis pathology, it is plausible that their interaction may influence the development and clinical outcome of the disease, although such an effect is yet to be fully characterised.

1.5 Hypothesis

While the cardioprotective and anti-atherosclerotic effects of long chain ω -3 PUFAs are well documented, the underlying cellular mechanisms conferring such benefits remain elusive. Given that there is an emerging body of evidence implicating the involvement of the endocannabinoid system in a variety of disease pathologies including atherosclerosis (Di Marzo, 2008), that preliminary evidence exists that dietary supplementation with long chain ω -3 PUFAs alters endocannabinoid levels in experimental animals (Berger *et al.*, 2001; Wood *et al.*, 2010) and that the metabolic pathways for both ω -3 PUFAs and endocannabinoids share some common steps, it is possible that some of the mechanisms underlying the anti-atherosclerotic and plaque stabilising properties of ω -3 PUFAs may involve components of the endocannabinoid system. This study therefore set out to test this hypothesis, with the following specific aims and objectives.

1.5.1 Objectives

The aim of the present study was to examine the potential mechanisms underlying the anti-atherosclerotic effects of the long chain ω -3 PUFAs EPA and DHA and to assess whether such effects are related to activation of the endocannabinoid system and/or cardiovascular remodelling. The key objectives of the project were as follows: -

- (i) To undertake studies using an *in vivo* model (high fat/high cholesterol fed ApoE^{-/-} mouse) to determine the effects of dietary supplementation with fish oil (containing EPA) on:
 - a. Hepatic lipid physiology and plasma lipoprotein profiles
 - b. Cardiac and vascular remodelling
 - c. Tissue endocannabinoid levels
 - d. Endothelial function
- (ii) To develop an *in vitro* model of lipid loading in a human monocytic cell line to allow investigation of:
 - a. The impact of cannabinoid receptor signalling on lipid accumulation and inflammatory marker production (MCP-1)
 - b. Endocannabinoid synthesis

Chapter 2: General Methods

2.1 *In Vitro* techniques

2.1.1 THP-1 cell resuscitation

Frozen human acute monocytic leukaemia (THP-1) cells were removed from liquid nitrogen storage and warmed to 37°C as quickly as possible. The contents of the warmed ampoule were transferred to 9ml of RPMI-1640 GlutaMAX medium supplemented with 10% heat-inactivated FBS and 1% penicillin streptomycin solution and centrifuged at 1200rpm for 5 minutes. Cell pellets were then resuspended in 2ml of medium and aliquots of 0.5ml were transferred to four 25cm² culture flasks. Cells were subsequently incubated in a humid atmosphere at 37°C with the addition of 5% carbon dioxide. Medium preparation as well as subsequent resuscitation and subculture was conducted within a Class II Microbiological Safety Unit (Aura 2000 M.A.C, Bioair Instruments, Italy).

2.1.2 THP-1 cell freezing

THP-1 cells were systematically frozen down at different passages in order to establish plentiful frozen supplies. Cells to be frozen were centrifuged at 1400rpm for 5 minutes and the pellet resuspended in 1ml fresh medium. Following assessment of cell numbers (method reported in section 2.1.4.1), cells were distributed to cryovials in aliquots of 1x10⁶ cells. In addition, freezing medium (10% dimethyl sulfoxide (DMSO) in fresh medium) was added to the cryovials to give a final volume of 1ml. Cells were incubated at -20°C for several hours in a Nalgene® cryogenic freezing container (Thermo Scientific, UK) and then stored at -80°C overnight. Following this incubation period, cells were transferred to liquid nitrogen storage.

2.1.3 THP-1 cell culture

THP-1 cells were purchased (ECACC, UK), resuscitated (see section 2.1.1) and sub-cultured as follows. Culture was conducted in T75cm² Nunc™ flasks (Nunc, Thermo Scientific, UK) and cells were maintained in the exponential phase of growth with numbers never exceeding 8x10⁵ cells/ml. Cells were sustained on RPMI-1640 GlutaMAX medium as described in section 2.1.1. To refresh medium, cells were collected and centrifuged at 1400rpm for 5 minutes. The pellet was resuspended in 1ml fresh medium and transferred to a new T75cm flask containing 15ml of fresh medium. Whole

medium changes were performed weekly and a 5ml top-up of fresh medium was added to each flask bi-weekly. Cell population size was regularly assessed using the method described in section 2.1.4.1.

2.1.4 Cell counting assays

2.1.4.1 Trypan blue staining

The size of individual cell populations was regularly assessed during routine culture using trypan blue – a stain derived from toluidine. Based on the dye exclusion method, viable cells were visualised and distinguished from non-viable cells which, due to the lack of a functional membrane, retained dye.

In order to count viable cells, a 1:4 dilution of cell suspension was prepared. During replenishment of medium, a 10µl aliquot was removed from the resuspended cells and transferred to an eppendorf containing 10µl fresh medium and 20µl 0.4% trypan blue stain. The solution was incubated for 5 minutes at room temperature then placed in a haemocytometer. In the central quadrant, unstained (viable) cells were enumerated while stained (dead) cells were not enumerated. This was repeated 3 times and the mean number of viable cells was thus calculated (Equation 2.1).

$$cell\ number \times dilution\ factor \times 10^4\ (1cm^2\ quadrant\ size) = cells/ml$$

Equation 2.1

2.1.4.2 Coomassie brilliant blue staining

Coomassie Brilliant Blue R-250 represents a popular dye for visualising proteins. The following method was employed to visualise and enumerate cell adherence in culture plates, as detailed in Chapter 3 section 3.2.1.

Five hundred millilitres of staining solution (see Table 2.1) and one litre of destain solution (see Table 2.1) were prepared. The staining solution was filtered through two filter paper sections (grade 1, Whatman) prior to use. Cells were fixed as described in section 2.1.5. One millilitre of staining solution was applied to each well for 20 minutes. The staining solution was aspirated off and each well rinsed with destain solution until the wells appeared clear. Stained cells were viewed under the microscope (x40 magnification) and within a designated 1cm² cube, 3 fields of vision were chosen at random. The number of adhered cells was enumerated.

Staining Solution (500ml)	35ml acetic acid, 175ml methanol and 2.5ml Coomassie Blue R-250 diluted in 287.5ml distilled H ₂ O
Destain Solution (500ml)	35ml acetic acid and 175ml methanol diluted in 290ml distilled H ₂ O
4% Paraformaldehyde	4g paraformaldehyde dissolved in 100ml PBS

Table 2.1 Coomassie Blue Stain: Preparation of staining solutions and fixative.

2.1.5 Cell fixation

Following completion of experimental protocols, cells were washed with 1ml room temperature phosphate buffered saline (PBS; see Table 2.2 for preparation) and were fixed in 1ml of 4% paraformaldehyde (at 4°C, see Table 2.1 for preparation) for 20 minutes at room temperature. Following fixation, cells were rinsed with 1ml distilled H₂O to remove any residual paraformaldehyde and the plates were allowed to dry for 30 minutes prior to beginning staining.

2.1.6 Bradford dye-binding assay

The Bradford dye-binding procedure constitutes an elegant colorimetric assay used to determine total protein concentrations. First described by Bradford (Bradford, 1976), the assay quantifies protein concentration through measuring the binding of Coomassie Brilliant Blue G-250 dye to basic and aromatic amino acid bases and comparing such binding to samples of known protein concentration. Binding can be visualised as a characteristic colour change from brown to blue.

In a 96 well microtiter plate, 50µl of the blank (deionised H₂O) and gamma globulin standards (prepared as in Table 2.3) were added to wells in quadruplicate. Samples were added to the plate in quadruplicate to a final volume of 50µl. Two hundred microlitres of Bradford reagent was added to each well and the plate was tapped gently to mix the solutions. The reaction was incubated for 5 minutes at room temperature and the absorbance was measured at 595nm using a 96-well plate reader (µQuant model, BioTek, UK).

2.1.7 Oil red O staining

Oil red O (ORO), a lysochrome diazo dye, was employed to selectively stain lipids thus enabling the study of lipid uptake in fixed cell populations as detailed in Chapter 3, section 3.2.2. The method is outlined as follows.

ORO stock solution was prepared (see Table 2.4) and stirred overnight at room temperature. The stock was then filtered through two filter paper sections (grade 1, Whatman) and stored at 4°C. Working ORO solution was prepared from the stock (as illustrated in Table 2.4) and filtered before use. Cells were washed and fixed in 4% paraformaldehyde as described in section 2.1.5. One millilitre room temperature ORO working solution was applied to each well for 10 minutes. Wells were

Phosphate Buffered Saline (PBS)	1 PBS Tablet was dissolved in 100ml distilled H ₂ O to give NaCl 8g/L, KCl 0.2g/L
---------------------------------	--

Table 2.2 Preparation of phosphate buffered saline.

Standard Concentration ($\mu\text{g/ml}$)	Volume of gamma globulin 0.1mg/ml (μl)	Volume of diluent: distilled H ₂ O (μl)
1	10	40
2	20	30
3	30	20
4	40	10
5	50	0

Table 2.3 Bradford Assay: Preparation of standards.

Oil Red O Stock Solution	0.35 grams ORO dissolved in 100ml 100% isopropanol
Oil Red O Working Solution	6 parts ORO stock solution and 4 parts distilled H ₂ O

Table 2.4 Oil red O: Preparation of ORO solutions.

immediately rinsed with distilled H₂O immediately following stain removal and the wells were allowed to air dry. The ORO stain was eluted using 1ml 100% isopropanol which was applied to each well for around 30 seconds. To quantify the lipid particle content of the sample, the optical density of eluted stain was measured at 510nm using a spectrophotometer (Helios Epsilon UV-visible, Thermo Scientific, UK). The blank was established using 100% isopropanol.

2.1.8 ELISA assay

Enzyme-linked immunosorbent assays (ELISAs) were employed to measure the presence and concentration of various proteins in cell culture supernates. DuoSet ELISA kits, buffer, wash solutions and stop solutions were purchased from R & D Systems (UK) and the standard method detailed in the kit protocol was conducted. Antibody (working) concentrations were kit specific and are not detailed below.

On a 96-well plate, wells were coated with 100µl of capture antibody and sealed with an adhesive plate cover for overnight incubation at room temperature with gentle agitation. Each well was aspirated and washed three times in 400µl of wash buffer (see Table 2.5), removing any residual wash buffer by inverting and blotting the plate against paper towels. Plates were blocked for a period of 1 hour by the addition of 300µl of reagent diluent (see Table 2.5) to each well. The aspiration and wash step was repeated. One hundred millilitres of standards and samples (diluted in reagent diluent if necessary) were added to the appropriate wells and the plate was sealed and incubated for 2 hours at room temperature. The aspiration and wash step was repeated. Wells were coated with 100µl of detection antibody and the plate was sealed and incubated for a further 2 hours at room temperature. A further aspiration and wash step was undertaken. Wells were coated with 100µl of streptavidin conjugated to horseradish-peroxidase and the plate was wrapped in foil (to avoid light interference) and incubated for a further 20 minutes at room temperature. A final aspiration and wash step was undertaken. Wells were coated with 100µl of substrate solution (see Table 2.5) and the plate incubated for a final 20 minutes at room temperature. Fifty microlitres of stop solution (see Table 2.5) was then added to each well and the well contents were gently mixed through tapping. The optical density of the samples was immediately measured at 450nm using a 96-well plate reader.

Wash Buffer	0.05% Tween® 20 in PBS (#WA126)
Reagent Diluent	1% BSA in PBS, pH7.2 – 7.4 (#DY995)
Substrate Solution	1:1 mixture of H ₂ O ₂ and tetramethylbenzidine (#DY999)
Stop Solution	2 N H ₂ SO ₄ (# DY994)

Table 2.5 ELISA Assay: Solutions purchased from R&D systems (catalogue numbers in brackets).

2.1.9 MTS assay

In order to assess cell viability and establish any cytotoxic effects of various compounds, CellTiter 96 AQueous One Solution reagent was used. The solution contains the key compound [3-(4, 5-dimethylthiazol-2-yl)-5-(3-carboxymethoxyphenyl)-2-(4-sulfophenyl)-2H-tetrazolium, inner salt; MTS^(a)] which is bio-reduced by viable cells to a coloured formazan product. The quantity of formazan product produced, which is determined by measuring absorbance at 490nm, is proportionately related to the number of viable cells in the sample. Cells were seeded onto a 96-well plate at a density of 20,000 cells per well, in a total volume of 100µl. A range of concentrations of the compound being assessed were applied to the cells in replicates of six. Twenty microlitres of the MTS solution was then applied to each sample and the cells were incubated for 2 hours at 37°C, in a humidified, 5% CO₂ atmosphere. Following completion of the incubation period, the absorbance was measured at 490nm using a 96-well plate reader.

2.2 In Vivo techniques

2.2.1 Animal sourcing and housing

Animals were purchased for subsequent procedures under project licence number 60/4231, granted by the Home Office in accordance with the Animals (Scientific Procedures) Act 1986. In addition, individual procedures were performed in accordance with the guidelines detailed in the Animals (Scientific Procedures) Act 1986 under personal licence, 60/11352. Male ApoE knockout (B6.129P2-Apoe^{tm1Unc/Crl*}) and wild type control (JAX® C57BL/6J) mice were purchased from Charles River Laboratories (UK) and housed at an external facility. Mice were housed in cages of 10 according to experimental group, in a temperature (21°C ± 2°C) and humidity (55% ±10%) regulated environment maintained by a TREND BSU Management System (Trend, UK). A 12 hour light/dark cycle was regulated by a Philips LightMaster system (Philips, UK). Lights were fully operational between the hours of 7am and 7pm. A ramping system, operational between the hours of 6.30am and 7am and 6.30pm and 7pm, mimicked “dawn” and “dusk” respectively. While housed, mice were allowed free access to chow and drinking water.

2.2.2 Dietary intervention

To conduct dietary intervention studies, specialised diets were developed to replace the regular chow. Each diet consisted of a purified powdered base (Diet W) containing 0.25% cholesterol w/w, 16% crude fat w/w supplemented with a specific additive. The diets were prepared as follows.

Agar ash was dissolved in distilled H₂O, to an end volume of 1 litre per kilogram of diet being produced. The agar solution was maintained in a liquid state at 60°C. Diet W was weighed out and systematically homogenised with the appropriate weight of supplement as detailed in Chapter 5, section 5.2.2. The agar solution was allowed to cool to 50°C and mixed with the powdered diet and supplement to form homogenous dough. Dough was spread on trays lined with baking paper to a height of 1 - 1.5cm and allowed to cool for 60 minutes. Grooves were cut into the chilled dough creating sections of 2 x 2cm and stored at -20°C overnight. Diet was broken into squares and freeze-dried for 2-3 days then moved to -80°C storage.

2.2.3 Surgical procedure for the measurement of haemodynamics

The following surgical protocol was used to prepare the mouse. Anaesthesia was induced using a combination of ketamine and xylazine, 120mg kg⁻¹ and 16mg kg⁻¹ respectively (injection volume of 0.1ml per 10g weight). Anaesthetic was prepared (as described in Table 2.6) and administered to the intra-peritoneal cavity. Induction was followed by a short stabilisation period during which depth of anaesthesia was assessed (pinch reflex) prior to beginning surgery. The neck area was sanitised with saline (see Table 2.6) and an incision made in the skin by blunt dissection. The carotid artery and jugular vein were isolated and cannulated for measurement of arterial blood pressure and drug administration respectively using flame-stretched Portex polythene tubing (0.58mm ID x 0.96mm OD; Scientific Laboratory Supplies, UK).

To measure arterial blood pressure, the arterial cannula was connected to a physiological pressure transducer which relayed signals through a Bridge Amplifier and Animal Bio Amplifier (ADInstruments, UK). Mean arterial blood pressure (MABP) was calculated using the following equation:

$$\frac{1}{3} (\text{Systolic BP} - \text{Diastolic BP}) + \text{Diastolic BP} = \text{MABP}$$

Equation 2.2

Saline Solution	0.9% sodium chloride (0.9g NaCl in 100ml distilled H ₂ O)
Heparinised Saline	20 units Heparin per 1ml of 0.9% NaCl solution
Anaesthetic Solution	0.6ml ketamine, 0.4ml xylazine diluted in 4ml distilled H ₂ O

Table 2.6: Surgical Procedure: Preparation of solutions used in surgery.

Heart rate (HR) was calculated from a Lead I electrocardiogram recorded from subcutaneous limb leads. Both arterial blood pressure (BP) and HR signals were acquired, visualised and continuously recorded using LabChart 5 software (ADInstruments, UK). The trachea was cannulated allowing respiration to be maintained artificially using a small animal ventilator (Harvard Apparatus, UK) operating at 120 strokes min^{-1} (stroke volume $100\mu\text{l } 10\text{g}^{-1}$). Core temperature was continuously monitored through a rectal thermometer and maintained at 37°C on a heat pad (Pico Services LTD, UK). Depth of anaesthesia was regularly assessed (pinch reflex and continuous monitoring of blood pressure) during the experimental protocol and, if required, an anaesthetic top-up of $50\mu\text{l}$ was administered to the intra-peritoneal cavity. To interpret BP responses accurately, BP was measured at fixed time points over a 420 second period, commencing just prior to the intra-venous injection of the pharmacological intervention. The absolute values (millimetres of mercury: mmHg) recorded were converted to a percentage change from the baseline (time point 0). The percentage changes were subjected to area under the curve (AUTC) analysis which enabled graphical presentation of reductions in BP.

2.2.4 Tissue harvest

Blood was withdrawn via the arterial cannula into 1ml syringes containing heparinised saline, and then centrifuged for 5 minutes at 13,000rpm at room temperature. The plasma fraction was collected from each sample and snap frozen in liquid nitrogen. The chest cavity was opened and the lungs removed and discarded. The thoracic aorta, liver and brain were removed and snap frozen. Hearts were removed and were fixed in either formalin or cryomatrix (Thermo Scientific, UK) for histology, or snap frozen for biochemical analysis. Following retrieval of all tissues, samples were moved to -80°C storage.

2.2.5 Blood sample analysis

A Konelab 30 discrete clinical analyser (Thermo Scientific, UK) constitutes an automated system capable of undertaking numerous sensitive assays with multiple applications. The clinical analyser was employed for the detection of cholesterol, lipoprotein sub-fractions (LDL and HDL) and triglycerides in the plasma fraction of blood samples. The samples, which were prepared as outlined in section 2.2.4, were placed in the analyser and the pre-programmed assays were allowed to run.

2.2.6 Tissue lipid extraction

Cellular lipids exist in close association with other non lipid cellular components e.g. sugars, polysaccharides and proteins. In order to be studied, lipids must be isolated from the aforementioned constituents. Extraction of lipids from hepatic tissue was achieved using an adapted version of the established Folch method (Folch *et al.*, 1957). Glass bottles containing 10µl internal standard (C:17:0, heptadecanoic acid) were placed on ice. A 200mg sample of the tissue being extracted was added to each bottle as well as 4ml chloroform: methanol (2:1). Each sample was homogenised for 2 minutes (ultra-turrax mixer). Following the addition of 2ml 0.9% sodium chloride, samples were homogenised for a further 30 seconds. Samples were centrifuged at 2500rpm for 10 minutes at 20°C. The aqueous layer was discarded and the underlying chloroform layer collected for solvent removal under nitrogen. The remaining extracted lipid was weighed and quantified as a percentage of the original tissue weight and stored at -20°C for further analysis.

2.2.7 FAME analysis

Determination of the fatty acid methyl ester (FAME) composition of crude lipid extracts, obtained as outlined in section 2.2.6, was undertaken using FAME analysis. A 20mg sample of lipid was dissolved in 0.5ml hexane with 2ml methanolic HCL (2ml of acetyl chloride added dropwise to 20ml of cooled methanol) and 10µl internal standard (C:19:0, nonadecanoic acid 2mg/ml in methanol). Samples were boiled for 2 hours followed by a cooling period. To each sample, 2.5ml of distilled, deionised H₂O and 2.5ml of hexane was added. Samples were then shaken vigorously for 15-20 seconds and centrifuged briefly at 3000rpm to separate layers. The top hexane layer was collected and the original sample re-extracted twice more using 2.5ml of diethyl-ether. The combined hexane/ether extract was washed with 4ml H₂O and vigorously shaken for 15-20 seconds. The aqueous layer was then removed via aspiration and the wash step repeated twice. The top solvent layer was dried with anhydrous sodium sulphate and evaporated under nitrogen at 40°C. The residue was then dissolved in 0.1ml of 0.02% 2, 6-di-tert-butyl-4-methyl phenol (BHT) in hexane and stored under nitrogen at 4°C.

Identification and quantification of the fatty acid methyl esters was achieved by separation using a 6890 gas chromatograph (GC; Agilent, UK). A 50m CP Sil-88 capillary column (Varian Chrompack, Kinesis, UK) with an inner diameter of 0.25mm and a film thickness of 0.20µm was fitted to the GC. Helium was passed through the system at an approximate rate of 0.6ml/min, at a constant pressure (14psi). The initial oven temperature of 80°C was increased to 160°C at a rate of 25°C/min, with a further increase to 190°C at a rate of 1°C/min followed by a final increase to 230°C at a rate of

10°C/min. Both the injector and flame-ionization detector were set at a temperature of 250°C, with a split mode ratio of 20:1. Samples were injected into the GC and peaks measured on the chromatogram were identified through comparison to peaks established from a standard FAME mixture. In addition, peaks were corrected for the BHT and/or any solvent peaks that may have been integrated. Peaks were then quantified as a percentage of the total sample using the following equation (Equation 2.3).

$$\frac{[\text{Peak Area of Fatty Acid } x] \times 100}{\text{Total (BHT) Corrected Peak Area}} = \% \text{ Fatty Acid } x$$

Equation 2.3

2.2.8 Endocannabinoid measurement

Solid phase extraction (SPE) and liquid chromatography-mass spectrometry (LC-MS) was employed to determine concentrations of both anandamide (AEA) and 2-arachidonoylglycerol (2-AG) in whole tissue samples and cellular extracts. Whole tissue samples were harvested, snap frozen and stored at -80°C prior to analysis. Cell extracts were obtained through washing treated cells three times in 1ml ice cold PBS and collecting and centrifuging the cells at 1400rpm for 5 minutes. The supernatant was discarded and the pellets stored at -80°C in preparation for analysis. The protocol was adapted from a method outlined by Giuffrida (Giuffrida *et al.*, 2000) and the assays were undertaken by Mr Gary Cameron of the Mass Spectrometry unit at Aberdeen University. In advance of the analysis being conducted, all samples were transferred to Aberdeen University on dry ice.

2.2.8.1 Extraction

Anandamide and 2-AG standards were prepared in acetonitrile. Samples were weighed and homogenised in 1.2ml of acetonitrile/H₂O (3:1 solution ratio) containing 6pmol of internal standard deuterated AEA (AEA-d₄). Samples were diluted in 0.6ml H₂O and immediately transferred to -80°C for storage until analysis was undertaken. For analysis, samples and standards were thawed and centrifuged at 3000 x g for 10 minutes at 4°C.

The resulting supernatant was applied to equilibrated 60mg/3ml Strata-X 33µm polymeric reversed-phase cartridges (Phenomenex, UK) on a Cerex SPE (positive-pressure) manifold (Crawford Scientific, UK) at a flow rate of 1ml/minute. Cartridges were systematically washed with 1ml of 30% methanol (in H₂O) and 2ml of 70% methanol (in H₂O) and dried under nitrogen. The samples were

eluted in 1ml methanol which was evaporated off under nitrogen. The remaining sample residue was resuspended in 50µl mobile phase of which 10µl was injected onto the chromatograph.

2.2.8.2 LC-MS/MS conditions

LC Column:	150mm x 2.1mm ACE 5µm C8 (Hichrom, Reading, UK)
Column Temperature:	30°C
Tray Temperature:	4°C
Nominal Flow Rate:	200µl/minute
Mobile Phase:	15% H ₂ O/85% methanol (both in 0.5% formic acid)
Mass Spectrometer (MS):	TSQ Quantum, triple quadrupole MS (Thermo Scientific, UK)
Interface:	Electrospray ionisation (positive ion mode)
Spray Voltage:	3500V
Sheath Gas:	Nitrogen (40, arbitrary units)
Auxiliary Gas:	Nitrogen (10, arbitrary units)
Capillary Temperature:	375°C
Collision Energy:	16V
Collision Gas Pressure:	1.3 milliTor (Argon)
Ion Transitions:	AEA: m/z 348.2 – 62.2 2-AG: m/z 379 – 287 AEA-d4: m/z 352.2 – 66.2

2.2.8.3 Analysis

Xcalibur 2.0.6 software (Thermo Scientific, UK) was used to conduct quantitative analysis of the LC-MS/MS output. Linear regression curves were produced from calculating the ratio of sample/internal

standard to the concentration of sample in the standard. The concentration of the sample extract was then determined from the curve.

2.2.9 Collagen and collagen cross-link measurement

Collagen and cross-link measurement, achieved using LC-MS, was undertaken by Dr Simon Robins of the Matrix Biochemistry research group within the Rowett Institute of Health and Nutrition (part of Aberdeen University). Whole tissue content of collagen (measured as total hydroxyproline), mature cross-links (pyridinoline [PYD], histidinohydroxylysinonorleucine [HHL] deoxypyridinoline [DPD]), elastin cross-links (desmosine [DES], isodesmosine [IDE]) and reduced intermediates (hydroxylysinonorleucine [HLNL], dihydroxylysinonorleucine [DHLNL]) were assessed. To prepare the tissue for analysis, samples were removed, 'processed' (fat and debris was removed from thoracic aorta samples and the upper atria section of heart samples was discarded), snap frozen and stored at -80°C as described in section 2.2.4. All samples for analysis were subsequently delivered to the Rowett Institute on ice.

2.2.9.1 Preparation of standards and samples

Deuterated internal standard, dideutero-dihydrodesmosine, was prepared from hydrolysates of bovine ligamentum nuchae previously reduced with sodium borodeuteride. PYD and DPD standards were isolated from bovine diaphyseal bone and were purified using their fluorescence by reverse-phase chromatography, the detailed method of which has been previously reported (Robins, 1996). DES and IDE were isolated from bovine ligamentum nuchae using similar procedures. HHL was isolated from ovine dermis and an HHL standard stock solution was prepared from the trihydrochloride salt (Robins *et al.*, 2003). Using previously described methods, DHLNL and HLNL were isolated from bovine bone reduced with potassium borohydride for the preparation of standards (Robins, 1982).

Samples were prepared for analysis as follows. The samples were rinsed repeatedly prior to equilibration in 20mM sodium phosphate (containing 140mM NaCl, pH 7.5) for a minimum of 2 hours. Potassium borohydride (in 20mM NaOH) to give a final concentration of 1.7mM was added to the sample suspension to reduce the immature-cross-links. Following 1 hour of stirring, excess borohydride was removed by lowering the pH to 4 using 3M acetic acid after which the tissue was rinsed with H₂O and lyophilized. Portions of the reduced tissue samples were weighed and hydrolysed in 5.7M HCl at 107°C for 21 hours after which time residual acid was removed by evaporation *in vacuo*.

Standards and sample hydrolysates (redissolved in H₂O) were fractionated using an adapted version of a method previously outlined by Pratt and colleagues (Pratt *et al.*, 1992). Prior to fractionation, stock solutions of standards were diluted to produce a range of concentrations from 0 to 100pmol. Partition chromatography using an SPE system (Gilson ASPEC II, Anachem Ltd, UK) incorporating cellulose CC31 columns with a mobile phase of butan-1-ol, acetic acid, H₂O (4:1:1 ratio by volume) was undertaken where processed standards/samples were eluted in 0.75ml of 50mM HCl. A 5301 concentrator (Eppendorf, UK) was used to reduce the eluates to a known volume (100µl - 200µl) determined by weight. From the concentration range of standards fractionated, a 6-point standard curve was constructed.

2.2.9.2 LC-MS/MS procedure

Fractionated eluates of standards and samples were mixed (9:1 v/v) with 10% pentafluoropropionic acid (PFPA) containing 30pmol/µl of internal standard, of which 20µl was injected onto the chromatograph (25cm x 0.2cm Aquasil C18 column, Thermo Scientific, UK). Mobile phases were 0.2% PFPA and acetonitrile: H₂O (75:25 v/v) containing 0.2% PFPA with a nominal flow rate maintained between 200µl-300µl/min. The column was coupled with a triple-quadrupole tandem mass spectrometer equipped with an electrospray ionisation interface operating in positive-ion mode (API4000 LC/MS/MS System, Applied Biosystems, UK). Data for each standard/sample was acquired using multiple reaction monitoring (MRM).

2.2.9.3 Analysis

Calibration curves were produced through comparison of the peak area ratio (MRM compound area/MRM internal standard area) against the standard concentration (standards run in duplicate). The concentrations of cross-links present in the samples were then calculated through interpolating the observed peak area ratio on the linear regression line of the corresponding calibration curve.

2.2.10 Western blotting

Western Blotting represents a powerful analytical tool for the detection of specific proteins in a sample of unknown protein composition. First developed within the biochemistry department of Stanford University (Renart *et al.*, 1979), the method involves separation of denatured proteins by gel electrophoresis and, following transfer to a membrane, antibody probing of the immobilised proteins to identify a specific protein of interest.

2.2.10.1 Protein extraction

Prior to undertaking the Western Blot process, it was necessary to establish the protein concentrations of the tissue samples. On ice, 150g of tissue was added to a flat-bottomed vial containing 600mg of 1mm zirconia beads (Thistle Scientific, UK) and 800µl of 10% protease inhibitor cocktail (complete tablet) diluted in 40mM Tris HCl (6.3g Trizma® Base in 1L distilled H₂O). Samples were homogenised for 30 seconds, a process which was repeated three times. Homogenised material was removed and centrifuged at 55,000rpm for 30 minutes at 4°C. The protein supernatant was collected in a clean microcentrifuge tube and both the pellet and supernatant stored at -80°C. Protein concentrations were then determined using the previously outlined Bradford assay method (see section 2.1.6).

2.2.10.2 Electrophoresis and immunoblotting

Sodium dodecyl sulphate polyacrylamide gel electrophoresis (SDS-PAGE) was used to separate the sample proteins by molecular weight. A 10% separating gel was prepared as described in Table 2.7. The gel was transferred into a glass casting stand and allowed to set at room temperature. Once set, a 5% stacker gel was added to the separating gel, prepared as illustrated in Table 2.7. A comb was inserted into the gel and the gel was allowed to set.

To load 150µg of sample per well, the samples were diluted (total protein concentration determined by Bradford Assay) in Laemmli buffer and boiled for 5 minutes on a heat block set at 100°C. Once the gel was set, the comb was gently removed and the glass casts moved to a gel tank. The gel tank was filled with SDS-PAGE running buffer (see Table 2.8) fully submerging the gel. Ten microlitres of protein standard (Precision Plus Dual Colour) was loaded into the first well. The remaining wells were loaded with 15µl of the denatured samples. The gel tank lid, which is attached to positive and negative electrodes, was placed on the gel tank and the leads were attached to a BioRad PowerPac 3000. 200mv of power was applied to the gel tank for 1 hour. Upon completion of electrophoresis, the gels were removed from the gel tank and the stacking gel and wells were cut off and discarded. The gels were placed in transfer buffer (see Table 2.8).

Sections of immobilon-P membrane (Millipore, UK) of roughly 5.5cm x 8.5cm were cut to size and submerged briefly in methanol until a colour change from opaque to a translucent grey was observed. Membranes were rinsed in distilled H₂O and placed in transfer buffer. In addition for each gel, two sponges and two sections of filter paper (cut to size) were also placed in transfer buffer.

Gel Constituent	Volume for 10% Separating Gel (mls)	Volume for 5% Stacking Gel (mls)
H ₂ O	8.1	6.1
1.5M Trizma® Base pH 8.8	5.0	-
0.5M Trizma® Base pH 6.6	-	2.5
sodium dodecyl sulphate	0.2	0.1
10% ammonium persulphate	0.1	0.05
TEMED	0.02	0.02
30% N,N-methylenebis/acrylamide	6.6	1.3

Table 2.7 Western Blot: Preparations of polyacrylamide gels.

SDS-PAGE Running Buffer	100ml of x 10 Tris-glycine buffer in 900ml distilled H ₂ O
5% milk powder	5g milk powder dissolved in 100mls 0.5% tween® in PBS
Transfer Buffer	3.05g Trizma® Base and 14.41g glycine dissolved in 200mls methanol and diluted in 800ml distilled H ₂ O

Table 2.8 Western Blot: Preparation of solutions required for Western Blotting.

The cassette was laid down flat, with the black side to the back. One sponge was placed on the cassette and a section of filter paper was placed on top of the sponge layer. A glass vial was gently rolled across the cassette to remove any air bubbles between the sponge and filter paper layers. The gel was carefully transferred onto the filter paper and the immobilon-P membrane placed on top of the gel. The rolling step was repeated to remove air bubbles. The second sponge was placed on the gel sandwich and a final rolling step was undertaken to remove any residual air bubbles. The cassette was placed in the transfer-electrode assembly, which was fitted in the gel tank along with an ice box. The tank was then filled with transfer buffer. The gel tank was closed and attached to a BioRad PowerPac 3000. One hundred mV of power was applied to the gel tank for 1 hour. Following transfer, the gel tank was opened and the cassette removed from the electrode assembly. The membrane was removed, briefly submerged in methanol and allowed to dry at room temperature for blotting at a later stage.

To undertake the immunoblot, the transferred membranes were briefly submerged in methanol and immediately placed in universals containing 20ml 5% milk powder solution (see Table 2.8) to block for 1 hour at room temperature with gentle agitation. Membranes were then transferred to bags containing the primary antibody diluted in 5% milk solution which were sealed. The antibody concentration, incubation length and temperature were dependant on the specific application of the protocol. Membranes were transferred to universals and washed with 10ml 0.5% tween® in PBS for 5 minutes. The wash step was repeated a further two times. The secondary antibody, diluted in 5% milk solution, was then added to the universal. The antibody concentration, incubation length and temperature were dependant on the specific application of the protocol. The PBS wash step was repeated three times. Membranes were placed on cling film, and coated in an equimolar solution of chemiluminescent substrate for band identification. Membranes were allowed to develop in chemiluminescent substrate for 3-5 minutes. Bands were visualised using a Fujifilm LAS-1000 Dark Box. Measurement of band width and intensity was undertaken using Aida Image Analyser software (version 3.5.2).

2.3 Materials

2.3.1 Antibodies and reagents

Abcam: Chicken polyclonal to ADFP, goat polyclonal secondary antibody to chicken IgY – H&L (HRP)

Bayer, UK: Xylazine hydrochloride 2% w/v (Rompun®)

BioRad, UK: Bradford reagent, protein standard (Precision Plus Dual Colour)

Cell Signalling Technology, UK: Cell lysis buffer (10X) [#9803]

Fisher Scientific, UK: Acetyl chloride, anhydrous sodium sulphate, heat-inactivated foetal bovine serum, hexane, methanol, penicillin streptomycin solution (1%), sodium chloride

Hayman's Ltd, UK: Absolute ethanol

Hope Farms, Netherlands: Diet W

Invitrogen, UK: Fungizone®, Hams F-12 nutrient mixture medium, RPMI-1640 GlutaMAX medium, Waymouths MB752/1 Medium

Marvel, UK: Milk powder

Millipore, UK: Accutase, ECL substrate (Immobilon Western)

Merial, UK: Pentobarbital sodium (Euthatal)

Oxoid, UK: Phosphate Buffered Saline

Promega, UK: CellTiter 96 AQueous One Solution reagent

Pfizer, UK: Ketamine hydrochloride (Vetalar™V)

Roche, UK: Protease inhibitor cocktail complete tablet

Severn Biotech: Ammonium persulphate, sodium dodecyl sulphate (10%), 30% N,N-methylenebis/acrylamide, 0.5% tween® in PBS

Sigma-Aldrich, UK: Agar ash 2-4%, coomassie brilliant blue R-250, chloroform, diethyl-ether, glycine, heparin, isopropanol, paraformaldehyde, sodium nitroprusside dihydrate ≥99.0%, trizma® base, trypan blue stain, oil red o, laemmli buffer , 2, 6-di-tert-butyl-4-methyl phenol (BHT), N,N,N', N'-Tetramethylethylenediamine (TEMED)

Tocris: Bradykinin

Chapter 3: Modelling lipid accumulation in the activated THP-1 macrophage

3.1 Introduction

3.1.1 Foam cell origin and development

As previously discussed in Chapter 1, the presence of lipid engorged macrophages or ‘foam cells’ in the subendothelial space constitutes the earliest visible manifestation of atherosclerosis, known as the fatty streak.

Macrophage foam cells are derived from blood monocytes. Prolonged influx, accumulation and retention of lipoproteins in the subendothelial space are synonymous with endothelial cell activation, to which circulatory monocytes are recruited. Monocytes represent a highly plastic cell population demonstrating phenotypic heterogeneity in both humans and mice. The monocytic sub-set from which foam cells originate remains under investigation. In apolipoprotein E-deficient (ApoE^{-/-}) mice fed a high fat diet, studies have reported rapid expansion of Ly6C^{high} monocytes, an effect which was not observed in the counter-part Ly6C^{low} population. Moreover, preferential recruitment and accumulation of Ly6C^{high} monocytes in atherosclerotic lesions was also demonstrated, suggesting a pro-atherogenic role of the Ly6C^{high} population (Swirski *et al.*, 2007; Tacke *et al.*, 2007).

Foam cell development thus stems from macrophage infiltration and phagocytic activity at sites of lipoprotein accumulation. Chemical modification, mainly oxidation, of low density lipoprotein (LDL) present in the vessel wall is pivotal to its uptake and contributes to its pro-inflammatory and pro-atherogenic profile (as reviewed in Levitan *et al.*, 2010). Uptake of modified LDL *via* scavenger receptors (discussed in Chapter 1, section 1.2.3) is genetically unregulated due to the lack of a sterol regulatory element in the scavenger receptor gene. In effect, and in contrast to the LDL receptor pathway, scavenger receptor expression is insensitive to intracellular cholesterol concentration and is not down-regulated by cholesterol loading (Han *et al.*, 1997). Persistent uptake and hydrolysis of modified LDL thus produces macrophages saturated in cholesteryl ester (CE) and free cholesterol (FC). Such macrophages are termed ‘foam cells’, in light of the ‘foam’ like appearance of CE rich lysosomes present in the cytoplasm.

Resulting foam cells serve as a potent source of pro-inflammatory cytokines and reactive oxygen species which promote local inflammation, further lipoprotein modification and trigger the activation of matrix metalloproteinases (MMPs): endopeptidases which facilitate the degradation of extracellular matrix (ECM) components (Dollery and Libby, 2006). MMP activity, in a highly regulated fashion, modulates the remodelling of tissue in essential processes such as organ development and wound healing. In the atherosclerotic plaque however, proteolytic degradation of the matrix reduces the

tensile strength conferred by collagenous material and ultimately reduces plaque integrity (Rekhter *et al.*, 2000). The degree of instability largely dictates the likelihood of plaque rupture and so in turn, the likelihood of a potentially fatal thrombogenic event.

3.1.2 Atherosclerosis and ω -3 PUFAs

In the setting of cardiovascular disease, the potentially beneficial properties of ω -3 PUFAs have been well investigated, including their ability to modify blood pressure and/or heart rate, cardiac function, triglyceride concentrations, platelet aggregation, inflammation and plaque stabilisation (as detailed in Chapter 1). Eicosapentaenoic acid (EPA) and docosahexaenoic acid (DHA) represent two key ω -3 PUFAs. As mentioned previously, fibrillar collagen provides tensile strength to the plaque microenvironment and therefore plaques with reduced collagen content will be less stable and more prone to rupture. In 2002, Kawano and colleagues demonstrated that EPA supplementation in high fat fed rabbits altered plaque composition. EPA treated animals displayed lesions mainly of type I and II classification (small foam cells, high collagen content) in contrast to lesions of control animals, which were mainly of type III and IV classification (large foam cells, poor collagen content). Subsequent human and murine studies have confirmed a direct association between EPA/DHA incorporation into lesions and reduced macrophage deposition, reduced macrophage cholesterol content, reduced markers of inflammation and an increased incidence of lesions with thick fibrous caps (Thies *et al.*, 2003; Wang *et al.*, 2009). Such findings support the notion that ω -3 PUFA incorporation into lesional macrophages triggers cellular events, perhaps related to cholesterol homeostasis, that confer plaque stabilising effects. The exact nature of these cellular mechanisms however has yet to be elucidated.

3.1.3 *In vitro* models of foam cell activity

To gain insight into the cellular events underpinning foam cell formation and activity *in vivo*: several *in vitro* models have evolved. A number of human myeloid cell lines are available, including KG-1, HL-60, U937 and THP-1, which are halted at different stages of differentiation (monoblast, pro-monocyte and monocyte). The use of cell lines offers several advantages over the use of human macrophage isolates, which can be difficult to expand *ex vivo*, carry risk of contamination and can exhibit phenotypic variation (donor variations). Immortalised cells are easily obtained, of plentiful supply and exhibit population homogeneity, a desirable characteristic for biochemical study (Daigneault *et al.*, 2010). With comparison to the aforementioned cell models, human monocytic leukaemia (THP-1) cells demonstrate physical and behavioural traits (morphology and secretory profiles) more similar to

native monocytes (Tsuchiya *et al.*, 1980 as reviewed by Auwerx, 1991). In response to treatment with differentiation agents, THP-1 cells express recognised markers of differentiation that are associated with macrophage development including scavenger receptor type A (SR-A), apolipoprotein E (ApoE) and lipoprotein lipase (LPL) (Tajima *et al.*, 1985; Hara *et al.*, 1987; Steinberg, 1987). Hence THP-1 cells are widely employed for the study of macrophage and/or foam cell behaviour.

Exposure of THP-1 macrophages to preparations of oxidised LDL (oxLDL) presents a well established method of inducing foam cell formation where the expression of scavenger receptors (notably CD36 and LOX-1), cytokines and growth factors associated with foam cells are increased with oxLDL loading (Han *et al.*, 1997; Nagy *et al.*, 1998; Malden *et al.*, 1991). The mechanisms underlying such effects are in part due to oxLDL activation of transcription factor peroxisome proliferator-activated receptor γ (PPAR γ) and possibly PPAR δ (Nagy *et al.*, 1998; Vosper *et al.*, 2001). Experimental production of oxLDL is a relatively inexpensive, but complex, procedure where the stage and extent of oxidation in individual preparations can vary substantially. In contrast, commercial production of oxLDL generates particles with heightened homogeneity and stability however the process is considerably more expensive. The present study sought to develop a model of lipid accumulation in activated macrophages. Lipid accumulation, quantified through measurement of the cellular content of fatty acid esters (primarily triglycerides), was achieved through exposure of cells to free fatty acids. Linoleic acid, an ω -6 PUFA, was employed as a lipid loading agent. Linoleic acid and its oxidised metabolites, 9- hydroxyoctadecadienoic acid (9-HODE) and 13-hydroxyoctadecadienoic acid (13-HODE), represent known components of oxLDL particles and have been shown to upregulate CD36 expression (Nagy *et al.*, 1998; Jostarndt *et al.*, 2002). While uptake and accumulation of free fatty acids does not constitute foam cell formation, modelling the accumulation of lipid in activated macrophages permitted further investigation of factors which influence this process including the potential involvement, if any, of the endocannabinoid system (discussed in Chapter 4).

3.2 Aims

The intent of this study was to develop a robust and reproducible *in vitro* model of lipid loading in differentiated THP-1 cells. In order to achieve the development of a sound model, the following aims were addressed 1) to determine the optimal conditions for lipid loading in activated THP-1 cells, using linoleic acid as a lipid loading agent; 2) to demonstrate the effect of ω -3 PUFAs on lipid

loading and 3) to employ the optimised model to investigate any effect of cannabinoid agents, be it beneficial or detrimental, on loading of ω -3 PUFAs into cells.

3.3 Methods

3.3.1 Optimisation of differentiation

Adherence of activated THP-1 cells to the plate surface was employed as a measurement of differentiation levels within the cell population. Determination of both optimum phorbol 12-myristate 13-acetate (PMA) concentration and incubation time was established using the following protocol.

THP-1 monocytic cells were acquired and sub-cultured as outlined in Chapter 2 (section 2.1.4). Six-well plates were seeded with 2×10^6 cells per well in a final volume of 4ml media containing 10% fetal bovine serum and 1% penicillin/streptomycin solution. Cells were treated with 1ng, 3ng, 5ng and 10ng of PMA per well (reconstituted in 100% ethanol, diluted in PBS) for a period of 3, 6, 10 or 24 hours in a humid atmosphere maintained at 37°C. At each time point, the cells were removed, washed and fixed as described in Chapter 2 (section 2.1.6). Enumeration of cells was achieved through staining with Coomassie Brilliant Blue. The final protocol for staining and enumeration was conducted as described in Chapter 2 (section 2.1.5.2). The full protocol was undertaken in three independent experiments (n=3).

3.3.2 Optimisation of lipid loading and quantification

3.3.2.1 Linoleic acid loading

Six-well plates were seeded with 2×10^6 cells per well in a final volume of 4ml media. Cells were treated with a range of concentrations of linoleic acid (LA): 0.5 μ M, 1 μ M, 10 μ M, 25 μ M and 50 μ M after which cells were incubated with 5ng PMA for a period of 24 hours, the optimal conditions determined by the findings from section 3.3.1. Following the 24 hour incubation conducted at 37°C, cells were washed and fixed as described previously (Chapter 2, section 2.1.6) and the plates were allowed to dry for 30 minutes. To analyse lipid accumulation, Oil red O (ORO) staining was then performed using the protocol described in Chapter 2 (section 2.1.8). The full protocol was undertaken in eight independent experiments (n=8).

3.3.2.2 Oleic acid loading: comparison to linoleic acid

Twenty-four-well plates were seeded with 1×10^6 cells per well in a final volume of 2ml media. Cells were treated with a range of concentrations of oleic acid (OA): 1 μ M, 5 μ M, 10 μ M, 25 μ M, 50 μ M and 100 μ M. Following OA treatment, cells were stimulated with 5ng PMA for a period of 24 hours in a humid environment at 37°C. Following the 24 hour incubation, cells were washed and fixed as described in Chapter 2 (section 2.1.6) and the plates were allowed to dry for 30 minutes. To stain and analyse lipid accumulation, Oil red O (ORO) staining was performed as per the optimised protocol described in Chapter 2 (section 2.1.8). The protocol was conducted once in triplicate (n=1).

3.3.2.3 ω -3 PUFA loading

Twenty-four-well plates were seeded with 1×10^6 cells per well in a final volume of 2ml fresh media. Cells were treated with 50 μ M of OA, EPA, DHA or the vehicle (ethanol, 0.1%). Following fatty acid treatment, cells were stimulated with 5ng PMA for a period of 24 hours at 37°C. Following the 24 hour incubation, cells were fixed as described in Chapter 2 (section 2.1.6) and stained with Oil red O (ORO) (see Chapter 2, section 2.1.8). Experiments were conducted three times and measured in triplicate (n=3).

3.4 Results

3.4.1 THP-1 monocyte differentiation

As shown in Figure 3.1, exposure to PMA elicited a concentration-dependent effect, where an increase in PMA concentration positively influenced cell adherence by increasing the number of adhered cells. This effect was evident at all assayed concentrations. A time dependent effect of PMA treatment was also observed. Increased exposure time to PMA (3, 6 and 10 hours) induced a directly proportionate increase in the number of adherent cells. Twenty-four hour exposure to PMA induced a plateau of maximum cell adhesion (133 \pm 21 cells) that was illustrated to occur even at the lowest concentration assayed, 0.4nM PMA (equivalent to 1ng per well). Exposure to 1, 3 and 5ng of PMA per well for 24 hours was strongly significant (p<0.001, p<0.01, p<0.05 respectively) in comparison to exposure of matching treatments for 3 hours. On the basis of these findings, treatment of cells with 5ng PMA for a period of 24 hours was defined as the optimum conditions for later experiments.

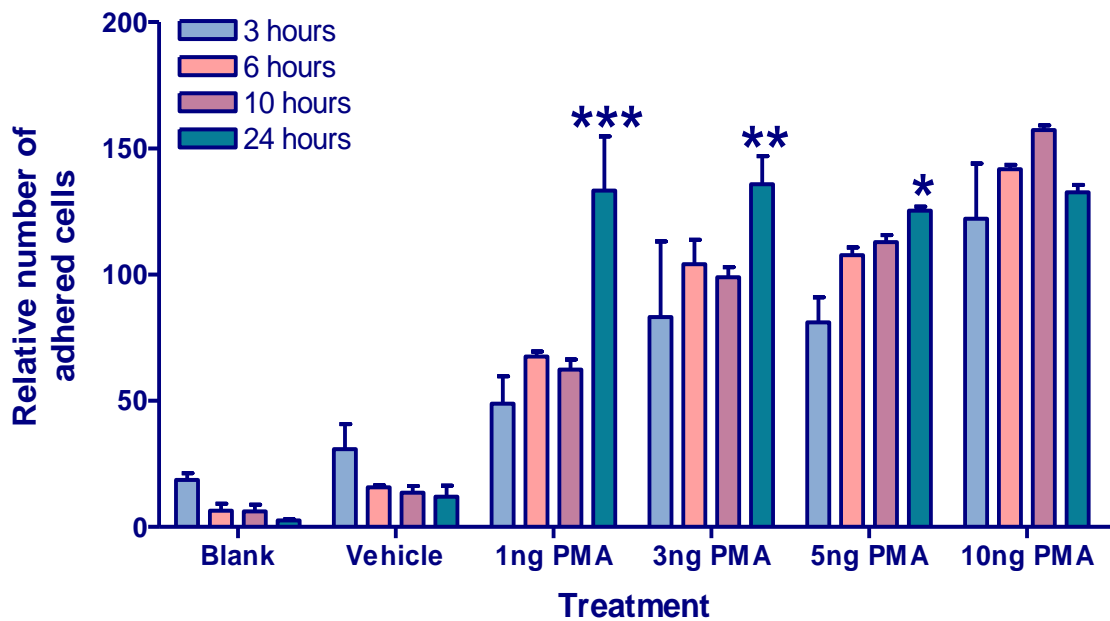


Figure 3.1 Optimisation of THP-1 monocyte differentiation: THP-1 monocytes, seeded at a density of 2×10^6 cells/well, were exposed to a range of PMA concentrations (1ng–10ng) across a range of timepoints (3-24 hours) in order to determine the optimal conditions for differentiation. Monocytes were between passages 32 and 34. Adherent cells were stained with Coomassie Brilliant Blue. A 1cm^2 area was designated at random and the cells within visualised and enumerated under $\times 40$ magnification. Enumeration was conducted in triplicate. The full protocol was conducted three times ($n=3$). * $p < 0.05$, ** $p < 0.01$, *** $p < 0.001$ vs respective concentration incubated for 3 hours (two-way ANOVA, Bonferroni's multiple comparison post-hoc test). Values represent mean \pm SEM.

3.4.2 Optimisation of lipid loading: linoleic acid

Lipid loading in differentiated cells was measured through staining with ORO – a fat soluble dye which stains cellular lipids. Figure 3.2 demonstrates the outcome of staining with ORO, where lipid droplets present in cells become red in colour. Loading of differentiated THP-1 cells with linoleic acid demonstrated a direct correlation between linoleic acid concentration and absorbance (see Figure 3.3). Across a concentration range of 0.5 μ M to 50 μ M LA, absorbance increased dose dependently. Exposure to 10 μ M, 25 μ M and 50 μ M LA induced significant increases in absorbance (0.51 \pm 0.10AU, 0.69 \pm 0.12AU and 0.73 \pm 0.10AU respectively) compared to 0.5 μ M LA (0.18 \pm 0.01AU; P<0.05). All data was corrected to baseline measurements (0 μ M LA). From the present findings, 50 μ M LA was deduced as the optimal fatty acid concentration to induce lipid accumulation.

3.4.3 Lipid loading: oleic acid

Figure 3.4 demonstrates the effects of loading differentiated THP-1 cells with OA. As observed with LA treatment, a concentration-dependent effect was observed with OA treatment. Across a concentration range of 1 μ M to 100 μ M OA, absorbance increased with increasing OA concentration. Comparative to the lowest assayed concentration of 1 μ M, marked increases in absorbance were noted at 50 μ M and 100 μ M OA. All data were corrected to baseline measurements (0 μ M OA). The results obtained confirmed the suitability of OA as a lipid loading agent thus 50 μ M OA was concluded as the optimal concentration to induce significant lipid accumulation.

3.4.4 Lipid loading: ω -3 PUFAs

The accumulation of 50 μ M EPA and DHA by activated THP-1 cells, compared with an equimolar concentration of OA, is illustrated in Figure 3.5. Data was corrected to the blank and expressed as a fold change in absorbency compared to the vehicle. The fold change in lipid uptake of OA (2.5 \pm 0.2), EPA (3.3 \pm 0.2) and DHA (3.9 \pm 0.4) was significantly increased (P<0.05) compared to the vehicle (0.1% ethanol). Statistical comparison between fatty acids revealed that DHA was more readily taken up by activated THP-1 macrophages than OA.

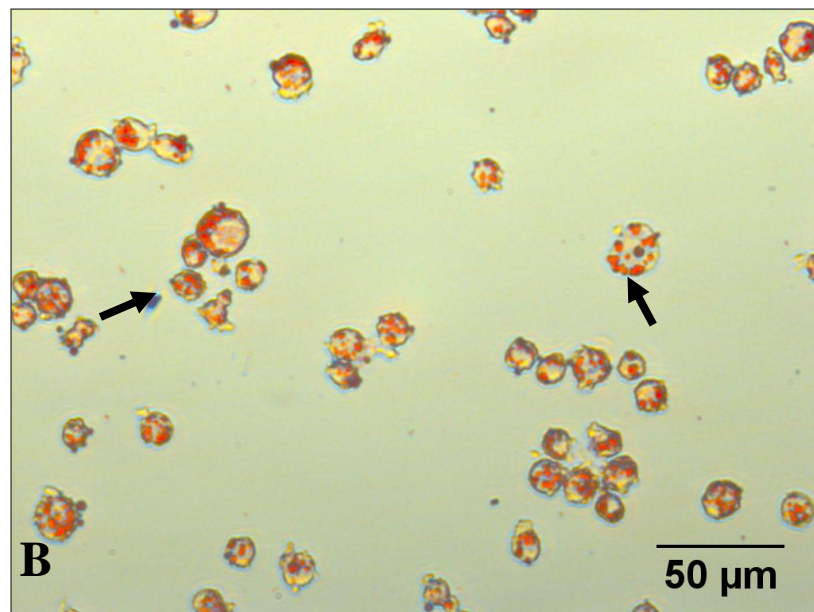
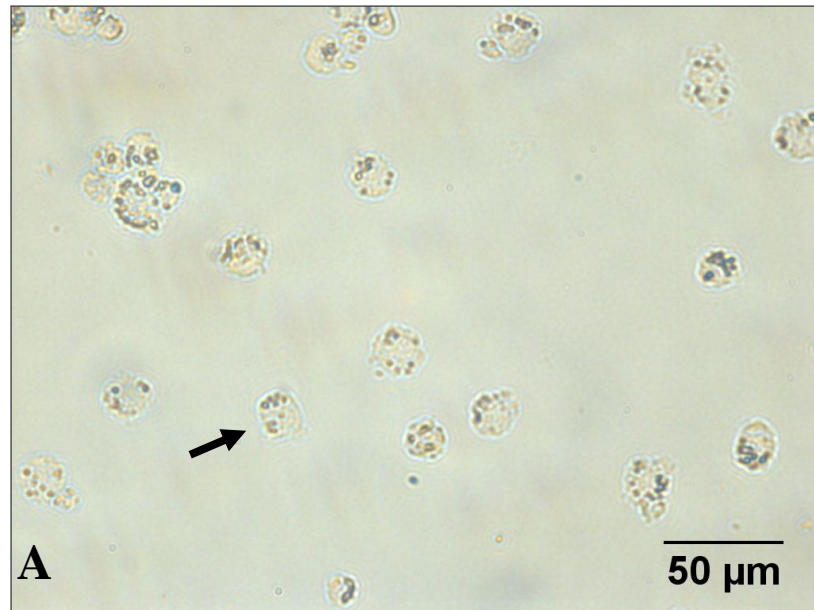


Figure 3.2 ORO staining of lipid accumulation in activated THP-1 cells: Image A displays unstained, activated THP-1 cells (see arrows). Image B demonstrates the accumulation of lipid in the cytoplasmic lysosomes (stained red) of activated THP-1 cells exposed to 10 μ M OA. Cells were at passage 35. Both images were viewed at 400 \times magnification.

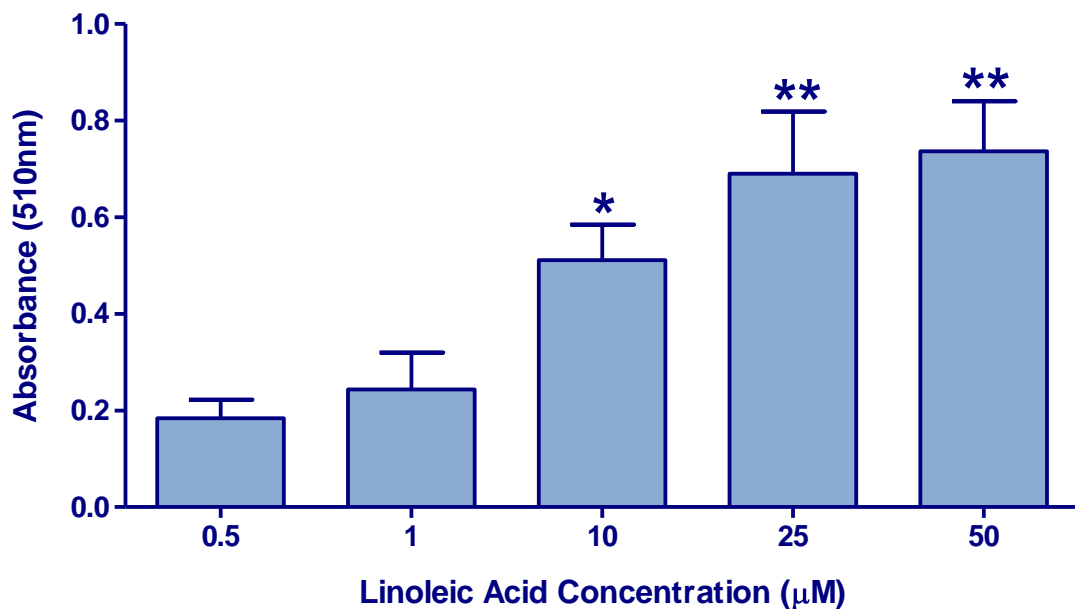


Figure 3.3 Optimisation of lipid accumulation in THP-1 cells using linoleic acid: THP-1 cells treated with 5ng PMA were incubated with a range of linoleic acid concentrations (0.5-50µM) for a period of 24 hours. Cells were rinsed in PBS, fixed in 4% paraformaldehyde and stained with ORO. The absorbance of eluted ORO stain was measured at 510nm, using isopropanol as blank. Cells used for experimentation were between passages 26-32). Data is corrected to the baseline, 0µM LA. The full protocol was conducted eight times n=8. *p<0.05, **p<0.01 vs 0.5µM LA (one-way ANOVA, Dunnett's multiple comparison post-hoc test). Values represent mean±SEM.

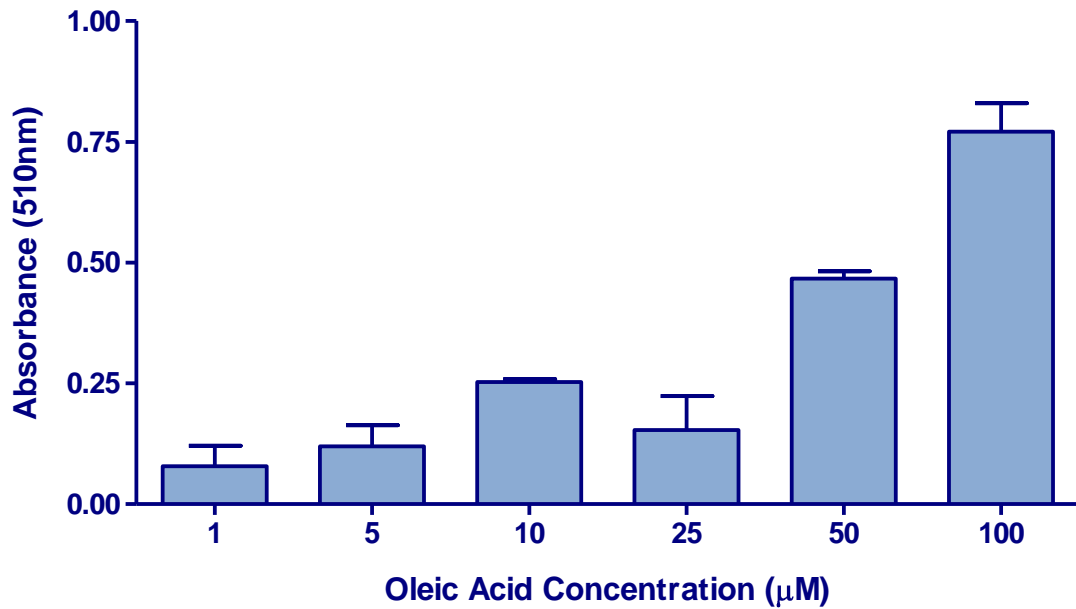


Figure 3.4 Lipid loading with oleic acid: Similar to linoleic acid treatment, THP-1 cells treated with 5ng PMA were incubated with a range of oleic acid concentrations (1-100µM) for a period of 24 hours. Cells were stained with ORO and the absorbance of eluted stain was quantified at 510nm. Cells used for experimentation were at passage 30. Data is corrected to the baseline, 0µM OA. The full protocol was conducted once with measurements made in triplicate (n=1). Values represent mean±SEM..

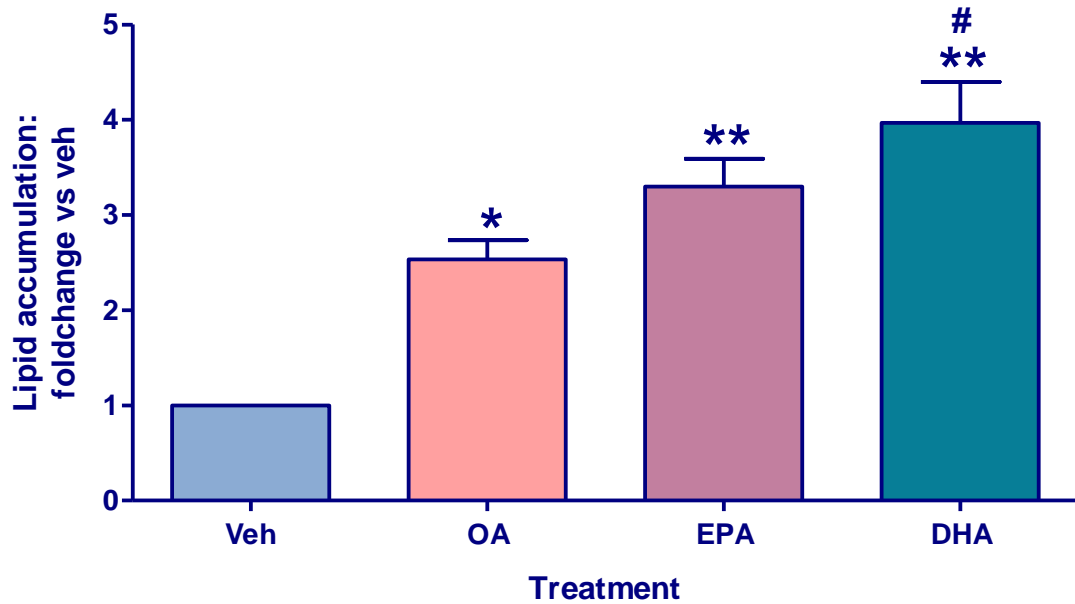


Figure 3.5 Lipid loading with omega-3 fatty acids: PMA (5ng) treated THP-1 cells were loaded with 50 μ M of either OA, EPA or DHA. Vehicle treated cells received 0.1% EtOH. Lipid accumulation was quantified with ORO staining. Absorbance was measured at 510nm and the values corrected to the baseline. Data was then expressed as a fold change in lipid accumulation compared to the vehicle. The full protocol was independently conducted three times with measurements made in triplicate (n=3). *p<0.05, **p<0.01 vs OA (one-way ANOVA, Dunnett's multiple comparison post-hoc test) and #p<0.05 vs OA (one-way ANOVA, Bonferroni's comparison post-hoc test). Values represent mean \pm SEM.

3.5 Discussion

The present study sought to develop a robust method of demonstrating lipid accumulation in activated macrophages. To generate a sensitive and reproducible model, the following parameters were investigated: differentiation conditions, optimal lipid loading concentration, optimal staining conditions and lipid loading with various fatty acids.

The cell seeding density chosen for the model was based on seeding densities reported in the methodology of similar studies in which THP-1 culture was conducted in 6-well plates (De Kimpe *et al.*, 1998; Zhao *et al.*, 2007) as well as methods used previously in the laboratory. Monocytes represent naturally non-adherent cells local to the blood and lymphatic system. To induce differentiation of the THP-1 monocytic cells experimentally, cells were exposed to PMA - a phorbol diester and potent activator of protein kinase C (Osto *et al.*, 2008). PMA has been demonstrated to trigger morphological and functional changes in THP-1 monocytes that include shape alteration, adherence capability, alteration in cellular structures, increased phagocytic activity and Fc γ receptor expression. Ultimately cells develop a phenotype mimicking that of an activated macrophage and, importantly, form an adherent monolayer (Tsuchiya *et al.*, 1982). Other archetypal differentiation agents are available such as 1,25-dihydroxyvitamin D₃ (VD₃). Respective to the THP-1 line however, VD₃-induced differentiation cannot induce adherence or phagocytic activity, does not alter proliferation and mediates only moderate expression of surface antigens CD11b and CD14 associated with macrophage differentiation (Schwende *et al.*, 1996). PMA which mediates reduced proliferation, increased adherence and enhanced surface antigen expression, presents a better candidate for this particular model. Thus, the relative number of cells that adhered to the plate surface was used as an indicator of the extent of differentiation. Quantification of cell numbers did however prove problematic. Two techniques (haematoxylin and eosin [H&E] staining and Bradford assay) were used to enumerate cell adhesion, however both failed to generate quantifiable results (data not shown). Increasing seeding density, renewing stain reagents (for H&E staining purposes only), different methods of detachment from plate surface and fixation methods were all attempted, none succeeded in rectifying the problem. Successful visualisation and enumeration of adhered cells was eventually achieved using Coomassie blue stain. From the results obtained, maximum differentiation was shown to occur following 24 hours of PMA exposure. Relative to incubation time, the concentration of PMA assayed had no significant effect on the extent of differentiation achieved. Treatment of cells with 5ng of PMA for a period of 24 hours was therefore deduced as the optimal conditions for induction of differentiation.

In light of the optimisation of differentiation, the next stage of model development was to load the THP-1 macrophages with lipid. Linoleic acid was employed as a lipid loading agent which (1) enabled determination of the optimal fatty acid concentration required to provoke significant lipid accumulation in the cells and (2) acted as a reference fatty acid, to which later studies with alternative fatty acids were contextualised but not statistically compared. Lipid uptake was quantified using the ORO staining protocol originally outlined by Ramirez-Zacarias *et al* (1992) which selectively stains triglycerides and some cholesteryl esters. Initial attempts of quantification encountered problems such as poor lipid recovery (out with lower detection limits of wavelength measurement) and high background staining (data not shown). To overcome these issues, the volumes of stain and wash agents used were refined to reflect the well surface and volume of the plate. From the results generated, maximum lipid retention was shown to occur in response to treatment with 50 μ M LA. This concentration (50 μ M) was therefore chosen as the optimum fatty acid concentration for loading the activated THP-1 cells.

Having refined a method for inducing fatty acid accumulation in THP-1 cells employing linoleic acid as a loading agent, the decision was made to convert to using oleic acid, a monounsaturated ω -9 PUFA. The decision to modify the experimental plan was made to improve continuity between the experimental approaches applied across the study as a whole, since oleic acid was to be used as control oil for the subsequent dietary intervention for the *in vivo* branch of the investigation. As linoleic acid could not therefore be used as a direct control, it was thus decided that oleic acid would replace linoleic acid as a reference fatty acid. It was not foreseen that loading of the cells with oleic acid, as opposed to linoleic acid, would result in any changes in uptake, however to negate any unexpected actions of oleic acid, a comparison experiment was conducted. Furthermore, to improve the reproducibility of the protocol, cells were seeded in 24-well plates as opposed to 6-well plates, thus allowing duplicate and triplicate treatments to be undertaken. To account for the loss of well surface area, the seeding density was reduced from 2×10^6 cells to 1×10^6 cells and the final volume was also reduced from 4ml to 2ml. As Figure 3.4 demonstrates, exposure to oleic acid elicited a trend mimicking that of exposure to linoleic acid. Compared to the lowest assayed concentration (1 μ M), significant increases in lipid uptake were observed at both 50 μ M and 100 μ M oleic acid. The observation that both linoleic and oleic acid induced similar responses in relation to lipid uptake confirmed no adverse actions of oleic acid nor any functional problems introduced to the protocol by changing the plate size. Therefore 50 μ M was chosen as the optimal loading concentration.

To standardise loading with ω -3 PUFAs, the accumulation of EPA and DHA was compared to oleic acid accumulation in the same experiment. The cellular uptake of EPA and DHA was significantly increased compared to the uptake of oleic acid. One potential mechanism to explain increased lipid

accumulation in EPA and DHA treated THP-1 macrophages may be EPA/DHA mediated dysregulation of cholesterol efflux. Reduced expression and accelerated degradation of ATP-binding cassette reporter (ABCA1) in EPA treated THP-1 macrophages has been reported in the literature (Hu *et al.*, 2009). As a membrane associated protein, ABCA1 facilitates the extrusion and association of cellular cholesterol with extracellular apolipoprotein-I (apoA-I), which combine to form high density lipoprotein particles (HDL). It is possible that, while normal cholesterol efflux is maintained in oleic acid treated macrophages; reduced cholesterol efflux in EPA- and DHA-treated macrophages is responsible for their heightened accumulation. Further studies examining ABCA1 mRNA and protein expression would be required in order to confirm such an effect.

On reflection, the outcome of this body of work was the production of a reproducible model of lipid loading in activated THP-1 macrophages, however, due to some inconsistency with the literature it is evident that the model is not without its limitations. One such limitation would be the use of ORO staining for the quantification of lipid accumulation. While ORO selectively stains triglycerides and cholesteryl esters, there is no option for differentiation between the two. Measuring the rate of formation and quantity of cholesterol esters, may provide a more accurate indicator of the involvement of a particular fatty acid in cholesterol homeostasis. As many studies have investigated fatty acid incubation periods in excess of 24 hours, discrepancy in findings may be the result of insufficient fatty acid exposure time. Therefore, investigation of the effect of increasing incubation times may be worthwhile. Moreover, the validity of the model could be further characterised by measuring the expression of markers of foam cell formation such as surface antigens (e.g. SRA, CD36 and LOX-1). In summary, a standardised protocol for the differentiation and loading of activated macrophages with lipid was developed. For intensive purposes, the model proved valuable, however further optimisation would generate a more sensitive, insightful method of detection.

Chapter 4: Role of the endocannabinoid system in lipid accumulation in the activated THP-1 macrophage

4.1 Introduction

4.1.1 The endocannabinoid system: an overview

Endocannabinoids (EC) represent endogenous lipid mediators with an extensive and diverse range of biological activities. Endocannabinoids, their cellular receptors and the proteins essential for their synthesis, transport and degradation together constitute the endocannabinoid system (ES). As reviewed in Chapter 1, endocannabinoids exert the majority of their effects through the CB₁ and CB₂ receptors; Gi/o protein coupled receptors present in central and peripheral tissue. The two most widely characterised ECs are arachidonoyl ethanolamide (AEA) and 2-arachidonoyl glycerol (2-AG): the synthesis, action and degradation of which is discussed in Chapter 1.

4.1.2 Endocannabinoids and disease pathology

Endocannabinoids have been implicated in a wide range of disease states where receptor studies and observed alterations in endocannabinoid concentrations have linked the ES to inflammation, pain, diabetes, cancer, obesity and, importantly, cardiovascular conditions (Mukhopadhyay *et al.*, 2010; Costa *et al.*, 2007; Annuzzi *et al.*, 2010; Guida *et al.*, 2010; Reidel *et al.*, 2009). The exact role of the endocannabinoids in disease is somewhat unclear as reported effects have been of both a beneficial and detrimental nature, dependent upon injury type, tissue type and/or the stage of disease development. In the setting of cardiovascular disease, ECs have been shown to influence hypotension induced by hemorrhagic shock (endotoxic and cardiogenic), myocardial ischemia and reperfusion injury, cardiac dysfunction and atherosclerosis (as reviewed by Pacher and Steffens, 2009 and Hiley, 2009).

4.1.3 Endocannabinoids and atherosclerosis

Both CB₁ and CB₂ receptors have been implicated in atherosclerosis development and progression. The majority of reports from the literature suggest a pro-atherosclerotic role of CB₁ receptor activation and an anti-atherosclerotic role of CB₂ receptor activation.

4.1.3.1 CB₁ receptor mediated effects

STRADIVARIUS, a randomized, double-blinded trial, examined the role of the CB₁ receptor in the progression of coronary artery disease in patients exhibiting abdominal obesity and metabolic syndrome. Pharmacological blockade of the CB₁ receptor using the antagonist rimonabant (20mg/day), significantly reduced normalised total atheroma volume in patients with high basal triglyceride levels (>140mg/dL) and in those not receiving statin treatment (Nissen *et al.*, 2008). Rimonabant treatment has been shown to dose dependently reduce atherosclerotic lesion progression in the aorta and aortic sinus of LDL receptor knockout mice (LDLr^{-/-}) fed a Western diet (Dol-Gleizes *et al.*, 2009). *In vitro*, it has been demonstrated that treatment of LPS-stimulated mouse peritoneal macrophages with rimonabant repressed the expression of pro-inflammatory cytokines IL-6, MCP-1 and TNF- α (Sugamura *et al.*, 2009). In vascular smooth muscle cells, a key cell type involved in atherosclerotic lesion progression and vessel restenosis, a recent study illustrated that CB₁ receptor antagonism (using rimonabant) inhibited platelet derived growth factor (PDGF) induced proliferation, migration and signalling in human coronary artery smooth muscle cells (Rajesh *et al.*, 2008a). Therefore it could be postulated that CB₁ receptor activation contributes to the progression of atherosclerosis, at least in part, through inflammatory mechanisms.

4.1.3.2 CB₂ receptor mediated effects

The first *in vivo* evidence of a direct effect of CB₂ receptor activation in atherosclerosis was provided by Steffens and colleagues (2005). It was noted that in apolipoprotein-E (ApoE^{-/-}) knockout mice treated with a daily oral dose (1 mg kg⁻¹) of Δ^9 - tetrahydrocannabinol (THC), a derivative of *Cannabis sativa*, lesion progression in the aortic root was significantly reduced compared to untreated controls. Through co-administration of THC with a CB₂ selective antagonist, SR144528, the lesion reducing effects of THC were completely abolished. Moreover, quantitative immunostaining of lesions revealed that THC treatment significantly lowered infiltration of macrophages, which highly express CB₂ receptors (Steffens *et al.*, 2005). Taken together, these findings strongly suggest a protective role of CB₂ receptor activation in preventing lesion progression. Similarly, a recent study reported that genetic ablation of the CB₂ receptor in high fat fed LDLr^{-/-} mice significantly aggravated progression of early lesions (Delsing *et al.*, 2011). Interestingly, absence of CB₂ receptor expression had no effect on late stage lesions (>12 weeks), a finding supported by observations in a similar LDLr^{-/-} study whereby supplementation of a high cholesterol diet with the CB₂ agonist, JWH133, for a period of 16 weeks had no effect on intimal lesion size or inflammatory profile (Willecke *et al.*, 2011).

In contrast, *in vitro* studies have implicated the involvement of activated CB₂ receptors in the inflammatory response within the atherosclerotic lesion. Treatment with selective CB₂ agonists was reported to attenuate TNF- α -induced migration and proliferation of coronary artery smooth muscle cells (Rajesh *et al.*, 2008b), reduce TNF- α -induced activation of coronary artery endothelial cells (reduced ICAM-1, VCAM-1 and MCP-1 expression) and reduce migration and adhesion of THP-1 monocytes (Rajesh *et al.*, 2007). While some conflict remains, the majority of the data suggests an anti-atherogenic role of CB₂ receptor activation.

4.1.3.3 Endocannabinoids and foam cell formation

In the setting of foam cell development, evidence of ES activation was provided by Jiang and colleagues (2009). *In vitro* studies demonstrated the ability of ox-LDL treatment to significantly increase AEA and 2-AG synthesis, to increase CB₁ and CB₂ receptor expression and importantly, promote cellular cholesterol accumulation (Jiang *et al.*, 2009). It was also observed that selective blockade of the CB₁ receptor (using AM251) reduced ox-LDL accumulation, suggesting that the process of cholesterol overload associated with foam cell development could be regulated by CB₁ receptor activation. While it appears that the endocannabinoid system plays a role in cholesterol loading of macrophages, it has yet to be documented if such an interaction is associated with the action of PUFAs.

4.2 Aims

In light of the optimisation of an *in vitro* model of lipid accumulation in the THP-1 macrophage described in Chapter 3, the central aim of this study was to further characterise the role of the ES in lipid accumulation and homeostasis in the THP-1 macrophage. The anti-atherosclerotic effects of the ω -3 PUFAs, EPA and DHA, which are discussed in detail in Chapters 1 and 3, are well documented. While the lesion-stabilising effects of these fatty acids have been reported, the underlying mechanisms conferring such effects remain unclear. Since there is evidence that ECs can influence the uptake of cholesterol into macrophages, and that EC levels are increased in response to LDL, it would be important to know whether ECs similarly affect ω -3 PUFA uptake, since this could limit their lesion-stabilising effects. Thus the present study sought to determine whether a) selective CB₁ and CB₂ receptor activation alters ω -3 PUFA accumulation and the production of inflammatory markers in macrophages and b) ω -3 PUFAs influence the production of endocannabinoids by macrophages.

4.3 Methods

4.3.1 Optimisation of drug pre-incubation period

To explore the effect of endocannabinoid and cannabinoid compounds on THP-1 macrophage activity and behaviour, it was first necessary to establish the optimal incubation period for drug exposure. A range of incubation times were established from the literature and were investigated as follows:

Twenty-four-well plates were seeded with 1×10^6 cells per well in a final volume of 2ml medium. Cells were pre-treated with ACEA or the vehicle (ethanol, 0.1%) for a period of 1, 3, 6 or 24 hours at 37°C. Following drug treatment, cells were treated with 50µM OA and stimulated with 5ng PMA for 24 hours. Following completion of the incubation period, cells were fixed as described in Chapter 2 (section 2.1.6) and stained with Oil red O (ORO) (see Chapter 2, section 2.1.8). The experiment was conducted independently three times in duplicate (n=3).

4.3.2 The effect of cannabinoid and endocannabinoid compounds on ω-3 PUFA accumulation

Twenty-four-well plates were seeded with 1×10^6 cells per well in a final volume of 2ml medium. Cells were pre-treated with either ACEA (synthetic CB₁ agonist), 2-AG (endogenous CB₁ and CB₂ receptor agonist), AEA (endogenous CB₁ and CB₂ receptor agonist) and JWH133 (synthetic CB₂ agonist) or vehicle (ethanol, 0.5%) for a period of 6 hours in a humidified atmosphere at 37°C. Following completion of the drug pre-treatment period, cells were exposed to 50µM OA, EPA or DHA and stimulated with 5ng PMA for a period of 24 hours at 37°C. Following completion of the incubation period, spent medium was removed and stored at -80°C for future protein analysis (see section 4.3.4). Cells were fixed as described in Chapter 2 (section 2.1.6) and stained with ORO (see Chapter 2, section 2.1.8). The experiment was conducted independently four times in duplicate (n=4).

4.3.3 The effect of cannabinoid and endocannabinoid compounds on cell viability

Cell viability was assessed by MTS as outlined in Chapter 2, section 2.1.11. Briefly, 96-well plates were seeded with 2×10^4 cells per well in a final volume of 100µl fresh medium. Cells were pre-treated with either AEA or JWH133 or vehicle (ethanol, 1%) for a period of 6 hours in a humidified atmosphere at 37°C. Following completion of the drug pre-treatment period, cells were exposed to 50µM DHA and stimulated with 5ng PMA for a period of 24 hours at 37°C. Following completion of

the incubation period, cells were incubated for 2 hours with MTS solution at 37°C. Following MTS exposure, the absorbance was measured at 490nm. The experiment was conducted independently three times with six replicates for each condition (n=3).

4.3.4 The effect of AEA and JWH133 on MCP-1 production

Spent medium was collected as described in section 4.3.2. The quantity of MCP-1 produced by the various cell treatments described in the previous section were assayed by ELISA, the protocol of which is outlined in Chapter 2, section 2.1.9. The assay was conducted three times in quadruplicate (n=3).

4.3.5 Endocannabinoid production in lipid loaded THP-1 macrophages

Twenty-four-well plates were seeded with 1×10^6 cells per well in a final volume of 2ml medium. Cells were treated with 50µM OA, EPA, DHA, fibrate or vehicle (ethanol, 0.1%) and stimulated with 5ng PMA for a period of 24 hours at 37°C. Following completion of the incubation period, cells were washed three times with ice cold PBS and scraped for collection in microcentrifuge tubes. Cells were then centrifuged at 14,000 rpm for 10 mins at 4°C. The resulting supernatant was discarded and the pellets were dried and stored at -80°C. Subsequently, cell pellets were lysed and endocannabinoid analysis was undertaken using LC-MS/MS (conducted by Mr Gary Cameron of Aberdeen University) as described in Chapter 2, section 2.2.8. The experiment was conducted independently four times in duplicate (n=4).

4.3.5.1 Endocannabinoid analysis: generation of the standard curve

Standards of varying concentrations and the internal standard were analysed using the previously described LC-MS/MS technique. The resultant peaks recorded (examples A-C in Figure 4.1) were further analysed by measuring the peak total area. The area ratio of each standard to the internal standard was then calculated (see Equation 4.1) and the value plotted against the concentration of the known standards. This enabled generation of a standard curve (see Figure 4.2). The area ratio of each sample (calculated as demonstrated in Equation 4.1, where the sample peak area replaced the EC peak area) was then determined from the total peak area (see Figure 4.3) and the ratio applied to the standard curve to establish the sample concentration.

$$\text{Area Ratio of Standard} = \frac{\text{Area of EC Standard Peak}}{\text{Area of Internal Standard Peak}}$$

Equation 4.1

4.3.5.2 Normalisation of endocannabinoid results

To accurately compare samples, it was first necessary to normalise the measured endocannabinoid concentrations to the original protein concentration present in the sample. This was achieved using the Bradford Assay where samples were normalised to pmol per 1mg total protein (see Equation 4.2).

$$\text{EC pmol per mg total protein} = \frac{\text{EC pmol} \times 1}{\text{Sample Total Protein}}$$

Equation 4.2

4.4 Results

4.4.1 Optimisation of drug pre-incubation

To optimise the conditions for drug pre-treatment, a range of incubation times were investigated using arachidonyl-2'-chloroethylamide (ACEA), a synthetic CB₁ agonist, in combination with OA as shown in Figure 4.4. There were no significant time-dependent differences in OA accumulation in any of the cell treatments exposed to ACEA for 1, 3 or 6 hours. This indicated that any differences observed in lipid accumulation were specific to the cell treatment, independent of time. Conversely, 24 hour pre-treatment with ACEA almost completely abolished lipid accumulation. This finding was attributed to widespread cell death, perhaps due to drug toxicity. Thus, based on the findings of this experiment, a pre-treatment time of 6 hours was deduced as the optimal condition for drug exposure. All data were expressed as a fold change in lipid accumulation over the stimulated cell controls.

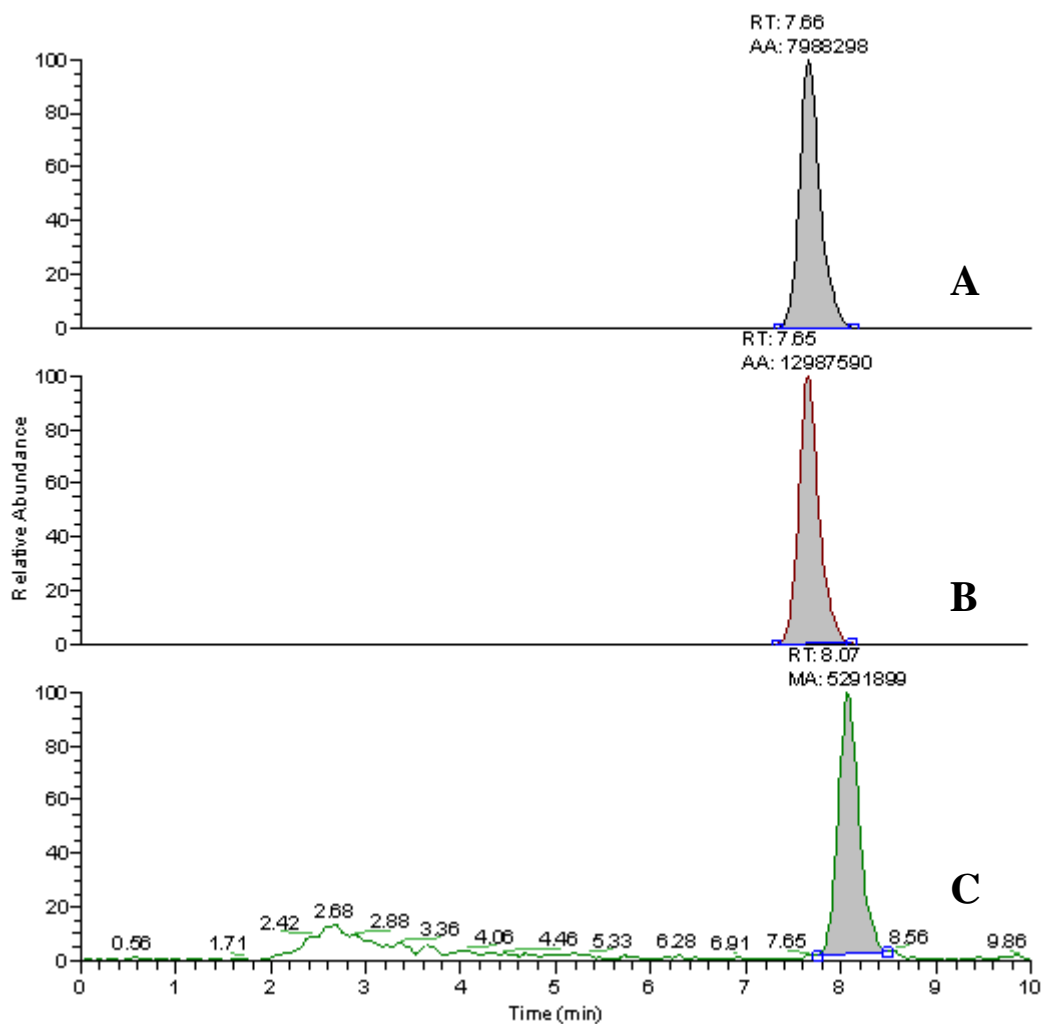


Figure 4.1 Original LC-MS/MS chromatograms of standards and internal standard: Example chromatograms demonstrating A) the peak produced by 5pmol of AEA standard; B) the peak produced by the internal standard, deuterated anandamide; C) the peak produced by 50pmol of 2-AG standard.

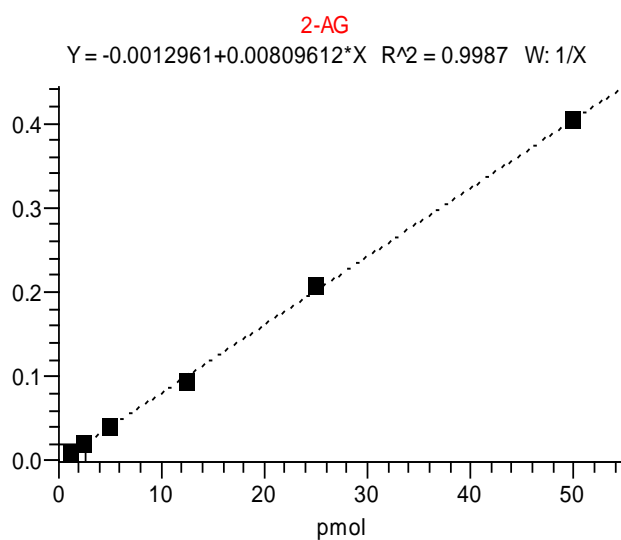
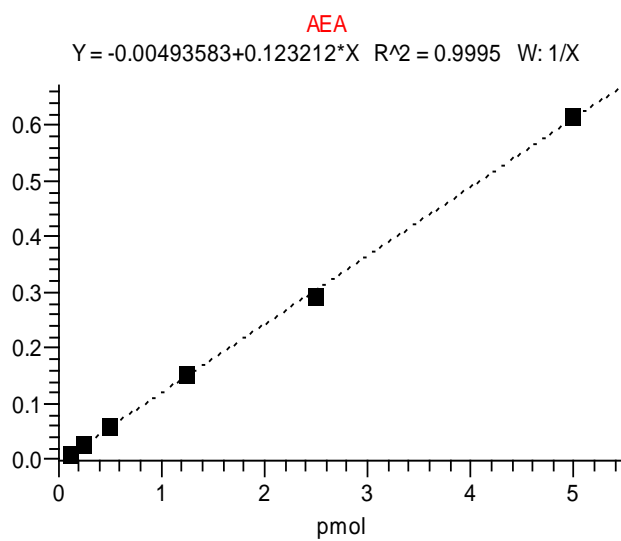


Figure 4.2 Example standard curves for AEA and 2-AG: Example standard curves produced for both AEA and 2-AG, generated through plotting the area ratio of known standard concentration/internal standard against standard concentration.

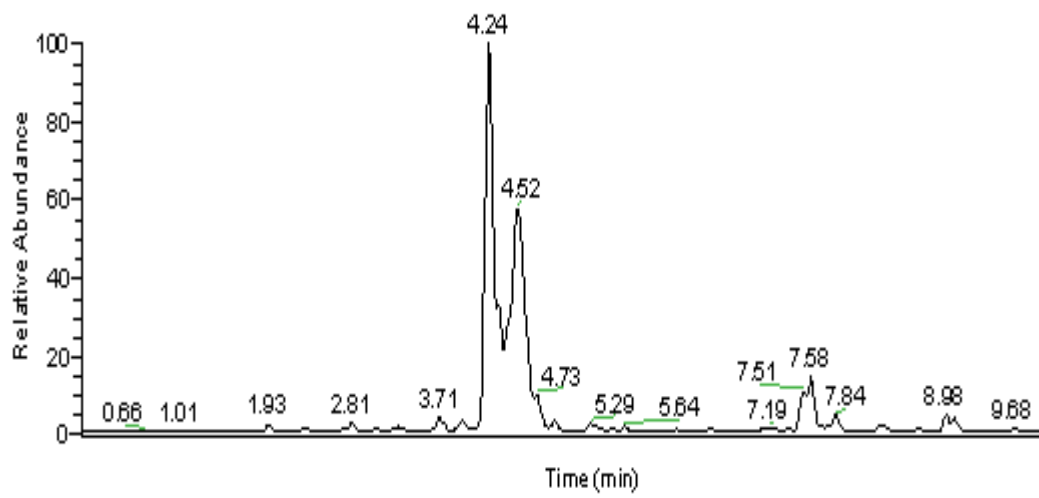


Figure 4.3 Original LC-MS/MS chromatogram outlining sample peak: Example peak recorded for a sample.

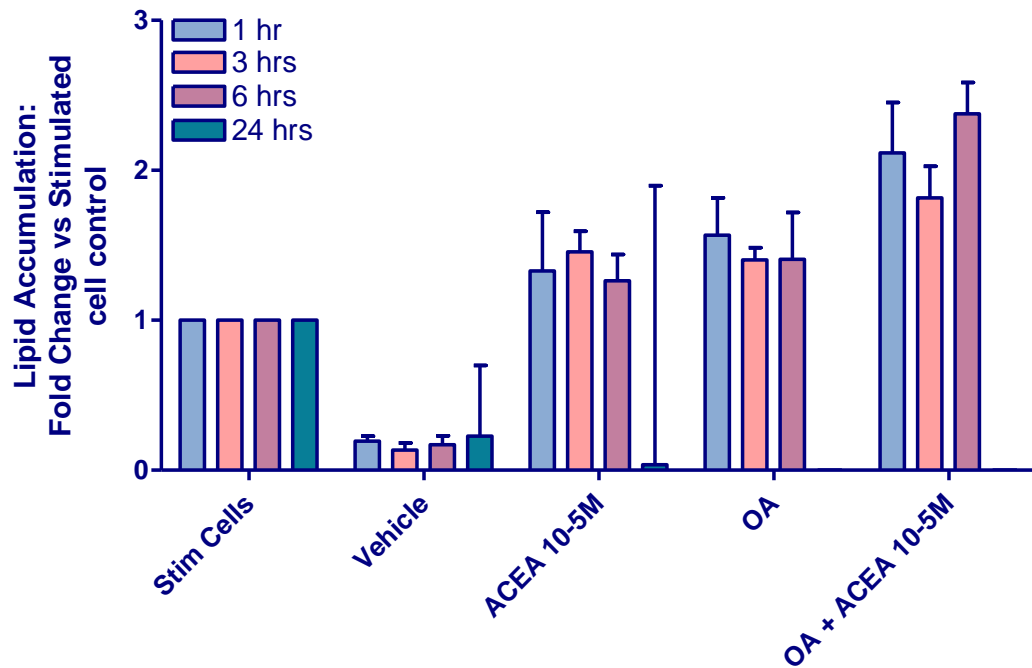


Figure 4.4 The time dependent effects of ACEA pre-treatment on OA uptake in THP-1 macrophages stimulated with PMA: THP-1 cells (1×10^6 cells/well) were pre-treated with either ACEA or vehicle (0.1% EtOH) for 1, 3, 6 or 24 hours. Cells were then stimulated with 5ng PMA and treated with oleic acid ($50\mu\text{M}$) for a further 24 hours. Lipid accumulation was quantified by ORO staining. Cells used in experiments were between passages 30 and 33. Data are expressed as a fold change in lipid accumulation compared to the control ('stim cells': cells stimulated with PMA). The full protocol was conducted independently three times in duplicate ($n=3$). Values represent mean \pm SEM.

4.4.2 The effect of endocannabinoid and cannabinoid compounds on OA accumulation in PMA-stimulated THP-1 macrophages

As illustrated in Figure 4.5 and Figure 4.6, OA treatment of cells resulted in significant lipid accumulation compared to stimulated cells. Neither ACEA nor 2-AG had any effect on the lipid accumulation in response to OA treatment (see Figure 4.5). Similarly, pre-treatment with either AEA or JWH133 failed to affect lipid accumulation in OA-treated THP-1 macrophages (see Figure 4.6). None of the cannabinoid ligands demonstrated any significant effect on basal lipid accumulation in the absence of OA.

4.4.3 MCP-1 production in OA and CB agonist treated THP-1 macrophages

As Figure 4.7 demonstrates, MCP-1 production in OA loaded cells (26 ± 3 pg/ml) was no different from that observed in stimulated cells (30 ± 3 pg/ml). Similarly, at a concentration of 10^{-5} M, AEA alone had negligible effects on MCP-1 production (24 ± 5 pg/ml) compared to stimulated cells. In contrast, an equimolar dose of JWH133 induced a significant increase in MCP-1 production (60 ± 14 pg/ml; $P<0.01$) compared to stimulated cells. Combined treatment of THP-1 macrophages with OA and either AEA or JWH133 had no significant effect on MCP-1 production beyond that of OA alone (Figure 4.8). Data is expressed as a fold change in lipid accumulation compared to stimulated cells.

4.4.4 Endocannabinoid production in OA loaded THP-1 macrophages

When the production of AEA and 2-AG by OA-loaded THP-1 macrophages was assessed, AEA levels were found to be below the lower detection limits of the assay and therefore could not be quantified. Figure 4.9 depicts the effect of OA loading of THP-1 macrophages on 2-AG production. Data is expressed as a fold change in 2-AG content (nmol/mg total protein) compared to unstimulated cells. Compared to unstimulated cells (1.08 ± 0.3 nmol/mg protein), stimulation of cells with PMA induced a fold increase in 2-AG production (2.08 ± 0.8 nmol/mg protein). Treatment of PMA stimulated cells with both vehicle (0.1% ethanol) and fibrate significantly reduced 2-AG production (1.09 ± 0.5 nmol/mg protein and 1.06 ± 0.5 nmol/mg protein respectively) compared to stimulated cells ($P<0.05$). OA treatment however, had no effect on PMA-stimulated 2-AG production.

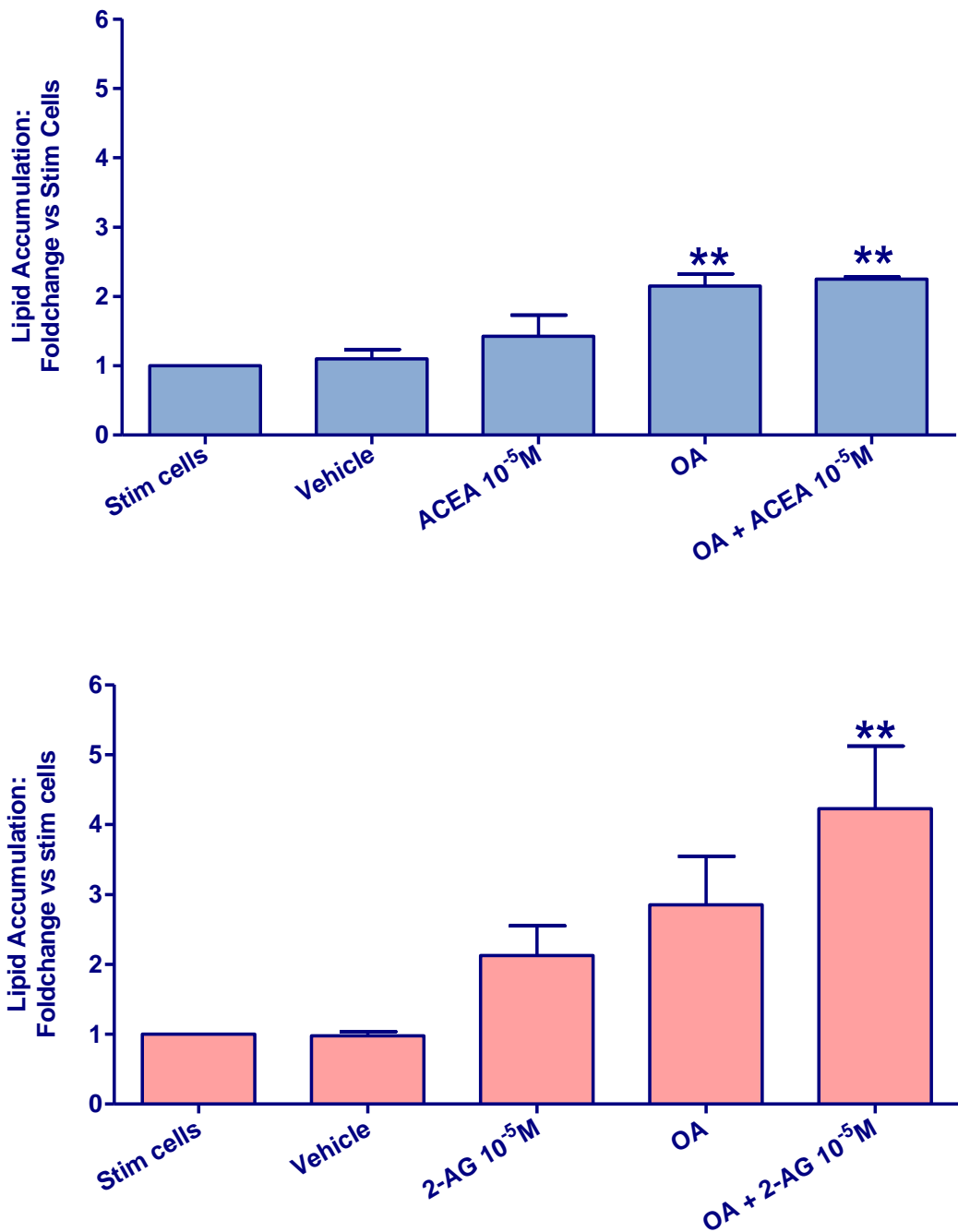


Figure 4.5 OA accumulation in ACEA and 2-AG treated THP-1 macrophages stimulated with PMA: THP-1 cells (1×10^6 cells/well) were pre-treated with ACEA, 2-AG or vehicle (0.1% ethanol) for 6 hours. Cells were then stimulated with 5ng PMA and treated with 50 μ M of OA for a further 24 hours. Lipid accumulation was quantified with ORO staining. Cells used were between passages 30 and 34. Data are expressed as a fold change in lipid accumulation compared to the control ('stim cells'). The full protocol was conducted independently four times in duplicate (n=4). **p<0.01 vs stim cells (one-way ANOVA, Dunnett's multiple comparison post-hoc test). Values represent mean \pm SEM.

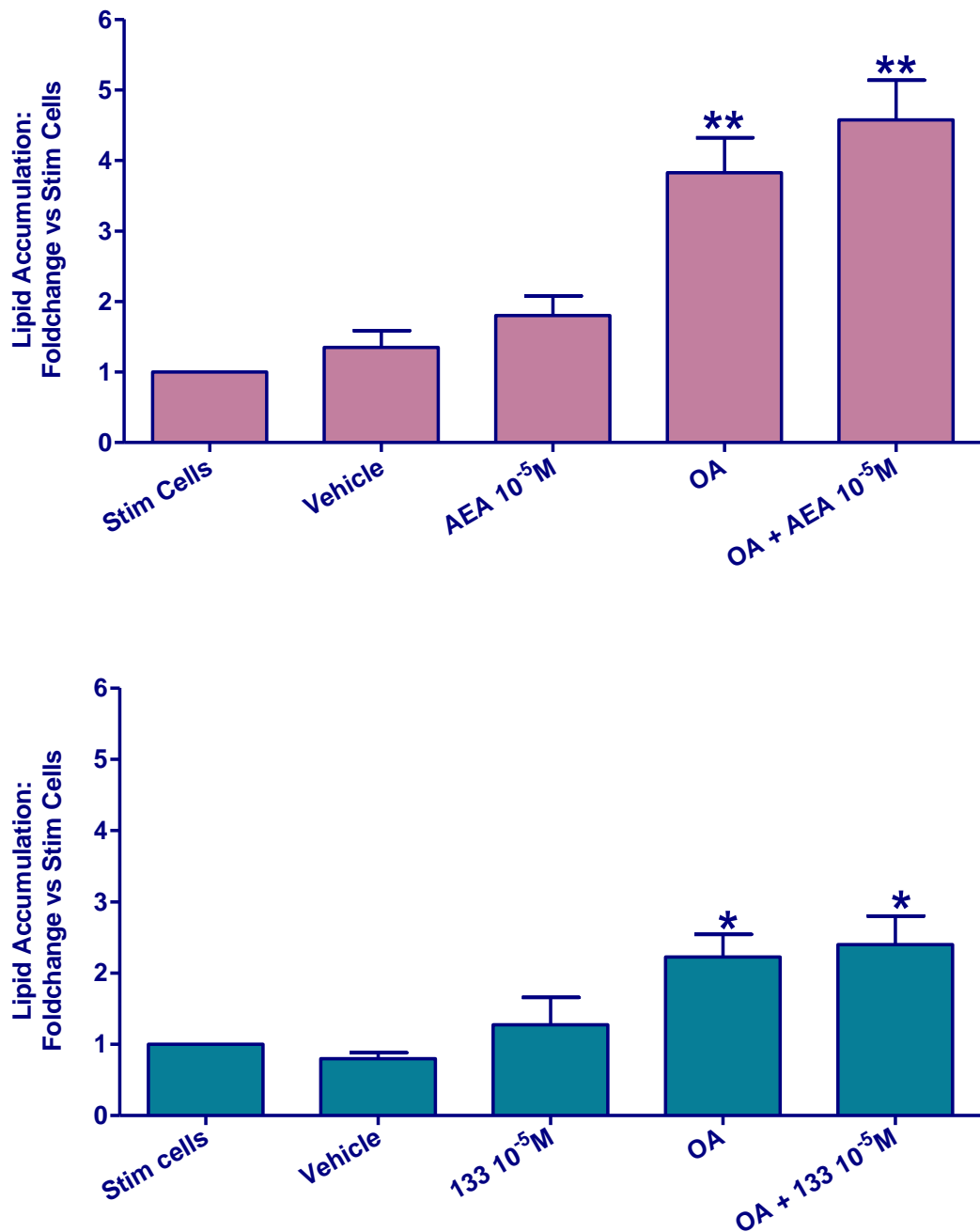


Figure 4.6 OA accumulation in AEA and JWH133 treated THP-1 macrophages stimulated with PMA: THP-1 cells (1×10^6 cells/well) were pre-treated with AEA, JWH133 or vehicle (0.1% ethanol) for 6 hours. Cells were then stimulated with 5ng PMA and treated with 50 μ M of OA for a further 24 hours. Lipid accumulation was quantified with ORO staining and expressed as described previously. Cells were used between passages 30 and 34. The full protocol was conducted independently four times in duplicate (n=4). *p<0.05, **p<0.01 vs stim cells (one-way ANOVA, Dunnett's multiple comparison post-hoc test). Values represent mean \pm SEM.

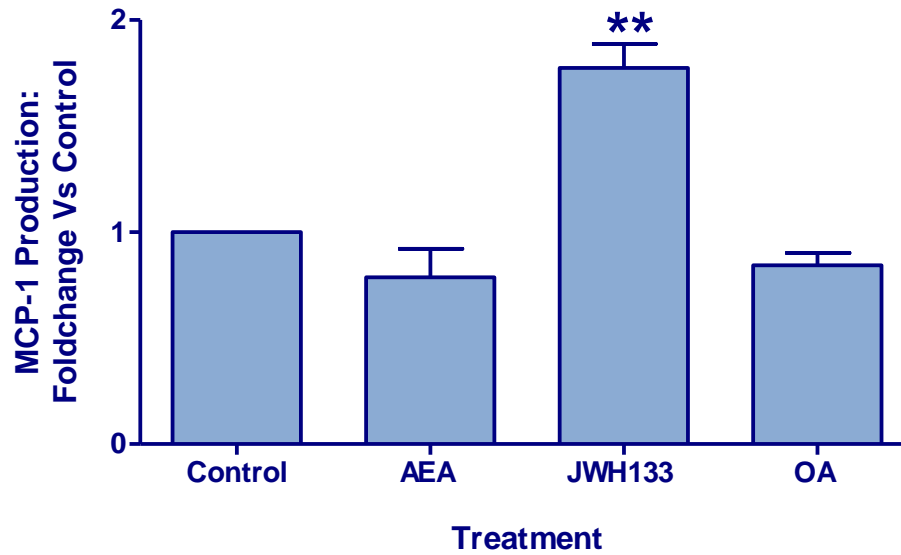


Figure 4.7 Baseline MCP-1 production in OA and drug treated THP-1 macrophages: MCP-1 production was measured in conditioned media retained from the previously described lipid accumulation studies. MCP-1 production, induced by OA, AEA and JWH133 treatment of THP-1 macrophages was assayed by ELISA. Data is expressed as a fold change in MCP-1 production compared to the control treatment (PMA stimulated cells; 30 ± 3 pg/ml). The full protocol was conducted independently three times in quadruplicate ($n=3$). ** $p < 0.01$ vs control (one-way ANOVA, Dunnett's multiple comparison post-hoc test). Values represent mean \pm SEM.

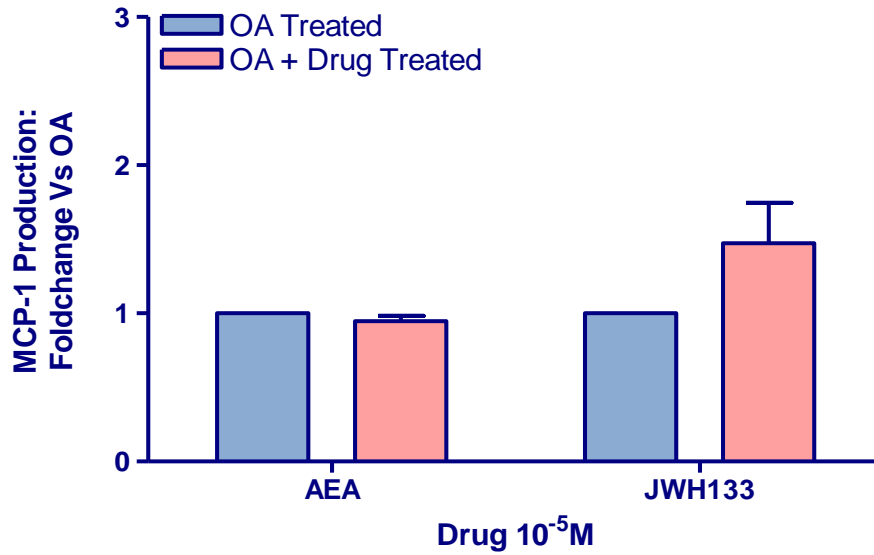


Figure 4.8 The effect of AEA/JWH133 on MCP-1 production in OA treated THP-1 macrophages: MCP-1 production was measured in conditioned media retained from the previously described lipid accumulation studies. MCP-1 production in OA and drug treated cells was assayed by ELISA. Data are expressed as a fold change in MCP-1 production compared to OA (26±3 pg/ml). The full protocol was conducted independently three times in quadruplicate (n=3). Values represent mean±SEM.

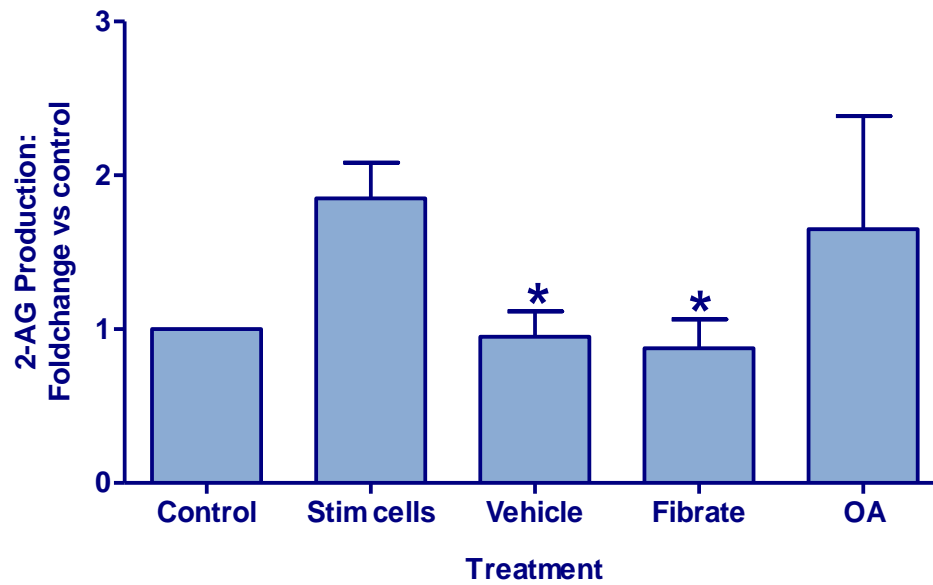


Figure 4.9 The effect of OA and fenofibrate on 2-AG production in PMA stimulated THP-1 macrophages: THP-1 cells (1×10^6 cells/well) were treated with 50 μ M fibrates, OA or vehicle (ethanol, 0.1%) and stimulated with 5ng PMA for 24 hours. Cells were collected and the 2-AG content quantified in the cell supernatant through LC-MS/MS analysis. Data are expressed as a fold change in 2-AG production compared to the control (unstimulated cells; 1082 ± 325 pmol/mg total protein). The full protocol was conducted independently four times in duplicate (n=4). *p<0.002 vs stimulated cells (unpaired t-test). Values represent mean \pm SEM.

4.4.5 The effect of endocannabinoid and cannabinoid compounds on EPA accumulation in PMA-stimulated THP-1 macrophages

As illustrated in Figure 4.10 and Figure 4.11, exposure of THP-1 macrophages to EPA resulted in significant lipid accumulation. Pre-treatment of EPA loaded cells with the various endocannabinoid and synthetic cannabinoid ligands (ACEA, 2-AG, AEA and JWH133) had no further impact on lipid accumulation.

4.4.6 MCP-1 production in EPA and CB agonist treated THP-1 macrophages

Figure 4.12 depicts the effect of EPA loading on MCP-1 production. With comparison to PMA stimulated cells (30 ± 3 pg/ml), EPA treatment of THP-1 macrophages was shown to increase MCP-1 production slightly (43 ± 9 pg/ml); however this effect was not significant. The compounding effect of exposure to EPA in conjunction with either AEA or JWH133 on MCP-1 production in macrophages is illustrated in Figure 4.13, where data have been normalised to EPA alone. Pre-treatment with AEA had no additional effect on EPA-induced MCP-1 production at either concentration tested. In contrast, JWH133 pre-treatment (10^{-5} M) significantly elevated MCP-1 production (74 ± 27 pg/ml) compared to EPA alone (43 ± 9 pg/ml; $P < 0.001$).

4.4.7 2-AG production in EPA treated THP-1 macrophages

Figure 4.14 depicts the production of 2-AG in EPA loaded THP-1 macrophages. Data is expressed as a fold change in 2-AG concentration (pmol/mg total protein) compared to unstimulated cells. As described previously, stimulation of cells with PMA induced a fold increase in 2-AG production (2.08 ± 0.8 nmol/mg protein) compared to unstimulated controls (1.08 ± 0.3 nmol/mg protein). EPA treatment had no effect on 2-AG production beyond the effects of PMA stimulation alone.

4.4.8 The effect of endocannabinoid and cannabinoid compounds on DHA accumulation in PMA-stimulated THP-1 macrophages

The impact of endocannabinoid and cannabinoid pre-treatment of DHA loaded cells is illustrated in Figure 4.15 and Figure 4.16. DHA treatment resulted in significant lipid accumulation compared to untreated cells. Neither ACEA, nor 2-AG pre-treatment had any effect on lipid accumulation.

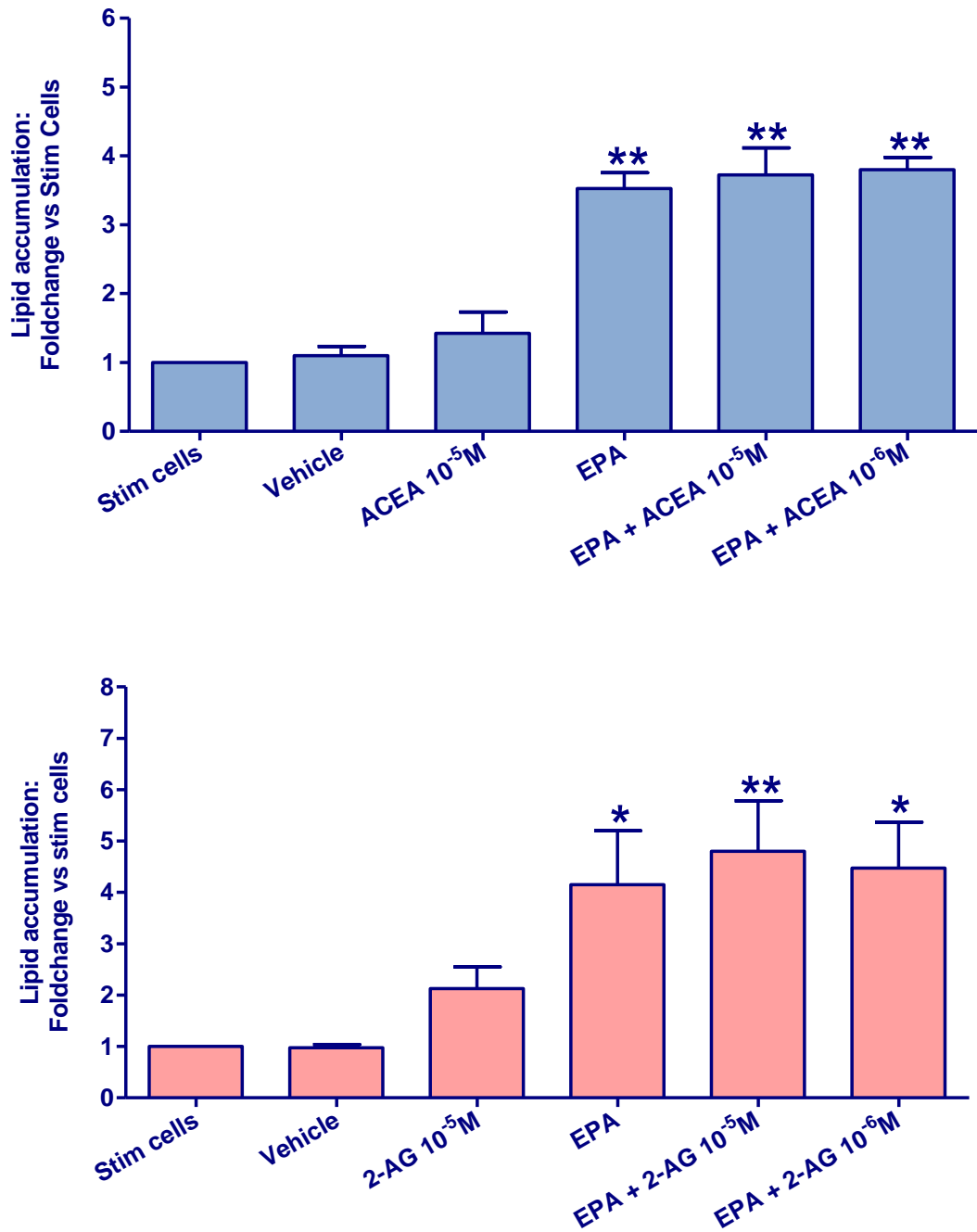


Figure 4.10 EPA accumulation in ACEA and 2-AG THP-1 macrophages stimulated with PMA: THP-1 cells (1×10^6 cells/well) were pre-treated with ACEA, 2-AG or vehicle (0.1% ethanol) for 6 hours. Cells were then stimulated with 5ng PMA and treated with 50 μ M of EPA for a further 24 hours. Lipid accumulation was quantified with ORO staining and expressed as described previously. Cells were used between passages 30 and 34. The full protocol was conducted independently four times and measured in duplicate. ** $p < 0.01$ vs stim cells (one-way ANOVA, Dunnett's multiple comparison post-hoc test). Values represent mean \pm SEM.

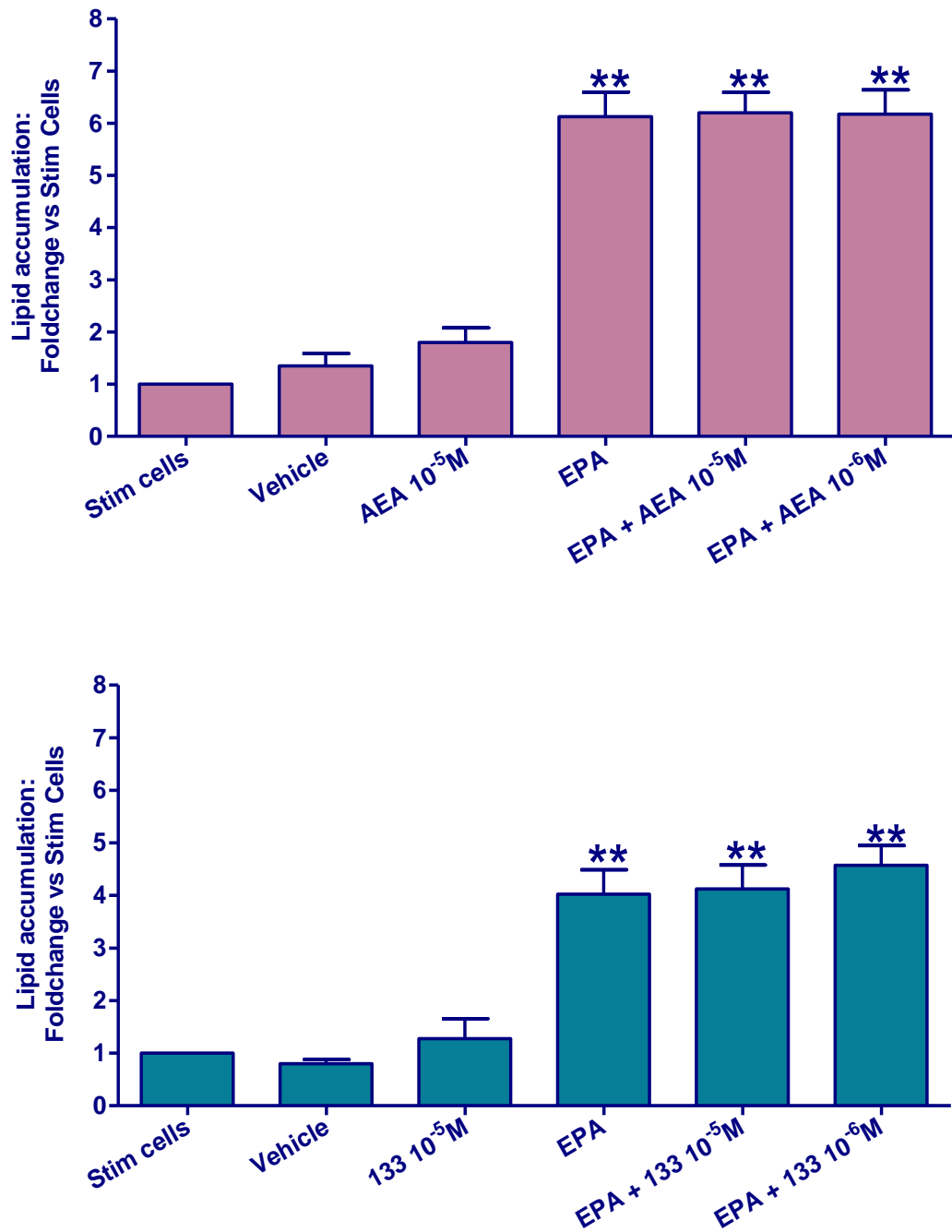


Figure 4.11 EPA accumulation in AEA and JWH133 treated THP-1 macrophages stimulated with PMA: THP-1 cells (1×10^6 cells/well) were pre-treated with AEA, JWH133 or vehicle (0.1% ethanol) for 6 hours. Cells were then stimulated with 5ng PMA and treated with 50 μ M of EPA for a further 24 hours. Lipid accumulation was quantified with ORO staining and expressed as described previously. Cells were used between passages 30 and 34. The full protocol was conducted independently four times in duplicate (n=4). *p<0.05; **p<0.01 vs stim cells (one-way ANOVA, Dunnett's multiple comparison post-hoc test). Values represent mean \pm SEM.

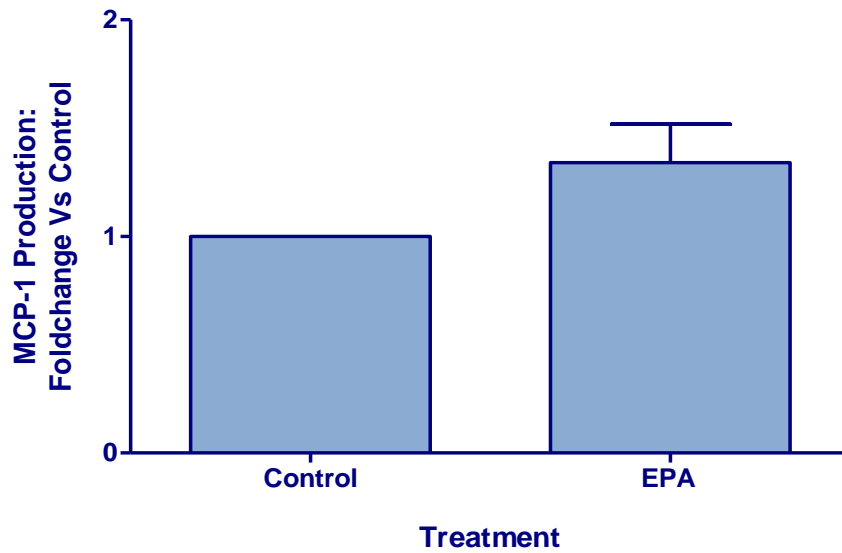


Figure 4.12 Baseline MCP-1 production in EPA loaded THP-1 macrophages: MCP-1 production was measured in conditioned media retained from the previously described lipid accumulation studies. MCP-1 production in EPA loaded THP-1 macrophages was assayed by ELISA. Data are expressed as a fold change in MCP-1 production compared to the control treatment (PMA stimulated cells; 30 ± 3 pg/mL). The full protocol was conducted independently three times in quadruplicate ($n=3$). Values represent mean \pm SEM.

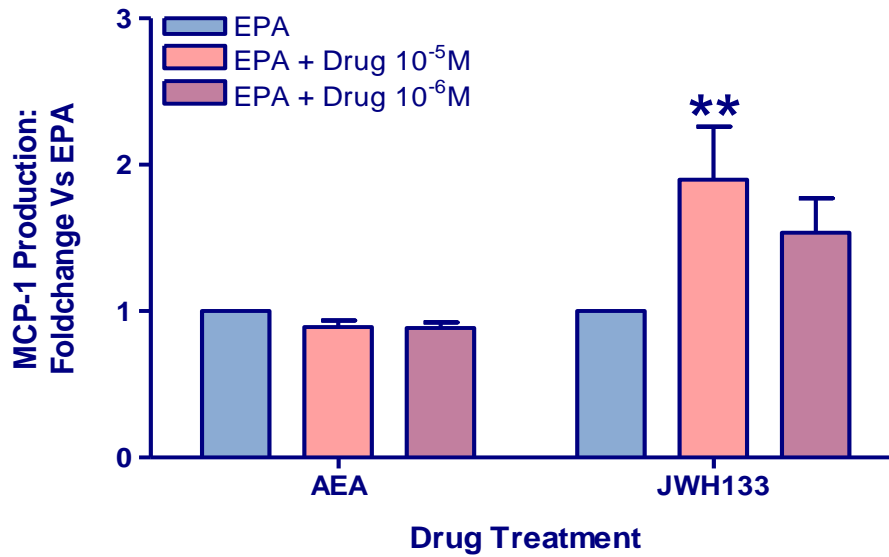


Figure 4.13 The effect of AEA/JWH133 pre-treatment on MCP-1 production in EPA loaded THP-1 macrophages: MCP-1 production in EPA- and drug-treated cells was assayed by ELISA. Data are expressed as a fold change in MCP-1 production compared to EPA (43±9 pg/mL). The full protocol was conducted independently three times in quadruplicate (n=3). **p<0.01 vs EPA alone (two-way ANOVA, Bonferroni post-hoc test). Values represent mean±SEM.

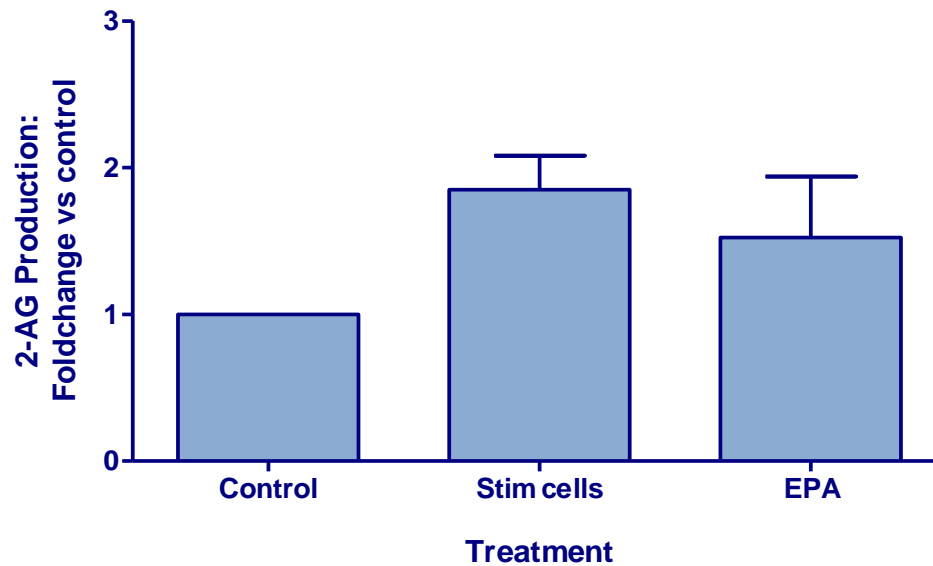


Figure 4.14 The effect of EPA accumulation on 2-AG production in PMA stimulated THP-1 macrophages: THP-1 cells (1×10^6 cells/well) were treated with $50\mu\text{M}$ EPA and stimulated with 5ng PMA for 24 hours. Cells were collected and the 2-AG content quantified as described previously. Data is expressed as a fold change in 2-AG production compared to the control (unstimulated cells; 1082 ± 325 pmol/mg total protein). The full protocol was conducted independently four times in duplicate ($n=4$). Values represent mean \pm SEM.

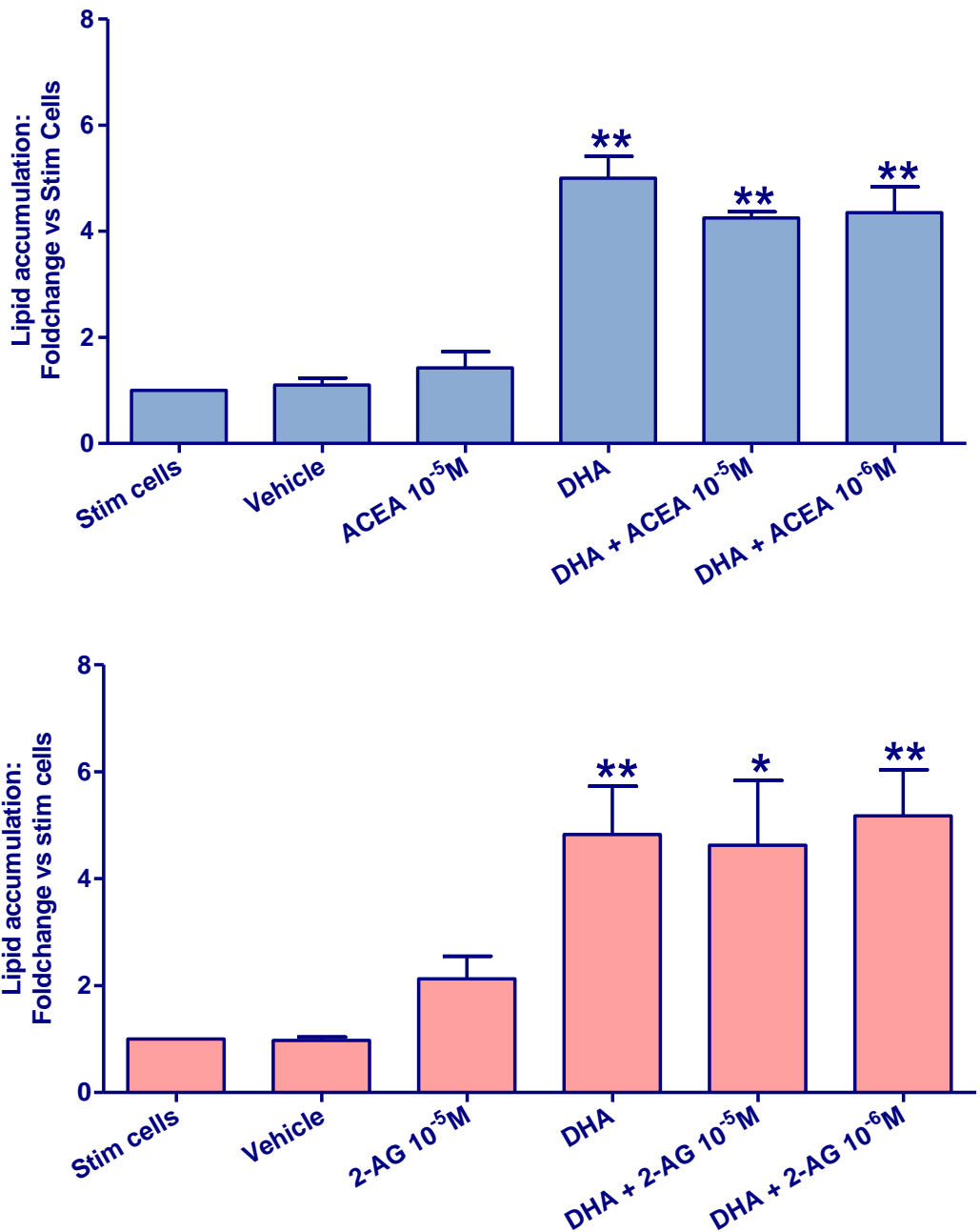


Figure 4.15 DHA accumulation in ACEA and 2-AG treated THP-1 macrophages stimulated with PMA: THP-1 cells (1×10^6 cells/well) were pre-treated with ACEA, 2-AG or vehicle (0.1% ethanol) for 6 hours. Cells were then stimulated with 5ng PMA and treated with 50 μ M of DHA for a further 24 hours. Lipid accumulation was quantified and expressed as described previously. Cells were used between passages 30 and 34. The full protocol was conducted independently four times in duplicate ($n=4$). * $p<0.05$; ** $p<0.01$ vs stim cells (one-way ANOVA, Dunnett's multiple comparison post-hoc test). Values represent mean \pm SEM.

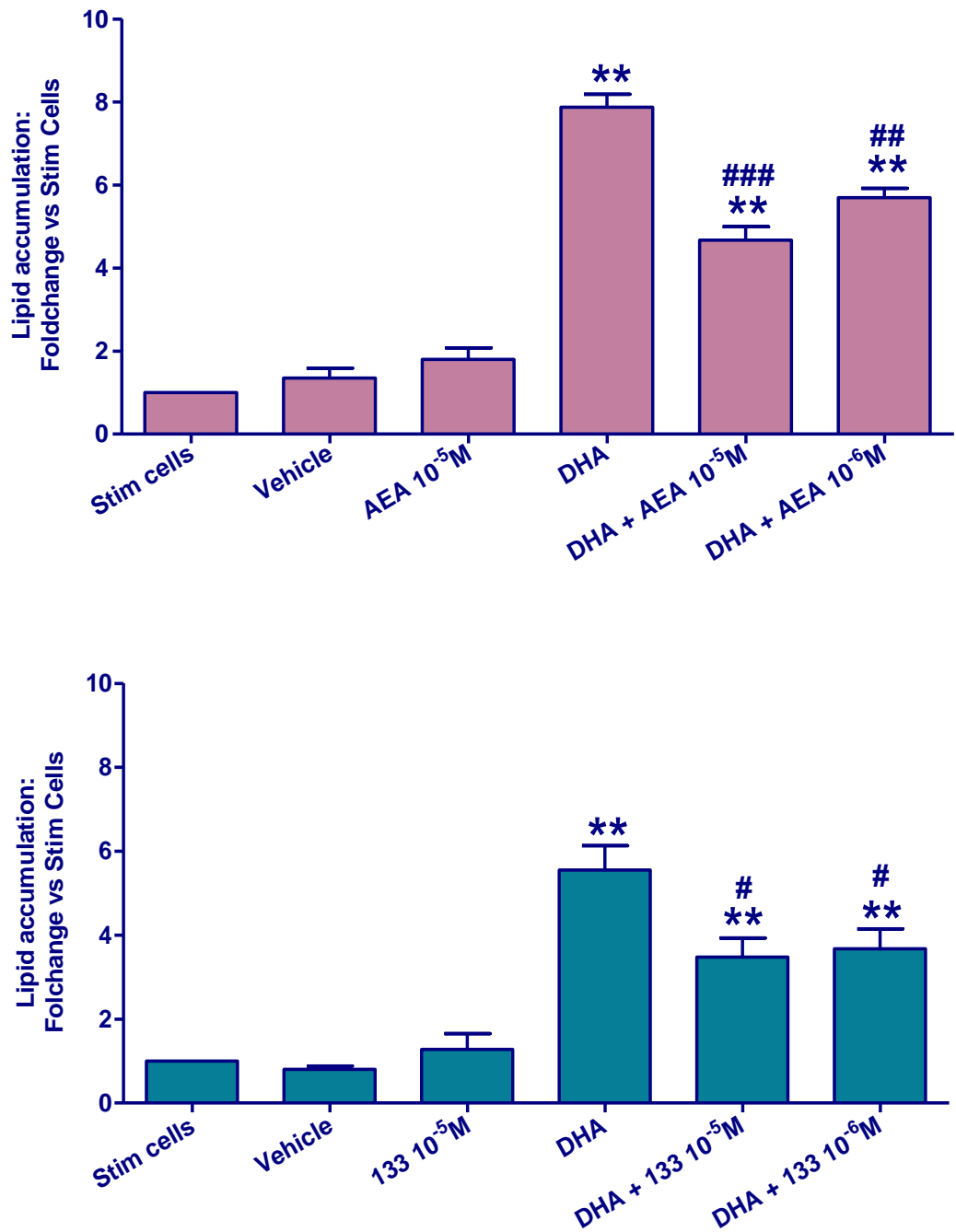


Figure 4.16 DHA accumulation in AEA and JWH133 treated THP-1 macrophages stimulated with PMA: THP-1 cells were pre-treated with AEA, JWH133 or vehicle as described previously. Cells were stimulated with 5ng PMA and treated with 50µM of DHA for a further 24 hours. Lipid accumulation was quantified and expressed as described previously. Cells were used between passages 30 and 34. The full protocol was conducted independently four times in duplicate. *p<0.05; **p<0.01 vs stim cells (one-way ANOVA, Dunnett’s multiple comparison post-hoc test). #p=0.395; ##p=0.012; ###p=0.0004 vs DHA (unpaired t-test). Values represent mean±SEM.

Pre-treatment of cells with AEA (10^{-5} M) significantly reduced DHA accumulation compared to DHA only treated cells (4.7 vs 7.9 respectively; $P=0.0004$). JWH133 pre-treatment also significantly reduced lipid accumulation compared to DHA only treated cells (3.4 vs 5.5 respectively; $P=0.0478$). All data were expressed as a fold change in lipid accumulation compared to the control treatment – PMA stimulated cells.

Figure 4.17 demonstrates the effect of AEA pre-treatment on cell viability. Exposure of DHA-treated cells to AEA, 10^{-9} M to 10^{-5} M, did not affect cell viability which did not fall below 95%. At 10^{-4} M, AEA, either alone or in combination with DHA significantly reduced cell viability to 30% ($P<0.01$). Treatment with the vehicle was shown to reduce cell viability to 67% ($P<0.05$). The effect of JWH133 pre-treatment on cell viability is illustrated in Figure 4.18. The viability of DHA treated cells exposed to JWH133 (10^{-9} M to 10^{-5} M) did not fall below 96%. JWH133 alone reduced cell viability to 79% while the vehicle significantly reduced cell viability to 71% ($P<0.05$). All data were normalised to the DHA treatment, where viability was deemed 100%.

4.4.9 MCP-1 production in DHA and CB agonist treated THP-1 macrophages

The production of MCP-1 by THP-1 macrophages loaded with DHA is shown in Figure 4.19. DHA was observed to have no impact on MCP-1 production beyond baseline MCP-1 production by untreated cells (29 ± 6 pg/ml vs 30 ± 3 pg/ml respectively). As demonstrated in Figure 4.20, pre-treatment of DHA loaded cells with AEA slightly elevated MCP-1 production with respect to DHA only treated cells, although this effect failed to reach statistical significance. Similarly, pre-treatment with JWH133 also induced a slight elevation of MCP-1 production however again, this effect lacked statistical significance.

4.4.10 2-AG production in DHA treated THP-1 macrophages

Figure 4.21 demonstrates the production of 2-AG in DHA loaded THP-1 macrophages. Data is expressed as a fold change over unstimulated cells. DHA treatment significantly reduced 2-AG production (0.89 ± 0.2 nmol/mg protein) compared to stimulated cells (2.08 ± 0.8 nmol/mg protein; $P<0.05$).

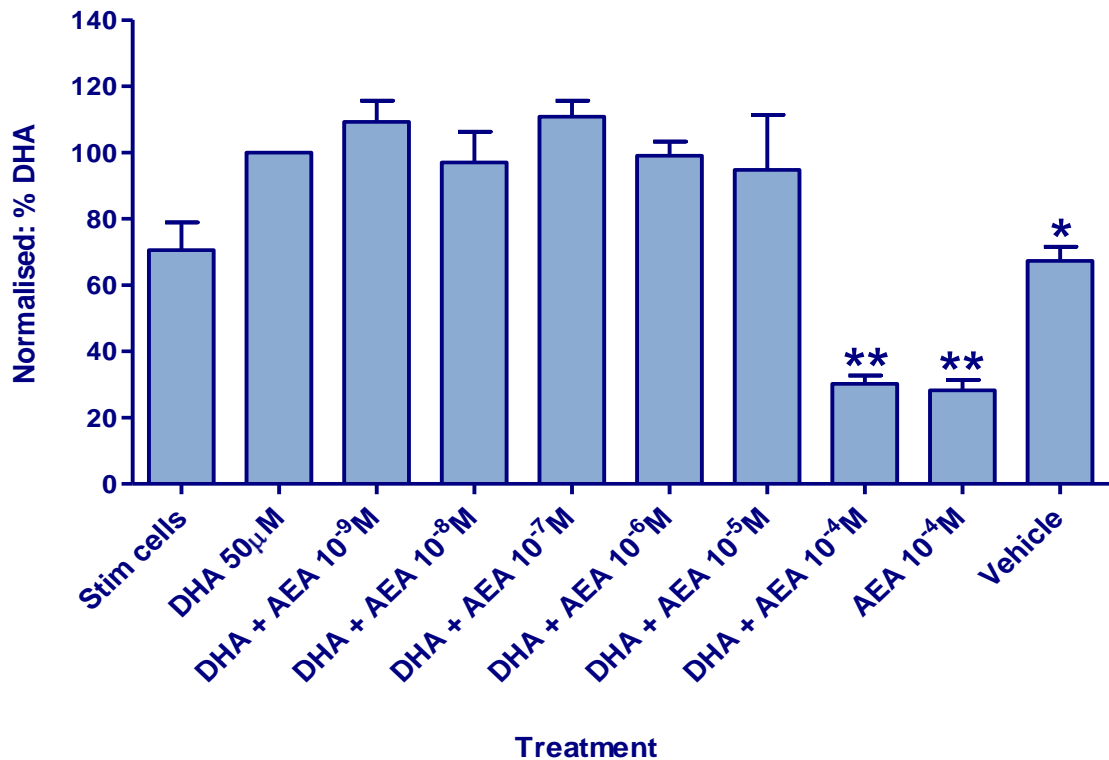


Figure 4.17 The effect of AEA treatment on the viability of PMA stimulated THP-1 macrophages: THP-1 cells (20,000 cells/well) were pre-treated with AEA or vehicle (1% ethanol) for 6 hours. Cells were stimulated with 5ng PMA and treated with 50µM DHA for a further 24 hours. MTS solution was applied to the cells for a further 2 hours and the absorbance measured at 490nm. Cells were between passages 32-35. Data were normalised to the DHA treatment, where viability was deemed 100%. The full protocol was conducted independently three times with six replicates for each treatment (n=3). *p<0.05; **p<0.01 vs DHA control (one-way ANOVA, Dunnett's Multiple Comparison post-hoc test). Values represent mean±SEM.

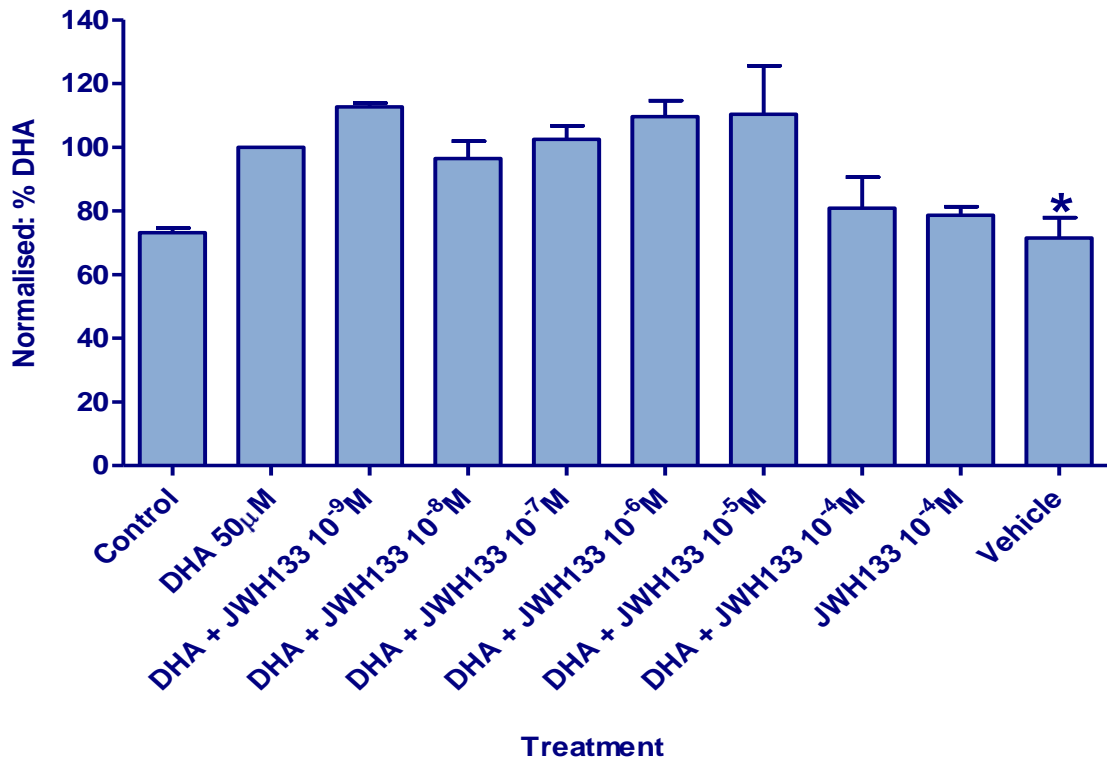


Figure 4.18 The effect of JWH133 treatment on the viability of PMA stimulated THP-1 macrophages: THP-1 cells (20,000 cells/well) were pre-treated with JWH133 or vehicle (1% ethanol) for 6 hours. Cells were stimulated with 5ng PMA and treated with 50µM DHA for a further 24 hours. MTS solution was applied to the cells for a further 2 hours and the absorbance measured at 490nm. Cells were between passages 32-35. Data were normalised to the DHA treatment (viability deemed 100%). The full protocol was conducted independently three times with each replicates for each treatment (n=3). *p<0.05; vs DHA control (one-way ANOVA, Dunnett's Multiple Comparison post-hoc test). Values represent mean±SEM.

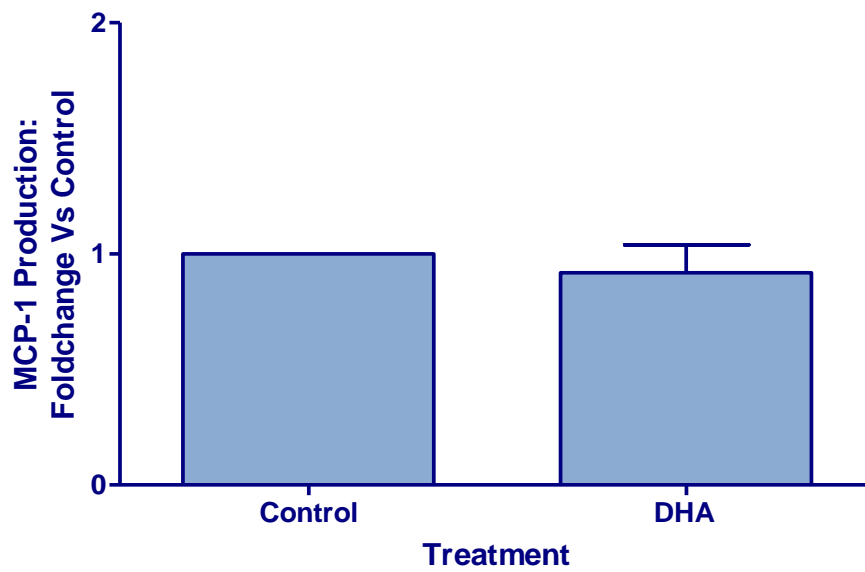


Figure 4.19 Baseline MCP-1 production in DHA loaded THP-1 macrophages: MCP-1 production was measured in conditioned media retained from the previously described lipid accumulation studies. MCP-1 production in DHA-loaded THP-1 macrophages was assayed by ELISA. Data were expressed as a fold change in MCP-1 production compared to the control treatment (PMA stimulated cells; 30 ± 3 pg/mL). The full protocol was conducted independently three times in quadruplicate ($n=3$). Values represent mean \pm SEM.

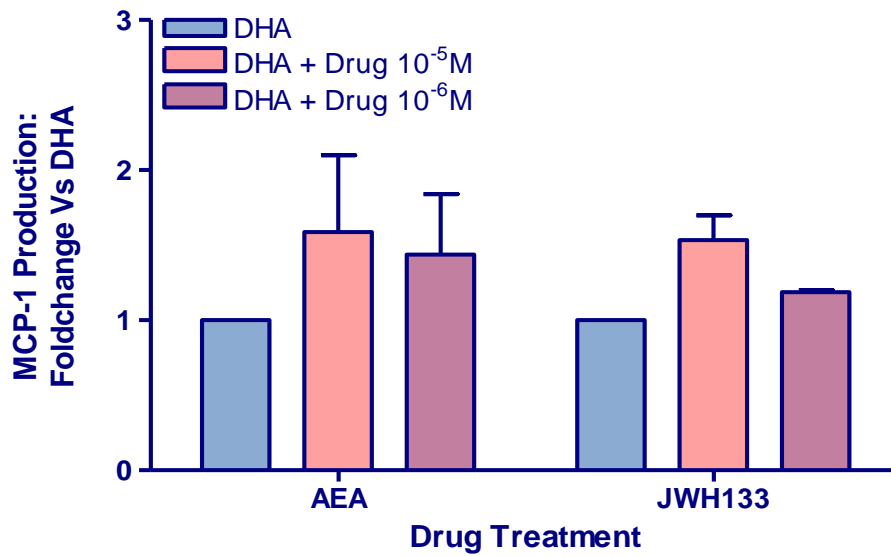


Figure 4.20 The effect of AEA/JWH133 on MCP-1 production in DHA loaded THP-1 macrophages: MCP-1 production in DHA and drug treated cells was assayed by ELISA. Data were expressed as a fold change in MCP-1 production compared to DHA (29 ± 6 pg/mL). The full protocol was conducted independently three times and in quadruplicate ($n=3$). Values represent mean \pm SEM.

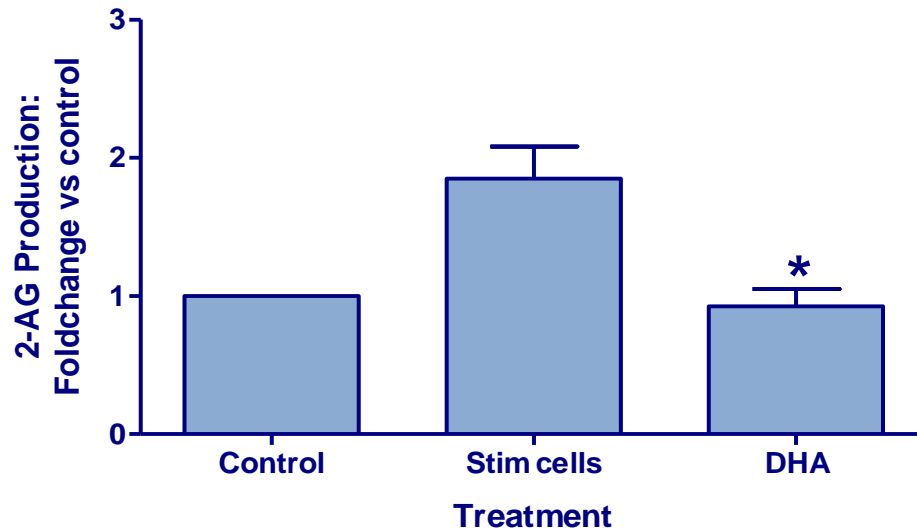


Figure 4.21 The effect of DHA accumulation on 2-AG production in PMA stimulated THP-1 macrophages: THP-1 cells (1×10^6 cells/well) were treated with the previously described controls or 50 μ M DHA and stimulated with 5ng PMA for 24 hours. Cells were collected and the 2-AG content quantified as described previously. Data is expressed as a fold change in 2-AG production compared to the control (unstimulated cells; 1082 ± 325 pmol/mg total protein). The full protocol was conducted independently four times in duplicate (n=4). *p=0.013 vs stimulated cells (unpaired t-test). Values represent mean \pm SEM.

4.5 Discussion

The intention of the present study was to identify an association, if existing, between the endocannabinoid system and ω -3 PUFAs, which are considered to be anti-inflammatory and anti-atherosclerotic, in the setting of the macrophage.

To allow investigation of the potential involvement of the endocannabinoid system in macrophage activity, it was necessary to optimise drug (cannabinoid and endocannabinoid ligands) treatment conditions in the model devised and described in Chapter 3. Based on dose response data obtained previously in the laboratory in combination with methodological approaches cited in the literature (Gokoh *et al.*, 2007; Correa *et al.*, 2005), drug doses of 10^{-5} M and 10^{-6} M were chosen for study. Although at the upper limit of the previously used dose range, high concentrations were chosen to increase the likelihood of observing any potential effects of the drugs. Figure 4.4 demonstrates the effect of 10^{-5} M ACEA on various cell treatments. The aim of the experiment was to assess any time dependent effects of the drug, thus allowing the optimal pre-treatment period to be deduced. It was found that there were no time-dependent effects observed with 1, 3 or 6 hour ACEA pre-treatment. The end-point of lipid accumulation did not significantly vary, time-dependently, between treatments. ACEA pre-treatment for a period of 24 hours did abolish lipid accumulation in certain treatments, an effect which was confirmed by light microscopy to be a result of extensive cell death. Therefore the pre-incubation period of 6 hours was chosen as the optimal incubation time for the following experiments.

4.5.1 The effect of endocannabinoids and cannabinoids on FA accumulation in THP-1 macrophages

Exposure of PMA-stimulated THP-1 macrophages to the various FAs examined significantly increased intracellular FA accumulation. While the medium in which the cells were suspended contained foetal bovine serum, which is known to contain free FAs, the control treatment (cells treated with only PMA) provided an indication of baseline FA uptake. Normalisation of the experimental FA data to this baseline negated any effects of the FAs present in the media. None of the ligands tested had a direct effect on lipid accumulation in the absence of FAs, this presented confirmation that any increases in lipid accumulation beyond that of the control treatment were a result of exposure to the experimental FA.

Activation of the CB₁ receptor using the CB₁ selective agonist ACEA ($K_i=1.4$ nM) had no impact on the cellular uptake of OA, EPA or DHA; an effect that would suggest in this set of experiments, that

CB₁ receptor activation did not influence FA accumulation. However, this finding may be specific to the experimental conditions of the present model. In RAW264.7 macrophages exposed to oxLDL (1-12µg/ml), Jiang and colleagues (2009) reported a significant increase in total and esterified cholesterol accumulation (measured by LC-MS/MS), following treatment with the selective CB₁ receptor agonist WIN,212-2 (1-20µM), an effect which was associated with increased CB₁ receptor expression. While the contrasting methodology and experimental conditions of the Jiang study do not permit its direct comparison to the present study, it is worthwhile to note the model specific differences.

CB₂ receptor activation using JWH133, a CB₂ selective agonist ($K_i=3.4\text{nM}$), induced a significant dose-dependent reduction in DHA uptake yet had no effect on OA or EPA uptake. Based on these findings, it could be postulated that the reduced accumulation of DHA was a result of CB₂ receptor activation. However, this proposed notion is complicated by the observation that the endocannabinoid AEA, an endogenous ligand of both CB₁ and CB₂ receptors, also significantly attenuated DHA uptake. In essence, it is not clear from these experiments whether the effect was mediated through the CB₁ or CB₂ receptor. However, the observation that ACEA (a CB₁ selective agonist) had no impact on lipid accumulation argues against the role of AEA-mediated activation of CB₁ receptors in this effect. Moreover, reported activity of AEA at the vanilloid receptor type-1 (TRPV1) and the gastrin-releasing peptide 55 (GPR55) receptors (Smart *et al.*, 2000; Ryberg *et al.*, 2007) suggests that, in this instance, AEA may be acting at receptors independent of the CB family entirely. It is intriguing that 2-AG, which is also an endogenous agonist of CB₁ and CB₂ receptors with a greater affinity for CB₂ (Mechoulam *et al.*, 1995), did not induce changes similar to that seen with JWH133 or AEA. However the lack of effect may be explained by the biological properties of 2-AG, given that 2-AG, in comparison to AEA, has a lower potency at the CB receptors (2-AG $EC_{50}=519, 618\text{nM}$ at CB₁ and CB₂ respectively vs AEA $EC_{50}=31, 27\text{nM}$ at CB₁ and CB₂ respectively).

To verify that the effects of JWH133 and AEA on DHA uptake were genuine, and not a result of drug induced cytotoxicity, their effect on cell viability was examined. Treatment of DHA-loaded cells with neither JWH133 nor AEA had any significant effect on cell viability at the concentrations shown to influence DHA uptake, although at a high concentration (10^{-4}M), AEA was demonstrated to induce a degree of cytotoxicity. Given that AEA has been reported to induce apoptotic body formation and DNA defragmentation (characteristic signs of programmed cell death) at micromolar concentrations (Maccarrone *et al.*, 2000), this finding was not unexpected. Importantly, the drug concentrations employed in the present assay did not reduce cell viability, thereby confirming the authenticity of the findings. The mechanism underlying the effect of AEA and JWH133 on DHA uptake remains unclear; however there are several potential explanations:

1) Since both cannabinoids and ω -3 PUFAs exert some of their actions through the nuclear PPAR pathways it is possible that the action of JWH133 and AEA on DHA uptake is the result of an overlapping role in PPAR signalling. DHA may be involved in regulating PPARs and their associated signalling pathways, since this has been reported with ω -3 PUFAs previously (Xu *et al.*, 1999). Indeed, DHA treatment has been reported to suppress protein expression of the CD36 scavenger receptor, a downstream target of PPAR α/γ signalling (Malfitano *et al.*, 2007), in human dermal microvascular endothelial cells, THP-1 cells and human colon tumour (HT116) cells (Lee and Hwang, 2002; Madonna *et al.*, 2011). This effect could be a direct regulation of PPAR protein expression or could be due to the action of a DHA metabolite, for example a transcription factor, nuclear hormone receptor or lipid second messenger. The capacity of several cannabinoid ligands to activate PPARs has also been previously documented (Bouaboula *et al.*, 2005; Sun *et al.*, 2007) and an *in vitro* study reported that treatment of peripheral blood mononuclear cells with anandamide (10 μ M) generated an increase in CD36 scavenger receptor mRNA expression. Consistent with this finding, WIN55,212-2 (CB₁ receptor agonist) has been shown to increase CD36 mRNA expression and to decrease ABCA1 mRNA expression in RAW264.7 macrophages, both of which occurred concomitantly with increased PPAR γ receptor expression (Jiang *et al.*, 2009). Since CD36 and ABCA1 represent the principal receptors involved in the regulation of macrophage cholesterol influx and efflux respectively, one might therefore expect cannabinoid treatment to increase FA uptake if DHA enters and leaves the cell by the same routes. However, the observation from the present studies that AEA and JWH133 reduced, rather than increased, DHA uptake suggest that a change in CD36 expression by these agents is unlikely to be fully responsible.

2) DHA mediated regulation of sterol regulatory-element binding protein (SREBP) could interfere with fatty acid and cholesterol metabolism. In response to intracellular sterol deprivation, SREBP undergoes various stages of cleavage to release n-SBREP, which binds to sterol regulatory elements (SREs) in the promoter region of genes regulating lipid metabolism pathways. *In vitro* studies on a range of cell types (African green monkey kidney, Chinese hamster ovary, human hepatoma and human non-hepatic cells) have demonstrated the ability of PUFAs, but not SFAs, to significantly reduce SREBP activation of SREs at micromolar concentrations (Worgall *et al.*, 1998; Hannah *et al.*, 2001). EPA, DHA and AA have been shown to have a greater inhibitory capacity than shorter chain fatty acids such as OA. In the present study, metabolism of AEA to AA may be acting independently or in combination with DHA, to regulate intracellular lipid metabolism. The observed effect of JWH133 may also be linked to the SREBP pathway. In colon cancer cell lines, CB₂ receptor agonist CB13 was recently demonstrated to induce a significant increase in intracellular ceramide production (Cianchi *et al.*, 2008); which has been reported to directly inhibit transcription of activated SBREP-1

and SBREP-2 though interference with sphingolipid synthesis (Worgall *et al.*, 2002). Thus it is possible that JWH133-induced stimulation of ceramide production could interfere indirectly with FA uptake.

While the discussed mechanisms do represent potential explanations for the current findings, it is worthwhile to note that these pathways could be extrapolated to the effects of ACEA and 2-AG and it is therefore curious that DHA uptake is not altered in these assays. It could be postulated that DHA may be influencing PPAR activation and/or SBREP activity under these conditions, however ACEA and 2-AG may have no pharmacological influence over the regulation of these pathways. Together these findings suggest that while CB receptor activation is capable of modulating intracellular FA uptake, the effect is dependent on the type of FA being internalised.

4.5.2 MCP-1 production in endocannabinoid and cannabinoid FA-loaded THP-1 macrophages

To assess the impact of CB receptor activation on inflammatory marker production in FA-loaded cells; production of monocyte chemoattractant protein-1 (MCP-1), a pro-inflammatory chemokine, was investigated. Over expression of MCP-1 by macrophages present in the atherosclerotic plaque has been demonstrated to promote atherosclerosis development in ApoE^{-/-} mice (Aiello *et al.*, 1999) while genetic deficiency of MCP-1 in LDLr^{-/-} mice fed a high fat diet, was reported to reduce atherosclerotic lesion development (Gu *et al.*, 1998). In stimulated THP-1 macrophages, CB₂ receptor activation significantly enhanced MCP-1 production compared to control cells. This is in contrast to recent studies, where CB₂ receptor activation has been associated with anti-inflammatory responses (Xu *et al.*, 2007; Montecucco *et al.*, 2008). However, *in vitro* studies in CB₂ receptor transfected HL60 (pro-myelocytic line) cells treated with nanomolar doses of CB₂ receptor agonist CP-55940 reported significant upregulation of MCP-1 mRNA and protein expression (Jbilo *et al.*, 1999; Derocq *et al.*, 2000). It was proposed that activation of the CB₂ receptor in undifferentiated HL60 cells induced a degree of differentiation, as exposure to CP-55940 upregulated cytokine production (MCP-1, IL-8, MIP-1 β and TNF- α) and the expression of cell differentiation factors (*junB* and *aldolase C*). Interestingly, exposure of HL60 cells to the differentiating stimulus Me₂SO revealed an inverse relationship between differentiation, progression and CB₂ receptor expression where maturation induced a systematic reduction in CB₂ mRNA expression and CP-55940 induced MCP-1 production (Derocq *et al.*, 2000). It could be postulated that in the present study, CB₂ receptor agonism with JWH133 induced further maturation of the THP-1 macrophages and in doing so, stimulated MCP-1 production. In contrast, there was no direct effect of AEA on MCP-1 production observed in the

present study. AEA, at a concentration of 10^{-5} M, has been previously demonstrated to reduce MCP-1 production in human gingival fibroblasts challenged with lipopolysaccharide (LPS; Yumiko *et al.*, 2006), however the lack of LPS challenge in the present study may have masked this action of AEA. As JWH133 selectively binds CB₂ receptors with a greater potency than AEA, this finding supports the notion that MCP-1 production is CB₂ receptor mediated in this particular experimental set-up.

Intracellular uptake of OA, EPA or DHA did not influence MCP-1 production in this model. This finding is in contrast to an earlier study in THP-1 monocytes, where DHA and EPA were demonstrated to suppress mRNA expression and protein production of several pro-inflammatory cytokines (TNF- α , IL-6 and IL-1 β ; Weldon *et al.*, 2006). However, the Weldon study did not examine the effects of the FAs on MCP-1 production, therefore the differential endpoint of the experiments does not allow for direct comparison of the results. Moreover, the fatty acid dose and exposure time employed in the Weldon study was 100 μ M for 48 hours respectively - double that of the current study (50 μ M for 24 hours). Therefore, it cannot be discounted that the differential outcomes of the two studies may be dependent on fatty acid exposure time and/or concentration. The most obvious methodological difference between the studies was the additional exposure of cells to LPS in the Weldon study. LPS exposure drastically elevated basal cytokine production which was significantly reduced by EPA/DHA pre-treatment. Perhaps the fundamental design difference in the current study, where cells were not challenged with LPS, masked the ability of the fatty acids to down-regulate cytokine production by not providing a cytokine stimulating factor.

Combined treatment of cells with AEA and FAs had no impact on MCP-1 production, an expected finding given that neither the drug alone, nor the individual FAs mediated any alteration to basal production. In the presence of FAs, JWH133 elevated MCP-1 production, an effect which was significant in EPA-loaded cells; however as this effect mirrored the magnitude of response to the ligand alone, it was most likely secondary to the drug mediated elevation in MCP-1 production. Further modification of the current cell model, perhaps considering fatty acid exposure time and concentration as well as including inflammatory stimulation, may provide a clearer insight into the inflammatory response occurring in this particular experimental set-up.

4.5.3 The effect of FA loading on endocannabinoid production

The production of 2-AG was significantly elevated in PMA-stimulated THP-1 macrophages compared to unstimulated cells; an effect which has been previously described in oxLDL stimulated RAW264.7 and rat peritoneal macrophages as well as rat microglial cells. This is thought to be a result of upregulated platelet-activating factor (PAF) receptor mediated phospholipases activation and

reduced degradation (Carrier *et al.*, 2004; Jiang *et al.*, 2009). AEA production in the present study was below the assay detection level, despite previous reports of AEA production in activated macrophages (Liu *et al.*, 2003; Carrier *et al.*, 2004; Jiang *et al.*, 2009). However in such studies, a higher quantity of cells was used for AEA extraction ($>2 \times 10^7$ in comparison to 1×10^6 cells used in the present study), and as AEA was found to be produced in lower quantities than 2-AG, it is likely that the quantity of cells used in the present protocol was not sufficient to detect alterations to AEA levels.

Treatment of cells with fenofibrate significantly lowered 2-AG production compared to stimulated cells, the first experimental evidence of such an action of fenofibrate. While the underlying mechanisms conferring such an effect have not been explored in the present study, it is possible that fenofibrate could be influencing the expression and/or activity of phospholipase C and diacylglycerol lipase, the enzymes which regulate the principle pathways of 2-AG synthesis, or it could be influencing the pool of 2-AG precursor phospholipids. Whether this effect is limited to the present model is currently unknown, therefore to fully characterise this novel action of fenofibrate warrants further investigation.

Intriguingly, DHA but not OA or EPA, significantly reduced 2-AG production in stimulated cells. Indeed, the elevated synthesis of 2-AG in stimulated cells was completely abolished in the presence of DHA where synthesis was equivalent to that of unstimulated cells. However, a similar effect was also observed in vehicle treated cells. While this response cannot be disregarded, the negligible impact of EPA or OA treatment alone on 2-AG production would suggest that the vehicle effect was not fully responsible for the effects of DHA treatment. In complement to the current findings, a recent study conducted in 3T3-F442A adipocytes reported that 72-hour treatment with 100 μ M DHA significantly reduced 2-AG synthesis (Matias *et al.*, 2008). It was also found that treatment of cells with EPA induced a slight, although not significant, reduction in 2-AG synthesis while OA failed to mediate any effects in this particular experimental set-up. The inconsistencies between these findings and the findings from the current study could be accounted for by the difference in cell phenotype as well as the concentration and incubation time of the fatty acids. As discussed in detail in Chapter 1 (section 1.4.2.2), 2-AG can be synthesised through several pathways from AA rich membrane phospholipids. The main pathway involves phospholipase C mediated hydrolysis of phospholipids to *sn*-1,2-diacylglycerol (DAG) which in turn reduced to 2-AG by the action of *sn*-1 specific DAG lipase (DAGL). An important structural feature of 2-AG is the unusual positioning of the glycerol/AA bond, which is esterified at the *sn*-2 position of the glycerol backbone. Matias and colleagues (2008) also observed an inverse correlation between DHA treatment and the occurrence of AA esterified at the *sn*-2 position of precursor DAGs. Hence DHA mediated reductions in 2-AG levels were accompanied with a reduction in the occurrence of *sn*-2 AA rich DAGs. It was thus proposed that DHA may reduce

2-AG synthesis by reducing the availability of the essential phospholipid precursors required for its production. This could be extrapolated to the current study, thus giving potential explanation for the reported reduction however in order to clarify such a proposal, further studies would be required.

4.5.4 Conclusion

In summary, the current study set out to investigate a potential association between the activity of the ES and the action of ω -3 PUFAs in the activated THP-1 macrophage. Activation of the endocannabinoid system was demonstrated to modulate FA homeostasis and pro-inflammatory cytokine production. CB receptor agonism reduced intracellular FA uptake; an effect which was ligand specific, FA specific and mediated, in part, through activation of the CB₂ receptor. Furthermore, a direct association between ω -3 PUFAs and the ES was demonstrated with the observation that DHA significantly attenuated macrophage endocannabinoid synthesis. Taken together, this evidence indicates a clear interaction of the ES with the function of ω -3 PUFAs in the activated THP-1 macrophage. As there is evidence to suggest ω -3 PUFAs may promote atherosclerotic plaque stability through both structural and anti-inflammatory mechanisms, the present findings suggest a potentially detrimental effect of endocannabinoid ligands in terms of plaque destabilisation.

Chapter 5: The physiological impact of chronic EPA intervention in a murine model of atherosclerosis

5.1 Introduction

5.1.1 Ω -3 fatty acids: *in vitro* to *in vivo* investigations

The *in vitro* observation (Chapter 4) that ω -3 PUFAs modulate lipid homeostasis in activated macrophages, an effect shown to involve components of the endocannabinoid system, and, that endocannabinoid synthesis is under the direct regulation of ω -3 PUFAs carries potential implications in terms of atherosclerosis development and progression. However to examine the actions of ω -3 PUFAs in a setting resembling the hemodynamic, immunological and haemorrhological conditions of the human vascular wall, requires the use of an *in vivo* model. This chapter describes the effect of long-term dietary intervention with EPA on the biochemical, structural and functional changes observed in atherosclerosis development in a mouse model, using fenofibrate as a hypolipidemic control. As discussed in the previous chapter, the observed interactions between the ω -3 PUFAs and endocannabinoid signalling were demonstrated to be DHA specific. DHA is synthesised endogenously from its metabolic precursor EPA, albeit *via* a relatively inefficient, and therefore slow, process. However, given the extended length of the dietary intervention (in which time EPA could be converted to DHA) and the potential effects of EPA *in vivo* which could not have been detected *in vitro*, EPA was employed as the intervention PUFA.

5.1.2 ApoE^{-/-} mice: a tool for atherosclerosis study

As described in Chapter 1 (section 1.2.7), numerous animal models are currently available for the study of experimental atherosclerosis and the action and efficacy of potential therapeutic agents. Mice models constitute a popular species of choice due to their low cost, ready availability, ease of handling and maintenance and, most importantly, easily manipulated genome. Such genetically engineered models include the LDL receptor deficient (LDLR^{-/-}) mouse, ApoE*3-Leiden (E3L) transgenic mouse, and apolipoprotein-E deficient (ApoE^{-/-}) mouse, which has been described in Chapter 1 (section 1.2.7).

ApoE^{-/-} mice are deficient in ApoE, a glycoprotein constituent of lipoproteins that binds to cell surface lipoprotein receptors (Mahley, 1988). Homozygous deletion of the ApoE gene prevents the hepatocyte mediated clearance of lipoprotein particles from the circulation and thus promotes development of a hyperlipidaemic profile. Moreover, atherosclerotic lesions develop spontaneously in ApoE^{-/-} mice, even when maintained on low fat chow (Plump *et al.*, 1992). In comparison to LDLR^{-/-} and E3L mice, the degree of hyperlipidaemia and lesion development in ApoE^{-/-} mice is considered

particularly severe. However the sequential events underpinning lesion formation and progression in ApoE^{-/-} mice, where initial aortic fatty streaks develop over time into complex lesions situated throughout the vasculature, is remarkably similar to that of humans (Zhang *et al.*, 1994; Nakashima *et al.*, 1994; Reddick *et al.*, 1994). Furthermore, analysis of the composition of advanced lesions from older ApoE^{-/-} mice has demonstrated a striking resemblance to the composition of vulnerable human lesions. Advanced lesions from ApoE^{-/-} mice were found to contain a necrotic core surrounded by smooth muscles cells, extracellular matrix proteins and evidence of lesion haemorrhage (Rosenfeld *et al.*, 2000).

Despite a number of limitations of the ApoE^{-/-} model (disease severity, differences in lipid particle physiology, potential influence on immune system through ApoE absence), ApoE^{-/-} mice constitute one of the most widely used animal models for atherosclerosis investigation. The current study required a model of progressive atherosclerosis in order to assess the effect of ω -3 PUFAs on the development process itself. As a result, the severity of the model was not of particular hindrance to this individual study as progression to the advanced lesion stage was desired. Furthermore, in light of similarities in disease development between ApoE^{-/-} mice and humans, the ApoE^{-/-} model was deemed a suitable model for use in this particular study.

5.1.3 Aims

As a continuation of the previously reported link between ω -3 PUFAs and the endocannabinoid system *in vitro* (see Chapter 4, section 4.4), the principle aim of this study was to further characterise such an interaction in the whole animal. ApoE^{-/-} mice maintained on an atherogenic diet were thus employed to determine the effect of long-term EPA supplementation on the following parameters 1) endothelial integrity, measured through blood pressure responses to vasodilators bradykinin and sodium nitroprusside; 2) blood plasma profiles of total cholesterol, LDL, HDL and triglycerides; 3) liver physiology; 4) tissue production of endocannabinoids AEA and 2-AG; 5) cardiac and vascular remodelling, measured as changes in collagen and collagen cross-linking, using fenofibrate as a control lipid lowering intervention.

5.2 Methods

5.2.1 Study Design

A total of sixty 5 week old male ApoE^{-/-} (B6.129P2-ApoE^{tm1Unc}/Cr1*) mice (Charles River Laboratories, UK) were purchased and maintained at the Medical Research Facility of the University of Aberdeen. Animals were housed for 180 days in conditions outlined in Chapter 2 (Section 2.2.1) during which the mice were randomly assigned to one of three study groups and given free access to a pre-prepared specialised diet. An allowance of 5 grams (wastage included) was allocated per mouse per day. Following completion of the 180-day intervention, animals were used for endpoint studies. To obtain control data from wild type mice fed a normal diet, 15 age-matched (6 months) male JAX® C57BL/6J (C57) mice fed regular chow (CRM irradiated pellets, Special Diets Service, UK) from weaning were purchased (Charles River Laboratories, UK) and the same endpoint studies undertaken.

5.2.2 Intervention diets

As outlined in Chapter 2, each diet was composed of a purified powdered base (Diet W) containing 0.25% cholesterol w/w, 16% crude fat w/w (of which 15% cocoa butter) and agar ash which was supplemented with the following additives (see Table 5.1):

Cohort 1: Control high fat diet (Diet W base) supplemented with 3% high oleic sunflower (HOSF) oil (Lipid Nutrition, Netherlands).

Cohort 2: Diet W supplemented with 3% eicosapentaenoic oil (EPA; 70% concentrate [additional ~10% DHA], Croda Chemicals, UK).

Cohort 3: Diet W supplemented with 3% high HOSF oil and 0.04% fenofibrate (Sigma, UK).

The percentage of energy provided by both HOSF and EPA oil was 4.2%. The level of anti-oxidants (alpha-tocopherol) present in the EPA oil was matched to that of the control HOSF oil. The specialised diets were prepared as previously described (Chapter 2, Section 2.2.2).

5.2.3 Endpoint Studies

5.2.3.1 Vascular function studies

Prior to commencement of the *in vivo* protocol, mice were fasted for a period of 2 hours. Induction and maintenance of anaesthesia and cannulation of the right carotid artery and left jugular vein (for blood pressure measurement and drug administration respectively) were performed using the surgical procedure detailed in Chapter 2, Section 2.2.3. Following completion of surgery, mice underwent a 15-minute stabilisation period.

Following measurement of baseline heart rate and arterial blood pressure, the endothelium dependent vasodilator bradykinin (BK) and the directly acting vasodilator sodium nitroprusside (SNP) were used to elicit changes in blood pressure (see Figure 5.1 for drug protocol). Bolus injections of $3\mu\text{g kg}^{-1}$, $30\mu\text{g kg}^{-1}$ and $300\mu\text{g kg}^{-1}$ drug (prepared in heparinised saline, see Chapter 2, Table 10) were administered intravenously (i.v.) with an injection volume of $10\mu\text{l}$ per 10g weight and a flush volume of $150\mu\text{l}$ heparinised saline. Between individual drug doses, mice underwent a 5-minute stabilisation period to allow blood pressure to return to baseline. For all experiments, drugs were administered in the order of BK followed by SNP due to the sustained hypotensive effect observed following administration of the higher SNP doses. Since the bulk of previous data pertaining to endothelial function in ApoE^{-/-} mice has been generated from *ex-vivo* studies, the dose range chosen for the protocol was extrapolated from concentrations used previously in murine *in vitro* studies (10^{-12}M – 10^{-4}M ; Viridis *et al.*, 2003; Liuba *et al.*, 2007; Xu *et al.*, 2007). Upon completion of the protocol, mice were euthanized via anaesthetic overdose and tissues were harvested (see Chapter 2, Section 2.2.4).

5.2.3.2 Lipid profiling

Blood samples were collected from the arterial cannula prior to termination of the *in vivo* protocol. Plasma levels of total cholesterol, low density lipoprotein (LDL), high density lipoprotein (HDL) and triglycerides were determined as detailed previously (Chapter 2, Section 2.2.5).

The crude lipid and triglyceride content of liver tissue was determined using the Folch method of fat extraction as described in Chapter 2 (Section 2.2.6). The fatty acid profiles of the liver samples were compiled using fatty acid methyl ester (FAME) analysis as previously described (Chapter 2, Section 2.2.7). The expression of adipose differentiation-related protein (ADFP) in liver tissue was visualised and quantified using Western Blotting. As detailed in Chapter 2, liver proteins were extracted

(described in Section 2.2.10.1) and electrophoresis and immunoblotting employed to separate and identify proteins (Section 2.2.10.2).

5.2.3.3 Endocannabinoid quantification

Brain, heart and thoracic aorta tissue was subjected to endocannabinoid quantification. The endocannabinoids, 2-arachidonoylglycerol (2-AG) and anandamide (AEA), were extracted from the tissues and quantified using LC-MS/MS methods detailed in Chapter 2 (Section 2.2.8). The assays were performed by Mr G Cameron, University of Aberdeen.

5.2.3.4 Collagen and collagen cross-link quantification

The remaining cardiac and thoracic aorta tissue was subjected to quantification of collagen and collagen cross-link content using HPLC and LC-MS/MS. The full protocol is described in Chapter 2 (Section 2.2.9). The assays were performed by Dr Simon Robins (The Rowett Institute of Health and Nutrition, Aberdeen University) and raw data provided for subsequent analysis and interpretation.

Experimental group	Total number of animals	Diet Details
ApoE ^{-/-} mice: high fat control	18*	Diet W + 3% HOSF oil
ApoE ^{-/-} mice: EPA	20	Diet W + 3% EPA oil
ApoE ^{-/-} mice: fibrate	20	Diet W + 3% HOSF oil + 0.04% fenofibrate
C57 mice: control	15	Regular chow

Table 5.1 Experimental group details: Details of experimental groups, total numbers and intervention diets. *Although 20 mice were originally planned for this group, 2 mice developed hydroencephalitis during transit from the supplier to the holding facility and therefore were humanely killed. Thus, the total number of animals successfully starting and completing this intervention was 18.

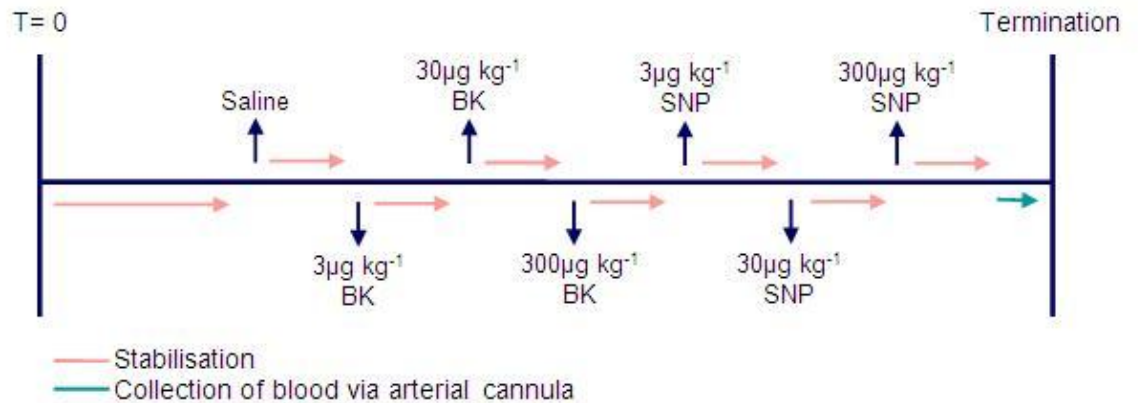


Figure 5.1 *In vivo* drug protocol: Following surgery (T=0), haemodynamic parameters were allowed to stabilise. BK and SNP (3-300µg kg⁻¹) were administered as bolus, I.V. injections. Between drug doses, haemodynamic parameters were allowed to return to pre-injection levels, (roughly 5 minutes stabilisation) prior to injection of subsequent doses.

5.3 Results

5.3.1 Baseline measurements

Body weight, heart weight, brain weight and resting blood pressure of mice from all study groups are presented in Table 5.2. With respect to mean body weight, no significant variations were observed between C57, control ApoE^{-/-} or EPA supplemented ApoE^{-/-} mice. In contrast, the mean body weight of fibrate supplemented ApoE^{-/-} mice (29.0±0.4 g) was slightly, but significantly, reduced compared to both C57 (30.8±0.5 g; P<0.01) and control ApoE^{-/-} mice (31.0±0.4 g; P<0.01).

Mean heart weights ranged between 187-215mg, however there were no significant differences between any study groups. Similarly, there was no statistically significant variation in mean brain weight or heart/body weight ratios between any study groups.

5.3.2 Hepatic lipid profiles

The content of total lipid present in liver samples is illustrated in Figure 5.2, where lipid content is expressed as a percentage of the original tissue weight. High fat feeding of ApoE^{-/-} mice (15.0±0.9%; P<0.001), significantly elevated the total lipid content of the liver compared to C57 mice (3.5±4.2%). Compared to control ApoE^{-/-} mice, both EPA (11.1±0.8%; P<0.001) and fibrate (9.5±1.4 %; P<0.01) supplementation significantly (P<0.05) attenuated the increased lipid content induced by high fat feeding by a similar magnitude, although these were still elevated compared to C57 mice fed standard laboratory chow.

The triglyceride content of liver samples is shown in Figure 5.3. High fat feeding of ApoE^{-/-} mice did not significantly vary the triglyceride content of the liver (6.9±0.6 mg/g tissue) from that of chow fed C57 mice (4.5±1.7 mg/g tissue). Similarly EPA supplemented ApoE^{-/-} mice demonstrated no variation (4.4±0.5 mg/g tissue). Conversely, fibrate supplemented ApoE^{-/-} mice exhibited significantly elevated triglycerides (12.1±1.2 mg/g tissue; P<0.01) compared to both C57 mice and control ApoE^{-/-} mice. Figure 5.4 depicts the expression of adipophilin protein in liver samples. Protein expression was quantified through conducting area under the curve analysis (presented in arbitrary units). Compared to high fat fed ApoE^{-/-} mice (2.4±0.6), fibrate, but not EPA, supplementation significantly elevated adipophilin expression (4.8±0.6).

Group	Body Weight (g)	Heart Weight (mg)	Brain Weight (g)	Heart/Body Weight Ratio (mg/g)
C57	30.8±0.5	215±12	0.39±0.01	7.0±0.4
ApoE ^{-/-} : High Fat	31.0±0.4	194±3	0.40±0.02	6.4±0.2
ApoE ^{-/-} : EPA	31.2±0.5	193±8	0.42±0.00	6.2±0.3
ApoE ^{-/-} : Fibrate	29.0±0.4* ^{##}	183±12	0.45±0.05	6.5±0.4

Table 5.2 Tissue weights in C57 and ApoE^{-/-} mice: Body weight was recorded at the end of the dietary intervention. Heart and brain weights were recorded following their removal. n=10-20. *P<0.05 vs C57 mice; ^{##}P<0.01 vs control ApoE^{-/-} mice (one-way ANOVA, Dunnett's Multiple Comparison post-hoc test). Values represent mean±SEM.

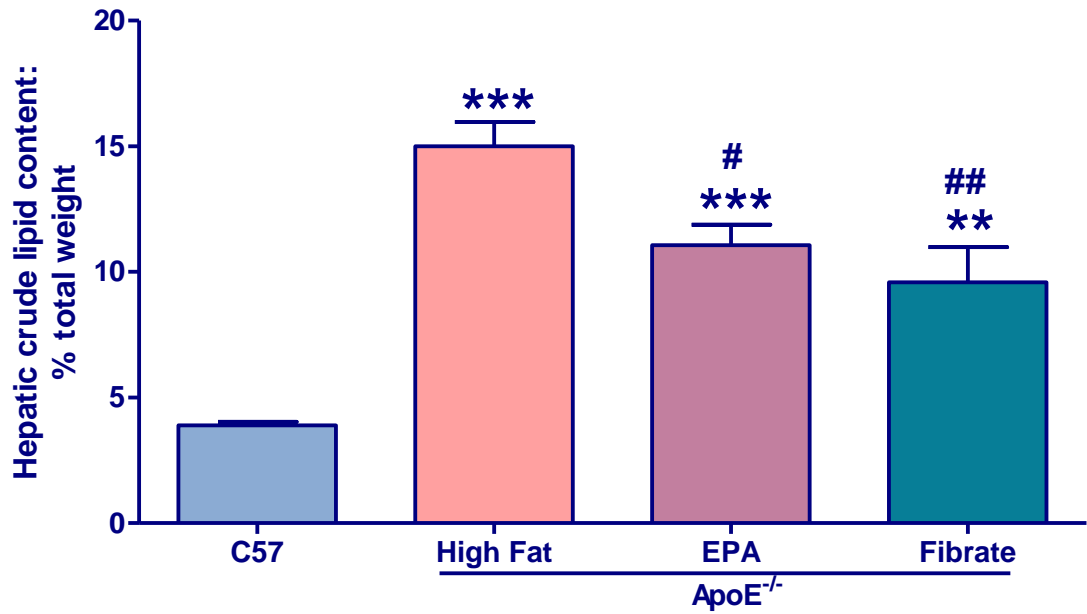


Figure 5.2 Hepatic lipid profiles - total lipid: The crude lipid content of liver samples collected from C57 and ApoE^{-/-} mice post dietary intervention were determined using the Folch method. Data is expressed as a percentage of the original sample weight. n=5-10 per group. **P<0.01, ***P<0.001 vs C57 mice; #P<0.05, ##P<0.01 vs control ApoE^{-/-} mice (one-way ANOVA, Dunnett's multiple comparison post-hoc test). Values represent mean±SEM..

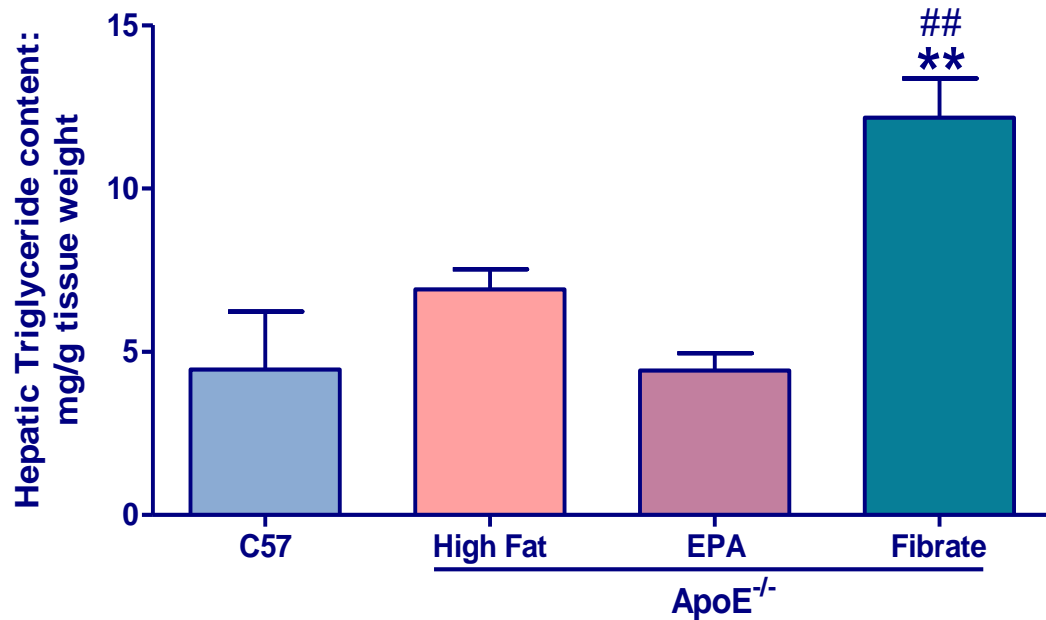


Figure 5.3 Hepatic lipid profiles - triglycerides: The triglyceride content of liver samples from C57 and ApoE^{-/-} mice was measured. Using the Folch method crude lipid was extracted from the liver samples, from which triglycerides were measured using a KoneLab 30 analyser. n=5-10 per group. **P<0.01 vs C57 mice; ##P<0.01 vs control ApoE^{-/-} mice (one-way ANOVA, Dunnett's multiple comparison post-hoc test). Values represent mean±SEM.

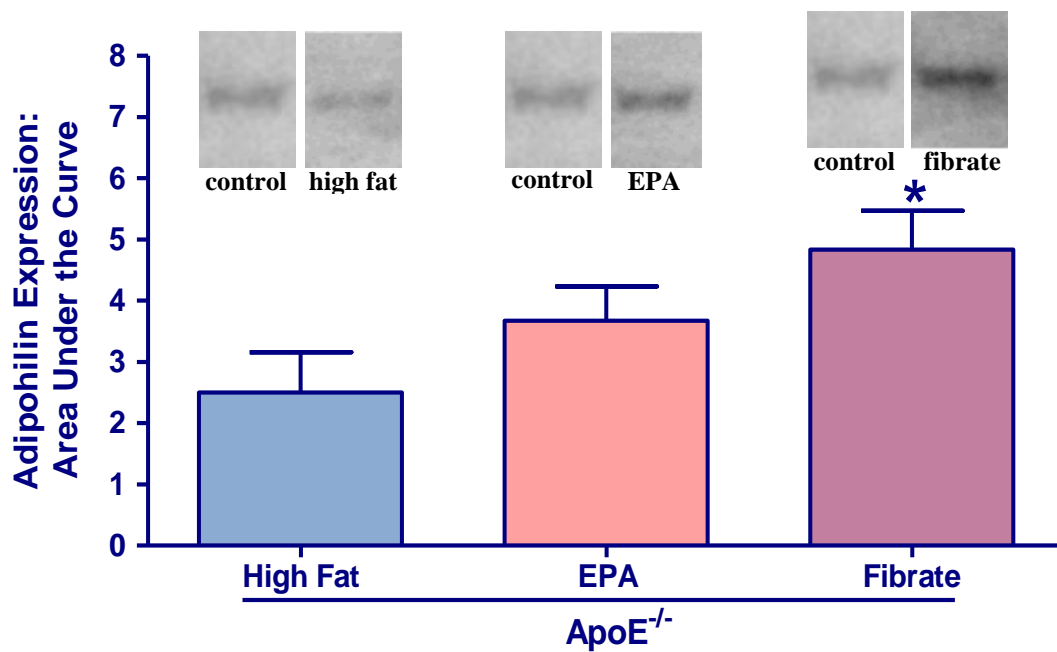


Figure 5.4 Hepatic lipid profiles - adipophilin expression: The expression of adipophilin protein in liver samples from ApoE^{-/-} mice was measured using Western Blotting. Bands corresponding to adipophilin expression were positively identified through comparison with bands from control tissue (heat shock protein 70; HSP). Band size and intensity was measured using Aida 3.52 software which converted the image to a histogram format. Area under the curve analysis enabled quantitative measurement of protein expression. n=5-10 per group. *P<0.05 vs control ApoE^{-/-} mice (one-way ANOVA, Dunnett's multiple comparison post-hoc test). Values represent mean±SEM.

Figure 5.5 illustrates the fatty acid profiles of liver samples from each study group. Fatty acids have been grouped into saturated, monounsaturated and polyunsaturated fatty acids (SFAs, MUFAs and PUFAs respectively). The profiles of C57 mice, which were fed a regular chow diet, demonstrated equal quantities of SFAs (39%) and PUFAs (44%), while MUFAs comprised only 17% of the profile. Of PUFAs, ω -6 (34%) predominate over ω -3 FAs (10%). Both control and fibrate supplemented ApoE^{-/-} mice, which were fed a ‘Western’ style base diet, had highly similar profiles composed mainly of MUFAs (53-54%), with 31-32% SFAs and only 15% PUFAs. Similar to C57 profiles, PUFAs were composed primarily of ω -6 FAs (11% vs 4% ω -3 FAs). In contrast, while EPA supplemented ApoE^{-/-} mice also had profiles dominated by SFAs (51%), they contained similar quantities of MUFAs (28%) and PUFAs (21%). Moreover, PUFAs were almost equally composed of ω -6 and ω -3 FAs (10% and 11% respectively).

The contribution of EPA and DHA to fatty acid profiles was determined and is illustrated in Figure 5.6. The DHA content of all ApoE^{-/-} groups was significantly higher than EPA compared to respective measurements in C57 mice. High fat feeding alone ($1.1\pm 0.1\%$), and in combination with fibrate supplementation ($1.4\pm 0.2\%$) exhibited significantly reduced hepatic DHA content of ApoE^{-/-} mice compared to C57 mice ($6.2\pm 0.3\%$; $P<0.01$). EPA supplemented ApoE^{-/-} mice, however, exhibited a significantly increased hepatic DHA content ($10.1\pm 0.3\%$; $P<0.05$) compared to both C57 and control ApoE^{-/-} mice. Hepatic EPA levels were significantly elevated in EPA supplemented ApoE^{-/-} mice compared to C57 mice. EPA levels in high fat fed and fibrate supplemented ApoE^{-/-} mice were below the minimum detection limits of the assay.

5.3.3 Blood plasma lipid profiles

The total cholesterol content of plasma from C57 and ApoE^{-/-} mice is illustrated in Figure 5.7. Compared to chow fed C57 mice, high fat feeding of ApoE^{-/-} mice significantly elevated cholesterol levels (0.89 ± 0.1 mmol/L vs 14.00 ± 2.6 mmol/L respectively; $P<0.01$). Both EPA and fibrate significantly attenuated the elevated cholesterol levels induced by high fat feeding to a similar degree (8.39 ± 1.7 mmol/L and 8.44 ± 0.99 mmol/L respectively vs 14.00 ± 2.6 mmol/L; $P<0.05$). A similar pattern was observed with low density lipoprotein (LDL) cholesterol levels (see Figure 5.8), where high fat feeding of ApoE^{-/-} mice significantly elevated LDL cholesterol levels (10.3 ± 1.8 mmol/L vs 0.12 ± 0.01 in C57 mice; $P<0.001$), while supplementation with EPA (4.4 ± 2.9 mmol/L) or fibrate (5.9 ± 4.2 mmol/L), significantly attenuated raised LDL cholesterol levels ($p<0.05$).

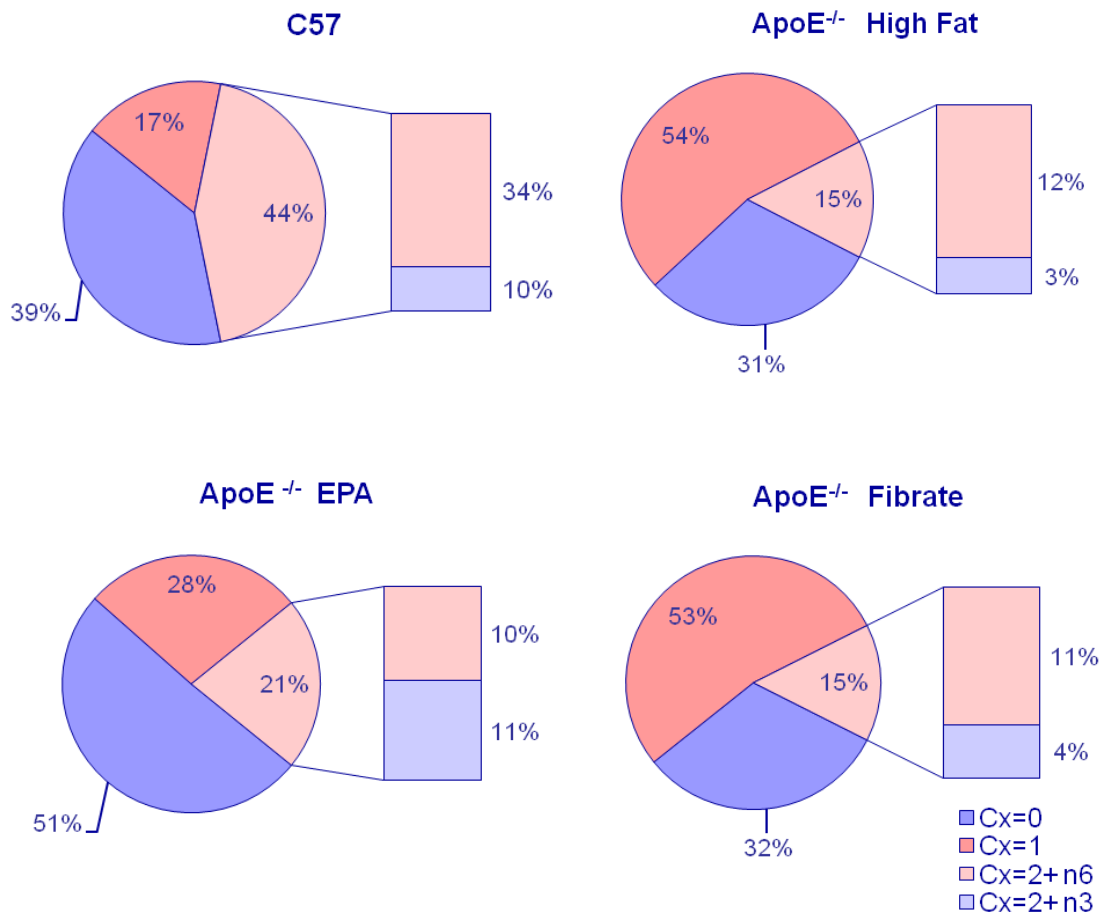


Figure 5.5 Hepatic lipid profiles - fatty acid profiling: Fatty acid methyl esters (FAME's) were prepared from crude lipid extracts and profiles compiled through conducting GC analysis. The quantity of each FAME identified was determined from the area of its corresponding peak. FAME's were then expressed as a percentage of the entire sample profile. Individual FAME's have been grouped into cohorts of saturated (Cx=0), monounsaturated (Cx=1) and polyunsaturated (Cx=2⁺ n6 and Cx=2⁺ n3) fatty acids. n=5-10 per group.

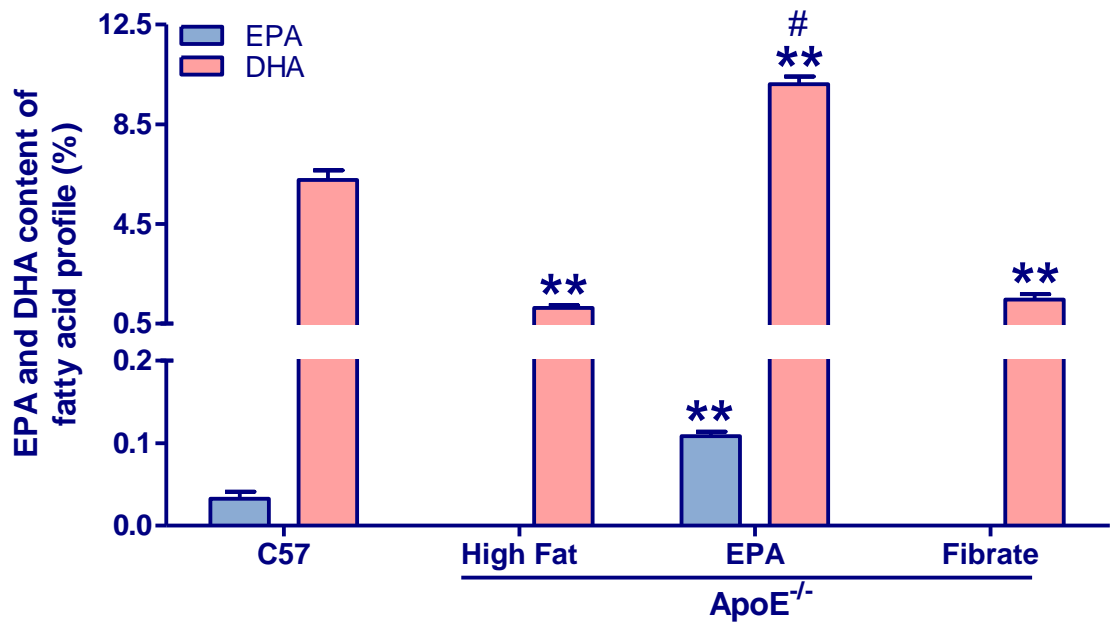


Figure 5.6 Hepatic lipid profiles – EPA and DHA content of hepatic fatty acid profiles: From the hepatic fatty acid profiles compiled previously, the EPA and DHA constituent of each profile was assessed. Data is expressed as a percentage of the complete fatty acid profile. n=5-10 per group. **P<0.01 vs C57 mice; #P<0.01 vs control ApoE^{-/-} mice (one-way ANOVA, Dunnett’s multiple comparison post-hoc test). Values represent mean±SEM.

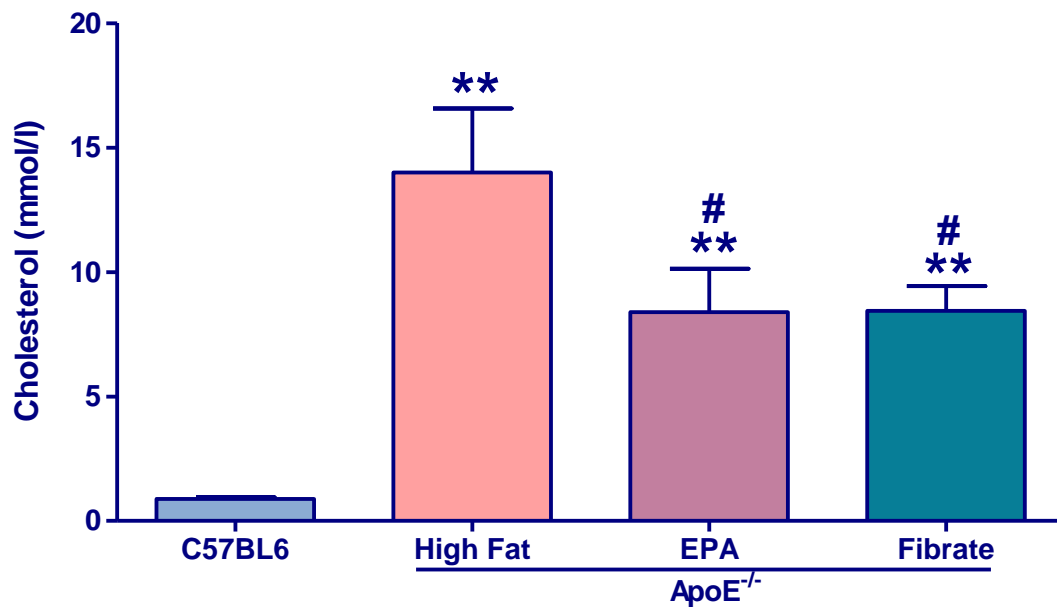


Figure 5.7 Plasma lipid profiles - total cholesterol: The cholesterol content of blood plasma collected from C57 and ApoE^{-/-} mice was measured. Blood samples were collected via arterial cannula and the plasma fraction isolated and snap frozen for subsequent analysis using a KoneLab 30 analyser. Samples were analysed in duplicate. n=7-10 per group. **P<0.01, ***P<0.001 vs C57 mice; #P<0.05 vs control ApoE^{-/-} mice (one-way ANOVA, Dunnett's multiple comparison post-hoc test). Values represent mean±SEM.

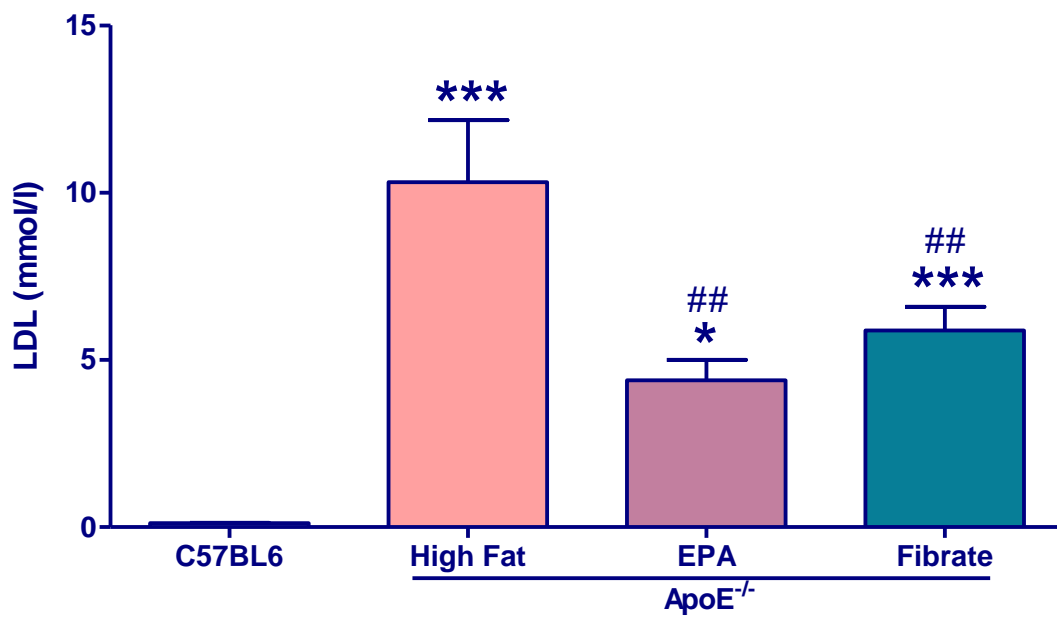


Figure 5.8 Plasma lipid profiles – LDL cholesterol: The low LDL cholesterol content of blood plasma collected from C57 and ApoE^{-/-} mice was measured and analysed as described previously. n=7-10 per group. *P<0.05, ***P<0.001 vs C57 mice; ##P<0.01 vs control ApoE^{-/-} mice (one-way ANOVA, Dunnett's multiple comparison post-hoc test). Values represent mean±SEM.

The high density lipoprotein (HDL) cholesterol content of plasma samples is illustrated in Figure 5.9. Compared to C57 mice fed standard laboratory chow, high fat feeding significantly elevated plasma HDL cholesterol in ApoE^{-/-} mice (P<0.01), which was unaffected by supplementation with either EPA or fibrate. The ratio of total cholesterol to HDL cholesterol was calculated and illustrated in Figure 5.10. High fat feeding of ApoE^{-/-} mice significantly increased the ratio of total cholesterol to HDL cholesterol compared to C57 mice fed standard laboratory chow. Although EPA supplementation tended to reduce the cholesterol to HDL cholesterol ratio, this was not statistically significant. In contrast, fibrate supplementation significantly lowered the ratio compared to control ApoE^{-/-} mice, to a value within the range of wild-type mice. Figure 5.11 depicts the triglyceride content of the plasma samples. Although high fat feeding alone had no significant effect on plasma triglycerides, these were significantly increased in EPA supplemented ApoE^{-/-} mice compared to both C57 and high fat fed ApoE^{-/-} mice (p<0.001).

5.3.4 Collagen and cross-link measurement

5.3.4.1 Cardiac Tissue

The total collagen content of cardiac tissue from all study groups is illustrated in Figure 5.12. Collagen content varied between 1.5-1.6% of the original dry tissue weights. There were no statistically significant variations between any of the experimental groups. Figures 5.13 and 5.14 demonstrate the formation of various cross-links in cardiac tissue. High fat feeding of ApoE^{-/-} mice significantly increased the formation of the intermediate cross-links DHLNL and HLNL (P<0.05; see Figure 5.13) and the mature cross-links PYD and DPD (P<0.01; Figure 5.14) compared to C57 mice. No significant effect of high fat diet was observed on the formation of the mature cross-link HHL, although there was a tendency for this to be increased in all ApoE^{-/-} mice. Moreover, the total content of elastin cross-links DES and IDE (P<0.01; see Figure 5.14) was significantly reduced in the control ApoE^{-/-} group. No statistically significant effects were observed on any cross-links in ApoE^{-/-} mice given EPA or fibrate supplementation, compared to control ApoE^{-/-} mice.

The ratio of mature to immature cross-linking was calculated and is presented in Figure 5.15. This ratio serves as an indicator of the rate of cross-link turnover from immature to mature conformations. C57 mice exhibited the highest ratio (2.0±0.5). Lower ratios were observed in all three ApoE^{-/-} groups, however this only reached statistical significance in the EPA supplemented mice (1.0±0.7).

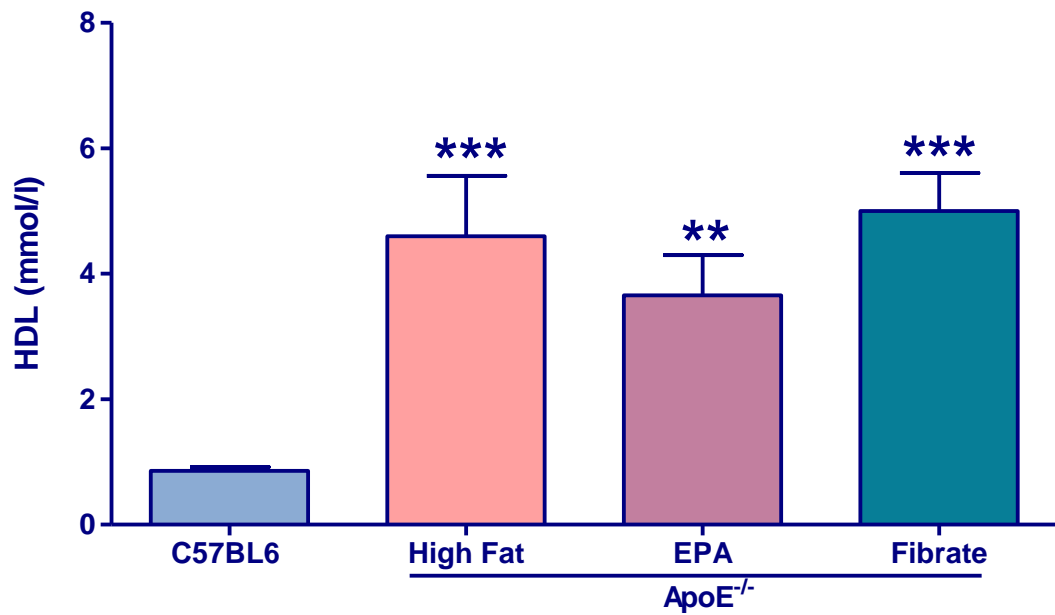


Figure 5.9 Plasma lipid profiles – HDL cholesterol: The blood plasma concentration of HDL cholesterol was measured and analysed as described previously. n=7-10 per group. **P<0.01, ***P<0.001 vs C57 mice (one-way ANOVA, Dunnett’s multiple comparison post-hoc test). Values represent mean±SEM.

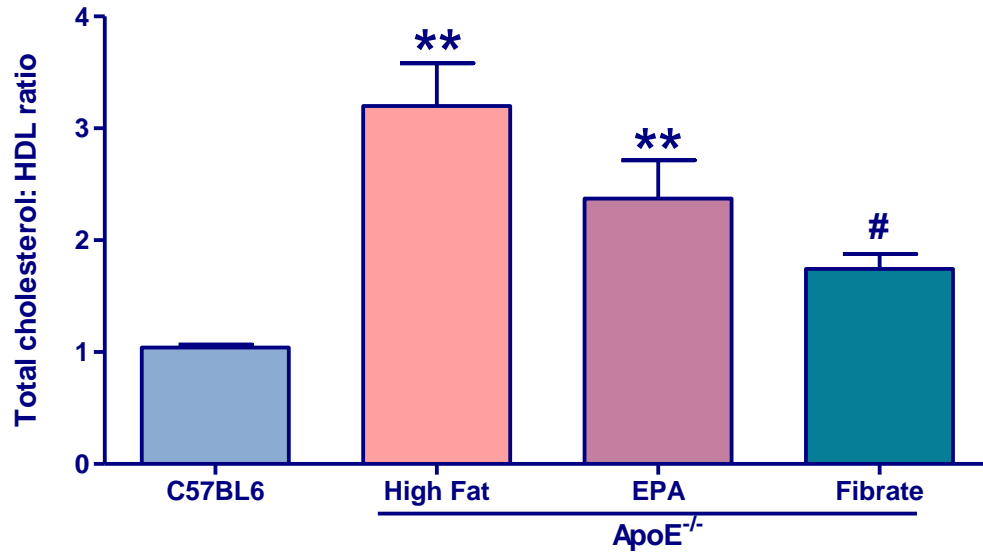


Figure 5.10 Plasma lipid profiles - total cholesterol/HDL cholesterol ratio: The ratio of total cholesterol to HDL cholesterol in the plasma of C57 and ApoE^{-/-} mice was calculated (calculated as total cholesterol value divided by HDL cholesterol value). n=7-10 per group. **P<0.01 vs C57 mice; #P<0.05 vs control ApoE^{-/-} mice (one-way ANOVA, Dunnett's multiple comparison post-hoc test). Values represent mean±SEM.

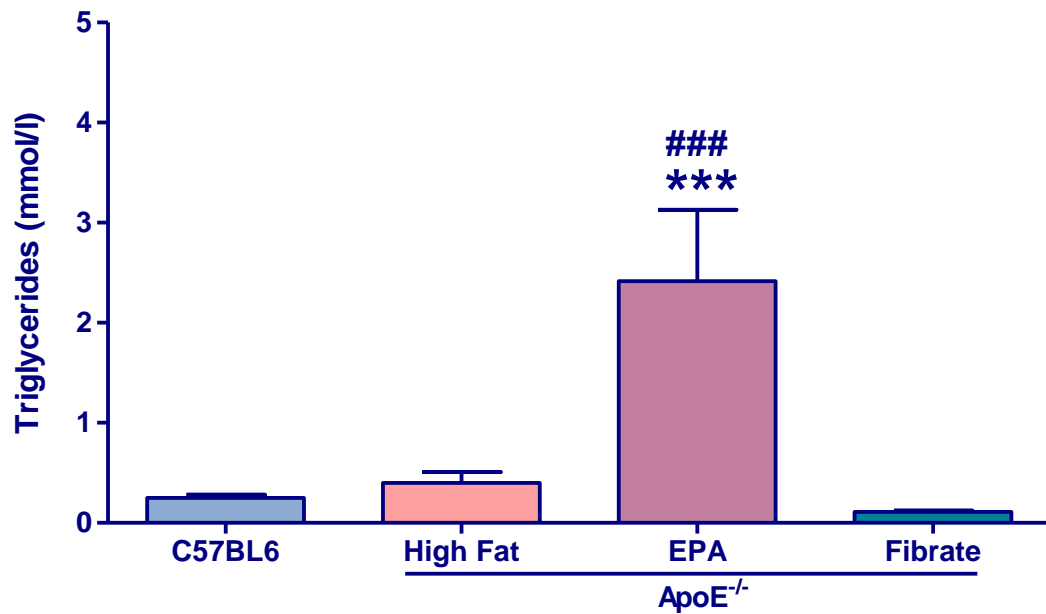


Figure 5.11 Plasma lipid profiles - triglycerides: The concentration of triglycerides present in the blood plasma of C57 and ApoE^{-/-} mice was measured as described previously. n=7-10 per group. ***P<0.001 vs C57 mice; ###P<0.001 vs control ApoE^{-/-} mice (one-way ANOVA, Dunnett's multiple comparison post-hoc test). Values represent mean±SEM.

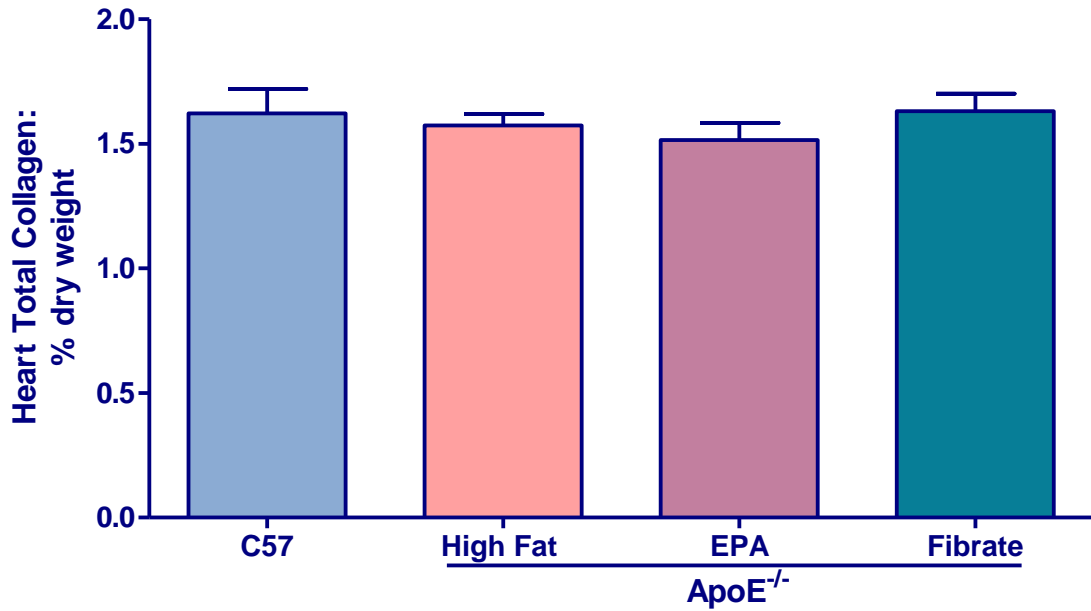


Figure 5.12 The total collagen content of C57 and ApoE^{-/-} mouse heart tissue: The collagen content of cardiac tissue from C57 and ApoE^{-/-} mice was measured. Post intervention, hearts were removed, the atria discarded and the ventricles snap frozen for analysis. Collagen content was determined from the total hydroxyproline content of the sample which was measured using LC-MS/MS. Data is expressed as a percentage of the original dry weight of sample – to which it is normalised. n=5-7 per group. Values represent mean±SEM.

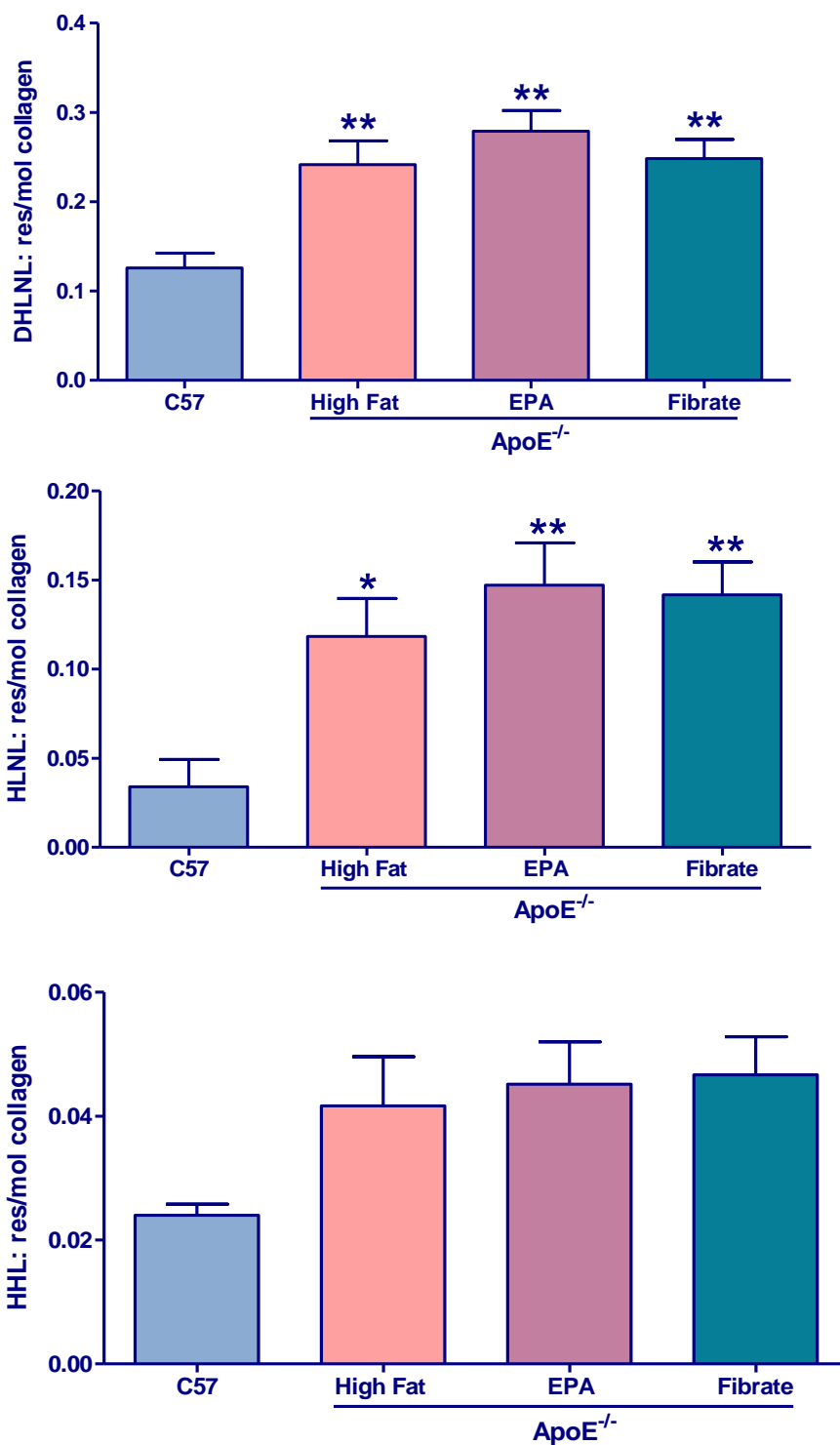


Figure 5.13 The DHLNL, HLNL and HHL content of C57 and ApoE^{-/-} mouse heart tissue: The presence and concentration of DHLNL, HLNL and HHL cross links in the heart samples collected and analysed as described previously were measured. n=5-7 per group. *P<0.05; **P<0.01 vs C57 mice (one-way ANOVA, Dunnett's multiple comparison post-hoc test). Values represent mean±SEM.

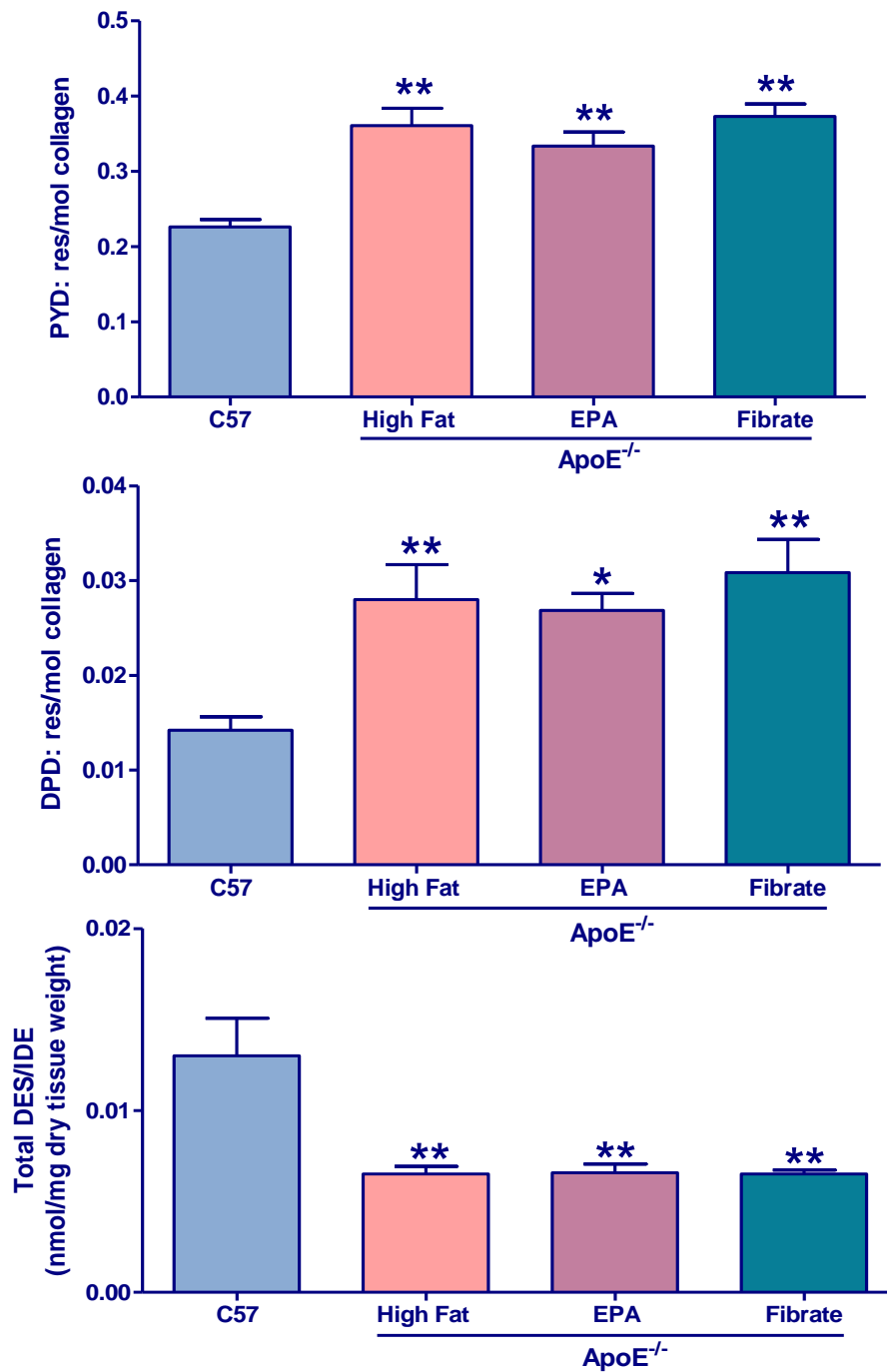


Figure 5.14 The PYD, DPD and total DES/IDE content of C57 and ApoE^{-/-} mouse heart tissue: The presence and concentration of PYD, DPD and the total DES/IDE cross links in heart samples collected and analysed as described previously were measured. n=5-7 per group. *P<0.05; **P<0.01 vs C57 mice (one-way ANOVA, Dunnett's multiple comparison post-hoc test). Values represent mean±SEM.

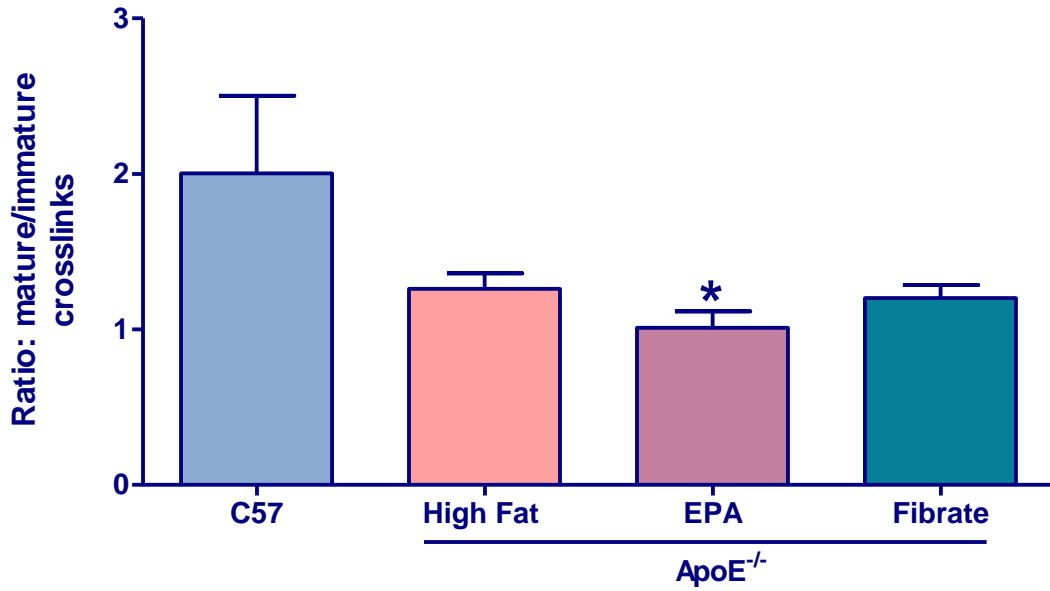


Figure 5.15 Mature:immature cross-link ratio in cardiac tissue: The ratio of mature to immature cross-links was calculated by dividing the total mature cross-link content (PYD, DPD and HHL) by the total immature cross-link content (DHLNL and HLNL). n=5-7 per group. *P<0.05 (one-way ANOVA, Dunnett's multiple comparison post-hoc test). Values represent mean±SEM.

5.3.4.2 Vascular Tissue

The total collagen content and collagen cross-link content of vascular tissue from ApoE^{-/-} mice is displayed in Table 5.3 and Table 5.4. No variations in total collagen content were observed between the ApoE^{-/-} mice interventions. Similarly, the cross-link content of vascular tissue did not vary significantly between ApoE^{-/-} mice intervention groups. Due to technical error, there was insufficient tissue retrieved from the C57 group to undertake collagen and cross-link analysis.

5.3.5 Tissue endocannabinoid levels

5.3.5.1 Thoracic aorta endocannabinoid levels

The concentration of 2-AG and AEA in vascular tissue is presented in Figure 5.16. High fat fed ApoE^{-/-} mice exhibited significantly elevated levels of both 2-AG (p<0.05) and AEA (P<0.01) compared to C57 mice fed standard laboratory chow. Compared to control ApoE^{-/-} mice, EPA supplementation significantly attenuated elevated 2-AG levels (3777±316 pmol/g; P<0.05) and reduced AEA levels, although this effect was not statistically significant. Conversely, fibrate supplementation significantly attenuated elevated AEA levels (6.8±1.5 pmol/g; P<0.05) but had no effect on 2-AG.

5.3.5.2 Brain endocannabinoid levels

The content of 2-AG and AEA present in brain tissue from C57 and ApoE^{-/-} mice is illustrated in Figure 5.17. High fat feeding of ApoE^{-/-} mice significantly elevated the concentration of 2-AG in brain tissue (34750±4521 pmol/g; P<0.05) compared to C57 mice (23074±1776 pmol/g) fed standard laboratory chow. Inclusion of EPA (36016±2843 pmol/g) or fibrate (43260±3424 pmol/g) in the diet had no effect on these elevated levels.

High fat feeding of ApoE^{-/-} mice also significantly elevated brain AEA levels (70.4±12.7 pmol/g; P<0.01) compared to C57 mice (35.0±3.2 pmol/g) fed standard laboratory chow. In contrast to 2-AG, EPA supplementation significantly attenuated (32.3±5.2 pmol/g; P<0.01) the enhanced AEA levels induced by high fat feeding. Fibrate supplementation also tended to reduce AEA levels compared to control ApoE^{-/-} mice, but this did not achieve statistical significance.

Group	Total Collagen: % Dry Weight
ApoE ^{-/-} High Fat	30.56±1.6
ApoE ^{-/-} EPA	32.33±1.8
ApoE ^{-/-} Fibrate	33.32±0.9

Table 5.3 Collagen content of ApoE^{-/-} mouse thoracic aorta tissue: Data is expressed as a percentage of the original sample dry weight. n=4-6 per group. Values represent mean±SEM.

Group	DHLNL (res/mol)	HLNL (res/mol)	HHL (res/mol)	PYD (res/mol)	DPD (res/mol)	Total DES/IDE (nmol/mg dry tissue)	Mature: immature cross-link ratio
ApoE ^{-/-} High Fat	0.33±0.02	0.26±0.03	0.04±0.03	0.30±0.02	0.02±0.0	1.02±0.1	0.61±0.04
ApoE ^{-/-} EPA	0.36±0.28	0.24±0.01	0.03±0.00	0.29±0.02	0.02±0.0	0.99±0.1	0.57±0.02
ApoE ^{-/-} Fibrate	0.24±0.18	0.22±0.03	0.04±0.03	0.26±0.01	0.02±0.0	0.98±0.1	0.73±0.07

Table 5.4 Collagen and elastin cross-link content of ApoE^{-/-} mouse tissue: Collagen and elastin cross-link concentrations were determined using LC-MS/MS as described previously. n=4-6 per group.

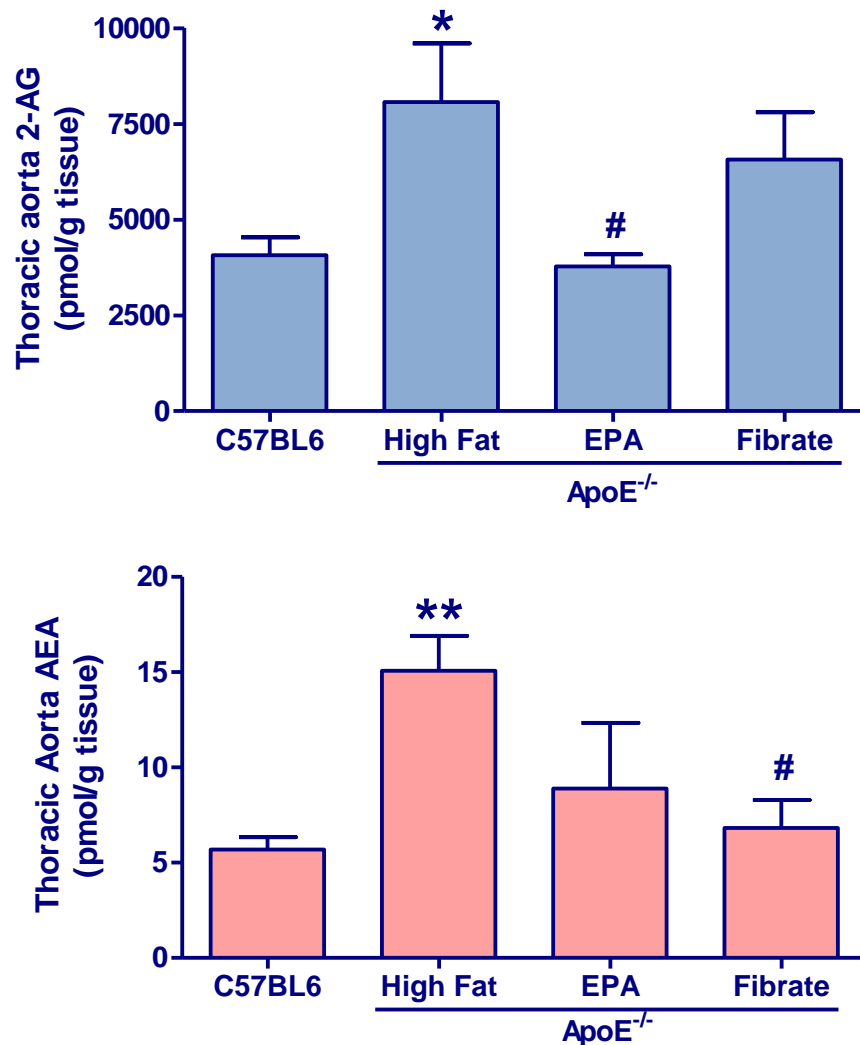


Figure 5.16 Endocannabinoid content of C57 and ApoE^{-/-} mouse vascular tissue: The 2-AG and AEA content of thoracic aorta tissue from C57 and ApoE^{-/-} mice was determined and analysed as described previously. n=9-10 per group. *P<0.05; **P<0.01 vs C57 mice; #P<0.05 vs control ApoE^{-/-} mice (one-way ANOVA, Dunnett's multiple comparison post-hoc test). Values represent mean±SEM.

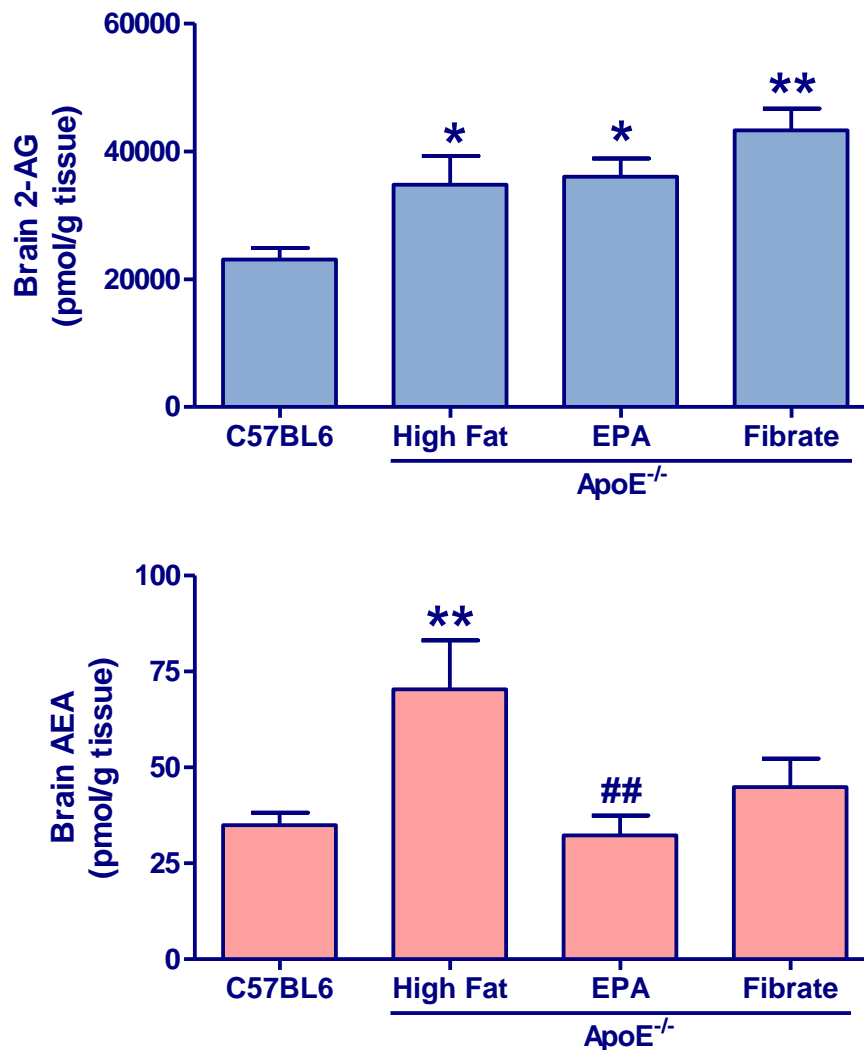


Figure 5.17 Endocannabinoid content of C57 and ApoE^{-/-} mouse brain tissue: The concentration of 2-AG and AEA present in brain tissue from C57 and ApoE^{-/-} mice was quantified. Brains were removed, rinsed in PBS and snap frozen. Tissue was analysed using LC-MS/MS. Data was normalised to the original tissue weight and expressed as pico mole per gram of tissue. n=9-10 per group. *P<0.05; **P<0.01 vs C57 mice; ##P<0.01 vs control ApoE^{-/-} mice (one-way ANOVA, Dunnett's multiple comparison post-hoc test). Values represent mean±SEM.

5.3.5.3 Heart endocannabinoid levels

Cardiac tissue from C57 mice fed standard laboratory chow contained 11163 ± 1168 pmol/g 2-AG (Figure 5.18). High fat feeding of ApoE^{-/-} mice, either alone or in combination with either EPA or fibrates, did not significantly affect 2-AG levels. In contrast, cardiac AEA was significantly elevated in high fat fed ApoE^{-/-} mice (22.1 ± 2.6 pmol/g; $P < 0.01$) compared to C57 mice (11.6 ± 2.1 pmol/g) fed standard laboratory chow. EPA supplemented ApoE^{-/-} mice exhibited cardiac AEA levels that were significantly lower (2.8 ± 0.8 pmol/g; $P < 0.01$) than in both C57 mice and control ApoE^{-/-} mice. Fibrate supplementation also significantly reduced AEA levels (14.5 ± 1.6 pmol/g; $P < 0.01$), but only in comparison with control ApoE^{-/-} mice.

5.3.6 Haemodynamic responses to bradykinin

Baseline haemodynamics in all groups is summarised in Table 5.5. Resting blood pressure and heart rate did not vary significantly between any of the experimental groups. Original traces showing examples of the saline response, depressor response to BK and depressor response to SNP are illustrated in Figures 5.19, 5.20 and 5.21 respectively. Figures 5.22 and 5.23 show the averaged time-dependent depressor responses to both saline (vehicle) and BK ($3 - 300 \mu\text{g kg}^{-1}$), where data is expressed as a percentage change in mean arterial blood pressure (MABP) from resting blood pressure (measured in millimetres of mercury; mmHg). Bradykinin was observed to induce a dose dependent reduction in MABP. Moreover, with increasing dose, the duration and magnitude of the response was augmented.

To account for the injection artefact, as observed with the response to saline, area under the curve (AUTC) analysis was conducted to quantify the blood pressure responses to BK in each study group (see Figure 5.24). In all study groups, BK induced a dose dependent increase in the AUTC. High fat feeding of ApoE^{-/-} mice significantly reduced the AUTC (4530 ± 945 AU; $P < 0.05$) response to $300 \mu\text{g kg}^{-1}$ BK compared to C57 mice (7903 ± 1202 AU). Fibrate supplementation restored this response (7470 ± 394 AU; $P < 0.05$), whereas EPA supplementation did not.

The effect of BK on heart rate is illustrated in Figure 5.25. Compared to saline, BK had no significant effect on heart rate at any dose, in any of the study groups.

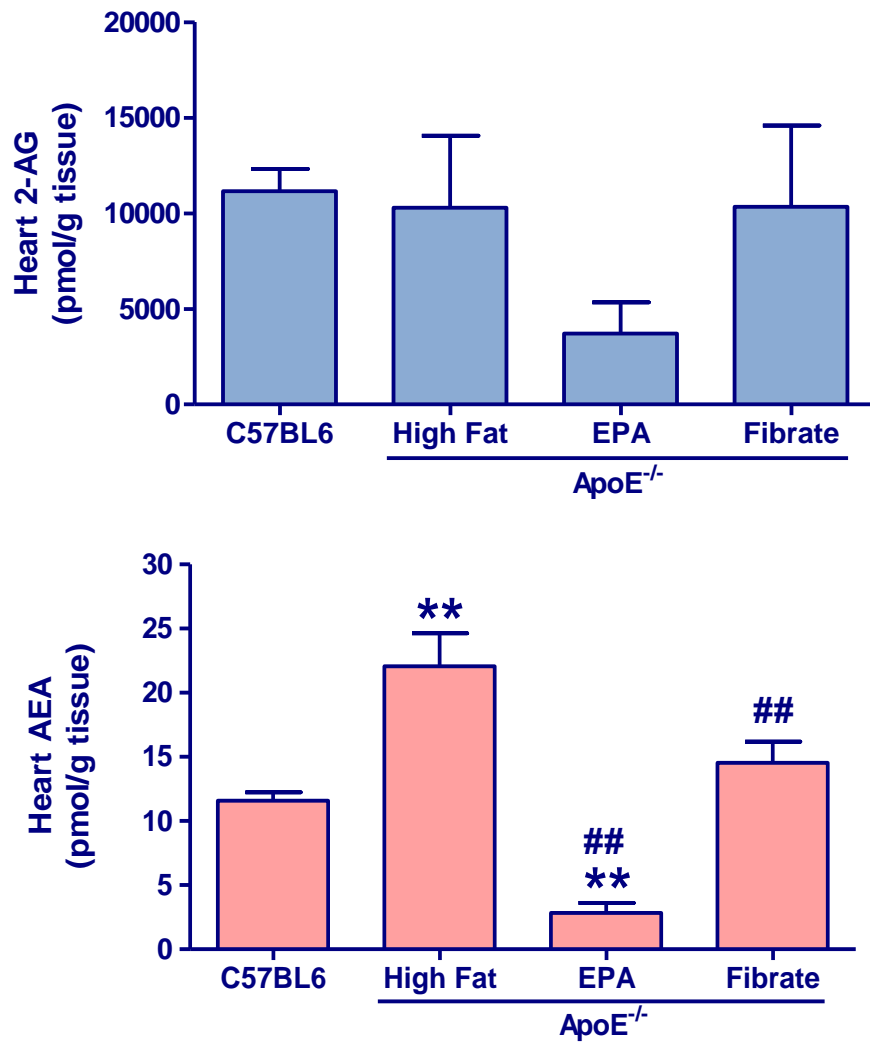


Figure 5.18 Endocannabinoid content of C57 and ApoE^{-/-} mouse cardiac tissue: 2-AG and AEA levels in cardiac tissue from C57 and ApoE^{-/-} mice were quantified and analysed as described previously. n=9-10 per group. **P<0.01 vs C57 mice; ##P<0.01 vs control ApoE^{-/-} mice (one-way ANOVA, Dunnett's multiple comparison post-hoc test). Values represent mean±SEM.

Group	Resting Blood Pressure (mmHg)	Resting Heart rate (BPM)
C57	90.7±4.7	360.2±18.28
ApoE ^{-/-} : High Fat	92.4±7.7	364.1±18.51
ApoE ^{-/-} : EPA	91.8±7.3	360.6±20.89
ApoE ^{-/-} : Fibrate	88.6±4.5	340.9±13.44

Table 5.5 Resting blood pressure and heart rate: Blood pressure (mmHg) and heart rate (BPM) was recorded at baseline (prior to drug administration). n=4-8 per group. Values represent mean±SEM.

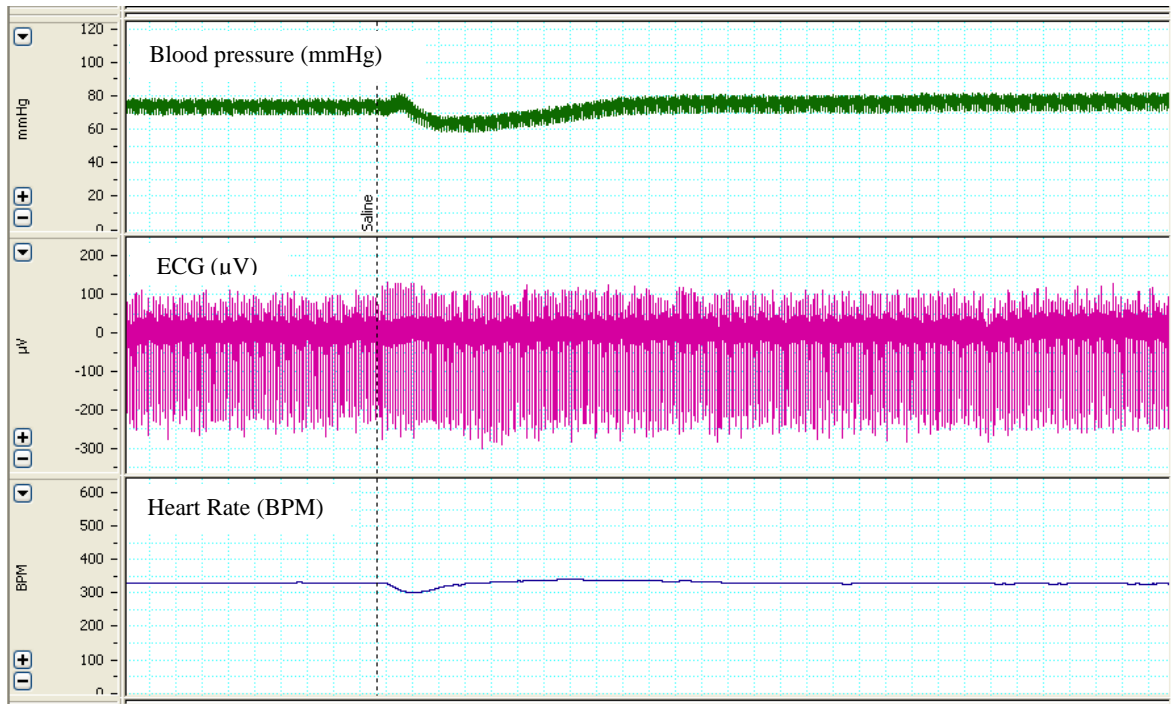


Figure 5.19 Original trace showing the haemodynamic response to heparinised saline: Heart rate (HR) was calculated by the software from the Lead I ECG (μV) recorded from subcutaneous limb leads. One hundred and fifty microlitres of saline (flush volume of drug) was administered I.V.

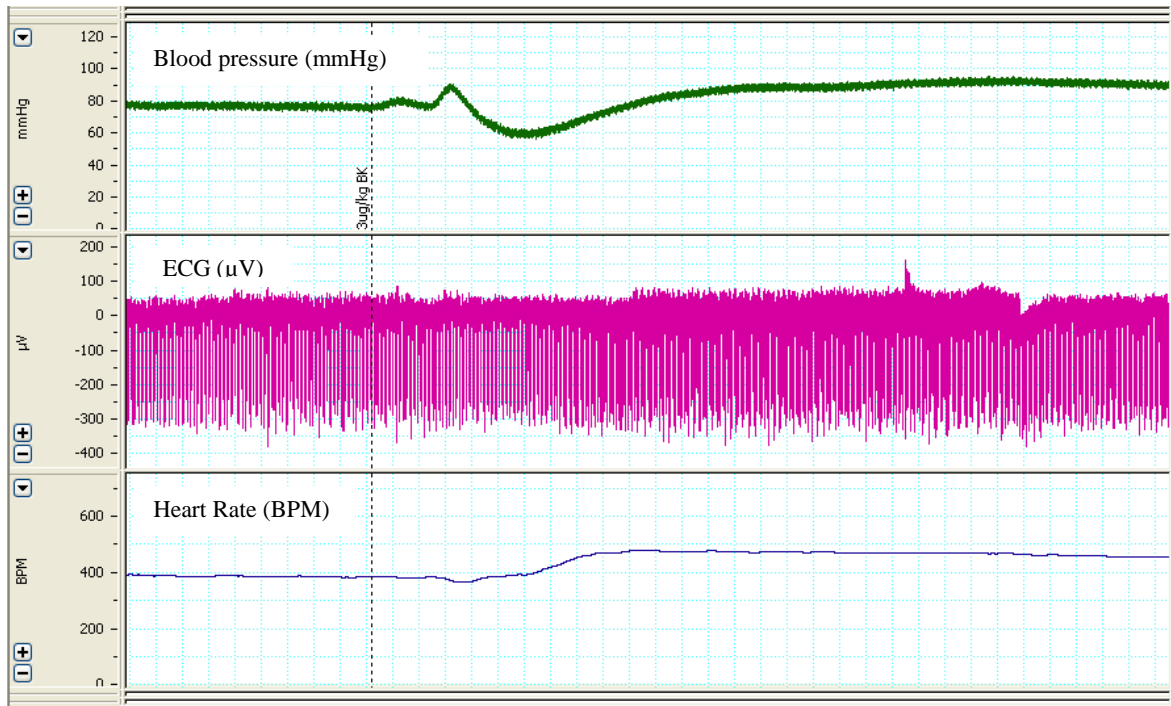


Figure 5.20 Original trace showing the depressor response to $3\mu\text{g kg}^{-1}$ bradykinin: Heart rate (HR) was calculated as described previously.

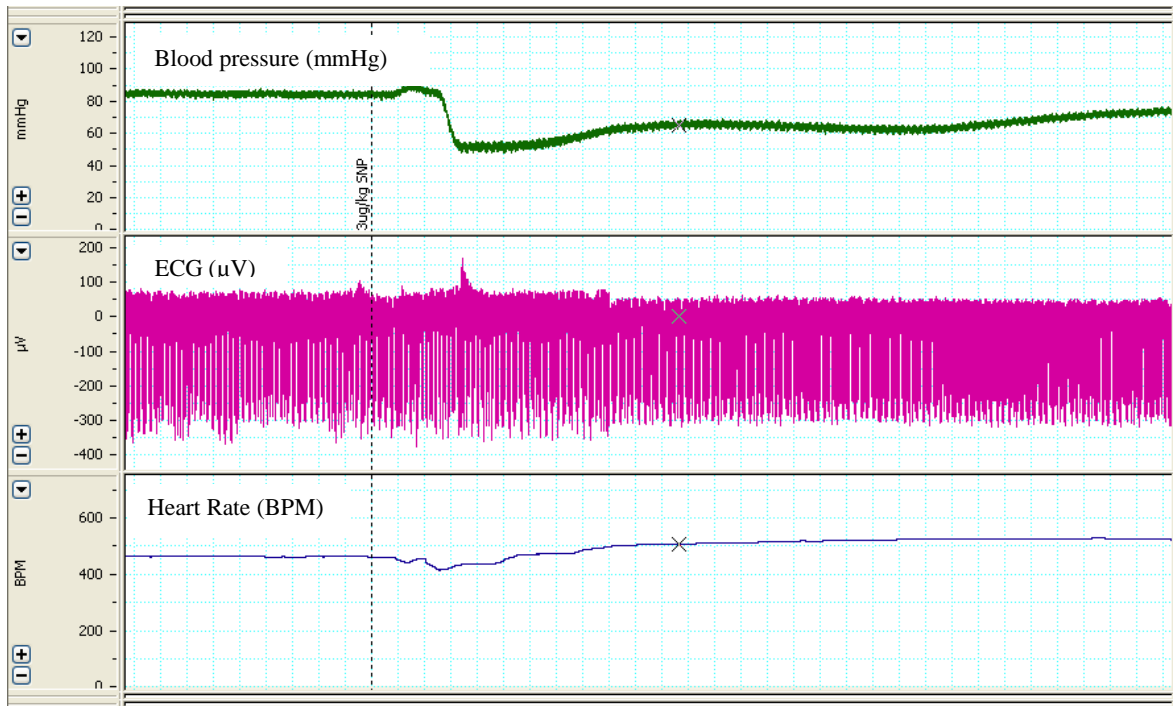


Figure 5.21 Original trace showing the depressor response to $3\mu\text{g kg}^{-1}$ sodium nitroprusside: HR was calculated as described previously.

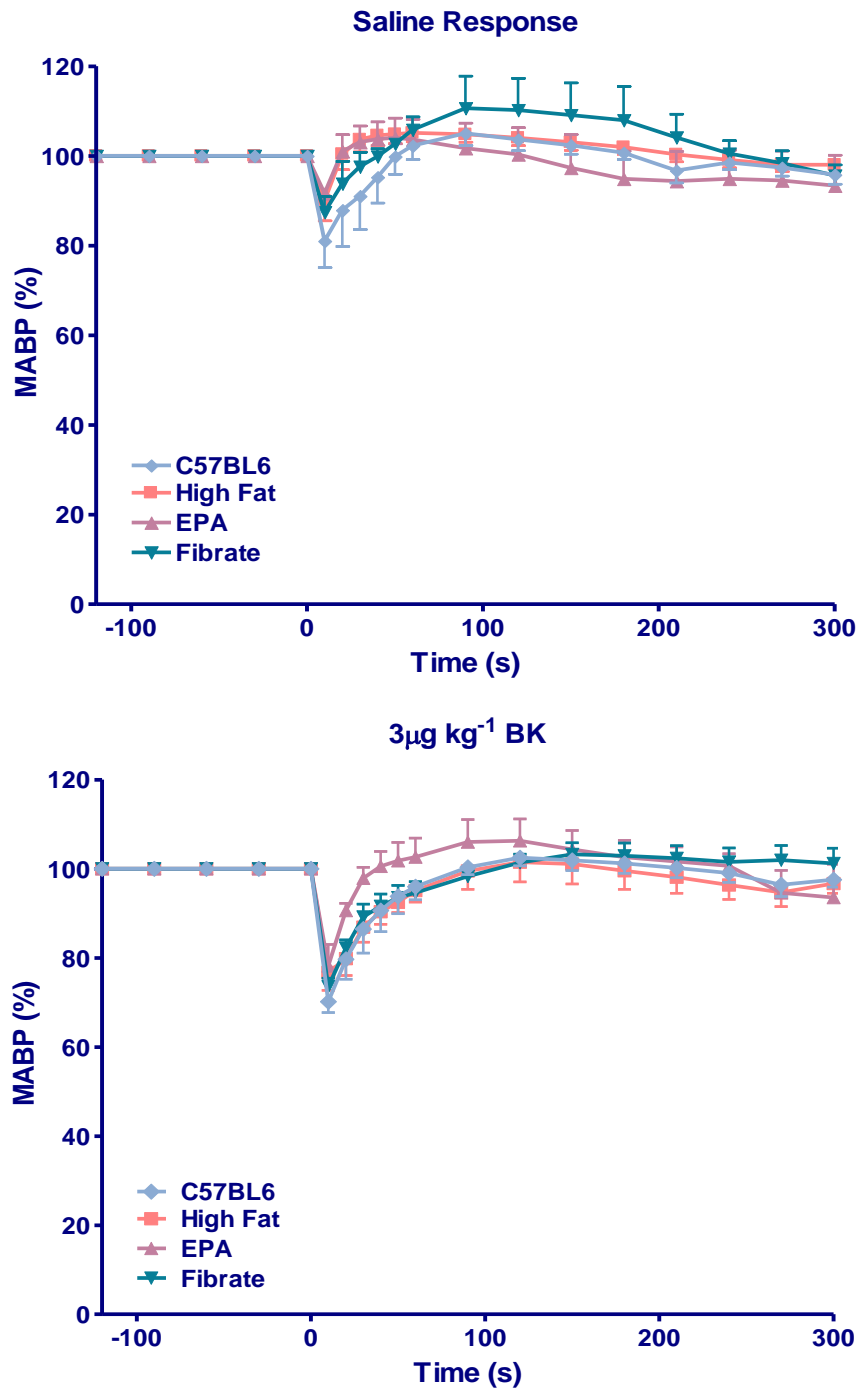


Figure 5.22 Blood pressure responses to bradykinin ($3\mu\text{g kg}^{-1}$): Depressor responses to endothelium dependent vasodilator bradykinin (BK) were recorded via a carotid artery cannula and presented as changes in mean arterial blood pressure (MABP; mmHg). Responses to saline and $3\mu\text{g kg}^{-1}$ BK are illustrated above. Data is expressed as a percentage fall in MABP respective to the resting blood pressure (denoted '100%'). $n=4-8$ per group. Values represent mean \pm SEM.

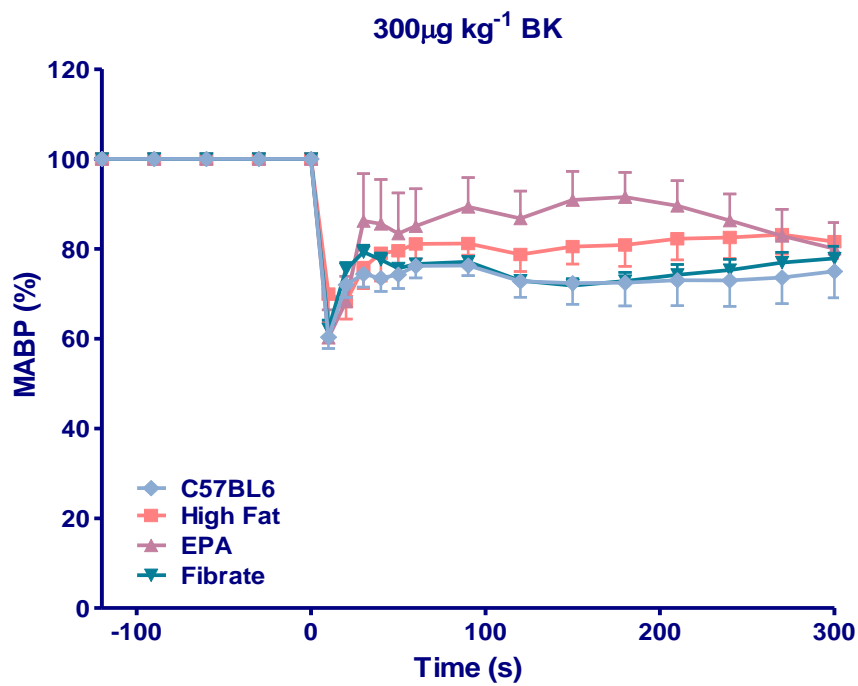
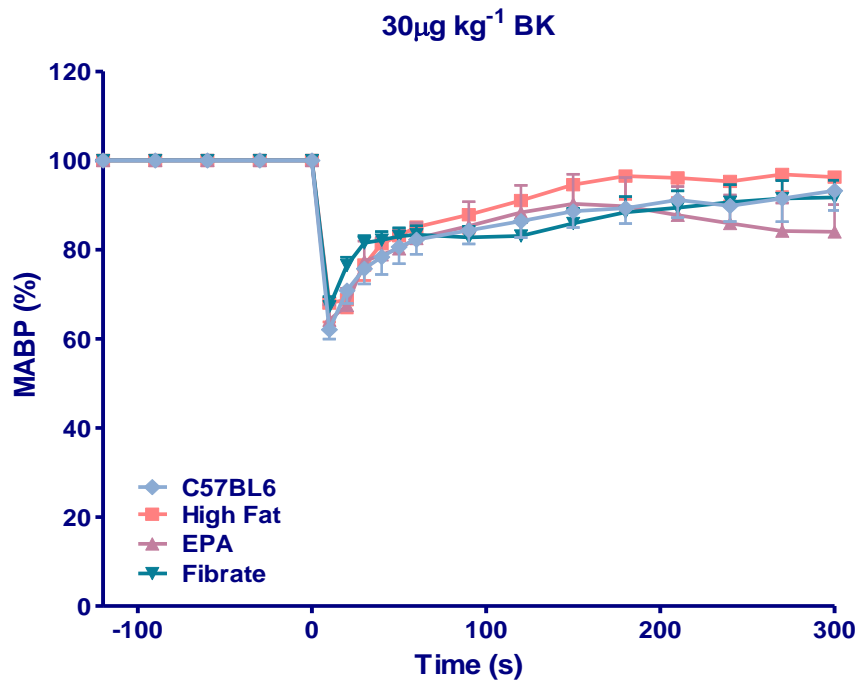


Figure 5.23 Blood pressure responses to bradykinin (30 and 300 $\mu\text{g kg}^{-1}$): Depressor responses to 30 and 300 $\mu\text{g kg}^{-1}$ BK were recorded via carotid artery cannula as described previously. Data is expressed as a percentage fall in MABP relative to resting blood pressure. n=4-8 per group. Values represent mean \pm SEM.

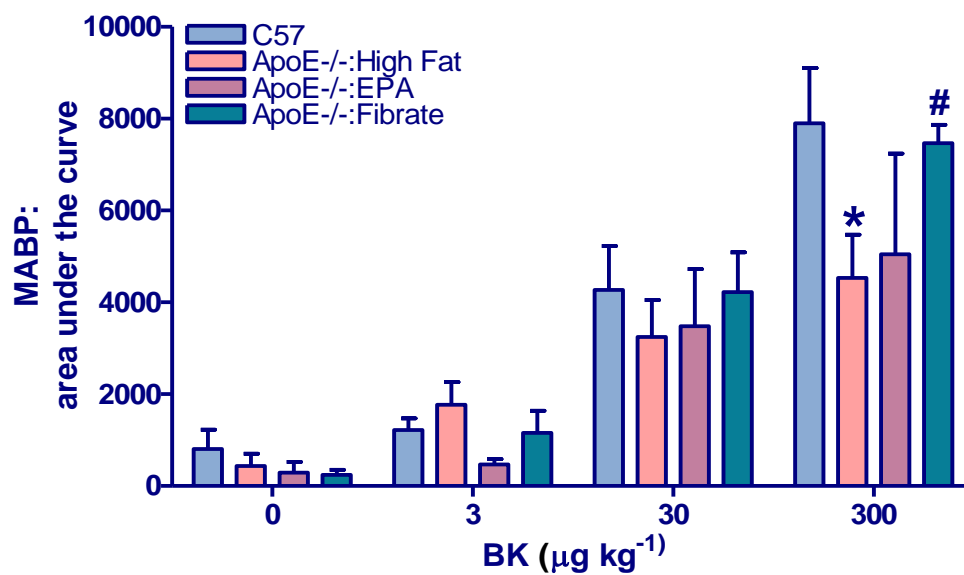


Figure 5.24 Area under the curve analysis of blood pressure responses to bradykinin: The depressor response to bradykinin was quantitatively measured through conducting area under the curve analysis. MABP data (expressed as % change) was inverted, where resting BP (denoted 100%) was denoted as '0'. n=4-8 per group. *P<0.05 vs C57 mice; #P<0.05 vs control ApoE^{-/-} mice (two-way ANOVA, Bonferroni post-hoc test). Values represent mean \pm SEM.

5.3.7 Haemodynamic responses to sodium nitroprusside

Figures 5.26 and 5.27 illustrate the time-dependent depressor responses to sodium nitroprusside (SNP; 3 - 300 $\mu\text{g kg}^{-1}$). A dose dependent response to SNP was not observed in any of the study groups, with a maximum reduction in MABP (40%) observed with 3 $\mu\text{g kg}^{-1}$ SNP. Subsequent AUTC analysis of the responses confirmed that there was no dose dependent response observed to SNP (Figure 5.28). Moreover, there was no effect of either high fat feeding, or EPA or fibrate supplementation, in any of the groups.

The effect of SNP on heart rate is shown in Figure 5.29. Compared to saline responses, heart rate was unaffected by increasing sodium nitroprusside administration. Moreover, there was no statistically significant variation in heart rate between any of the treatment groups.

5.4 Discussion

In light of the findings from Chapter 4 that indicated the existence of interaction between ω -3 PUFAs and endocannabinoids at the cellular level, the principle aim of this part of the thesis was to determine whether dietary supplementation with EPA (using fenofibrate as a lipid lowering control) has any effect on the endocannabinoid system *in vivo*. In order to assess this, it was necessary to first determine the impact of a high fat diet intervention alone on tissue endocannabinoid levels alongside the development of hyperlipidaemia, vascular dysfunction and tissue remodelling, and to compare these changes in high fat fed mice supplemented with EPA and fenofibrate.

The ApoE^{-/-} mouse was utilised as an *in vivo* model of hyperlipidaemia and its development, a process which was hastened by maintenance on an atherogenic diet. The composition of the atherogenic diet used in the current study was based on the widely used semi-synthetic 'Paigen' diet. First formulated in the laboratory of Paigen and colleagues in 1990 (Nishina *et al.*, 1990), the original Paigen diet contained 15% fat (cocoa or butter fat), 1.25% cholesterol, 1% corn oil and 0.5% sodium cholate. For the present study, the diet was modified to contain a marginally higher quantity of fat (16%, sourced from cocoa butter), a reduced quantity of cholesterol (0.25%) and without cholate due to its confounding influence on the genetic regulation of inflammation, cholesterol processing and lipoprotein metabolism (Vergnes *et al.*, 2003; Lambert *et al.*, 2003). Corn oil was substituted with 3% high oleic sunflower (HOSF) oil, the purpose of which was to prevent polyunsaturated fatty acid deficiency (the predominant fat present in the diet was derived from saturated fatty acids) and to equal the content of polyunsaturated fatty acids present in the EPA oil supplemented diet.

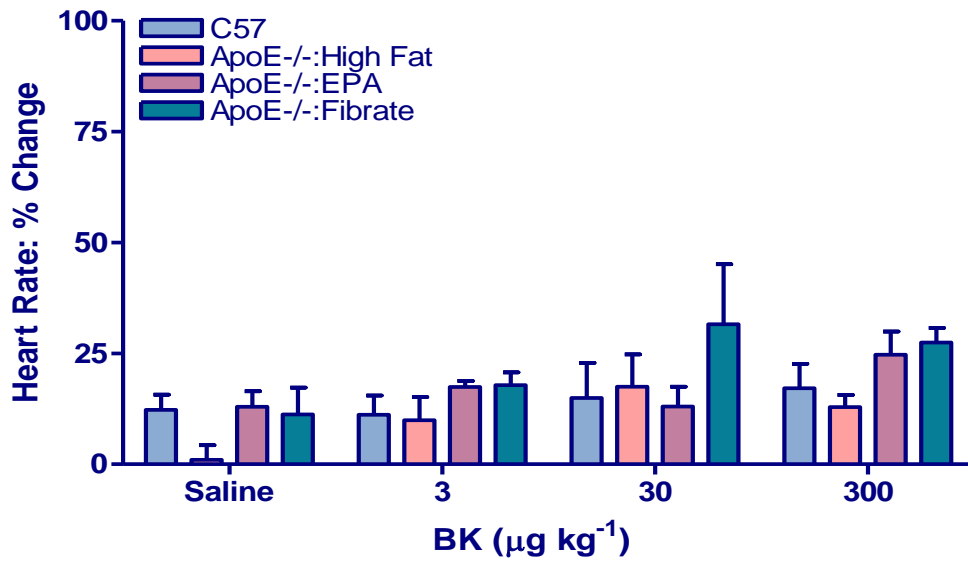


Figure 5.25 Heart rate responses to bradykinin: The effect of BK (3-300µg kg⁻¹) on HR was measured. Data was recorded as beats per minute (BPM) through Lead I ECG limb leads. Data was expressed as a percentage change in HR compared to baseline HR. n=4-8 per group. Values represent mean±SEM.

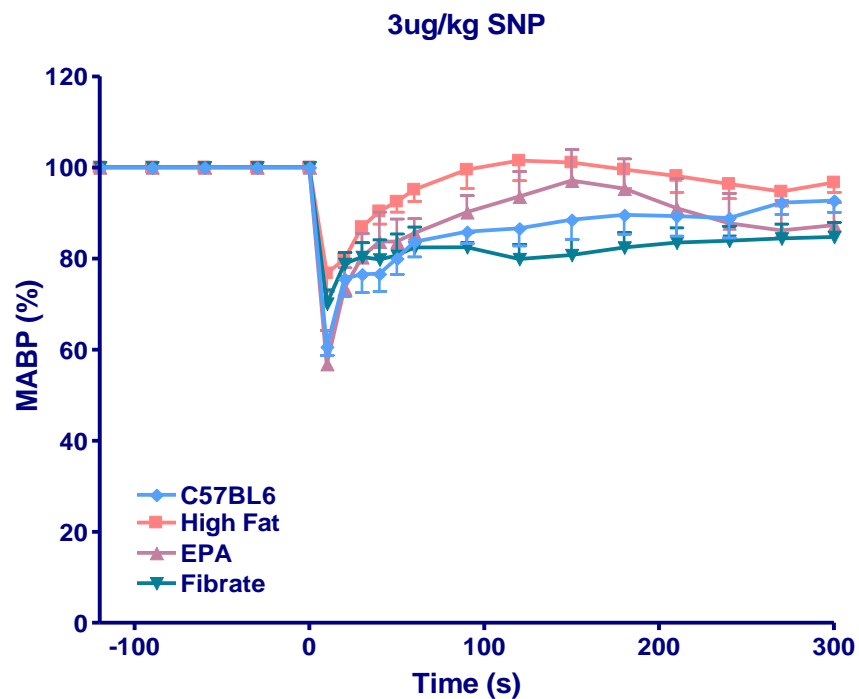
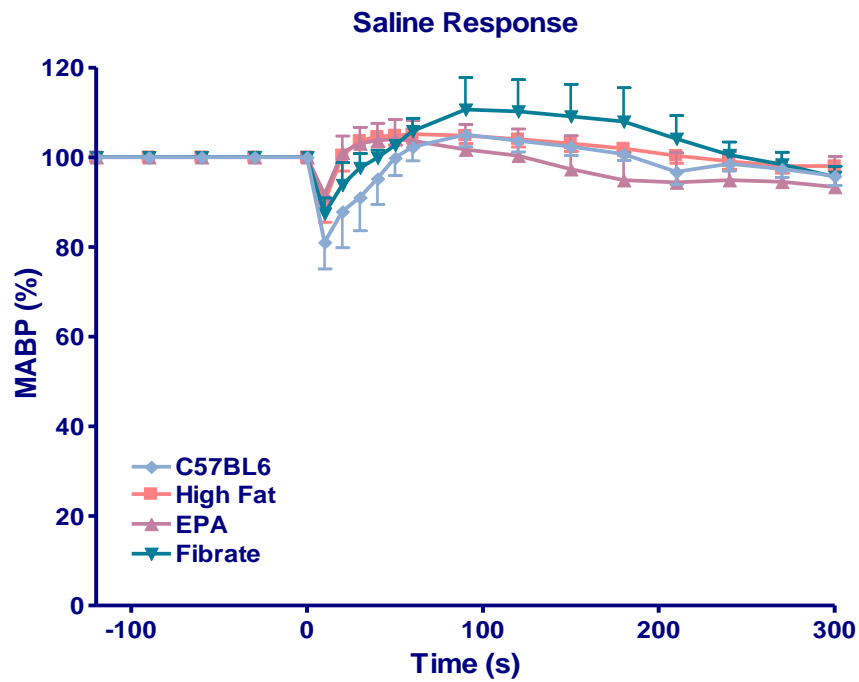


Figure 5.26 Blood pressure responses to sodium nitroprusside ($3\mu\text{g kg}^{-1}$): Depressor responses to endothelium independent vasodilator SNP were recorded across a 300 second sampling period as described previously. Responses to saline and $3\mu\text{g kg}^{-1}$ are shown above, expressed as a percentage fall in MABP relative to resting blood pressure. $n=4-8$ per group. Values represent mean \pm SEM.

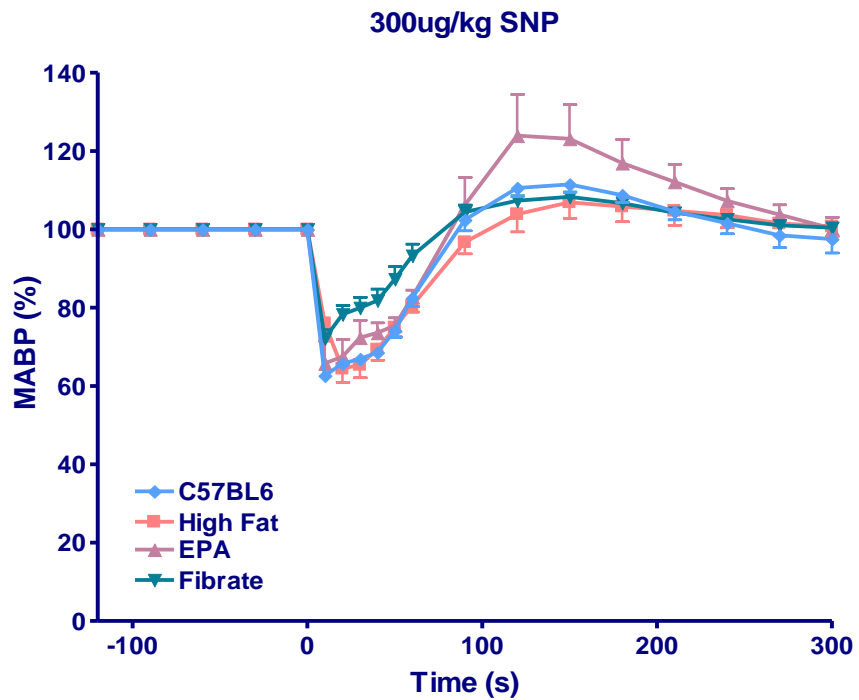
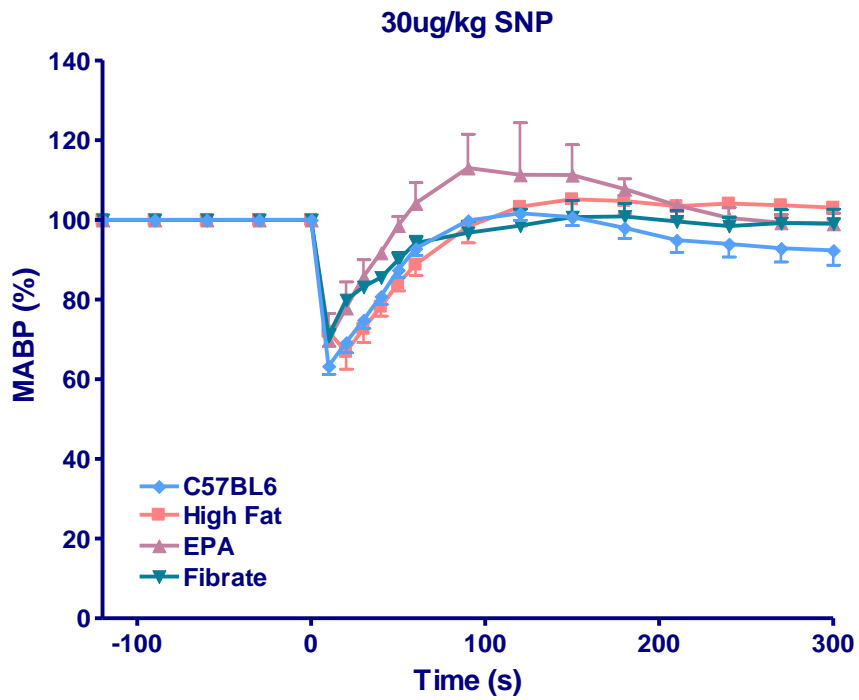


Figure 5.27 Blood pressure responses to sodium nitroprusside (30 and 300µg kg⁻¹): Depressor responses to 30 and 300µg kg⁻¹ SNP were recorded and analysed as described previously. n=4-8 per group. Values represent mean±SEM.

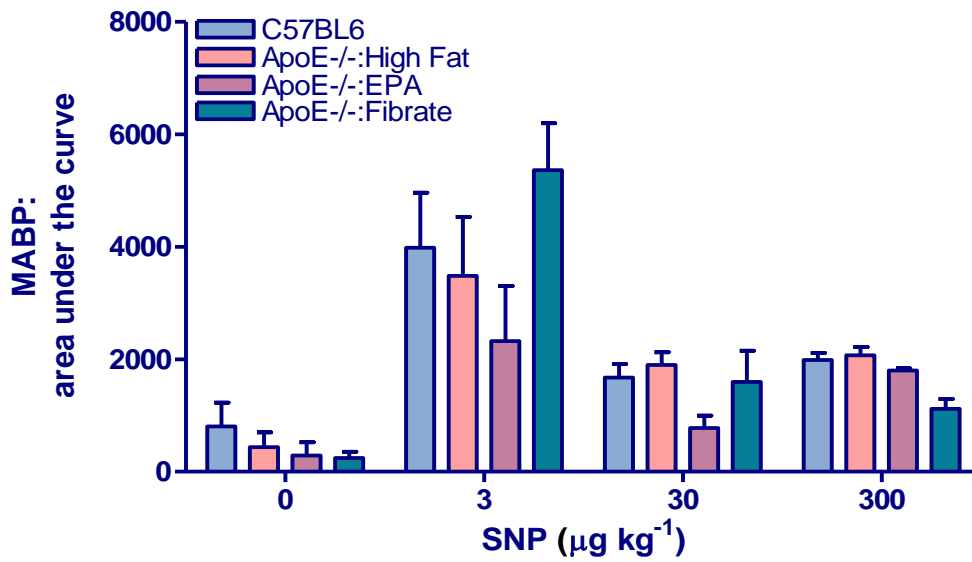


Figure 5.28 Area under the curve analysis of blood pressure responses to sodium nitroprusside: Depressor responses to SNP were measured quantitatively using area under the curve analysis as described previously. n=4-8 per group. Values represent mean \pm SEM.

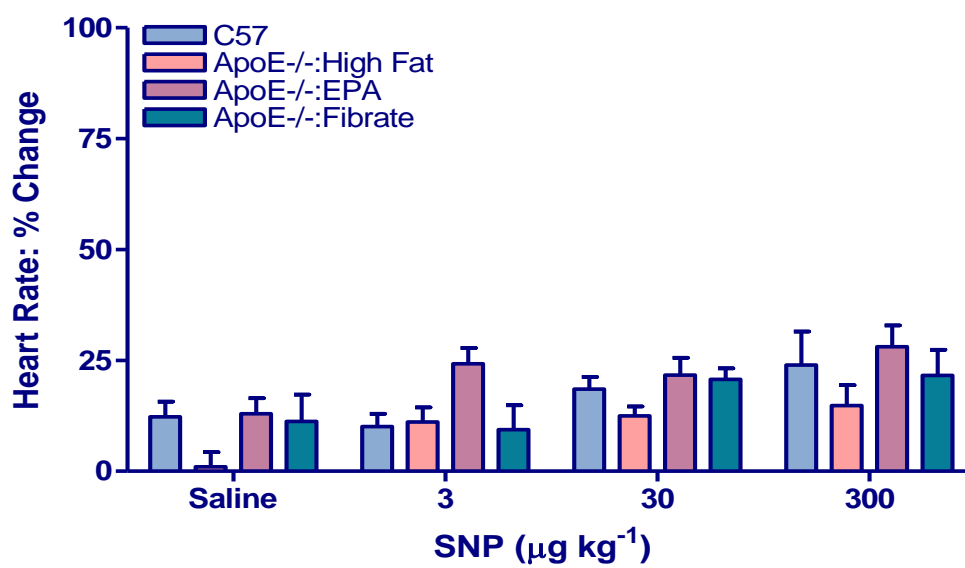


Figure 5.29 Heart rate responses to sodium nitroprusside: The effect of SNP (3-300µg kg⁻¹) on HR was measured and analysed as described previously. n=4-8 per group Values represent mean±SEM.

As outlined in the methods section, one ApoE^{-/-} cohort received 3% EPA oil in addition to the atherogenic diet. Investigations of the effects of dietary EPA oil have been conducted in numerous animal studies in which intervention doses have been within the range of 1% to 5% (w/w) of total food intake (Xu *et al.*, 2007; Matsumoto *et al.*, 2008; Mavrommatis *et al.*, 2010; Burri *et al.*, 2011). Therefore based on the literature, a dose of 3% EPA oil was chosen for the current study. A final ApoE^{-/-} cohort received the atherogenic diet supplemented with 0.04% fenofibrate: an established lipid lowering drug from the fibrate class of amphipathic carboxylic acids (refer to chapter 1 for details). The dose of fenofibrate employed in the present study was based on a previously used dose (de Roos *et al.*, 2005).

5.4.1 The impact of dietary intervention on baseline physiology in the ApoE^{-/-} mouse

Although it might be expected that maintenance on a high fat diet would increase mean body weight, when compared with age-matched wild-type mice fed regular chow, high fat feeding of ApoE^{-/-} mice did not influence mean body weight. However, as ApoE^{-/-} mice primarily represent a model of hyperlipidaemia and not obesity, the current result is not entirely unexpected and is consistent with previous dietary studies that have indicated no significant effect of high fat feeding on ApoE^{-/-} body weight (Davis *et al.*, 2001; Harrington *et al.*, 2007; Nakagami *et al.*, 2009), suggesting that these mice follow a normal body weight pattern irrespective of diet. Of the other baseline characteristics measured, there was negligible variation in mean heart weights between wild-type mice and ApoE^{-/-} mice. Additionally, there was no variation in heart/body weight ratios. Together this evidence demonstrates that there is no impact of high fat feeding on cardiac mass. This finding is in contrast to those of a study conducted by Hartley *et al.* (2000), which reported significant cardiac hypertrophy in chow fed ApoE^{-/-} mice compared to wild-type mice. Interestingly, mice used in the Hartley study were 13 months of age, which is considerably older than those used in the current study (6 months), suggesting that development of cardiac hypertrophy in the ApoE^{-/-} mouse is influenced by age rather than diet.

EPA supplementation had no effect on mean body weight, a finding which is reported inconsistently in the literature. Studies in ApoE^{-/-} mice have reported no effect of fish oil supplementation on mean body weight (Xu *et al.*, 2007). In wild-type mice however, inclusion of EPA in the diet was reported to significantly increase body weight (Halade *et al.*, 2010), suggesting the discrepancy could be strain specific. EPA supplementation did not alter either mean heart weight or heart/body weight ratios, while fenofibrate supplementation modestly, but significantly, lowered mean body weight compared with both wild-type mice and high fat fed ApoE^{-/-} mice. This latter observation is supported by

findings from multiple studies in wild-type and genetic knockout murine strains and is thought to arise from PPAR- α mediated induction of hepatic fatty acid metabolism (Mancini *et al.*, 2001; Jeong *et al.*, 2004; Motawi *et al.*, 2009). Fenofibrate supplementation had no impact on mean heart weights or mean heart/body weight ratios.

5.4.2 The impact of an atherogenic diet on lipid metabolism in the ApoE^{-/-} mouse

In terms of hepatic lipid physiology, the observation that the atherogenic diet significantly elevated the hepatic crude lipid levels of ApoE^{-/-} mice compared to chow fed wild-type mice, is consistent with the notion that a high fat diet is conducive to altered hepatic lipid metabolism and accumulation in this model. These findings are in agreement with similar studies in C57BL/6J mice and Wistar rats (Kim *et al.*, 2004; Vijaimohan *et al.*, 2006). However, hepatic triglyceride levels were unaltered by the atherogenic diet, suggesting that the observed changes in hepatic lipid levels were independent of triglyceride synthesis. This finding is in contrast to previous reports of a positive association between high fat feeding and hepatic triglyceride synthesis, where 6 weeks of high fat feeding in 3 month old C57BL/6J mice was shown to significantly elevate hepatic triglyceride levels (Oosterveer *et al.*, 2009), although this difference could be accounted for by different mouse strains. Genetic ablation of the apoE impairs hepatic clearance of both chylomicron remnants and LDL, generating a hyperlipidaemic profile. It is possible that such elevated levels of circulating chylomicrons, combined with an increased pool of exogenously derived triglycerides, could induce negative feedback inhibition whereby *de novo* hepatic triglyceride synthesis is down-regulated. Analysis of hepatic fatty acid composition of the ApoE^{-/-} mice in this study revealed that the high fat diet markedly increased the quantity of MUFAs, a finding which has been previously reported in C57BL/6J mice (Oosterveer *et al.*, 2009). In contrast, the overall proportion of PUFAs was decreased and there was a shift in PUFA composition towards profound ω -6 predominance, an effect that has been linked to atherosclerotic lesion progression (Wang *et al.*, 2008; Wan *et al.*, 2010) and suggests an increased abundance of the metabolic products of ω -6 PUFAs (arachidonic acid (AA) derived prostaglandins, thromboxanes, leukotrienes, lipoxins).

In relation to plasma lipid profiles, maintenance on the atherogenic diet significantly elevated total cholesterol and LDL-cholesterol, an effect which is consistent with reports in high fat fed ApoE^{-/-} mice (Moghadasian *et al.*, 2001; Guo *et al.*, 2005) and represents a widely recognised risk factor for coronary artery disease. Absolute HDL-cholesterol levels were also significantly increased - an effect which could suggest a beneficial action of the diet. However, in light of the elevated total cholesterol:HDL ratio, it is likely that the increase was secondary to the overall elevation of total cholesterol and

that the majority of circulating cholesterol was confined to the lower density, pro-atherogenic particles. Indeed, elevated LDL-cholesterol measured in the present study, together with previous reports of elevated VLDL-cholesterol in high fat fed ApoE^{-/-} mice support this notion (Guo *et al.*, 2005). The observation that the atherogenic diet induced a slight, although not significant, increase in plasma triglycerides was not unexpected considering the negligible effect of the diet on hepatic triglyceride synthesis.

5.4.2.1 EPA supplementation and lipid metabolism in the ApoE^{-/-} mouse

The present finding that supplementation with EPA significantly reduced hepatic lipid levels is consistent with previously reported studies in mice and rats (De Roos *et al.*, 2005; Vijaimohan *et al.*, 2006). The current study found that EPA supplementation had a negligible impact on hepatic triglyceride levels, while causing a significant rise in serum triglycerides. This is in contrast to the well accepted hypotriglyceridaemic effects of EPA (Chapter 1, Section 1.3.4), which are thought to be the result of reduced hepatic VLDL assembly and secretion and, increased chylomicron and VLDL clearance (Harris *et al.*, 1997; Yongsoon and Harris, 2003). Thus a potential explanation for the failure of EPA to influence hepatic triglyceride levels in ApoE^{-/-} mice could be due to impaired hepatic clearance of chylomicrons due to the apoE deficiency characteristic of this strain. Consistent with previous findings (De Roos *et al.*, 2005), EPA supplementation raised hepatic PUFA composition considerably, an effect which was accompanied by a favourable increase in the ω -3/ ω -6 PUFA ratio. Moreover, hepatic EPA and DHA levels were significantly elevated in the EPA supplemented group, which strongly suggests that the supplementation was sufficient to effect alterations in tissue fatty acid composition.

In terms of plasma profiles, EPA supplementation moderately improved the lipid profile. Compared to high fat fed ApoE^{-/-} mice, total cholesterol and LDL-cholesterol levels were significantly reduced. While the cholesterol lowering effects of ω -3 PUFAs have been reported previously (Illingworth *et al.*, 1984; De Roos *et al.*, 2005), data concerning the impact of ω -3 PUFA supplementation on LDL-cholesterol levels remains inconsistent. Indeed high, often supraphysiological, doses (Illingworth *et al.*, 1984) have been reported to significantly lower LDL-cholesterol while low to moderate doses paradoxically often induce an increase in LDL-cholesterol levels (Radack *et al.*, 1990; Suzukawa *et al.*, 1995). Negligible variation in absolute HDL-cholesterol levels, in combination with a moderately reduced total cholesterol: HDL cholesterol ratio (insignificant), suggested minimal impact of EPA supplementation on the plasma HDL fraction in this model. In contradiction, EPA supplementation significantly enhanced plasma triglyceride levels. This finding is in stark contrast to an abundance of previous studies describing the hypotriglyceridemic actions of ω -3 PUFAs, which have been largely

attributed to decreased hepatic assembly and secretion of triglyceride rich VLDL particles secondary to decreased triglyceride synthesis. However, given that EPA supplementation had no impact on hepatic triglyceride synthesis, the observed increase is yet more puzzling. It is possible that this finding is strain specific, a notion supported by a dietary study in high fat fed ApoE^{-/-} mice which reported a significant elevation of plasma triglyceride levels following fish oil supplementation (Xu *et al.*, 2007). Moreover, in light of the observation that fish oil supplementation significantly reduced hepatocyte LDL receptor mRNA and protein expression (Lindsey *et al.*, 1992), fish oil supplementation of ApoE^{-/-} mice may serve to augment impaired chylomicron and IDL clearance through a lack of functional apoE combined with reduced LDL-receptor availability.

5.4.2.2 Fenofibrate supplementation and lipid metabolism in the ApoE^{-/-} mouse

Fenofibrate supplementation significantly lowered total hepatic lipids compared to high fat fed mice, although hepatic triglyceride levels were significantly elevated compared to wild-type and high fat fed ApoE^{-/-} mice. This latter observation is a curious finding considering the established capacity of fibrates to lower serum triglycerides, a process that has been linked to increased hepatic uptake and β -oxidation of free fatty acids (Schoonjans *et al.*, 1995; Martin *et al.*, 1997) resulting in reduced bioavailability of fatty acids for hepatic triglyceride synthesis. However, a similar effect has been observed in chow fed Wistar rats where hepatic triglyceride levels were significantly augmented by fenofibrate (0.5%) supplementation (Waterman and Zammit, 2002). One explanation for this could be a consequence of PPAR- α mediated overexpression of adipose differentiation-related protein (ADRP), a perilipin surface protein expressed on lipid droplets (Listenberger *et al.*, 2007). In support of this, in the present study, hepatic ADRP protein expression was found to be significantly elevated in the fenofibrate supplemented group (but not EPA), implying this was an effect specific to fenofibrate and not due to non-specific effects of lipid lowering. While PPAR- α stimulation has previously been shown to modulate hepatic ADRP mRNA and protein expression in humans (Liu *et al.*, 2003; Schadinger *et al.*, 2005; Inoue *et al.*, 2005) and C57BL/6J mice (Edvardsson *et al.*, 2005), the current findings are the first to suggest that the same effect may occur in the ApoE^{-/-} mouse and warrants further investigation.

Fenofibrate supplementation had negligible effects on hepatic fatty acid composition, a finding that is in disagreement with a study conducted in chow fed C57BL/6J mice where 0.2% fenofibrate supplementation significantly enhanced hepatic MUFA composition (Oosterveer *et al.*, 2009). One possible explanation for this discrepancy is that the capacity of fenofibrate to elevate hepatic MUFAs may have been shrouded by the parallel actions of the high fat diet alone, or that the dose used in the

present study may have been too low to achieve such an effect, but this clearly warrants further investigation before any firm conclusion can be reached.

In terms of plasma profiles, fenofibrate supplementation significantly attenuated diet induced hypercholesterolemia in the present model. Total cholesterol and LDL-cholesterol were significantly reduced compared to the high fat fed group – an effect consistent with previous studies (Caslake *et al.*, 1993 Guerin *et al.*, 2003). Such actions are thought to be mediated, at least in part, through PPAR- α mediated stimulation of lipoprotein lipase activity and repression of hepatic ApoC-III expression, which together, enhance VLDL (and ultimately LDL) hydrolysis (Staels *et al.*, 1995; Schoonjans *et al.*, 1996). Therefore the present findings are most likely the result of transcriptional modulation of VLDL metabolism. Interestingly, fenofibrate supplementation mediated a modest, although not significant, reduction in plasma triglyceride levels compared to wild-type and high fat fed ApoE^{-/-} mice. In light of the observation that fenofibrate supplementation significantly elevated hepatic triglyceride levels, sequestration of triglycerides from VLDL assembly through their cytosolic storage could in effect reduce hepatic VLDL secretion, representing a possible mechanism for the hypolipidemic action of fenofibrate in this model.

5.4.3 The impact of an atherogenic diet on cardiac and vascular remodelling

As described in Chapter 1 (Section 1.1.3), cardiac fibrosis is due to the progressive accumulation of fibrous collagen in the heart and is associated with increased myocardial stiffness (Conrad *et al.*, 1995; Norton *et al.*, 1997) and cardiac dysfunction (Kuwahara *et al.*, 2002). Therefore, cardiac collagen content was measured in the present study to ascertain whether high fat feeding induced cardiac fibrosis. Although hypercholesterolemia was recently demonstrated to induce collagen deposition in the hearts of LDLr^{-/-} mice (Kang *et al.*, 2009), few studies have examined the association between high fat feeding and cardiac remodelling in the ApoE^{-/-} model. In the present study, maintenance of ApoE^{-/-} mice on a high fat/high cholesterol diet had no impact on cardiac collagen deposition compared to chow fed wild-type mice. This finding is in disagreement with a very recent study conducted in ApoE^{-/-} mice fed a Western style diet (21% fat, 0.15% cholesterol) which reported an age-dependent increase in heart/body weight ratio and left ventricular (LV) collagen volume fraction after 32 weeks feeding and a significant increase in LV wall thickness after 40 weeks feeding, when compared to baseline measurements at 24 weeks (Qin *et al.* 2010). Thus since the present study was terminated at 24 weeks, it is likely that this was too early to detect the development of significant cardiac remodelling and the lack of effect of high fat feeding on heart/body weight ratios in the present study is supportive of this notion.

However, although total collagen levels were not affected by high fat feeding, the quantity of both mature (DPD, PYD, HHL) and immature (DHLNL, HLNL) collagen cross-links were significantly elevated in cardiac tissue compared to matched measurements in wild-type mice. This is an interesting finding considering the mounting evidence that suggests myocardial stiffness arises from increased collagen cross-link formation and not absolute collagen levels per se (Norton *et al.*, 1997; Woodiwiss *et al.*, 2001). Indeed, the observed elevation in mature cross-links (DPD, PYD, HHL), together with the significant reduction in elastin cross-links, might imply increased ventricular stiffness and, in effect, reduced cardiac contractility. However, this notion is undermined by the observation that the atherogenic diet also elevated immature cross-link formation and resulted in a lower mature: immature cross-link ratio – findings which could imply impaired maturation of collagen and ultimately, greater ventricular compliance. The dichotomous effect of the atherogenic diet on cross-link maturation may be explained by abnormal structural rearrangements of cross-links. The process of cross-link maturation, detailed in Chapter 1 (Section 1.1.3.2), imparts tensile strength to collagen by forming covalent intermolecular bonds between protein sub-units. Immature cross-links stabilise collagen microfibrils, quasi-hexagonal units containing five tropocollagen monomers (Orgel *et al.*, 2001), by forming intermolecular bonds between the tropocollagen monomers of the microfibril structure (Kang, 1972; Nicholls and Bailey, 1980; see Figure 5.30A). Individual microfibrils are then further stabilised by mature cross-links, which constitute intermolecular bonds between microfibril units (Figure 5.30B) that together comprise the mature collagen fibril (Light and Bailey, 1985). Conversion of the difunctional, immature cross-links to trifunctional, mature cross-links normally allows the formation of a complete inter-microfibrillar network of cross-links (Fig 5.29B). In the present study, it is postulated that, perhaps because of structural changes within the tissue, formation of mature cross-links occurs within, as opposed to between, individual microfibrils, thus providing an explanation as to the anomaly in cross-link measurements (Figure 5.30C).

While it is clear that cross-link formation, but not total collagen, is altered by an atherogenic diet in the ApoE^{-/-} model, the present study was not designed to assess the implication of these changes in terms of cardiac function. However, other studies from this laboratory have shown that 24 weeks of high fat feeding in ApoE^{-/-} mice results in changes in various load-dependent measures of cardiac function including a significant reduction in end diastolic volume (EDV) combined with a significant elevation of end diastolic pressure (EDP), implying increased ventricular stiffness (Walsh and Wainwright, unpublished). Furthermore, an increase in the slope (leftward shift) of the end diastolic pressure volume relationship (EDPVR) indicates reduced LV compliance, possibly as a consequence of adverse ventricular remodelling. These findings are not in isolation, as similar alterations to cardiac function have been measured in high fat fed, ageing C57BL/6J mice; effects which were also

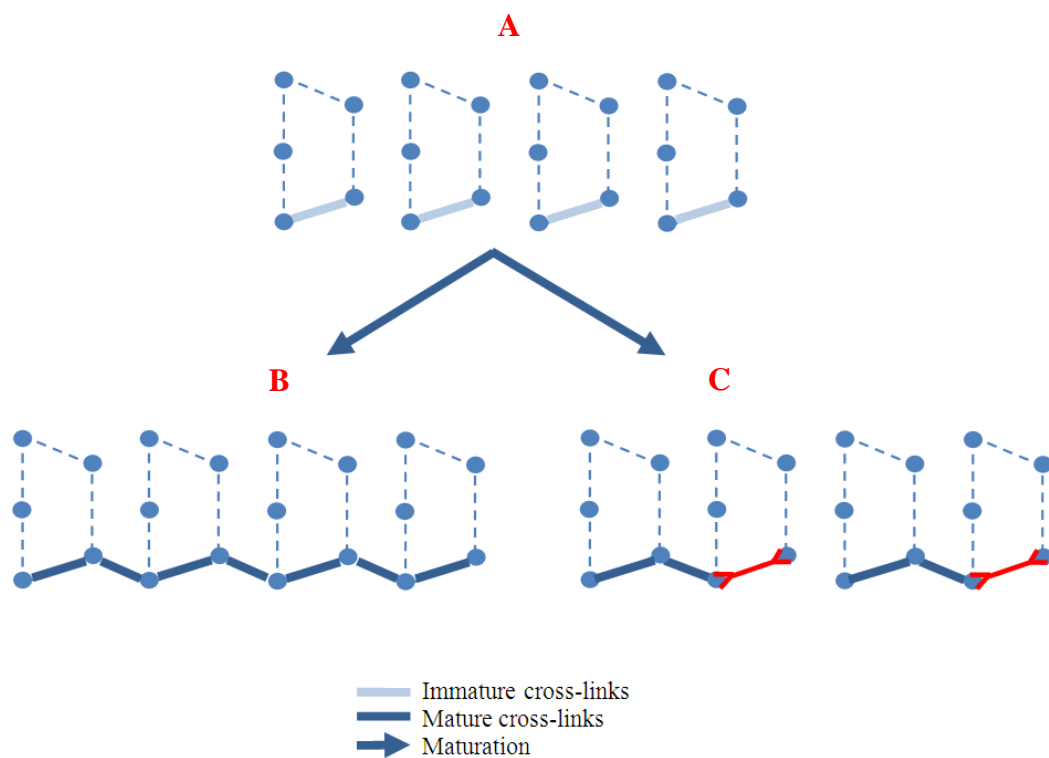


Figure 5.30 Schematic representation of cardiac collagen cross-link formation Diagram details structural placement of A) immature cross-links within individual microfibrils; B) mature cross-links between microfibrils; C) Postulated re-arrangement of intra-fibrillar cross-links in ApoE^{-/-} model of hyperlipidaemia.

accompanied by an increase in collagen cross-linking (Zibadi *et al.*, 2009). Moreover, the proposed link between cardiac fibrosis and altered cardiac function has also been described previously in pig and human models (Martos *et al.*, 2007; Zhu *et al.*, 2007). Together this data suggests that in the ApoE^{-/-} model, hyperlipidaemia induced alterations to the underlying structure and quality of cardiac collagen may alter normal cardiac function. From the present study, there is a clear requirement for full characterisation of the functional implication of abnormal cross-linking.

Considering the mounting evidence of a direct association between hyperlipidaemia and plaque instability, it was considered likely that high fat feeding would lower total aortic collagen levels. Indeed, it has been confirmed in both murine and rabbit models, that hyperlipidaemia reduces the collagen content of plaques and likewise its reversal results in increased collagen content of plaques (Aikawa *et al.*, 1998; Rekhter *et al.*, 2000; Feig *et al.*, 2011) since lipid lowering has been observed to reduce lesional macrophage numbers and thus the activation and secretion of collagen degrading MMP's (Aikawa *et al.*, 1998). In terms of cross-link formation, a recent study demonstrated that cross-link maturation was reduced in advanced plaques from human carotid arteries (Hector *et al.*, 2010), a finding which would imply reduced tensile strength and an increased likelihood of rupture in these plaques. In contrast, Rekhter *et al.* (2000) reported no change in cross-link levels (albeit measured as the ratio of hydroxyproline/pyridinoline) between cholesterol fed and chow fed rabbits, despite a time-dependent reduction in the total collagen content of aortic plaques from cholesterol fed animals. However, due to a technical error, no aortic collagen data was collected from the wild-type group which presents a major limitation of the present study. The nature of this limitation prevented comparison of the high fat diet and its effects on baseline vascular collagen levels.

5.4.3.1 EPA supplementation and cardiac and vascular remodelling

EPA supplementation had no impact on either cardiac collagen or cross-link levels in the present study – a finding which is not entirely unexpected given that the atherogenic diet alone had no impact on total cardiac collagen. This data implies no effect of EPA supplementation on remodelling in the ApoE^{-/-} heart, an effect which may be species specific given the recent report that fish oil supplementation (5% EPA + DHA) significantly attenuated LV collagen deposition induced by corn oil feeding in ageing C57BL/6 mice (Halade *et al.*, 2011). However, while the murine model could account for the inconsistency between the studies, the substantially higher dose of ω-3 PUFAs and different method of collagen quantification used in the Halade study cannot be overlooked. Furthermore, in studies of pressure-overload induced cardiac dysfunction, fish oil supplementation has been shown to attenuate cardiac fibrosis and improve contractile function in both rat and mouse

models (Duda *et al.*, 2009; Chen *et al.*, 2011). Both of these studies support the theory that the lack of impact of EPA on cardiac collagen in the present study could be specific to the ApoE^{-/-} model.

In terms of vascular remodelling, EPA supplementation had a negligible effect on total collagen and cross-link levels in the aorta compared to high fat fed mice. This finding is somewhat surprising in view of the propounded plaque stabilising properties of fish oil which have been attributed to modulation of macrophage numbers and activity, attenuation of MMP expression, and reduced adhesion molecule expression (Thies *et al.*, 2003; Matsumoto *et al.*, 2008). In support of this, Matsumoto *et al.* (2008) reported increased collagen content of aortic root plaques in high fat fed ApoE^{-/-} mice supplemented with 5% EPA respective to high fat fed controls. However, in that study collagen levels were assessed qualitatively, using Sirius red polarisation microscopy of stained aortic sections, whereas the present study employed a more robust, quantitative measurement of total collagen; hence contrast in methodological approaches may explain the equivocal results. The high dose of EPA used in the Matsumoto study also suggests a greater dose than that used in the present study may be required to elicit alterations to aortic plaque morphology. However, it is the brachiocephalic artery, and not the aorta, that represents the major location of plaque rupture predilection in the ApoE^{-/-} mouse (Johnson and Jackson, 2001). Therefore it is possible that any effects of EPA on hyperlipidaemia induced vascular remodelling would be more likely to be detected in these vessels, although considering the small size of this vessel, biochemical quantification of collagen and associated cross-links was not possible.

5.4.3.2 Fenofibrate supplementation and cardiac and vascular remodelling

Parallel to the findings with EPA, fenofibrate supplementation had no impact on the total collagen and cross-link content of either cardiac or aortic tissue in the present study, which together implies a lack of effect of fenofibrate on cardiac and vascular remodelling in the ApoE^{-/-} model. Reports of the effect of fenofibrate on cardiac function are sparse and, of the studies which have examined these variables, the results are equivocal. In keeping with the present findings, fenofibrate supplementation (160mg/d) failed to improve LV diastolic dysfunction in type 2 diabetes patients (Chew *et al.*, 2008). In contrast, fenofibrate supplementation (80mg/kg/day) significantly attenuated myocardial fibrosis and endothelial dysfunction in hypertensive rats; an effect that was attributed, in part, to modulation of the NF-κB pathway (Ogata *et al.*, 2004). Interestingly, fenofibrate supplementation was observed to significantly exacerbate LV fibrosis in pressure overloaded PPAR-α deficient rats (Duhaney *et al.*, 2007). From these studies, it is apparent that the pleiotropic actions of fenofibrate in the heart are further complicated by differences in technical approach and drug doses employed in these studies.

In relation to vascular remodelling, Corti and colleagues (2007) reported a significant increase in the collagen content of aortic plaque sections in ageing New Zealand white rabbits maintained on a high cholesterol diet supplemented with fenofibrate, an effect that was not observed in the present study. The considerably different study designs, together with species variation, may explain this inconsistency between the Corti study and findings from the present study. Indeed, as mentioned above, if it had been possible to measure collagen and cross-links in the plaque rupture-prone brachiocephalic artery, some effect may have been observed.

5.4.4 The impact of an atherogenic diet on tissue endocannabinoid levels

Given that the major endocannabinoids, AEA and 2-AG, are synthesised from AA and that tissue fatty acid content is influenced by diet, the impact of the atherogenic diet on tissue endocannabinoid levels was assessed. Interestingly, maintenance of ApoE^{-/-} mice on the atherogenic diet significantly elevated endocannabinoid levels in the brain, heart and thoracic aorta compared to chow fed wild type mice. These findings correlate with previous studies, which have highlighted an association between high fat/high cholesterol feeding and modulation of endocannabinoid levels in peripheral tissues, the majority of which report elevated endocannabinoids in heart, thoracic aorta, kidney, skeletal muscle and brown adipose tissue and reduced endocannabinoid levels in thyroid and subcutaneous white adipose tissue (Matias *et al.*, 2008; Starowicz *et al.*, 2008; Montecucco *et al.*, 2009; Bartelt *et al.*, 2011). However, to our knowledge, this is the first study to demonstrate a rise in brain endocannabinoid levels (both AEA and 2-AG) in response to a high fat diet.

In terms of brain endocannabinoid levels, the diet induced elevation of both 2-AG and AEA observed in the present study was supported, in part, by the findings of a dietary study in rats where maintenance on a high fat diet enriched with oleic acid increased the levels of 2-AG, but not AEA in the brain (Artmann *et al.*, 2008). In the latter study however, the dietary intervention period was substantially shorter than that of the present study (1 week), which may offer a possible explanation for the lack of impact of the diet on AEA levels. Conversely, ketogenic and/or food restriction diets have been reported to lower brain endocannabinoids (Hanus *et al.*, 2003; Hansen *et al.*, 2009). Together these findings present further confirmation of the modulation of central endocannabinoid levels by diet. The functional implications of elevated brain endocannabinoids, although not examined in the present study, would most likely reflect the action of endocannabinoids on food intake, appetite regulation and mood. The observation that CB₁ receptors are expressed in regions of the brain that control food intake (hypothalamus, nucleus accumbens shell and vagus nerve), combined with reports that hypothalamic endocannabinoid levels (both AEA and 2-AG) are increased

during fasting suggests a regulatory role of endocannabinoids in food intake (Kirkham *et al.*, 2002; Robbe *et al.*, 2002; Burdyga *et al.*, 2004). Indeed, the observation that injection of a CB₁ receptor agonist (anandamide) directly into the hypothalamus induced hyperphagia in satiated rats, while a CB₁ receptor antagonist (rimonabant) reduced appetite, combined with the observation that systemic administration of rimonabant reduced food intake in fasted rats, support this notion (Jamshidi and Taylor, 2001; Gomez *et al.*, 2002). Excessive brain endocannabinoid production, as observed in response to hyperlipidaemia in the present study, could generate dysregulation of food intake and energy expenditure by over stimulation of the CB₁ receptor and its associated pathways. In terms of mood responses, altered endocannabinoid signalling has been reported in schizophrenia, anxiety and depression (Guiffrida *et al.*, 2004; Gobbi *et al.*, 2005), conditions which could thus be affected by overproduction of endocannabinoids in the brain.

In the present study, the observed elevation of AEA in the heart following high fat/high cholesterol feeding is in agreement with the findings of a previous dietary study in C57BL/6J mice (Matias *et al.*, 2008). The endocannabinoid system is known to be activated in the heart under pathological conditions, including experimental models of endotoxic, hemorrhagic and septic shock and heart failure, where the activity of endocannabinoids (whether beneficial or detrimental) remains a point of contention. Several studies have implicated CB₁ receptor activation in the exacerbation of certain cardiac pathologies. In a murine model of doxorubicin (DOX) induced ventricular dysfunction, CB₁ receptor blockade with either rimonabant or AM251, alleviated cardiac dysfunction (Mukhopadhyay *et al.*, 2007), while abolition of fatty acid amide hydrolase, the enzyme responsible for AEA metabolism, potentiated myocardial injury in DOX treated mice (Mukhopadhyay *et al.*, 2011). Furthermore, chronic treatment with rimonabant (CB₁ selective antagonist) reduced infarct size in a murine model of myocardial infarction (Lim *et al.*, 2009). In contrast, the presence and activation of CB₂ receptors is generally thought to be cardioprotective. Indeed in the setting of experimental myocardial ischaemia, CB₂ receptors have been implicated in the preconditioning response where CB₂ receptor agonism has been observed to reduce infarct size, oxidative stress and neutrophil infiltration in the infarcted myocardium, effects which were abolished by CB₂, but not CB₁, receptor blockade (Montecucco *et al.*, 2009). In relation to studies in heart failure, genetic abolition of the CB₂ receptor has been demonstrated to induce significant cardiac remodelling in mice (Defer *et al.*, 2009). Elevated endocannabinoids and upregulated CB₂ receptor expression have also been measured in patients with chronic heart failure, an effect which was proposed as detrimental in this model whereby receptor activation, through inhibitory G protein signalling and reduced cAMP levels, could propagate negative inotropic conditions that would further weaken the failing ventricles (Weis *et al.*, 2010). Overproduction of endocannabinoids in response to an atherogenic diet, as observed in the

present study, implies increased activation of the endocannabinoid system. While activation of CB₂ receptors may confer protection in some cardiac pathologies, the deleterious effects of CB₁ receptor activation cannot be ignored and, as AEA has a greater affinity for CB₁ receptors, it is not unreasonable to suggest that the observed elevation of cardiac AEA seen in response to a high fat/high cholesterol diet in the present study may suggest high fat intake predisposes the heart to additional pathological stress beyond the development of atheroma.

The significant elevation in aortic content of AEA and 2-AG measured in response to the atherogenic diet supports the findings of a similar study conducted in ApoE^{-/-} mice, where maintenance on a high cholesterol diet elevated the aortic content of 2-AG, although AEA levels were out-with detection limits (Montecucco *et al.*, 2009). In the latter study, a lack of impact of the cholesterol enriched diet on endocannabinoid levels in wild-type mice led the authors to assume that the elevation in endocannabinoids was independent of the effects of the diet. However, since high fat feeding in wild type mice does not induce the same degree of hyperlipidaemia as that seen in the ApoE^{-/-} mouse, it is possible that a critical cholesterol/LDL level must be reached to activate increased endocannabinoid synthesis. Moreover, as the endocannabinoid system is known to be activated in pathological conditions, the lack of atherosclerosis pathology in the wild-type strain could also account for the negligible increase in endocannabinoids. The physiological impact of activation of the endocannabinoid system in the aorta has been linked to atherogenesis. In patients with coronary artery disease, CB₁ receptor expression was significantly increased in coronary plaques, while circulating endocannabinoid levels were also significantly elevated, providing evidence of activation of the endocannabinoid system in atherosclerosis pathology (Sugamura *et al.*, 2009). Subsequently, it has been demonstrated that CB₁ receptor agonism most likely propagates atherogenesis since, in LDLr^{-/-} mice fed a Western style diet, CB₁ receptor blockade with rimonabant dose dependently reduced atherosclerotic lesion progression in the aorta and aortic sinus, an effect that implicates CB₁ receptor agonism in the progression of the condition (Dol-Gleizes *et al.*, 2009). In line with this notion, *in vitro* studies revealed that blockade of the CB₁ receptor inhibited PDGF-induced proliferation and migration of human coronary artery smooth muscle cells (Rajesh *et al.*, 2008), key events in plaque progression and vessel restenosis. Furthermore AEA, at micromolar concentrations, has been observed to promote reactive oxygen species (ROS) generation and apoptotic cell death in human coronary artery endothelial cells; an effect which was significantly attenuated by CB₁ receptor antagonism (Rajesh *et al.*, 2010). While key observations in studies using synthetic cannabinoids have provided evidence of an anti-atherosclerotic and anti-inflammatory role of CB₂ receptor activation where lesion development and pro-inflammatory cytokine activity is downregulated by receptor signalling (Steffens *et al.*, 2005; Rajesh *et al.*, 2007), other studies have demonstrated that

endogenous activation of these receptors can induce both pro- and anti-inflammatory actions depending on the concentration and biosynthetic origin of the endocannabinoid (Gallily *et al.*, 2000; Gokoh *et al.*, 2005).

5.4.4.1 EPA supplementation and tissue endocannabinoid levels

In the present study, supplementation of the atherogenic diet with EPA significantly attenuated the diet induced elevation of endocannabinoids in all tissues examined. Concomitant with its hypolipidaemic effects, EPA supplementation significantly lowered elevated AEA levels in the brain and heart, and lowered 2-AG levels in the vasculature. The ability of EPA to modulate tissue endocannabinoid levels is not unexpected given that incorporation of ω -3 PUFAs into membrane phospholipids alters the ω -3/ ω -6 PUFA ratio and thus the availability of arachidonic acid for endocannabinoid biosynthesis (both AEA and 2-AG), an effect which has been previously reported in brain tissue of mice fed a DHA-enriched diet (Wood *et al.*, 2010). In contrast, a dietary study in Sprague-Dawley rats observed no change in brain endocannabinoids in response to a fish oil enriched diet (Artmann *et al.*, 2008). However as the intervention period lasted only 7 days, these findings would suggest a substantially longer time period is required for the alteration of tissue phospholipid content and ultimately, endocannabinoid content. Moreover, these studies were undertaken in normocholesterolaemic animals.

Normalisation of the hyperlipidaemia-activated endocannabinoid system in the heart may represent one of the underlying mechanisms in which the propounded cardioprotective effects of EPA supplementation are conferred. Indeed, several studies have reported a beneficial effect of ω -3 PUFAs in experimental myocardial infarction, where ω -3 PUFA supplementation or an increase in the ω -3/ ω -6 PUFA ratio has been shown to reduce infarct size and systemic inflammatory marker circulation, an effect which was linked to activation of the reperfusion injury salvage kinase (RISK) pathway (Abdukeyum, Owen and McLennan, 2008; Rondeau *et al.*, 2011). Furthermore, studies have reported beneficial effects of EPA supplementation on both atrial and ventricular arrhythmias in several animal models (Yang *et al.*, 1993; Tsuburaya *et al.*, 2011). As previously discussed, CB₁ receptor activation has been linked to exacerbation of myocardial injury and heart failure. In light of the observation that EPA supplementation significantly attenuated the hyperlipidaemia induced elevation of cardiac AEA levels in the present study, this finding suggests that a potential cardioprotective mechanism of EPA could be to reduce endocannabinoid mediated CB₁ receptor activation.

The anti-atherosclerotic effects of ω -3 PUFAs at the level of the blood vessel have been attributed to plaque stabilisation and modulation of the atherosclerotic inflammatory response, including decreased

pro-inflammatory cytokine production (TNF- α , IL-8), decreased monocyte infiltration (reduced MCP-1, VCAM-1, ICAM-1 expression) and decreased platelet activation (Yaqoob and Calder, 1995; Zhao *et al.*, 2004; Yamada *et al.*, 2008). Indeed a correlation between low serum ω 3/ ω 6 PUFA ratios and vulnerable plaques has been identified in patients exhibiting CAD (Kashiyama *et al.*, 2011). Although CB₂ receptor activation has been shown to mediate anti-atherosclerotic actions in some studies, the observation from the present studies (Chapter 4) that activation of CB₂ receptors with JWH133 causes an increased release of MCP-1 from activated macrophages, coupled with the observed reduction in vascular 2-AG and AEA levels by EPA *in vivo*, is suggestive of an interaction between EPA and the endocannabinoids playing a part in the anti-atherosclerotic effects of ω -3 PUFAs. This notion is further supported by the observation from the present studies that DHA directly inhibited endocannabinoid production by activated macrophages *in vitro* (Chapter 4). It is possible therefore that the macrophage is one of the sources of the vascular endocannabinoids.

5.4.4.2 Fenofibrate supplementation and tissue endocannabinoid levels

The present study provided the novel finding that fenofibrate supplementation significantly alters the concentrations of endocannabinoids in tissues from hyperlipidaemic ApoE^{-/-} mice. While several endogenous and synthetic endocannabinoid ligands have been demonstrated to activate PPARs (Sun *et al.*, 2007), the current findings represent the first *in vivo* evidence of PPAR associated modulation of tissue endocannabinoids. Compared to ApoE^{-/-} mice fed the atherogenic diet alone, fenofibrate supplementation significantly attenuated elevated AEA concentrations in brain and aortic tissue and substantially, albeit not significantly, in cardiac tissue. The effect of fenofibrate on 2-AG tissue concentrations however, was minimal. From the present study, it is not clear whether fenofibrate is influencing endocannabinoid synthesis directly, through PPAR α agonism, or indirectly via non-specific lipid lowering. It was previously reported that both fenofibrate and EPA treatment attenuated hyperlipidaemia to a similar degree. While both fenofibrate and EPA lowered tissue endocannabinoid concentrations, they exerted different effects in terms of the endocannabinoid being reduced (either AEA or 2-AG, or both) which was dependent upon the tissue type being examined. If the effects of fenofibrate were due solely to non-specific lipid lowering, it could be assumed that both fenofibrate and EPA would exert similar effects on tissue endocannabinoids; therefore it is possible that fenofibrate may be mediating its effects, at least in part, via PPAR α agonism. Indeed, evidence that PPARs are expressed in the heart (Braissant *et al.*, 1996) and in blood vessels (coronary artery and aortic endothelial cells and vascular smooth muscle cells) supports this notion (Inoue *et al.*, 1998; Marx *et al.*, 1998).

Taberero et al. (2002) observed reduced myocardial infarct size and improved contractile function following ischemia/reperfusion induced injury in fenofibrate supplemented C57BL/6J mice, compared to sham controls. Moreover, upregulation of PPAR α mRNA and protein expression was linked to a reduced occurrence of severe ventricular arrhythmias following ischemia/reperfusion induced injury in normocholesterolaemic rats (Ravingerová *et al.*, 2009); a finding which would suggest agonism of this receptor could have a similar effect. Fenofibrate was also demonstrated to attenuate the development of heart failure in Dahl salt sensitive rats fed a high salt diet (Ichihara *et al.*, 2006). In the setting of atherosclerosis, fenofibrate treatment has been demonstrated to enhance plaque stability. In a rabbit model of experimental atherosclerosis, fenofibrate supplementation induced significant regression of established plaques; an effect associated with reduced macrophage infiltration and increased smooth muscle cell and collagen content of plaques (Corti *et al.*, 2007). Furthermore it was demonstrated in a rabbit model of plaque rupture, that fenofibrate supplementation improved re-endothelialisation and attenuated arterial tissue factor expression, findings which together suggest increased plaque stability and reduced thrombogenicity (Jeanpierre *et al.*, 2009).

The mechanism(s) underlying the described cardioprotective and anti-atherosclerotic actions of fenofibrate remain under scrutiny. In the present study, hyperlipidaemia was demonstrated to induce overactivation of the endocannabinoid system which, as described previously, may be conducive to cardiac and vasculature disease pathology. It is possible that fenofibrate mediated normalisation of elevated tissue endocannabinoid concentrations, either through the non-specific effects of lipid lowering or through direct PPAR α agonism, could represent a possible mechanism in which fenofibrate mediates its beneficial effects.

5.4.5 The impact of an atherogenic diet on endothelial function

Endothelial dysfunction, characterised by abnormal vascular vasoreactivity, has been reported in the coronary and peripheral circulation of patients with established coronary artery disease. Moreover, vasodilatory dysfunction has been deemed a predictor of increased cardiovascular risk (Suwaidi *et al.*, 2000; Heitzer *et al.*, 2001). Compared to baseline measurements obtained in chow fed wild-type mice, high fat feeding of ApoE^{-/-} mice significantly blunted depressor responses to the endothelium dependent vasodilator bradykinin – an indication of impaired vasorelaxation and endothelial dysfunction in these animals. This finding represents the first *in vivo* demonstration of an association between hypercholesterolemia and endothelial dysfunction in the ApoE^{-/-} model; an association which has previously only been described in ApoE^{-/-} mice *ex vivo* using aortic ring preparations. However, this finding is in complement to a wealth of *in vivo* studies using both human and animal (porcine,

non-human primate, rabbit and murine) models (Cohen *et al.*, 1988; Creager *et al.*, 1990; Sellke *et al.*, 1990; Laight *et al.*, 1996; D'Uscio, Smith and Katusic, 2001).

Administration of the NO-donor, sodium nitroprusside, induced a vasodepressor response in both control and hypercholesterolaemic mice, an effect which has been previously reported in *ex vivo* studies using vessels from high fat fed ApoE^{-/-} mice (Deckert *et al.*, 1999; Kaul *et al.*, 2004). This finding suggests that, in the ApoE^{-/-} group, the underlying vascular smooth muscle cells remained responsive to NO, and that the impaired vasodilatation observed in response to bradykinin administration was specific to endothelial activity. Heart rate was not found to vary significantly between experimental groups during endothelial function studies, which would suggest that the depressor responses induced by both bradykinin and sodium nitroprusside were likely mediated via an effect on the vasculature and not in response to a fall in heart rate. Furthermore, there was no significant compensatory increase in heart rate associated with the depressor responses.

Although it was not explored in the present study, the mechanism(s) underlying the impaired endothelium dependent vasodilation associated with hyperlipidaemia could be attributed to the modulation of several pathways, including (a) a change in bradykinin receptor (BR) expression; (b) nitric oxide production (endothelial nitric oxide synthase (eNOS) activity); (c) ROS generation; (d) anti-oxidant enzymatic activity and (e) oxidation of plasma lipoproteins. Reduced NO production, due to reduced eNOS activity and/or increased sequestration of NO by ROS may lead to reduced NO availability and hence reduced NO mediated vasodilation. Indeed in the ApoE^{-/-} model, studies have suggested a decreased availability of NO as a key mechanism underlying hypercholesterolemia mediated endothelial dysfunction. Maintenance of ApoE^{-/-} mice on a Western style diet was observed to upregulate the expression of NADPH oxidase 2 (Nox2), a ROS generating membrane bound enzyme expressed on endothelial cells, and concomitantly, to decrease NO bioavailability (Judkins *et al.*, 2010). Furthermore, the progression of atherosclerosis was impaired in high fat fed ApoE^{-/-} mice deficient in NADPH oxidase (Barry-Lane *et al.*, 2001). Thus it is likely that upregulated ROS production plays a role in endothelial dysfunction in the ApoE^{-/-} mouse.

5.4.5.1 EPA/ fenofibrate supplementation and endothelial function

As previously discussed, both EPA and fenofibrate supplementation of high fat fed ApoE^{-/-} mice induced significant lipid-lowering effects leading to a marked improvement of the hyperlipidaemia induced by the atherogenic diet. In particular, EPA and fenofibrate were observed to lower plasma total cholesterol and LDL-cholesterol levels to a similar degree. Given the reported inverse association between plasma cholesterol levels and endothelial dependent vasodilation (Steinberg *et*

al., 1997), and the observation that hyperlipidaemia in the present study was associated with endothelial dysfunction, it may seem likely that both agents would improve endothelial vasoreactivity as a consequence of their effects on lipid profiles.

However, EPA supplementation had no significant effect on hypercholesterolaemia induced endothelial dysfunction. This finding is in agreement with evidence from human studies that indicate negligible benefit of ω -3 PUFA supplementation (doses ranging from 0.45g/d – 3.4g/d EPA + DHA) on endothelial function (Anderson *et al.*, 2010; Sanders *et al.*, 2011; Skulas-ray *et al.*, 2011). In contrast, fenofibrate supplementation significantly attenuated the diet induced endothelial dysfunction observed in control ApoE^{-/-} mice. This finding complements a study conducted by Olukman *et al.* (2010) who reported that fenofibrate supplementation improved endothelial function in diabetic rats; an effect associated with increased aortic NO production and gene expression of anti-oxidant enzymes (superoxide dismutase and catalase). Given that both EPA and fenofibrate improved hypercholesterolaemia, but only fenofibrate improved endothelial function, this may suggest that the vasculoprotective effects of the latter are independent of its effects on lipid-lowering.

The clear disparity between the ability of EPA and fenofibrate to preserve endothelial function may be linked to their opposing effects on vascular endocannabinoid concentrations: EPA supplementation significantly attenuated 2-AG levels whereas fenofibrate supplementation significantly attenuated AEA levels. Together these findings suggest that, in the present study, the reduction of vascular AEA levels may explain the improved endothelial function associated with fenofibrate supplementation. Activation of CB₁ receptors is known to promote oxidative stress and apoptosis in cells of the vascular wall. Studies have demonstrated an increase in inflammatory marker production (TNF- α , MCP-1, IL-1 β , IL-6 and IL-8), ROS generation and the activation of p38/Jun N-terminal kinase (JNK) mitogen-activated protein kinases (MAPKs), kinases involved in cell death pathways, in response to CB₁ receptor activation in macrophages and endothelial cells (Han *et al.*, 2009; Sagamura *et al.*, 2009; Rajesh *et al.*, 2010). Given that AEA preferentially binds CB₁ receptors, and increases ROS generation dose dependently (Rajesh *et al.*, 2010), it is possible that excessive production of AEA in the vasculature in response to hypercholesterolaemia may contribute to endothelial dysfunction through the promotion of oxidative stress and inflammation. However, as the differential effects of EPA and fenofibrate supplementation on vascular AEA concentrations are very subtle (EPA also reduces the concentration of vascular AEA, although not significantly), the discrepancy between their effects on endothelial function are unlikely to be explained solely by modulation of vascular AEA concentrations. Further investigation is therefore essential to determine the mechanism underlying the differential effects of EPA and fibrate on endothelial function.

5.4.6 Conclusion

In summary, maintenance of ApoE^{-/-} mice on an atherogenic diet induced marked hyperlipidaemia, altered cardiac collagen cross-linking, induced significant endothelial dysfunction and elevated tissue reservoirs of endocannabinoids. Intriguingly, endothelial dysfunction was associated with significantly elevated AEA and 2-AG levels in the vasculature, which could be interpreted as suggestive of a detrimental role of these mediators on endothelial function. Moreover, while supplementation of the atherogenic diet with EPA had a moderate lowering effect on hyperlipidaemia, it had no effect on endothelial dysfunction or on 2-AG or AEA levels in the vasculature. In contrast, fenofibrate supplementation significantly improved the hyperlipidaemic profile and endothelial dysfunction, an effect which was in association with significantly attenuated AEA levels in the vasculature. Therefore it is postulated that ligands of the endocannabinoid system may play a role in hyperlipidaemia induced endothelial dysfunction. Furthermore, the hyperlipidaemia induced elevation of cardiac endocannabinoid concentrations was normalised through dietary intervention with both EPA and fibrate. As these agents have been reported as beneficial in the setting of myocardial ischaemia and the associated adverse electrophysiological events (i.e. ventricular arrhythmias), it is possible that such cardioprotective effects are related to attenuation of the overactive endocannabinoid system.

Chapter 6: General Discussion

6.1 Key Findings

The benefits of PUFA consumption were first highlighted by Dyerberg and colleagues, who demonstrated that Greenland Inuit populations exhibit low mortality rates from coronary heart disease despite consuming a diet rich in fat; a finding which was attributed to the predominance of PUFAs as opposed to SFAs in the diet (Dyerberg, Bang and Hjorne, 1975). Anti-atherosclerotic actions of ω -3 PUFAs have subsequently been demonstrated (Thies *et al.*, 2003; Matsumoto *et al.*, 2008), although the mechanisms are not yet fully understood. In light of reports that increased dietary intake of ω -3 PUFAs influences endocannabinoid levels (Wood *et al.*, 2010), and that synthetic cannabinoids exert anti-atherosclerotic actions (Steffens *et al.*, 2005), the present study was designed to examine the anti-atherosclerotic effects of ω -3 PUFAs in 1) an *in vitro* model of macrophage activity and 2) a murine model of atherosclerosis and to determine whether or not these effects involve a functional role of the endocannabinoid system. The present study has demonstrated, at the cellular level, that activation of the endocannabinoid system altered intracellular uptake of the ω -3 PUFA, DHA, in activated macrophages, signifying a functional role of the endocannabinoid system in the activity of these cells. Moreover, DHA was found to inhibit macrophage synthesis of 2-AG, evidence of a direct association between the endocannabinoid system and the ω -3 PUFAs, an effect which was mimicked by the PPAR α agonist, fenofibrate. In an *in vivo* model of atherosclerosis, maintenance on an atherogenic diet induced significant hyperlipidaemia, an effect which was associated with endothelial dysfunction, cardiac remodelling, and elevated tissue endocannabinoid levels. Supplementation of the atherogenic diet with the ω -3 PUFA, EPA, while having minimal impact on endothelial dysfunction or cardiac remodelling, moderately improved the hyperlipidaemic profile and significantly attenuated elevated tissue endocannabinoid levels. Finally, supplementation of the atherogenic diet with fenofibrate significantly attenuated hyperlipidaemia, endothelial dysfunction and elevated endocannabinoids although no effect on cardiac remodelling was observed.

6.1.1 Activated endocannabinoid system in stimulated THP-1 macrophages

Functional activity of the endocannabinoid system was detected in activated THP-1 macrophages. The concentration of the endocannabinoid 2-AG was significantly elevated in PMA stimulated cells, compared to unstimulated cells. This finding is in agreement with a number of studies that have reported basal 2-AG production in both macrophages (RAW264.7, J774, microglial and rat peritoneal) and endothelial cells which is upregulated in response to a number of stimulants including

ionomycin, lipopolysaccharide (LPS) and thrombin (Sugira *et al.*, 1998; Di Marzo *et al.*, 1999; Carrier *et al.*, 2004; Jiang *et al.*, 2009). Neither basal nor altered synthesis of AEA was detected in the present study. This finding is in disagreement with other studies that have demonstrated the production of AEA in macrophages stimulated with LPS or oxLDL (Liu *et al.*, 2003; Carrier *et al.*, 2004; Jiang *et al.*, 2009). However, the lack of inclusion of an inflammatory stimulus in the present study is a likely source of this discrepancy.

6.1.2 Regulation of endocannabinoid synthesis

Evidence of a direct regulation of endocannabinoid activation by ω -3 PUFAs was discovered. DHA was found to exert a significant inhibitory effect on 2-AG synthesis in stimulated macrophages which reduced production to basal levels measured in unstimulated cells. To our knowledge, this finding presents the first demonstration of such an effect in macrophages although DHA has been shown to reduce 2-AG synthesis in adipocytes (Matias *et al.*, 2008). Of the other FAs examined in the present study, neither OA nor EPA had any significant impact on 2-AG synthesis, a finding which was also described in the Matias study. A possible mechanism through which DHA reduced 2-AG synthesis could be to alter the bioavailability of the phospholipid precursors essential for 2-AG production.

Fenofibrate, at equimolar concentrations to DHA, significantly attenuated 2-AG synthesis in stimulated macrophages. This finding constitutes the first reported link of PPAR α agonism and endocannabinoid synthesis in the macrophage. The present study did not investigate the mechanism underpinning this effect however it is possible that fenofibrate is influencing the enzymatic regulation of 2-AG synthesis and/or the pre-cursor pool. As ω -3 PUFAs are also known agonists of PPAR receptors (Xu *et al.*, 1999), DHA and fenofibrate may be influencing endocannabinoid synthesis through the modulation of common cell signalling pathways.

6.1.3 Activated endocannabinoid system and dysregulated FA uptake

Activation of cannabinoid (CB) receptors using a range of endogenous and synthetic CB ligands was demonstrated to influence the process of FA uptake in activated THP-1 macrophages. Selective activation of the CB₁ receptor had no impact on FA uptake, despite a previous report of increased cholesterol uptake in macrophages treated with the CB₁ selective agonist WIN,212-2 (Jiang *et al.*, 2009). Selective activation of the CB₂ receptor significantly attenuated FA uptake. The non-selective CB agonist AEA, which is reported to act at receptors independent of the CB family including TRPV1 and GPR55 (Smart *et al.*, 2000; Ryberg *et al.*, 2007), also induced a significant reduction in

FA uptake. Modulation of FA uptake in activated THP-1 macrophages was thus concluded to be mediated in part, through CB₂ receptor signalling, although other target receptors may also play a role in this effect.

In addition to these findings, it was also discovered that modulation of FA uptake was dependent upon the FA being internalised, as the aforementioned effects were only observed in macrophages exposed to DHA, and not OA or EPA. The mechanism conferring this effect was not investigated in the present study however speculation can be drawn from evidence provided in the literature. Direct activation of PPAR receptors by ω -3 PUFAs and CB ligands (both endogenous and synthetic) has previously been documented (Xu *et al.*, 1999; Bouaboula *et al.*, 2005; Sun *et al.*, 2007). CB₁ receptor activation increases CD36 scavenger receptor mRNA expression, one of the downstream targets of PPAR signalling, in macrophages and peripheral blood mononuclear cells (Malfitano *et al.*, 2007; Jiang *et al.*, 2009). DHA treatment of human colon cancer cells suppresses CD36 scavenger receptor mRNA expression (Madonna *et al.*, 2011). Therefore an overlapping role in PPAR signalling and its regulation of intracellular cholesterol influx/efflux may underlie the present findings.

6.1.4 Hypercholesterolaemia in a murine model of atherosclerosis

The present study demonstrated that maintenance of ApoE^{-/-} mice on an atherogenic diet induced marked hyperlipidaemia. Plasma cholesterol and LDL-cholesterol was significantly elevated by the consumption of a high fat/high cholesterol diet. These findings are in agreement with several studies in ApoE^{-/-} mice fed a high fat diet (Moghadasian *et al.*, 2001; Guo *et al.*, 2005).

The induction of hyperlipidaemia in ApoE^{-/-} mice was associated with a degree of cardiac remodelling. There was no evidence of collagen deposition in the ApoE^{-/-} heart compared to the chow fed wild-type controls, despite previous reports that hypercholesterolaemia induces cardiac fibrosis in LDLr^{-/-} mice and ageing ApoE^{-/-} mice (Kang *et al.*, 2009; Qin *et al.* 2010). However, it was discovered that collagen cross-link levels were elevated and cross-link maturation reduced. While fibrosis has been linked to impaired cardiac function in humans and pigs (Martos *et al.*, 2007; Zhu *et al.*, 2007), the functional impact of remodelling in the ApoE^{-/-} model was not assessed. However evidence from other studies have provided a basis for speculation. In C57BL6 and ApoE^{-/-} mice, high fat feeding was associated with altered cardiac function indicative of increased ventricular stiffness and reduced compliance (Zibadi *et al.*, 2009; Walsh and Wainwright, unpublished).

Hyperlipidaemia in the ApoE^{-/-} mouse was associated with elevated endocannabinoid concentrations in both central (brain) and peripheral (heart and aorta) tissue compared to chow fed wild-type mice, a

finding which is in agreement with a large body of evidence that describes increased tissue endocannabinoid concentrations in pathological conditions (reviewed by Di Marzo, 2008).

Endothelial function was found to be significantly impaired in hyperlipidaemic ApoE^{-/-} mice - the first *in vivo* evidence of a direct correlation between hyperlipidaemia and vasodilatory dysfunction in the ApoE^{-/-} model. These findings are however in complement to a wealth of *in vitro* and *in vivo* observations in both human and animal models (Cohen *et al.*, 1988; Creager *et al.*, 1990; Sellke *et al.*, 1990; Laight *et al.*, 1996; Xu *et al.*, 2007). Although not examined in the present study, evidence from the literature suggests endothelial dysfunction in the ApoE^{-/-} mouse is due to ROS production and reduced NO bioavailability. Enzymatic activity of NADPH oxidase was upregulated in ApoE^{-/-} mice fed a Western style diet, while plaque progression was retarded in ApoE^{-/-} mice genetically deficient of NADPH oxidase (Barry-Lane *et al.*, 2001; Judkins *et al.*, 2010).

6.1.5 EPA supplementation in the hyperlipidaemic ApoE^{-/-} mouse

Supplementation of the atherogenic diet with EPA had a modest impact on ApoE^{-/-} mouse physiology. EPA supplementation moderately attenuated hyperlipidaemia in accordance with previous studies which have reported cholesterol lowering properties of ω -3 PUFAs (Illingworth *et al.*, 1984; De Roos *et al.*, 2005). Paradoxically, EPA supplementation induced a significant elevation of plasma triglycerides. Given the quantity of experimental and clinical evidence supporting a hypotriglyceridaemic action of the ω -3 PUFAs (as reviewed by Roth and Harris, 2010), this finding was unexpected. However, fish oil supplementation was previously demonstrated to elevate plasma triglycerides in high fat fed ApoE^{-/-} mice (Xu *et al.*, 2007), and as fish oil was demonstrated to reduce LDL receptor activity (Lindsey *et al.*, 1992), it is possible that ω -3 PUFAs augment impaired chylomicron clearance in the ApoE^{-/-} mouse - an anomaly of the model.

EPA supplementation had no impact on hyperlipidaemia associated cardiac remodelling in the ApoE^{-/-} mouse. There are no reports of the effects of ω -3 PUFA supplementation on cardiac remodelling in the ApoE^{-/-} model in which to compare this finding. However, EPA supplementation has been demonstrated to attenuate cardiac fibrosis in ageing, hyperlipidaemic C57BL/6J mice (Halade *et al.*, 2011) and in murine models of pressure overload induced cardiac dysfunction (Duda *et al.*, 2009; Chen *et al.*, 2011).

EPA supplementation significantly attenuated elevated endocannabinoid concentrations in brain, cardiac and aortic tissue. While there are no reports of the effects of EPA on tissue endocannabinoid concentrations in the setting of experimental hyperlipidaemia, the cardioprotective and anti-

atherosclerotic actions of ω -3 PUFAs are well documented. Evidence from animal models indicates that ω -3 PUFA supplementation reduces infarct size in experimental myocardial infarction, reduces systemic inflammatory marker circulation and is beneficial in arrhythmia prevention (Abdukeyum *et al.*, 2008; Mayyas *et al.*, 2011; Rondeau *et al.*, 2011; Tsuburaya *et al.*, 2011). In atherosclerosis pathology, a low serum ω -3/ ω -6 PUFA ratio has been correlated with plaque instability in patients with advanced CAD while direct incorporation of EPA into plaques reduces macrophage infiltration and inflammatory marker production (Thies *et al.*, 2003; Wang *et al.*, 2009; Kashiyaama *et al.*, 2011). Lowering the excessive production of endogenous cannabinoids as observed in the hyperlipidaemic ApoE^{-/-} model, could represent one of the underlying mechanisms conferring the protective effects of EPA.

Endothelial dysfunction in the hyperlipidaemic ApoE^{-/-} mouse was unaltered by supplementation with EPA. Despite the absence of information in the literature regarding the effect of EPA on endothelial function in the ApoE^{-/-} mouse, this finding contributes to a mounting body of evidence from human studies that indicate a negligible effect of ω -3 PUFA supplementation (0.45g/d – 3.4g/d EPA + DHA) on endothelial function (Anderson *et al.*, 2010; Sander *et al.*, 2011; Skulas-ray *et al.*, 2011).

6.1.6 Fenofibrate supplementation in the hyperlipidaemic ApoE^{-/-} mouse

In the hyperlipidaemic ApoE^{-/-} mouse, fenofibrate supplementation of the atherogenic diet was demonstrated to markedly attenuate plasma total and LDL-cholesterol and to moderately reduce plasma triglycerides - findings which are supportive of the hypolipidaemic action of fenofibrate documented in humans (Caslake *et al.*, 1993; Guerin *et al.*, 2003; Davidson *et al.*, 2006).

The study demonstrated that, while improving the hyperlipidaemic profile, fenofibrate treatment did not have any significant impact on hyperlipidaemia induced cardiac remodelling. Reports of the effects of fenofibrate on cardiac remodelling are equivocal. In type 2 diabetes patients, fenofibrate supplementation had a negligible impact on LV diastolic dysfunction (Chew *et al.*, 2008). However, in murine models of hypertension (aldosterone or DOCA-salt induced), fenofibrate attenuated LV hypertrophy and myocardial fibrosis (Ogata *et al.*, 2004; LeBrasseur *et al.*, 2007). Take together, the effect of fenofibrate on structural and functional remodelling in the heart is not yet clear and the disparity between reports may be due to variation in species dependent disease pathology.

The present study provided the novel finding that fenofibrate supplementation influences tissue endocannabinoid concentrations. Hypercholesterolaemia associated elevations in the AEA, but not 2-AG, content of brain and aortic tissue was significantly attenuated by dietary supplementation with

fenofibrate. It is unlikely that the aforementioned effects of fenofibrate were due solely to non-specific lipid lowering since both EPA and fenofibrate attenuated hyperlipidaemia to a similar degree, yet exerted differential effects on endocannabinoid concentrations. As fenofibrate represents a selective agonist of PPAR α receptors, it is possible that activation of PPARs may play a role in modulating tissue endocannabinoid concentrations.

Finally, fenofibrate supplementation significantly attenuated hyperlipidaemia induced endothelial dysfunction. Given that the present study provided the first *in vivo* evidence of an association between hyperlipidaemia and endothelial dysfunction in the ApoE^{-/-} mouse, this effect of fenofibrate represents a novel observation in the ApoE^{-/-} model. However, the vasorelaxant properties of fenofibrate have been previously reported *ex vivo*, in vessel studies from normotensive and hypertensive rats (Li *et al.*, 2010; Olukman *et al.*, 2010). The capacity of fenofibrate to preserve endothelial function in the hyperlipidaemic ApoE^{-/-} mouse was unlikely to be related to its hypolipidaemic actions, as EPA also normalised the hyperlipidaemic profile yet failed to modulate endothelial function. It is possible therefore, that the effects of fenofibrate are, in part, due to its influence of vascular AEA levels, which in the present study, were not significantly altered by EPA supplementation. AEA is known to directly enhance the generation of ROS and activation of apoptosis pathways in macrophages and endothelial cells (Rajesh *et al.*, 2010). Moreover, studies have implicated a pro-inflammatory and pro-oxidative role of CB₁ receptor agonism in cells of the vascular wall (Han *et al.*, 2009; Sagamura *et al.*, 2009). Therefore, one possible mechanism by which fenofibrate preserves endothelial function in the ApoE^{-/-} model may involve normalisation of the excessive vascular AEA levels that characterise the hyperlipidaemic profile of these mice.

6.2 Future studies

6.2.1 Histological examination of atherosclerotic lesion development

The ApoE^{-/-} mouse represents, primarily, a model of atherosclerosis development. While the present study demonstrated the induction of marked hypercholesterolaemia and endothelial dysfunction in response to maintenance on an atherogenic diet, the presence and extent of lesion formation in the vasculature was not assessed. The lack of histological data prevented further characterisation of the high fat diet intervention and importantly, investigation of the effects, if any, of EPA and fenofibrate on lesion formation. Furthermore, it would be of interest to examine the composition of lesions, in order to assess the effect of the interventions on markers of stability (i.e. presence of a lipid core, collagen deposition). The upper section of heart samples (including the attached aorta and

brachiocephalic artery) collected from the dietary study were retained and, while atherosclerotic lesion development in the aortic root and brachiocephalic artery (the prominent site of lesion formation and rupture) was to be assessed histologically, time did not permit the undertaking of these experiments. In the brachiocephalic artery, treatment of serial sections with Masson's Trichrome stain would enable visualisation and comparison of the collagen content (appears blue) and connective tissue (cell nuclei, cytoplasm and surrounding tissue) content (appears red) of lesions. Moreover Oil red O staining, which dyes neutral lipids red, could be employed to identify the lipid content of innominate artery lesions. Quantification of morphological differences in serial sections of vessels would be conducted using Leica Q-Win software.

6.2.2 Cannabinoid receptor antagonist studies

While the present study has demonstrated an association between tissue endocannabinoid levels and endothelial dysfunction, it is not known which cannabinoid receptors are involved in mediating these effects. As there is growing evidence to suggest a detrimental role of CB₁ receptor signalling in many pathologies, including atherosclerosis development, examining the impact of CB₁ receptor blockade may further understanding of its role in the effects described in the current study. Repeating the dietary intervention with the additional inclusion of a CB₁ selective antagonist (e.g. rimonabant) would allow the involvement of this receptor in mediating endothelial dysfunction to be characterised. In addition, the involvement of specific cannabinoid receptors could be further investigated by conducting immunostaining of serial sections collected from the brachiocephalic artery and aortic root sections as described previously. Labelling of sections with CB₁ and CB₂ receptor specific antibodies would allow visualisation of the localisation and extent of CB receptor expression, data which together with the aforementioned antagonist studies would provide an understanding of the specific receptors mediating the effects described in the present study.

6.3 Conclusion

In conclusion, despite the well documented anti-atherosclerotic and cardioprotective effects of long chain ω -3 PUFAs, the exact underlying mechanisms have yet to be fully elucidated. Using both *in vitro* and *in vivo* approaches, the present study demonstrated an association between the effects of ω -3 PUFAs and functional modulation of the endocannabinoid system, the latter of which has been implicated in numerous disease pathologies (Di Marzo, 2008). The *in vitro* experiments conducted in this study demonstrated the capacity of DHA to significantly attenuate the production of 2-AG in

activated THP-1 macrophages. Moreover, exogenous CB receptor signalling interfered with DHA uptake in activated macrophages, an effect which was shown to be mediated, in part, via the CB₂ receptor. In the ApoE^{-/-} mouse, a murine model of atherosclerosis development, maintenance on an atherogenic diet induced marked hypercholesterolaemia, endothelial dysfunction and elevated tissue concentrations of the endocannabinoids AEA and 2-AG. Taken together, these findings suggest a detrimental involvement of the endocannabinoid system and its activation in hypercholesterolaemia in the ApoE^{-/-} model. Supplementation of the atherogenic diet with EPA significantly attenuated hypercholesterolaemia and normalised tissue endocannabinoid levels, specifically AEA in the brain and heart, and 2-AG in the vasculature, although there was no alleviation of endothelial dysfunction. Given the mounting body of evidence that suggests dysregulation of the endocannabinoid system is conducive to the progression of certain disease pathologies, manipulation of its activity through long chain ω-3 PUFA administration may have therapeutic potential.

Chapter 7: References

- GISSI-Prevenzione Investigators. Dietary supplementation with n-3 polyunsaturated fatty acids and vitamin E after myocardial infarction: results of the GISSI-Prevenzione trial. 1999. *The Lancet*, 354(9177), pp. 447-455
- AIELLO, R.J. et al., 1999. Monocyte Chemoattractant Protein-1 Accelerates Atherosclerosis in Apolipoprotein E-Deficient Mice. *Arteriosclerosis, Thrombosis, and Vascular Biology*, 19(6), pp. 1518-1525
- AIKAWA, M. et al., 1998. Lipid Lowering by Diet Reduces Matrix Metalloproteinase Activity and Increases Collagen Content of Rabbit Atheroma : A Potential Mechanism of Lesion Stabilization. *Circulation*, 97(24), pp. 2433-2444
- ALLAVENA, P. et al., 1998. IL-10 prevents the differentiation of monocytes to dendritic cells but promotes their maturation to macrophages. *European journal of immunology*, 28(1), pp. 359-369
- AMENTO, E. et al., 1991. Cytokines and growth factors positively and negatively regulate interstitial collagen gene expression in human vascular smooth muscle cells. *Arteriosclerosis, Thrombosis, and Vascular Biology*, 11(5), pp. 1223-1230
- ANDERSON, J.S. et al., 2010. Relation of omega-3 fatty acid and dietary fish intake with brachial artery flow-mediated vasodilation in the Multi-Ethnic Study of Atherosclerosis. *The American Journal of Clinical Nutrition*, 92(5), pp. 1204-1213
- ANNUZZI, G. et al., 2010. Differential alterations of the concentrations of endocannabinoids and related lipids in the subcutaneous adipose tissue of obese diabetic patients. *Lipids in Health and Disease*, 9(43),
- ANZINGER, J.J. et al., 2010. Native Low-Density Lipoprotein Uptake by Macrophage Colony-Stimulating Factor-Differentiated Human Macrophages Is Mediated by Macropinocytosis and Micropinocytosis. *Arteriosclerosis, Thrombosis, and Vascular Biology*, 30(10), pp. 2022-2031
- ARRIBAS, S.M., HINEK, A. and GONZÁLEZ, M.C., 2006. Elastic fibres and vascular structure in hypertension. *Pharmacology & therapeutics*, 111(3), pp. 771-791
- ARTMANN, A. et al., 2008. Influence of dietary fatty acids on endocannabinoid and N-acylethanolamine levels in rat brain, liver and small intestine. *Biochimica et Biophysica Acta (BBA) - Molecular and Cell Biology of Lipids*, 1781(4), pp. 200-212
- AUWERX, J.H., 1991. The human leukemia cell line, THP-1: A multifaceted model for the study of monocyte-macrophage differentiation. *Experientia*, 47(1), pp. 22-31
- BALL, R.Y. et al., 1995. Evidence that the death of macrophage foam cells contributes to the lipid core of atheroma. *Atherosclerosis*, 114(1), pp. 45-54
- BARRY-LANE, P.A. et al., 2001. p47^{phox} is required for atherosclerotic lesion progression in *ApoE*^{-/-} mice. *The Journal of Clinical Investigation*, 108(10), pp. 1513-1522

- BARTELT, A. et al., 2011. Altered endocannabinoid signalling after a high-fat diet in *ApoE*^{-/-} mice: relevance to adipose tissue inflammation, hepatic steatosis and insulin resistance. *Diabetologia*, 54(11), pp. 2900-2910
- BÁTKAI, S. et al., 2007. Cannabinoid-2 receptor mediates protection against hepatic ischemia/reperfusion injury. *The FASEB Journal*, 21(8), pp. 1788-1800
- BÁTKAI, S. et al., August 2007. Decreased age-related cardiac dysfunction, myocardial nitrate stress, inflammatory gene expression, and apoptosis in mice lacking fatty acid amide hydrolase. *American Journal of Physiology - Heart and Circulatory Physiology*, 293(2), pp. H909-H918
- BAUMANN, K.H. et al., 1999. Dietary Ω -3, Ω -6, and Ω -9 Unsaturated Fatty Acids and Growth Factor and Cytokine Gene Expression in Unstimulated and Stimulated Monocytes : A Randomized Volunteer Study. *Arteriosclerosis, Thrombosis, and Vascular Biology*, 19(1), pp. 59-66
- BELLAMY, G. and BORNSTEIN, P., 1971. Evidence for Procollagen, a Biosynthetic Precursor of Collagen. *Proceedings of the National Academy of Sciences of the United States of America*, 68(6), pp. 1138-1142
- BENDITT, E.P. and BENDITT, J.M., 1973. Evidence for a monoclonal origin of human atherosclerotic plaques. *Proceedings of the National Academy of Sciences of the United States of America*, 70(6), pp. 1753-1756
- BERGER, A. et al., 2001. Anandamide and diet: Inclusion of dietary arachidonate and docosahexaenoate leads to increased brain levels of the corresponding N-acyl ethanolamines in piglets. *Proceedings of the National Academy of Sciences*, 98(11), pp. 6402-6406
- BERGER, C. et al., 2004. Massive accumulation of N-acyl ethanolamines after stroke. Cell signalling in acute cerebral ischemia? *Journal of neurochemistry*, 88(5), pp. 1159-1167
- BIRGIT, F. and POBER, J.S., 2012. Vascular Endothelial Cells as Immunological Targets in Atherosclerosis. In: G. WICK and C. GRUNDTMAN, eds. *Inflammation and Atherosclerosis*. Springer Vienna. pp. 87-114
- BISOGNO, T. et al., 2003. Cloning of the first sn1-DAG lipases points to the spatial and temporal regulation of endocannabinoid signaling in the brain. *The Journal of cell biology*, 163(3), pp. 463-468
- BLANKMAN, J.L., SIMON, G.M. and CRAVATT, B.F., 2007. A Comprehensive Profile of Brain Enzymes that Hydrolyze the Endocannabinoid 2-Arachidonoylglycerol. *Chemistry and Biology*, 14(12), pp. 1347-1356
- BOUABOULA, M. et al., 2005. Anandamide induced PPAR γ transcriptional activation and 3T3-L1 preadipocyte differentiation. *European journal of pharmacology*, 517(3), pp. 174-181
- BOUHLEL, M.A. et al., 2007. PPAR γ Activation Primes Human Monocytes into Alternative M2 Macrophages with Anti-inflammatory Properties. *Cell Metabolism*, 6(2), pp. 137-143

- BOYLE, J.J. et al., 2009. Coronary Intraplaque Hemorrhage Evokes a Novel Atheroprotective Macrophage Phenotype. *The American Journal of Pathology*, 174(3), pp. 1097-1108
- BRAISSANT, O. et al., 1996. Differential expression of peroxisome proliferator-activated receptors (PPARs): tissue distribution of PPAR-alpha, -beta, and -gamma in the adult rat. *Endocrinology*, 137(1), pp. 354-366
- BRAUD, S. et al., 2000. Activation of rabbit blood platelets by anandamide through its cleavage into arachidonic acid. *FEBS letters*, 471(1), pp. 12-16
- BRENNAN, J.T. et al., 2009. α -Linolenic acid supplementation and conversion to n-3 long-chain polyunsaturated fatty acids in humans. *Prostaglandins, Leukotrienes and Essential Fatty Acids*, 80(2-3), pp. 85-91
- BUETTNER, R. et al., 2006. Defining high-fat-diet rat models: metabolic and molecular effects of different fat types. *Journal of Molecular Endocrinology*, 36(3), pp. 485-501
- BURDYGA, G. et al., 2004. Expression of cannabinoid CB1 receptors by vagal afferent neurons is inhibited by cholecystokinin. *The Journal of neuroscience: the official journal of the Society for Neuroscience*, 24(11), pp. 2708-2715
- BURR, M.L. et al., 1989. Effects of changes in fat, fish, and fibre intakes on death and myocardial reinfarction:diet and reinfarction trial (DART). *The Lancet*, 334(8666), pp. 757-761
- BURRI, L. et al., 2011. Differential effects of krill oil and fish oil on the hepatic transcriptome in mice. *Frontiers in Genetics*, 2, DOI: 10.3389/fgene.2011.00045
- CARRIER, E.J. et al., 2004. Cultured Rat Microglial Cells Synthesize the Endocannabinoid 2-Arachidonylglycerol, Which Increases Proliferation via a CB2 Receptor-Dependent Mechanism. *Molecular pharmacology*, 65(4), pp. 999-1007
- CASLAKE, M. et al., 1993. Fenofibrate and LDL metabolic heterogeneity in hypercholesterolemia. *Arteriosclerosis, Thrombosis, and Vascular Biology*, 13(5), pp. 702-711
- CASLAKE, M. et al., 1993. Fenofibrate and LDL metabolic heterogeneity in hypercholesterolemia. *Arteriosclerosis, Thrombosis, and Vascular Biology*, 13(5), pp. 702-711
- CAWOOD, A.L. et al., 2010. Eicosapentaenoic acid (EPA) from highly concentrated n-3 fatty acid ethyl esters is incorporated into advanced atherosclerotic plaques and higher plaque EPA is associated with decreased plaque inflammation and increased stability. *Atherosclerosis*, 212(1), pp. 252-259
- CHAPMAN, M.J. et al., 2010. Cholesteryl ester transfer protein: at the heart of the action of lipid-modulating therapy with statins, fibrates, niacin, and cholesteryl ester transfer protein inhibitors. *European Heart Journal*, 31(2), pp. 149-164

- CHEN, J. et al., 2011. Omega-3 Fatty Acids Prevent Pressure Overload–Induced Cardiac Fibrosis Through Activation of Cyclic GMP/Protein Kinase G Signaling in Cardiac Fibroblasts / Clinical Perspective. *Circulation*, 123(6), pp. 584-593
- CHEN, X. et al., 2007. Oxidized low density lipoprotein receptor-1 mediates oxidized low density lipoprotein-induced apoptosis in human umbilical vein endothelial cells: Role of reactive oxygen species. *Vascular Pharmacology*, 47(1), pp. 1-9
- CHEW, G.T. et al., August 2008. Hemodynamic Effects of Fenofibrate and Coenzyme Q10 in Type 2 Diabetic Subjects With Left Ventricular Diastolic Dysfunction. *Diabetes care*, 31(8), pp. 1502-1509
- CHO, H.P., NAKAMURA, M.T. and CLARKE, S.D., 1999. Cloning, Expression, and Nutritional Regulation of the Mammalian Δ -6 Desaturase. *Journal of Biological Chemistry*, 274(1), pp. 471-477
- CIANCHI, F. et al., 2008. Cannabinoid Receptor Activation Induces Apoptosis through Tumor Necrosis Factor α -Mediated Ceramide De novo Synthesis in Colon Cancer Cells. *Clinical Cancer Research*, 14(23), pp. 7691-7700
- COHEN, R. et al., 1988. Loss of selective endothelial cell vasoactive functions caused by hypercholesterolemia in pig coronary arteries. *Circulation research*, 63(5), pp. 903-910
- COMINACINI, L. et al., 2000. Oxidized Low Density Lipoprotein (ox-LDL) Binding to ox-LDL Receptor-1 in Endothelial Cells Induces the Activation of NF- κ B through an Increased Production of Intracellular Reactive Oxygen Species. *Journal of Biological Chemistry*, 275(17), pp. 12633-12638
- CONRAD, C.H. et al., 1995. Myocardial Fibrosis and Stiffness With Hypertrophy and Heart Failure in the Spontaneously Hypertensive Rat. *Circulation*, 91(1), pp. 161-170
- CORREA, F. et al., 2005. Activation of cannabinoid CB2 receptor negatively regulates IL-12p40 production in murine macrophages: role of IL-10 and ERK1/2 kinase signaling. *British journal of pharmacology*, 145(4), pp. 441-448
- CORTI, R. et al., 2007. Fenofibrate induces plaque regression in hypercholesterolemic atherosclerotic rabbits: In vivo demonstration by high-resolution MRI. *Atherosclerosis*, 190(1), pp. 106-113
- COSTA, B. et al., 2007. The non-psychoactive cannabis constituent cannabidiol is an orally effective therapeutic agent in rat chronic inflammatory and neuropathic pain. *European journal of pharmacology*, 556(1-3), pp. 75-83
- CRAVATT, B.F. et al., 2001. Supersensitivity to anandamide and enhanced endogenous cannabinoid signaling in mice lacking fatty acid amide hydrolase. *Proceedings of the National Academy of Sciences of the United States of America*, 98(16), pp. 9371-9376
- CREAGER, M.A. et al., 1990. Impaired vasodilation of forearm resistance vessels in hypercholesterolemic humans. *The Journal of Clinical Investigation*, 86(1), pp. 228-234

- D'USCIO, L.V., SMITH, L.A. and KATUSIC, Z.S., 2001. Hypercholesterolemia Impairs Endothelium-Dependent Relaxations in Common Carotid Arteries of Apolipoprotein E-Deficient Mice. *Stroke*, 32(11), pp. 2658-2664
- DAIGNEAULT, M. et al., 2010. The Identification of Markers of Macrophage Differentiation in PMA-Stimulated THP-1 Cells and Monocyte-Derived Macrophages. *PLoS ONE*, 5(1),
- DAUGHERTY, A. et al., 2005. Thematic review series: The Immune System and Atherogenesis. Cytokine regulation of macrophage functions in atherogenesis. *Journal of lipid research*, 46(9), pp. 1812-1822
- DAVIS, H.R. et al., 2001. Ezetimibe, a Potent Cholesterol Absorption Inhibitor, Inhibits the Development of Atherosclerosis in ApoE Knockout Mice. *Arteriosclerosis, Thrombosis, and Vascular Biology*, 21(12), pp. 2032-2038
- DE GRAAF, J. et al., 1993. Identification of multiple dense LDL subfractions with enhanced susceptibility to in vitro oxidation among hypertriglyceridemic subjects. Normalization after clofibrate treatment. *Arteriosclerosis, Thrombosis, and Vascular Biology*, 13(5), pp. 712-719
- DE KIMPE, S.J., ÄNGGÅRD, E.E. and CARRIER, M.J., 1998. Reactive Oxygen Species Regulate Macrophage Scavenger Receptor Type I, but Not Type II, in the Human Monocytic Cell Line THP-1. *Molecular pharmacology*, 53(6), pp. 1076-1082
- DE ROOS, B. et al., 2005. Response of apolipoprotein E*3-Leiden transgenic mice to dietary fatty acids: combining liver proteomics with physiological data. *The FASEB Journal*, 19(7), pp. 813-815
- DECKERT, V. et al., 1999. Impairment of Endothelium-Dependent Arterial Relaxation By High-Fat Feeding in ApoE-Deficient Mice: Toward Normalization By Human ApoA-I Expression. *Circulation*, 100(11), pp. 1230-1235
- DECLERCQ, V. et al., 2005. Paradoxical Effects of Fenofibrate and Nicotinic Acid in Apo E-Deficient Mice. *Journal of Cardiovascular Pharmacology*, 46(1), pp. 18-24
- DEFER, N. et al., 2009. The cannabinoid receptor type 2 promotes cardiac myocyte and fibroblast survival and protects against ischemia/reperfusion-induced cardiomyopathy. *The FASEB Journal*, 23(7), pp. 2120-2130
- DELERIVE, P. et al., 1999. Peroxisome Proliferator-activated Receptor α Negatively Regulates the Vascular Inflammatory Gene Response by Negative Cross-talk with Transcription Factors NF- κ B and AP-1. *Journal of Biological Chemistry*, 274(45), pp. 32048-32054
- DELNESTE, Y. et al., 2003. Interferon- γ switches monocyte differentiation from dendritic cells to macrophages. *Blood*, 101(1), pp. 143-150
- DELSING, D.J.M. et al., 2011. Cannabinoid Receptor 2 Deficiency in Haematopoietic cells Aggravates Early Atherosclerosis in LDL Receptor Deficient Mice. *The Open Cardiovascular Medicine Journal*, 5, pp. 15-21

- DEROCQ, J. et al., 2000. Genomic and Functional Changes Induced by the Activation of the Peripheral Cannabinoid Receptor CB2 in the Promyelocytic Cells HL-60. *Journal of Biological Chemistry*, 275(21), pp. 15621-15628
- DEVANE, W.A. et al., 1992. Isolation and structure of a brain constituent that binds to the cannabinoid receptor. *Science*, 258(5090), pp. 1946-1949
- DI MARZO, V. et al., 1994. Formation and inactivation of endogenous cannabinoid anandamide in central neurons. *Nature*, 327(6507), pp. 686-691
- DI MARZO, V. et al., 1999. Biosynthesis and inactivation of the endocannabinoid 2-arachidonoylglycerol in circulating and tumoral macrophages. *European Journal of Biochemistry*, 264(1), pp. 258-267
- DINH, T.P. et al., 2002. Brain monoglyceride lipase participating in endocannabinoid inactivation. *Proceedings of the National Academy of Sciences*, 99(16), pp. 10819-10824
- DINH, T.P., KATHURIA, S. and PIOMELLI, D., 2004. RNA Interference Suggests a Primary Role for Monoacylglycerol Lipase in the Degradation of the Endocannabinoid 2-Arachidonoylglycerol. *Molecular pharmacology*, 66(5), pp. 1260-1264
- DOKHOLYAN, R.S. et al., 2004. A trial of omega-3 fatty acids for prevention of hypertension. *The American Journal of Cardiology*, 93(8), pp. 1041-1043
- DOL-GLEIZES, F. et al., 2009. Rimonabant, a Selective Cannabinoid CB1 Receptor Antagonist, Inhibits Atherosclerosis in LDL Receptor-Deficient Mice. *Arteriosclerosis, Thrombosis, and Vascular Biology*, 29(1), pp. 12-18
- DOL-GLEIZES, F. et al., 2009. Rimonabant, a Selective Cannabinoid CB1 Receptor Antagonist, Inhibits Atherosclerosis in LDL Receptor-Deficient Mice. *Arteriosclerosis, Thrombosis, and Vascular Biology*, 29(1), pp. 12-18
- DOLLERY, C.M. and LIBBY, P., 2006. Atherosclerosis and proteinase activation. *Cardiovascular research*, 69(3), pp. 625-635
- DUDA, M.K. et al., 2009. Fish oil, but not flaxseed oil, decreases inflammation and prevents pressure overload-induced cardiac dysfunction. *Cardiovascular research*, 81(2), pp. 319-327
- DUHANEY, T.S. et al., 2007. Peroxisome Proliferator-Activated Receptor α -Independent Actions of Fenofibrate Exacerbates Left Ventricular Dilation and Fibrosis in Chronic Pressure Overload. *Hypertension*, 49(5), pp. 1084-1094
- DURANTE, W. et al., 2001. Transforming Growth Factor- β 1 Stimulates L-Arginine Transport and Metabolism in Vascular Smooth Muscle Cells : Role in Polyamine and Collagen Synthesis. *Circulation*, 103(8), pp. 1121-1127

- DYERBERG, J., BANG, H. and HJORNE, N., 1975. Fatty acid composition of the plasma lipids in Greenland Eskimos. *The American Journal of Clinical Nutrition*, 28(9), pp. 958-966
- EDVARDSSON, U. et al., 2006. PPAR α activation increases triglyceride mass and adipose differentiation-related protein in hepatocytes. *Journal of lipid research*, 47(2), pp. 329-340
- EGHBALI, M. et al., 1989. Collagen accumulation in heart ventricles as a function of growth and aging. *Cardiovascular research*, 23(8), pp. 723-729
- FABRICANT, C.G. et al., 1978. Virus-induced atherosclerosis. *The Journal of experimental medicine*, 148(1), pp. 335-340
- FEIG, J.E. et al., 2011. Reversal of Hyperlipidaemia With a Genetic Switch Favorably Affects the Content and Inflammatory State of Macrophages in Atherosclerotic Plaques / Clinical Perspective. *Circulation*, 123(9), pp. 989-998
- FOLCH, J., LEES, M. and STANLEY, G.H.S., 1957. A simple method for the isolation and purification of total lipids from animal tissues. *Journal of Biological Chemistry*, 226(1), pp. 497-509
- FOLCIK, V.A. et al., 1995. Lipoxygenase contributes to the oxidation of lipids in human atherosclerotic plaques. *The Journal of Clinical Investigation*, 96(1), pp. 504-510
- FRANK, P.G. et al., 2004. Genetic Ablation of Caveolin-1 Confers Protection Against Atherosclerosis. *Arteriosclerosis, Thrombosis, and Vascular Biology*, 24(1), pp. 98-105
- FRONTINI, M.J. et al., 2009. Lipid Incorporation Inhibits Src-Dependent Assembly of Fibronectin and Type I Collagen by Vascular Smooth Muscle Cells. *Circulation research*, 104(7), pp. 832-841
- FRY, D., HERDERICK, E. and JOHNSON, D., 1993. Local intimal-medial uptakes of 125I-albumin, 125I-LDL, and parenteral Evans blue dye protein complex along the aortas of normocholesterolemic minipigs as predictors of subsequent hypercholesterolemic atherogenesis. *Arteriosclerosis, Thrombosis, and Vascular Biology*, 13(8), pp. 1193-1204
- FU, M. et al., 2001. Peroxisome Proliferator-activated Receptor γ Inhibits Transforming Growth Factor β -induced Connective Tissue Growth Factor Expression in Human Aortic Smooth Muscle Cells by Interfering with Smad3. *Journal of Biological Chemistry*, 276(49), pp. 45888-45894
- FUJIMOTO, D. et al., 1978. The structure of pyridinoline, a collagen crosslink. *Biochemical and biophysical research communications*, 84(1), pp. 52-57
- GALLILY, R., BREUER, A. and MECHOULAM, R., 2000. 2-Arachidonylglycerol, an endogenous cannabinoid, inhibits tumor necrosis factor- α production in murine macrophages, and in mice. *European journal of pharmacology*, 406(1), pp. R5-R7
- GELEIJNSE, J.M. et al., 2002. Blood pressure response to fish oil supplementation: metaregression analysis of randomized trials. *Journal of Hypertension*, 20(8), pp. 1493-1499

- GIUFFRIDA, A. et al., 2004. Cerebrospinal anandamide levels are elevated in acute schizophrenia and are inversely correlated with psychotic symptoms. *Neuropsychopharmacology*, 29(11), pp. 2108-2114
- GLASS, M. and FELDER, C.C., 1997. Concurrent Stimulation of Cannabinoid CB1 and Dopamine D2 Receptors Augments cAMP Accumulation in Striatal Neurons: Evidence for a G_s Linkage to the CB1 Receptor. *The Journal of neuroscience: the official journal of the Society for Neuroscience*, 17(14), pp. 5327-5333
- GOBBI, G. et al., 2005. Antidepressant-like activity and modulation of brain monoaminergic transmission by blockade of anandamide hydrolysis. *Proceedings of the National Academy of Sciences of the United States of America*, 102(51), pp. 18620-18625
- GOKOH, M. et al., 2007. 2-Arachidonoylglycerol Enhances the Phagocytosis of Opsonized Zymosan by HL-60 Cells Differentiated into Macrophage-Like Cells. *Biological & pharmaceutical bulletin*, 30(7), pp. 1199-1205
- GOKOH, M. et al., 2005. 2-Arachidonoylglycerol, an endogenous cannabinoid receptor ligand, enhances the adhesion of HL-60 cells differentiated into macrophage-like cells and human peripheral blood monocytes. *FEBS letters*, 579(28), pp. 6473-6478
- GÓMEZ, R. et al., 2002. A Peripheral Mechanism for CB1 Cannabinoid Receptor-Dependent Modulation of Feeding. *The Journal of neuroscience: the official journal of the Society for Neuroscience*, 22(21), pp. 9612-9617
- GREAVES, D.R. and GORDON, S., 2009. The macrophage scavenger receptor at 30 years of age: current knowledge and future challenges. *Journal of lipid research*, 50(Supplement), pp. S282-S286
- GU, L. et al., 1998. Absence of Monocyte Chemoattractant Protein-1 Reduces Atherosclerosis in Low Density Lipoprotein Receptor-Deficient Mice. *Molecular cell*, 2(2), pp. 275-281
- GUERIN, M. et al., 2002. Dose-dependent action of atorvastatin in type IIB hyperlipidaemia: preferential and progressive reduction of atherogenic apoB-containing lipoprotein subclasses (VLDL-2, IDL, small dense LDL) and stimulation of cellular cholesterol efflux. *Atherosclerosis*, 163(2), pp. 287-296
- GUERIN, M. et al., 2003. Action of Ciprofibrate in Type IIB Hyperlipoproteinemia: Modulation of the Atherogenic Lipoprotein Phenotype and Stimulation of High-Density Lipoprotein-Mediated Cellular Cholesterol Efflux. *Journal of Clinical Endocrinology & Metabolism*, 88(8), pp. 3738-3746
- GUIDA, M. et al., 2010. The Levels of the Endocannabinoid Receptor CB2 and Its Ligand 2-Arachidonoylglycerol Are Elevated in Endometrial Carcinoma. *Endocrinology*, 151(3), pp. 921-928
- GUO, Y. et al., 2005. Morphological and functional alterations of the cochlea in apolipoprotein E gene deficient mice. *Hearing research*, 208(1-2), pp. 54-67
- GÜRTEL, B. et al., 2009. Apoptosis and fibrosis are early features of heart failure in an animal model of metabolic cardiomyopathy. *International Journal of Experimental Pathology*, 90(3), pp. 338-346

- GUYTON, J.R. and KLEMP, K.F., 1993. Transitional features in human atherosclerosis. Intimal thickening, cholesterol clefts, and cell loss in human aortic fatty streaks. *The American Journal of Pathology*, 143(5), pp. 1444-1457
- HAJRASOULIHA, A.R. et al., 2008. Endogenous cannabinoids contribute to remote ischemic preconditioning via cannabinoid CB2 receptors in the rat heart. *European journal of pharmacology*, 579(1-3), pp. 246-252
- HALADE, G.V. et al., 2011. Fish oil decreases inflammation and reduces cardiac remodeling in rosiglitazone treated aging mice. *Pharmacological Research*, 63(4), pp. 300-307
- HAN, J. et al., 1997. Native and Modified Low Density Lipoproteins Increase the Functional Expression of the Macrophage Class B Scavenger Receptor, CD36. *Journal of Biological Chemistry*, 272(34), pp. 21654-21659
- HANNAH, V.C. et al., 2001. Unsaturated Fatty Acids Down-regulate SREBP Isoforms 1a and 1c by Two Mechanisms in HEK-293 Cells. *Journal of Biological Chemistry*, 276(6), pp. 4365-4372
- HANSEN, S.L. et al., 2009. Ketogenic diet is antiepileptogenic in pentylenetetrazole kindled mice and decrease levels of N-acyl ethanolamines in hippocampus. *Neurochemistry international*, 54(3-4), pp. 199-204
- HANUS, L. et al., 2001. 2-Arachidonyl glyceryl ether, an endogenous agonist of the cannabinoid CB₁ receptor. *Proceedings of the National Academy of Sciences of the United States of America*, 98(7), pp. 3662-3665
- HANUS, L. et al., 2003. Short-term fasting and prolonged semistarvation have opposite effects on 2-AG levels in mouse brain. *Brain research*, 983(1-2), pp. 144-151
- HARIZI, H., CORCUFF, J. and GUALDE, N., 2008. Arachidonic-acid-derived eicosanoids: roles in biology and immunopathology. *Trends in molecular medicine*, 14(10), pp. 461-469
- HARRINGTON, S.C., SIMARI, R.D. and CONOVER, C.A., 2007. Genetic Deletion of Pregnancy-Associated Plasma Protein-A Is Associated With Resistance to Atherosclerotic Lesion Development in Apolipoprotein E-Deficient Mice Challenged With a High-Fat Diet. *Circulation research*, 100(12), pp. 1696-1702
- HARRIS, W.S. et al., 1997. N-3 fatty acids and chylomicron metabolism in the rat. *Journal of lipid research*, 38(3), pp. 503-515
- HARRIS, W.S., POSTON, W.C. and HADDOCK, C.K., 2007. Tissue n - 3 and n - 6 fatty acids and risk for coronary heart disease events. *Atherosclerosis*, 193(1), pp. 1-10
- HARRIS, W., 1997. n-3 fatty acids and serum lipoproteins: human studies. *The American Journal of Clinical Nutrition*, 65(5), pp. 1645S-1654S

- HARTLEY, C.J. et al., 2000. Hemodynamic changes in apolipoprotein E-knockout mice. *American Journal of Physiology - Heart and Circulatory Physiology*, 279(5), pp. H2326-H2334
- HARTWICH, J. et al., 2009. The effect of the plasma n-3/n-6 polyunsaturated fatty acid ratio on the dietary LDL phenotype transformation – Insights from the LIPGENE study. *Clinical Nutrition*, 28(5), pp. 510-515
- HAZEN, S.L. and HEINECKE, J.W., 1997. 3-Chlorotyrosine, a specific marker of myeloperoxidase-catalyzed oxidation, is markedly elevated in low density lipoprotein isolated from human atherosclerotic intima. *The Journal of Clinical Investigation*, 99(9), pp. 2075-2081
- HECTOR, E.E. et al., 2010. Quantitative measurement of mature collagen cross-links in human carotid artery plaques. *Atherosclerosis*, 211(2), pp. 471-474
- HEEBA, G. et al., 2009. Anti-atherogenic effect of statins: role of nitric oxide, peroxynitrite and haem oxygenase-1. *British journal of pharmacology*, 156(8), pp. 1256-1266
- HEITZER, T. et al., 2001. Endothelial Dysfunction, Oxidative Stress, and Risk of Cardiovascular Events in Patients With Coronary Artery Disease. *Circulation*, 104(22), pp. 2673-2678
- HIGASHIKATA, T. et al., 2006. Altered expression balance of matrix metalloproteinases and their inhibitors in human carotid plaque disruption: Results of quantitative tissue analysis using real-time RT-PCR method. *Atherosclerosis*, 185(1), pp. 165-172
- HILEY, C.R., 2009. Endocannabinoids and the Heart. *Journal of Cardiovascular Pharmacology*, 53(4), pp. 267-276
- HOJIMA, Y., VAN DER REST, M. and PROCKOP, D.J., 1985. Type I procollagen carboxyl-terminal proteinase from chick embryo tendons. Purification and characterization. *Journal of Biological Chemistry*, 260(29), pp. 15996-16003
- HONG, S. et al., 2003. Novel Docosatrienes and 17S-Resolvins Generated from Docosahexaenoic Acid in Murine Brain, Human Blood, and Glial Cells. *Journal of Biological Chemistry*, 278(17), pp. 14677-14687
- HU, Y. et al., 2009. Eicosapentaenoic acid reduces ABCA1 serine phosphorylation and impairs ABCA1-dependent cholesterol efflux through cyclic AMP/protein kinase A signaling pathway in THP-1 macrophage-derived foam cells. *Atherosclerosis*, 204(2), pp. e35-e43
- IKARI, Y. et al., 1999. Neonatal Intima Formation in the Human Coronary Artery. *Arteriosclerosis, Thrombosis, and Vascular Biology*, 19(9), pp. 2036-2040
- ILLINGWORTH, D., HARRIS, W. and CONNOR, W., 1984. Inhibition of low density lipoprotein synthesis by dietary omega-3 fatty acids in humans. *Arteriosclerosis, Thrombosis, and Vascular Biology*, 4(3), pp. 270-275

- INOUE, I. et al., 1998. Expression of Peroxisome Proliferator-Activated Receptor α (PPAR α) in Primary Cultures of Human Vascular Endothelial Cells. *Biochemical and biophysical research communications*, 246(2), pp. 370-374
- INOUE, M. et al., 2005. Increased expression of PPAR γ in high fat diet-induced liver steatosis in mice. *Biochemical and biophysical research communications*, 336(1), pp. 215-222
- ISHIBASHI, S. et al., 1993. Hypercholesterolemia in low density lipoprotein receptor knockout mice and its reversal by adenovirus-mediated gene delivery. *The Journal of Clinical Investigation*, 92(2), pp. 883-893
- JAMSHIDI, N. and TAYLOR, D.A., 2001. Anandamide administration into the ventromedial hypothalamus stimulates appetite in rats. *British journal of pharmacology*, 134(6), pp. 1151-1154
- JÁRAI, Z. et al., 2000. Cardiovascular Effects of 2-Arachidonoyl Glycerol in Anesthetized Mice. *Hypertension*, 35(2), pp. 679-684
- JBILLO, O. et al., 1999. Stimulation of peripheral cannabinoid receptor CB2 induces MCP-1 and IL-8 gene expression in human promyelocytic cell line HL60. *FEBS letters*, 448(2-3), pp. 273-277
- JEANPIERRE, E. et al., 2009. Beneficial effects of fenofibrate on plaque thrombogenicity and plaque stability in atherosclerotic rabbits. *Cardiovascular Pathology*, 18(3), pp. 140-147
- JEONG, S. et al., 2004. Effects of fenofibrate on high-fat diet-induced body weight gain and adiposity in female C57BL/6J mice. *Metabolism*, 53(10), pp. 1284-1289
- JIANG, L. et al., 2009. Role of activated endocannabinoid system in regulation of cellular cholesterol metabolism in macrophages. *Cardiovascular research*, 81(4), pp. 805-813
- JOHNSON, J.L. and JACKSON, C.L., 2001. Atherosclerotic plaque rupture in the apolipoprotein E knockout mouse. *Atherosclerosis*, 154(2), pp. 399-406
- JOSTARNDT, K. et al., 2002. Dissociation of Apoptosis Induction and CD36 Upregulation by Enzymatically Modified Low-Density Lipoprotein in Monocytic Cells. *Biochemical and biophysical research communications*, 290(3), pp. 988-993
- JUDKINS, C.P. et al., January 2010. Direct evidence of a role for Nox2 in superoxide production, reduced nitric oxide bioavailability, and early atherosclerotic plaque formation in ApoE $^{-/-}$ mice. *American Journal of Physiology - Heart and Circulatory Physiology*, 298(1), pp. H24-H32
- KANG, A.H., 1972. Studies on the location of intermolecular crosslinks in collagen. Isolation of a cyanogen bromide peptide containing δ -hydroxylysino-norleucine. *Biochemistry*, 11(10), pp. 1828-1835
- KASHIYAMA, T. et al., 2011. Relationship between coronary plaque vulnerability and serum n-3/n-6 polyunsaturated fatty acid ratio. *Circulation journal: official journal of the Japanese Circulation Society*, 75(10), pp. 2432-2438

- KAUL, S. et al., 2004. Rapid reversal of endothelial dysfunction in hypercholesterolemic apolipoprotein E-null mice by recombinant apolipoprotein A-IMilano-phospholipid complex. *Journal of the American College of Cardiology*, 44(6), pp. 1311-1319
- KAWANO, H. et al., 2002. Changes in Aspects Such as the Collagenous Fiber Density and Foam Cell Size of Atherosclerotic Lesions Composed of Foam Cells, Smooth Muscle Cells and Fibrous Components in Rabbits Caused by All-*cis*-5, 8, 11, 14, 17-icosapentaenoic Acid. *Journal of Atherosclerosis and Thrombosis*, 9(4), pp. 170-177
- KAWASHIMA, Y., MUSOH, K. and KOZUKA, H., 1990. Peroxisome proliferators enhance linoleic acid metabolism in rat liver. Increased biosynthesis of omega 6 polyunsaturated fatty acids. *Journal of Biological Chemistry*, 265(16), pp. 9170-9175
- KELLER, H. et al., 1993. Fatty acids and retinoids control lipid metabolism through activation of peroxisome proliferator-activated receptor-retinoid X receptor heterodimers. *Proceedings of the National Academy of Sciences of the United States of America*, 90(6), pp. 2160-2164
- KIM, H., TAKAHASHI, M. and EZAKI, O., 1999. Fish Oil Feeding Decreases Mature Sterol Regulatory Element-binding Protein 1 (SREBP-1) by Down-regulation of SREBP-1c mRNA in Mouse Liver. *Journal of Biological Chemistry*, 274(36), pp. 25892-25898
- KIM, S. et al., 2004. Hepatic gene expression profiles in a long-term high-fat diet-induced obesity mouse model. *Gene*, 340(1), pp. 99-109
- KIRKHAM, T.C. et al., 2002. Endocannabinoid levels in rat limbic forebrain and hypothalamus in relation to fasting, feeding and satiation: stimulation of eating by 2-arachidonoyl glycerol. *British Journal of Pharmacology*, 136(4), pp. 550-557
- KLOUCHE, M. et al., 2000. Enzymatically Degraded, Nonoxidized LDL Induces Human Vascular Smooth Muscle Cell Activation, Foam Cell Transformation, and Proliferation. *Circulation*, 101(15), pp. 1799-1805
- KOBAYASHI, N. et al., 2006. Effect of Altering Dietary ω -6/ ω -3 Fatty Acid Ratios on Prostate Cancer Membrane Composition, Cyclooxygenase-2, and Prostaglandin E2. *Clinical Cancer Research*, 12(15), pp. 4662-4670
- KOHN, L.D. et al., 1974. Calf tendon procollagen peptidase: its purification and endopeptidase mode of action. *Proceedings of the National Academy of Sciences of the United States of America*, 71(1), pp. 40-44
- KONDO, S. et al., 1998. 2-Arachidonoylglycerol, an endogenous cannabinoid receptor agonist: identification as one of the major species of monoacylglycerols in various rat tissues, and evidence for its generation through Ca²⁺-dependent and -independent mechanisms. *FEBS letters*, 429(2), pp. 152-156
- KUNJATHOOR, V.V. et al., 2002. Scavenger Receptors Class A-I/II and CD36 Are the Principal Receptors Responsible for the Uptake of Modified Low Density Lipoprotein Leading to Lipid Loading in Macrophages. *Journal of Biological Chemistry*, 277(51), pp. 49982-49988

- KUWAHARA, F. et al., 2002. Transforming Growth Factor- β Function Blocking Prevents Myocardial Fibrosis and Diastolic Dysfunction in Pressure-Overloaded Rats. *Circulation*, 106(1), pp. 130-135
- LAFLAMME, K. et al., 2006. Adventitia contribution in vascular tone: insights from adventitia-derived cells in a tissue-engineered human blood vessel. *The FASEB Journal*, 20(8), pp. 1245-1247
- LAIGHT, D.W. et al., 1996. Investigation of endogenous nitric oxide vascular function in the carotid artery of cholesterol-fed rabbits. *British Journal of Pharmacology*, 117(7), pp. 1471-1474
- LAKE, K.D. et al., 1997. Cannabinoid-induced hypotension and bradycardia in rats is mediated by CB1-like cannabinoid receptors. *Journal of Pharmacology and Experimental Therapeutics*, 281(3), pp. 1030-1037
- LAKE, K.D. et al., 1997. Cannabinoid-Induced Hypotension and Bradycardia in Rats Is Mediated by CB1-Like Cannabinoid Receptors. *Journal of Pharmacology and Experimental Therapeutics*, 281(3), pp. 1030-1037
- LAMBERT, G. et al., 2003. The Farnesoid X-receptor Is an Essential Regulator of Cholesterol Homeostasis. *Journal of Biological Chemistry*, 278(4), pp. 2563-2570
- LEBRASSEUR, N.K. et al., 2007. Effects of Fenofibrate on Cardiac Remodeling in Aldosterone-Induced Hypertension. *Hypertension*, 50(3), pp. 489-496
- LEE, J.Y. and HWANG, D.H., 2002. Docosahexaenoic acid suppresses the activity of peroxisome proliferator-activated receptors in a colon tumor cell line. *Biochemical and biophysical research communications*, 298(5), pp. 667-674
- LEEUWENBURGH, C. et al., 1997a. Reactive Nitrogen Intermediates Promote Low Density Lipoprotein Oxidation in Human Atherosclerotic Intima. *Journal of Biological Chemistry*, 272(3), pp. 1433-1436
- LEEUWENBURGH, C. et al., 1997b. Mass Spectrometric Quantification of Markers for Protein Oxidation by Tyrosyl Radical, Copper, and Hydroxyl Radical in Low Density Lipoprotein Isolated from Human Atherosclerotic Plaques. *Journal of Biological Chemistry*, 272(6), pp. 3520-3526
- LEUNG, D. et al., 2006. Inactivation of *N*-Acyl Phosphatidylethanolamine Phospholipase D Reveals Multiple Mechanisms for the Biosynthesis of Endocannabinoids *Biochemistry*, 45(15), pp. 4720-4726
- LEVITAN, I., VOLKOV, S. and SUBBIAIAH, P.V., 2010. Oxidized LDL: Diversity, Patterns of Recognition, and Pathophysiology. *Antioxidants & Redox Signaling*, 13(1), pp. 39-75
- LI, D. and MEHTA, J.L., 2000. Antisense to LOX-1 Inhibits Oxidized LDL-Mediated Upregulation of Monocyte Chemoattractant Protein-1 and Monocyte Adhesion to Human Coronary Artery Endothelial Cells. *Circulation*, 101(25), pp. 2889-2895
- LI, S. et al., 1999. Evidence From a Novel Human Cell Clone That Adult Vascular Smooth Muscle Cells Can Convert Reversibly Between Noncontractile and Contractile Phenotypes. *Circulation research*, 85(4), pp. 338-348

- LIGHT, N. and BAILEY, A.J., 1985. Collagen cross-links: location of pyridinoline in type I collagen. *FEBS letters*, 182(2), pp. 503-508
- LIM, S.Y. et al., 2009. The cannabinoid CB1 receptor antagonist, rimonabant, protects against acute myocardial infarction. *Basic research in cardiology*, 104(6), pp. 781-792
- LINDSEY, S., PRONCZUK, A. and HAYES, K.C., 1992. Low density lipoprotein from humans supplemented with n-3 fatty acids depresses both LDL receptor activity and LDLr mRNA abundance in HepG2 cells. *Journal of lipid research*, 33(5), pp. 647-658
- LISTENBERGER, L.L. et al., 2007. Adipocyte differentiation-related protein reduces the lipid droplet association of adipose triglyceride lipase and slows triacylglycerol turnover. *Journal of lipid research*, 48(12), pp. 2751-2761
- LIU, J.C. et al., 2011. Long-chain omega-3 fatty acids and blood pressure. *American Journal of Hypertension*, 24(10), pp. 1121-1126
- LIU, J. et al., 2003. Lipopolysaccharide Induces Anandamide Synthesis in Macrophages via CD14/MAPK/Phosphoinositide 3-Kinase/NF- κ B Independently of Platelet-activating Factor. *Journal of Biological Chemistry*, 278(45), pp. 45034-45039
- LIU, J. et al., 2008. Multiple pathways involved in the biosynthesis of anandamide. *Neuropharmacology*, 54(1), pp. 1-7
- LIU, J. et al., 2006. A biosynthetic pathway for anandamide. *Proceedings of the National Academy of Sciences*, 103(36), pp. 13345-13350
- LIU, J. et al., 2006. A biosynthetic pathway for anandamide. *Proceedings of the National Academy of Sciences*, 103(36), pp. 13345-13350
- LIU, P.C.C. et al., 2003. Induction of endogenous genes by peroxisome proliferator activated receptor alpha ligands in a human kidney cell line and in vivo. *The Journal of steroid biochemistry and molecular biology*, 85(1), pp. 71-79
- LIUBA, P. et al., 2007. Effects of Bradykinin on Aortic Endothelial Function in ApoE-Knockout Mice With Chronic Chlamydia Pneumoniae Infection. *71*, 9, pp. 1480-1484
- LOPPNOW, H. and LIBBY, P., 1990. Proliferating or interleukin 1-activated human vascular smooth muscle cells secrete copious interleukin 6. *The Journal of clinical investigation*, 85(3), pp. 731-738
- LUC, G. et al., 2002. Value of HDL Cholesterol, Apolipoprotein A-I, Lipoprotein A-I, and Lipoprotein A-I/A-II in Prediction of Coronary Heart Disease. *Arteriosclerosis, Thrombosis, and Vascular Biology*, 22(7), pp. 1155-1161
- MACCARRONE, M. et al., 2001. Human platelets bind and degrade 2-arachidonoylglycerol, which activates these cells through a cannabinoid receptor. *European Journal of Biochemistry*, 268(3), pp. 819-825

- MACCARRONE, M. et al., 2000. Anandamide Induces Apoptosis in Human Cells via Vanilloid Receptors. *Journal of Biological Chemistry*, 275(41), pp. 31938-31945
- MACKAY, I. et al., 2012. Effect of Omega-3 fatty acid supplementation on markers of platelet and endothelial function in patients with peripheral arterial disease. *Atherosclerosis*, 221(2), pp. 514-520
- MADONNA, R. et al., 2011. Omega-3 fatty acids attenuate constitutive and insulin-induced CD36 expression through a suppression of PPAR α/γ activity in microvascular endothelial cells. *Thrombosis and Haemostasis*, 106(3), pp. 500-510
- MAHLEY, R., 1988. Apolipoprotein E: cholesterol transport protein with expanding role in cell biology. *Science*, 240(4852), pp. 622-630
- MALDEN, L.T. et al., 1991. The influence of oxidatively modified low density lipoproteins on expression of platelet-derived growth factor by human monocyte-derived macrophages. *The Journal of Biological Chemistry*, 266(21), pp. 13901-13907
- MALFITANO, A.M. et al., 2007. Arvanil and anandamide up-regulate CD36 expression in human peripheral blood mononuclear cells. *Immunology letters*, 109(2), pp. 145-154
- MANCINI, F.P. et al., 2001. Fenofibrate prevents and reduces body weight gain and adiposity in diet-induced obese rats. *FEBS letters*, 491(1-2), pp. 154-158
- MANNING-TOBIN, J.J. et al., 2009. Loss of SR-A and CD36 Activity Reduces Atherosclerotic Lesion Complexity Without Abrogating Foam Cell Formation in Hyperlipidemic Mice. *Arteriosclerosis, Thrombosis, and Vascular Biology*, 29(1), pp. 19-26
- MARION M., B., 1976. A rapid and sensitive method for the quantitation of microgram quantities of protein utilizing the principle of protein-dye binding. *Analytical Biochemistry*, 72(1-2), pp. 248-254
- MARTIN, G. et al., 1997. Coordinate Regulation of the Expression of the Fatty Acid Transport Protein and Acyl-CoA Synthetase Genes by PPAR α and PPAR γ Activators. *Journal of Biological Chemistry*, 272(45), pp. 28210-28217
- MARTIN, G. et al., 1997. Coordinate Regulation of the Expression of the Fatty Acid Transport Protein and Acyl-CoA Synthetase Genes by PPAR α and PPAR γ Activators. *Journal of Biological Chemistry*, 272(45), pp. 28210-28217
- MARTOS, R. et al., 2007. Diastolic Heart Failure. *Circulation*, 115(7), pp. 888-895
- MARX, N. et al., 1998. Peroxisome Proliferator-Activated Receptor Gamma Activators Inhibit Gene Expression and Migration in Human Vascular Smooth Muscle Cells. *Circulation research*, 83(11), pp. 1097-1103
- MATIAS, I. et al., 2008. Effect of polyunsaturated fatty acids on endocannabinoid and N-acyl-ethanolamine levels in mouse adipocytes. *Biochimica et Biophysica Acta (BBA) - Molecular and Cell Biology of Lipids*, 1781(1-2), pp. 52-60

- MATIAS, I. et al., 2008. Dysregulation of peripheral endocannabinoid levels in hyperglycemia and obesity: Effect of high fat diets. *Molecular and cellular endocrinology*, 286(1–2, Supplement 1), pp. S66-S78
- MATSUDA, L.A. et al., 1990. Structure of a cannabinoid receptor and functional expression of the cloned cDNA. *Nature*, 346(6284), pp. 561-564
- MATSUMOTO, M. et al., 2008. Orally administered eicosapentaenoic acid reduces and stabilizes atherosclerotic lesions in ApoE-deficient mice. *Atherosclerosis*, 197(2), pp. 524-533
- MAVROMMATIS, Y. et al., 2010. Intervention with fish oil, but not with docosahexaenoic acid, results in lower levels of hepatic soluble epoxide hydrolase with time in apoE knockout mice. *British Journal of Nutrition*, 103(1), pp. 16-24
- MECHOULAM, R. et al., 1995. Identification of an endogenous 2-monoglyceride, present in canine gut, that binds to cannabinoid receptors. *Biochemical pharmacology*, 50(1), pp. 83-90
- MECHOULAM, R. et al., 1995. Identification of an endogenous 2-monoglyceride, present in canine gut, that binds to cannabinoid receptors. *Biochemical pharmacology*, 50(1), pp. 83-90
- MESTAS, J. and LEY, K., 2008. Monocyte-Endothelial Cell Interactions in the Development of Atherosclerosis. *Trends in cardiovascular medicine*, 18(6), pp. 228-232
- MIETUS-SNYDER, M., GOWRI, M.S. and PITAS, R.E., 2000. Class A Scavenger Receptor Up-regulation in Smooth Muscle Cells by Oxidized Low Density Lipoprotein. *Journal of Biological Chemistry*, 275(23), pp. 17661-17670
- MOGHADASIAN, M.H. et al., 2001. Pathophysiology of apolipoprotein E deficiency in mice: relevance to apo E-related disorders in humans. *The FASEB Journal*, 15(14), pp. 2623-2630
- MONTECUCCO, F. et al., 2008. CB2 cannabinoid receptor agonist JWH-015 modulates human monocyte migration through defined intracellular signaling pathways. *American Journal of Physiology - Heart and Circulatory Physiology*, 294(3), pp. H1145-H1155
- MONTECUCCO, F. and DI MARZO, V., At the heart of the matter: the endocannabinoid system in cardiovascular function and dysfunction. *Trends in pharmacological sciences*, (0),
- MONTECUCCO, F. et al., 2009. Regulation and possible role of endocannabinoids and related mediators in hypercholesterolemic mice with atherosclerosis. *Atherosclerosis*, 205(2), pp. 433-441
- MOORE, R.E. et al., 2003. Apolipoprotein A-I Deficiency Results in Markedly Increased Atherosclerosis in Mice Lacking the LDL Receptor. *Arteriosclerosis, Thrombosis, and Vascular Biology*, 23(10), pp. 1914-1920
- MOREL, D., DICORLETO, P. and CHISOLM, G., 1984. Endothelial and smooth muscle cells alter low density lipoprotein in vitro by free radical oxidation. *Arteriosclerosis, Thrombosis, and Vascular Biology*, 4(4), pp. 357-364

- MOTAWI, T.M.K. et al., 2009. Comparative study between the effect of the peroxisome proliferator activated receptor-alpha ligands fenofibrate and n-3 polyunsaturated fatty acids on activation of 5'-AMP-activated protein kinase-alpha1 in high-fat fed rats. *Journal of Pharmacy and Pharmacology*, 61(10), pp. 1339-1346
- MOTOMURA, W. et al., 2006. Up-regulation of ADRP in fatty liver in human and liver steatosis in mice fed with high fat diet. *Biochemical and biophysical research communications*, 340(4), pp. 1111-1118
- MOZAFFARIAN, D. et al., 2005. Effect of Fish Oil on Heart Rate in Humans. *Circulation*, 112(13), pp. 1945-1952
- MUCCIOLI, G.G., 2010. Endocannabinoid biosynthesis and inactivation, from simple to complex. *Drug discovery today*, 15(11-12), pp. 474-483
- MUERHOFF, A.S., GRIFFIN, K.J. and JOHNSON, E.F., 1992. The peroxisome proliferator-activated receptor mediates the induction of CYP4A6, a cytochrome P450 fatty acid omega-hydroxylase, by clofibrac acid. *Journal of Biological Chemistry*, 267(27), pp. 19051-19053
- MUKHOPADHYAY, P. et al., 2007. Pharmacological Inhibition of CB1 Cannabinoid Receptor Protects Against Doxorubicin-Induced Cardiotoxicity. *Journal of the American College of Cardiology*, 50(6), pp. 528-536
- MUKHOPADHYAY, P. et al., 2011. Fatty acid amide hydrolase is a key regulator of endocannabinoid-induced myocardial tissue injury. *Free Radical Biology and Medicine*, 50(1), pp. 179-195
- MUKHOPADHYAY, P. et al., 2010. CB1 cannabinoid receptors promote oxidative/nitrosative stress, inflammation and cell death in a murine nephropathy model. *British journal of pharmacology*, 160(3), pp. 657-668
- MUNRO, S., THOMAS, K.L. and ABU-SHAAR, M., 1993. Molecular characterization of a peripheral receptor for cannabinoids. *Nature*, 365(6441), pp. 61-65
- NAGY, L. et al., 1998. Oxidized LDL Regulates Macrophage Gene Expression through Ligand Activation of PPAR γ . *Cell*, 93(2), pp. 229-240
- NAKAGAMI, H. et al., 2009. Vascular protective effects of ezetimibe in ApoE-deficient mice. *Atherosclerosis*, 203(1), pp. 51-58
- NAKAJIMA, Y. et al., 2006. Endocannabinoid, anandamide in gingival tissue regulates the periodontal inflammation through NF- κ B pathway inhibition. *FEBS letters*, 580(2), pp. 613-619
- NAKASHIMA, Y. et al., 2002. Distributions of diffuse intimal thickening in human arteries: preferential expression in atherosclerosis-prone arteries from an early age. *Virchows Archiv: An International Journal of Pathology*, 441(3), pp. 279-288
- NAKASHIMA, Y. et al., 1994. ApoE-deficient mice develop lesions of all phases of atherosclerosis throughout the arterial tree. *Arteriosclerosis, Thrombosis, and Vascular Biology*, 14(1), pp. 133-140

- NAKASHIMA, Y. et al., 2007. Early Human Atherosclerosis. *Arteriosclerosis, Thrombosis, and Vascular Biology*, 27(5), pp. 1159-1165
- NAPOLI, C. et al., 1997. Fatty streak formation occurs in human fetal aortas and is greatly enhanced by maternal hypercholesterolemia. Intimal accumulation of low density lipoprotein and its oxidation precede monocyte recruitment into early atherosclerotic lesions. *The Journal of Clinical Investigation*, 100(11), pp. 2680-2690
- NETEA, M.G. et al., 2008. Interleukin-32 induces the differentiation of monocytes into macrophage-like cells. *Proceedings of the National Academy of Sciences*, 105(9), pp. 3515-3520
- NEWBY, A.C. et al., 2009. Vulnerable atherosclerotic plaque metalloproteinases and foam cell phenotypes. *Thrombosis and Haemostasis*, 101(6), pp. 1006-1011
- NICHOLLS, A.C. and BAILEY, A.J., 1980. Identification of cyanogen bromide peptides involved in intermolecular cross-linking of bovine type III collagen. *Biochemical Journal*, 185(1), pp. 195-201
- NISHINA, P.M., VERSTUYFT, J. and PAIGEN, B., 1990. Synthetic low and high fat diets for the study of atherosclerosis in the mouse. *Journal of lipid research*, 31(5), pp. 859-869
- NISSEN, S.E. et al., 2008. Effect of Rimonabant on Progression of Atherosclerosis in Patients With Abdominal Obesity and Coronary Artery Disease. *JAMA: The Journal of the American Medical Association*, 299(13), pp. 1547-1560
- NORDESTGAARD, B., TYBJAERG-HANSEN, A. and LEWIS, B., 1992. Influx in vivo of low density, intermediate density, and very low density lipoproteins into aortic intimas of genetically hyperlipidemic rabbits. Roles of plasma concentrations, extent of aortic lesion, and lipoprotein particle size as determinants. *Arteriosclerosis, Thrombosis, and Vascular Biology*, 12(1), pp. 6-18
- NORTON, G.R. et al., 1997. Myocardial Stiffness Is Attributed to Alterations in Cross-Linked Collagen Rather Than Total Collagen or Phenotypes in Spontaneously Hypertensive Rats. *Circulation*, 96(6), pp. 1991-1998
- O'BRIEN, K.D. et al., 1998. Comparison of Apolipoprotein and Proteoglycan Deposits in Human Coronary Atherosclerotic Plaques : Colocalization of Biglycan With Apolipoproteins. *Circulation*, 98(6), pp. 519-527
- OGATA, T. et al., 2004. Myocardial fibrosis and diastolic dysfunction in deoxycorticosterone acetate-salt hypertensive rats is ameliorated by the peroxisome proliferator-activated receptor-alpha activator fenofibrate, partly by suppressing inflammatory responses associated with the nuclear factor-kappa-b pathway. *Journal of the American College of Cardiology*, 43(8), pp. 1481-1488
- OGAWA, T. et al., 1982. A novel fluor in insoluble collagen: A crosslinking moiety in collagen molecule. *Biochemical and biophysical research communications*, 107(4), pp. 1252-1257
- OHARA, Y., PETERSON, T.E. and HARRISON, D.G., 1993. Hypercholesterolemia increases endothelial superoxide anion production. *The Journal of Clinical Investigation*, 91(6), pp. 2546-2551

- OKAMOTO, Y. et al., 2005. Mammalian cells stably overexpressing *N*-acylphosphatidylethanolamine-hydrolysing phospholipase D exhibit significantly decreased levels of *N*-acylphosphatidylethanolamines. *The Biochemical Journal*, 389(1), pp. 241-247
- OLIN-LEWIS, K. et al., 2002. ApoC-III content of apoB-containing lipoproteins is associated with binding to the vascular proteoglycan biglycan. *Journal of lipid research*, 43(11), pp. 1969-1977
- OMURA, M. et al., 2001. Eicosapentaenoic acid (EPA) induces Ca²⁺-independent activation and translocation of endothelial nitric oxide synthase and endothelium-dependent vasorelaxation. *FEBS letters*, 487(3), pp. 361-366
- OOSTERVEER, M.H. et al., 2009. High Fat Feeding Induces Hepatic Fatty Acid Elongation in Mice. *PLoS One*, 4(6), pp. e6066
- ORBE, J. et al., 2003. Different expression of MMPs/TIMP-1 in human atherosclerotic lesions. Relation to plaque features and vascular bed. *Atherosclerosis*, 170(2), pp. 269-276
- ORGEL, J.P.R.O. et al., 2001. The In Situ Supermolecular Structure of Type I Collagen. *Structure*, 9(11), pp. 1061-1069
- OSTO, E. et al., 2008. Inhibition of Protein Kinase C β Prevents Foam Cell Formation by Reducing Scavenger Receptor A Expression in Human Macrophages. *Circulation*, 118(21), pp. 2174-2182
- PACHER, P. and STEFFENS, S., 2009. The emerging role of the endocannabinoid system in cardiovascular disease. *Seminars in Immunopathology*, 31(1), pp. 63-77
- PACHER, P., BÁTKAI, S. and KUNOS, G., 2004. Haemodynamic profile and responsiveness to anandamide of TRPV1 receptor knock-out mice. *The Journal of physiology*, 558(2), pp. 647-657
- PAIGEN, B. et al., 1987. Ath-1, a gene determining atherosclerosis susceptibility and high density lipoprotein levels in mice. *Proceedings of the National Academy of Sciences*, 84(11), pp. 3763-3767
- PAOLETTI, R., CORSINI, A. and BELLOSTA, S., 2002. Pharmacological interactions of statins. *Atherosclerosis Supplements*, 3(1), pp. 35-40
- PARK, Y. and HARRIS, W.S., 2003. Omega-3 fatty acid supplementation accelerates chylomicron triglyceride clearance. *Journal of lipid research*, 44(3), pp. 455-463
- PARK, Y. and HARRIS, W.S., 2003. Omega-3 fatty acid supplementation accelerates chylomicron triglyceride clearance. *Journal of lipid research*, 44(3), pp. 455-463
- PARTHASARATHY, S. et al., 1986. Macrophage oxidation of low density lipoprotein generates a modified form recognized by the scavenger receptor. *Arteriosclerosis, Thrombosis, and Vascular Biology*, 6(5), pp. 505-510
- PERTWEE, R.G. and ROSS, R.A., 2002. Cannabinoid receptors and their ligands. *Prostaglandins, Leukotrienes and Essential Fatty Acids*, 66(2-3), pp. 101-121

- PERTWEE, R.G. and ROSS, R.A., 2002. Cannabinoid receptors and their ligands. *Prostaglandins, Leukotrienes and Essential Fatty Acids*, 66(2–3), pp. 101-121
- PLUMP, A.S. et al., 1992. Severe hypercholesterolemia and atherosclerosis in apolipoprotein E-deficient mice created by homologous recombination in ES cells. *Cell*, 71(2), pp. 343-353
- PODREZ, E.A. et al., 2000. Macrophage scavenger receptor CD36 is the major receptor for LDL modified by monocyte-generated reactive nitrogen species. *The Journal of Clinical Investigation*, 105(8), pp. 1095-1108
- PORTER, A.C. et al., 2002. Characterization of a Novel Endocannabinoid, Virodhamine, with Antagonist Activity at the CB1 Receptor. *Journal of Pharmacology and Experimental Therapeutics*, 301(3), pp. 1020-1024
- PRATT, D.A. et al., 1992. Automated analysis of the pyridinium crosslinks of collagen in tissue and urine using solid-phase extraction and reversed-phase high-performance liquid chromatography. *Analytical Biochemistry*, 207(1), pp. 168-175
- QIN, Y. et al., 2010. Simvastatin inhibited cardiac hypertrophy and fibrosis in apolipoprotein E-deficient mice fed a “Western-style diet” by increasing PPAR α and γ expression and reducing TC, MMP-9, and Cat S levels. *Acta Pharmacologica Sinica*, 31(10), pp. 1350-1358
- QIU, X., HONG, H. and MACKENZIE, S.L., 2001. Identification of a $\Delta 4$ Fatty Acid Desaturase from *Thraustochytrium* sp. Involved in the Biosynthesis of Docosahexanoic Acid by Heterologous Expression in *Saccharomyces cerevisiae* and *Brassica juncea*. *Journal of Biological Chemistry*, 276(34), pp. 31561-31566
- RADACK, K., DECK, C. and HUSTER, G., 1990. n-3 fatty acid effects on lipids, lipoproteins, and apolipoproteins at very low doses: results of a randomized controlled trial in hypertriglyceridemic subjects. *The American Journal of Clinical Nutrition*, 51(4), pp. 599-605
- RAJESH, M. et al., 2008a. Cannabinoid CB₁ receptor inhibition decreases vascular smooth muscle migration and proliferation. *Biochemical and Biophysical Research Communications*, 377(4), pp. 1248-1252
- RAJESH, M. et al., 2008. CB₂ cannabinoid receptor agonists attenuate TNF- α -induced human vascular smooth muscle cell proliferation and migration. *British journal of pharmacology*, 153(2), pp. 347-357
- RAJESH, M. et al., 2012. Cannabinoid 1 Receptor Promotes Cardiac Dysfunction, Oxidative Stress, Inflammation, and Fibrosis in Diabetic Cardiomyopathy. *Diabetes*, 61(3), pp. 716-727
- RAJESH, M. et al., 2007. CB₂-receptor stimulation attenuates TNF- α -induced human endothelial cell activation, transendothelial migration of monocytes, and monocyte-endothelial adhesion. *American Journal of Physiology - Heart and Circulatory Physiology*, 293(4), pp. H2210-H2218

- RAJESH, M. et al., 2010. Cannabinoid-1 receptor activation induces reactive oxygen species-dependent and -independent mitogen-activated protein kinase activation and cell death in human coronary artery endothelial cells. *British journal of pharmacology*, 160(3), pp. 688-700
- RAMÍREZ-ZACARÍAS, J.L., CASTRO-MUÑOZLEDO, F. and KURI-HARCUCH, W., 1992. Quantitation of adipose conversion and triglycerides by staining intracytoplasmic lipids with oil red O. *Histochemistry*, 97(6), pp. 493-497
- REDDICK, R., ZHANG, S.H. and MAEDA, N., 1994. Atherosclerosis in mice lacking apo E. Evaluation of lesional development and progression. *Arteriosclerosis, Thrombosis, and Vascular Biology*, 14(1), pp. 141-147
- REKHTER, M.D. et al., 2000. Hypercholesterolemia Causes Mechanical Weakening of Rabbit Atheroma: Local Collagen Loss as a Prerequisite of Plaque Rupture. *Circulation research*, 86(1), pp. 101-108
- RENART, J., REISER, J. and STARK, G.R., 1979. Transfer of proteins from gels to diazobenzoyloxymethyl-paper and detection with antisera: a method for studying antibody specificity and antigen structure. *Proceedings of the National Academy of Sciences*, 76(7), pp. 3116-3120
- RIDKER, P.M. et al., 2008. Rosuvastatin to Prevent Vascular Events in Men and Women with Elevated C-Reactive Protein. *N Engl J Med*, 359(21), pp. 2195-2207
- RIEDEL, G. et al., 2009. Synthetic and plant-derived cannabinoid receptor antagonists show hypophagic properties in fasted and non-fasted mice. *British Journal of Pharmacology*, 156(7), pp. 1154-1166
- ROBBE, D. et al., 2002. Endogenous cannabinoids mediate long-term synaptic depression in the nucleus accumbens. *Proceedings of the National Academy of Sciences of the United States of America*, 99(12), pp. 8384-8388
- ROBINS, S.P., 1982. Analysis of the crosslinking components in collagen and elastin. *Methods of Biochemical Analysis*, 28, pp. 329-379
- ROBINS, S.P. et al., 1996. Standardization of pyridinium crosslinks, pyridinoline and deoxypyridinoline, for use as biochemical markers of collagen degradation. *Clinical chemistry*, 42(10), pp. 1621-1626
- ROBINS, S.P. et al., 2003. Increased Skin Collagen Extractability and Proportions of Collagen Type III Are Not Normalized after 6 Months Healing of Human Excisional Wounds. *Journal of Investigative Dermatology*, 121(2), pp. 267-272
- RONG, J.X. et al., 2003. Transdifferentiation of mouse aortic smooth muscle cells to a macrophage-like state after cholesterol loading. *Proceedings of the National Academy of Sciences*, 100(23), pp. 13531-13536
- ROSENFELD, M.E. et al., 2000. Advanced Atherosclerotic Lesions in the Innominate Artery of the ApoE Knockout Mouse. *Arteriosclerosis, Thrombosis, and Vascular Biology*, 20(12), pp. 2587-2592

- ROSS, R. and GLOMSET, J.A., 1973. Atherosclerosis and the arterial smooth muscle cell: Proliferation of smooth muscle is a key event in the genesis of the lesions of atherosclerosis. *Science*, 180(4093), pp. 1332-1339
- ROUZER, C.A. and MARNETT, L.J., 2011. Endocannabinoid oxygenation by cyclooxygenases, lipoxygenases, and cytochromes P450: cross-talk between the eicosanoid and endocannabinoid signaling pathways. *Chemical Reviews*, 111(10), pp. 5899-5921
- RUSSO, G.L., 2009. Dietary n – 6 and n – 3 polyunsaturated fatty acids: From biochemistry to clinical implications in cardiovascular prevention. *Biochemical pharmacology*, 77(6), pp. 937-946
- RYBERG, E. et al., 2007. The orphan receptor GPR55 is a novel cannabinoid receptor. *British journal of pharmacology*, 152(7), pp. 1092-1101
- SAGE, H., TRÜEB, B. and BORNSTEIN, P., 1983. Biosynthetic and structural properties of endothelial cell type VIII collagen. *Journal of Biological Chemistry*, 258(21), pp. 13391-13401
- SANDERS, T.A. et al., 2011. Effect of low doses of long-chain n–3 PUFAs on endothelial function and arterial stiffness: a randomized controlled trial. *The American Journal of Clinical Nutrition*, 94(4), pp. 973-980
- SAYANOVA, O.V. and NAPIER, J.A., 2004. Eicosapentaenoic acid: biosynthetic routes and the potential for synthesis in transgenic plants. *Phytochemistry*, 65(2), pp. 147-158
- SCHADINGER, S.E. et al., 2005. PPAR γ 2 regulates lipogenesis and lipid accumulation in steatotic hepatocytes. *American Journal of Physiology - Endocrinology And Metabolism*, 288(6), pp. E1195-E1205
- SCHOENHAGEN, P., TUZCU, E.M. and ELLIS, S.G., 2002. Plaque Vulnerability, Plaque Rupture, and Acute Coronary Syndromes. *Circulation*, 106(7), pp. 760-762
- SCHOONJANS, K. et al., 1996. PPAR α and PPAR γ activators direct a distinct tissue-specific transcriptional response via a PPRE in the lipoprotein lipase gene. *The EMBO Journal*, 15(19), pp. 5336-5348
- SCHOONJANS, K. et al., 1995. Induction of the Acyl-Coenzyme A Synthetase Gene by Fibrates and Fatty Acids Is Mediated by a Peroxisome Proliferator Response Element in the C Promoter. *Journal of Biological Chemistry*, 270(33), pp. 19269-19276
- SCHOONJANS, K. et al., 1995. Induction of the Acyl-Coenzyme A Synthetase Gene by Fibrates and Fatty Acids Is Mediated by a Peroxisome Proliferator Response Element in the C Promoter. *Journal of Biological Chemistry*, 270(33), pp. 19269-19276
- SCHWENDE, H. et al., 1996. Differences in the state of differentiation of THP-1 cells induced by phorbol ester and 1,25-dihydroxyvitamin D₃. *Journal of leukocyte biology*, 59(4), pp. 555-561

- SCHWENKE, D. and CAREW, T., 1989. Initiation of atherosclerotic lesions in cholesterol-fed rabbits. I. Focal increases in arterial LDL concentration precede development of fatty streak lesions. *Arteriosclerosis, Thrombosis, and Vascular Biology*, 9(6), pp. 895-907
- SEHAYEK, E. et al., 2001. Hyodeoxycholic acid efficiently suppresses atherosclerosis formation and plasma cholesterol levels in mice. *Journal of lipid research*, 42(8), pp. 1250-1256
- SEKIKAWA, A. et al., 2008. Marine-Derived n-3 Fatty Acids and Atherosclerosis in Japanese, Japanese-American, and White Men: A Cross-Sectional Study. *Journal of the American College of Cardiology*, 52(6), pp. 417-424
- SELLKE, F., ARMSTRONG, M. and HARRISON, D., 1990. Endothelium-dependent vascular relaxation is abnormal in the coronary microcirculation of atherosclerotic primates. *Circulation*, 81(5), pp. 1586-1593
- SERHAN, C.N. et al., 2000. Novel Functional Sets of Lipid-Derived Mediators with Antiinflammatory Actions Generated from Omega-3 Fatty Acids via Cyclooxygenase 2–Nonsteroidal Antiinflammatory Drugs and Transcellular Processing. *The Journal of experimental medicine*, 192(8), pp. 1197-1204
- SERHAN, C.N. et al., 2003. Reduced Inflammation and Tissue Damage in Transgenic Rabbits Overexpressing 15-Lipoxygenase and Endogenous Anti-inflammatory Lipid Mediators. *The Journal of Immunology*, 171(12), pp. 6856-6865
- SHEKHONIN, B.V. et al., 1985. Distribution of type I, III, IV and V collagen in normal and atherosclerotic human arterial wall: immunomorphological characteristics. *Collagen and related research*, 5(4), pp. 355-368
- SHI, Y. et al., 1997. Origin of Extracellular Matrix Synthesis During Coronary Repair. *Circulation*, 95(4), pp. 997-1006
- SHIFFMAN, D. et al., 2000. Large Scale Gene Expression Analysis of Cholesterol-loaded Macrophages. *Journal of Biological Chemistry*, 275(48), pp. 37324-37332
- SHOULDERS, M.D. and RAINES, R.T., 2009. Collagen Structure and Stability. *Annual review of biochemistry*, 78, pp. 929-958
- SIMON, G.M. and CRAVATT, B.F., 2006. Endocannabinoid Biosynthesis Proceeding through Glycerophospho-N-acyl Ethanolamine and a Role for α/β -Hydrolase 4 in This Pathway. *Journal of Biological Chemistry*, 281(36), pp. 26465-26472
- SINGH, T.U. et al., 2010. Eicosapentaenoic acid-induced endothelium-dependent and -independent relaxation of sheep pulmonary artery. *European journal of pharmacology*, 636(1–3), pp. 108-113
- SKÅLÉN, K. et al., 2002. Subendothelial retention of atherogenic lipoproteins in early atherosclerosis. *Nature*, 417(6890), pp. 750-754

- SKULAS-RAY, A.C. et al., 2011. Dose-response effects of omega-3 fatty acids on triglycerides, inflammation, and endothelial function in healthy persons with moderate hypertriglyceridemia. *The American Journal of Clinical Nutrition*, 93(2), pp. 243-252
- SMART, D. et al., 2000. The endogenous lipid anandamide is a full agonist at the human vanilloid receptor (hVR1). *British journal of pharmacology*, 129(2), pp. 227-230
- SMIRNOVA, I.V. et al., 2004. Asymmetric dimethylarginine upregulates LOX-1 in activated macrophages: role in foam cell formation. *American Journal of Physiology - Heart and Circulatory Physiology*, 287(2), pp. H782-H790
- SMITH, J.D. et al., 1995. Decreased atherosclerosis in mice deficient in both macrophage colony-stimulating factor (op) and apolipoprotein E. *Proceedings of the National Academy of Sciences of the United States of America*, 92(18), pp. 8264-8268
- SOSKIĆ, S.S. et al., 2011. Peroxisome Proliferator-Activated Receptors and Atherosclerosis. *Angiology*, 62(7), pp. 523-534
- STAELS, B. et al., 1995. Fibrates downregulate apolipoprotein C-III expression independent of induction of peroxisomal acyl coenzyme A oxidase. A potential mechanism for the hypolipidemic action of fibrates. *The Journal of Clinical Investigation*, 95(2), pp. 705-712
- STAELS, B. et al., 1995. Fibrates downregulate apolipoprotein C-III expression independent of induction of peroxisomal acyl coenzyme A oxidase. A potential mechanism for the hypolipidemic action of fibrates. *The Journal of Clinical Investigation*, 95(2), pp. 705-712
- STAELS, B. et al., 1998. Mechanism of Action of Fibrates on Lipid and Lipoprotein Metabolism. *Circulation*, 98(19), pp. 2088-2093
- STAROWICZ, K.M. et al., 2008. Endocannabinoid Dysregulation in the Pancreas and Adipose Tissue of Mice Fed With a High-fat Diet *Obesity*, 16(3), pp. 553-565
- STARY, H. et al., 1992. A definition of the intima of human arteries and of its atherosclerosis-prone regions. A report from the Committee on Vascular Lesions of the Council on Arteriosclerosis, American Heart Association. *Arteriosclerosis, Thrombosis, and Vascular Biology*, 12(1), pp. 120-134
- STARY, H. et al., 1994. A definition of initial, fatty streak, and intermediate lesions of atherosclerosis. A report from the Committee on Vascular Lesions of the Council on Arteriosclerosis, American Heart Association. *Arteriosclerosis, Thrombosis, and Vascular Biology*, 14(5), pp. 840-856
- STARY, H.C. et al., 1995. A Definition of Advanced Types of Atherosclerotic Lesions and a Histological Classification of Atherosclerosis : A Report From the Committee on Vascular Lesions of the Council on Arteriosclerosis, American Heart Association. *Circulation*, 92(5), pp. 1355-1374
- STEFFENS, S. et al., 2005. Low dose oral cannabinoid therapy reduces progression of atherosclerosis in mice. *Nature*, 434(7034), pp. 782-786

- STEINBERG, H.O. et al., 1997. Endothelial Dysfunction Is Associated With Cholesterol Levels in the High Normal Range in Humans. *Circulation*, 96(10), pp. 3287-3293
- STEINBRECHER, U.P. et al., 1984. Modification of low density lipoprotein by endothelial cells involves lipid peroxidation and degradation of low density lipoprotein phospholipids. *Proceedings of the National Academy of Sciences of the United States of America*, 81(12), pp. 3883-3887
- STILLWELL, W. and WASSALL, S.R., 2003. Docosahexaenoic acid: membrane properties of a unique fatty acid. *Chemistry and physics of lipids*, 126(1), pp. 1-27
- STRITTMATTER, F. et al., 2012. Expression of Fatty Acid Amide Hydrolase (FAAH) in Human, Mouse, and Rat Urinary Bladder and Effects of FAAH Inhibition on Bladder Function in Awake Rats. *European urology*, 61(1), pp. 98-106
- STRITTMATTER, F. et al., 2012. Expression of Fatty Acid Amide Hydrolase (FAAH) in Human, Mouse, and Rat Urinary Bladder and Effects of FAAH Inhibition on Bladder Function in Awake Rats. *European urology*, 61(1), pp. 98-106
- SUGAMURA, K. et al., 2009. Activated Endocannabinoid System in Coronary Artery Disease and Antiinflammatory Effects of Cannabinoid 1 Receptor Blockade on Macrophages. *Circulation*, 119(1), pp. 28-36
- SUGAMURA, K. et al., January 6/13, 2009. Activated Endocannabinoid System in Coronary Artery Disease and Antiinflammatory Effects of Cannabinoid 1 Receptor Blockade on Macrophages. *Circulation*, 119(1), pp. 28-36
- SUGIURA, T. et al., 1998. Detection of an Endogenous Cannabimimetic Molecule, 2-Arachidonoylglycerol, and Cannabinoid CB1 Receptor mRNA in Human Vascular Cells: Is 2-Arachidonoylglycerol a Possible Vasomodulator? *Biochemical and biophysical research communications*, 243(3), pp. 838-843
- SUGIURA, T. and WAKU, K., 2002. Cannabinoid Receptors and Their Endogenous Ligands. *Journal of Biochemistry*, 132(1), pp. 7-12
- SUMPIO, B.E., TIMOTHY RILEY, J. and DARDIK, A., 2002. Cells in focus: endothelial cell. *The international journal of biochemistry & cell biology*, 34(12), pp. 1508-1512
- SUN, Y.X. et al., 2004. Biosynthesis of anandamide and *N*-palmitoylethanolamine by sequential actions of phospholipase A₂ and lysophospholipase D. *The Biochemical Journal*, 380(3), pp. 749-756
- SUN, Y. et al., 2007. Cannabinoid activation of PPAR α ; a novel neuroprotective mechanism. *British journal of pharmacology*, 152(5), pp. 734-743
- SUWAIDI, J.A. et al., 2000. Long-Term Follow-Up of Patients With Mild Coronary Artery Disease and Endothelial Dysfunction. *Circulation*, 101(9), pp. 948-954

- SUZUKAWA, M. et al., 1995. Effects of fish oil fatty acids on low density lipoprotein size, oxidizability, and uptake by macrophages. *Journal of lipid research*, 36(3), pp. 473-484
- SWIRSKI, F.K. et al., 2007. Ly-6C^{hi} monocytes dominate hypercholesterolemia-associated monocytosis and give rise to macrophages in atheromata. *The Journal of Clinical Investigation*, 117(1), pp. 195-205
- TACKE, F. et al., 2007. Monocyte subsets differentially employ CCR2, CCR5, and CX3CR1 to accumulate within atherosclerotic plaques. *The Journal of Clinical Investigation*, 117(1), pp. 185-194
- TALMUD, P.J. et al., 2002. Nonfasting Apolipoprotein B and Triglyceride Levels as a Useful Predictor of Coronary Heart Disease Risk in Middle-Aged UK Men. *Arteriosclerosis, Thrombosis, and Vascular Biology*, 22(11), pp. 1918-1923
- TENGER, C. and ZHOU, X., 2003. Apolipoprotein E modulates immune activation by acting on the antigen-presenting cell. *Immunology*, 109(3), pp. 392-397
- THEOBALD, H.E. et al., April 2007. Low-Dose Docosahexaenoic Acid Lowers Diastolic Blood Pressure in Middle-Aged Men and Women. *The Journal of nutrition*, 137(4), pp. 973-978
- THIES, F. et al., 2003. Association of n-3 polyunsaturated fatty acids with stability of atherosclerotic plaques: a randomised controlled trial. *The Lancet*, 361(9356), pp. 477-485
- TOKUNO, A. et al., 2007. The effects of statin and fibrate on lowering small dense LDL- cholesterol in hyperlipidemic patients with type 2 diabetes. *Journal of Atherosclerosis and Thrombosis*, 14(3), pp. 128-132
- TORNQVIST, H. and BELFRAGE, P., 1976. Purification and some properties of a monoacylglycerol-hydrolyzing enzyme of rat adipose tissue. *Journal of Biological Chemistry*, 251(3), pp. 813-819
- TRUSKEY, G. et al., 1992. Measurement of endothelial permeability to 125I-low density lipoproteins in rabbit arteries by use of en face preparations. *Circulation research*, 71(4), pp. 883-897
- TSUBURAYA, R. et al., 2011. Eicosapentaenoic acid reduces ischemic ventricular fibrillation via altering monophasic action potential in pigs. *Journal of Molecular and Cellular Cardiology*, 51(3), pp. 329-336
- TSUCHIYA, S. et al., 1982. Induction of Maturation in Cultured Human Monocytic Leukemia Cells by a Phorbol Diester. *Cancer research*, 42(4), pp. 1530-1536
- TSUCHIYA, S. et al., 1980. Establishment and characterization of a human acute monocytic leukemia cell line (THP-1). *International Journal of Cancer*, 26(2), pp. 171-176
- TVRZICKA, E. et al., 2011. Fatty acids as biocompounds: their role in human metabolism, health and disease--a review. Part 1: classification, dietary sources and biological functions. *Biomedical Papers of the Medical Faculty of the University Palacky, Olomouc, Czechoslovakia*, 155(2), pp. 117-130

- TWIGG, M.W. et al., 2012. The LOX-1 Scavenger Receptor and Its Implications in the Treatment of Vascular Disease. *Cardiology Research and Practice*, 2012
- UEDA, H. et al., 1993. A possible pathway of phosphoinositide metabolism through EDTA-insensitive phospholipase A1 followed by lysophosphoinositide-specific phospholipase C in rat brain. *Journal of Neurochemistry*, 61(5), pp. 1874-1881
- VAN SICKLE, M.D. et al., 2005. Identification and functional characterization of brainstem cannabinoid CB2 receptors. *Science*, 310(5746), pp. 329-332
- VAN VLIJMEN, B.J. et al., 1994. Diet-induced hyperlipoproteinemia and atherosclerosis in apolipoprotein E3-Leiden transgenic mice. *The Journal of Clinical Investigation*, 93(4), pp. 1403-1410
- VARGA, K. et al., 1995. Novel antagonist implicates the CB1 cannabinoid receptor in the hypotensive action of anandamide. *European journal of pharmacology*, 278(3), pp. 279-283
- VARGA, K. et al., 1998. Platelet- and macrophage-derived endogenous cannabinoids are involved in endotoxin-induced hypotension. *The FASEB Journal*, 12(11), pp. 1035-1044
- VEMURI, V.K., JANERO, D.R. and MAKRIYANNIS, A., 2008. Pharmacotherapeutic targeting of the endocannabinoid signaling system: Drugs for obesity and the metabolic syndrome. *Physiology & Behavior*, 93(4-5), pp. 671-686
- VERGNES, L. et al., 2003. Cholesterol and Cholate Components of an Atherogenic Diet Induce Distinct Stages of Hepatic Inflammatory Gene Expression. *Journal of Biological Chemistry*, 278(44), pp. 42774-42784
- VIJAIMOHAN, K. et al., 2006. Beneficial effects of alpha linolenic acid rich flaxseed oil on growth performance and hepatic cholesterol metabolism in high fat diet fed rats. *Life Sciences*, 79(5), pp. 448-454
- VILAHUR, G., PADRO, T. and BADIMON, L., 2011. Atherosclerosis and Thrombosis: Insights from Large Animal Models. *Journal of Biomedicine and Biotechnology*, 2011
- VIRDIS, A. et al., 2003. Effect of Hyperhomocystinemia and Hypertension on Endothelial Function in Methylene tetrahydrofolate Reductase-Deficient Mice. *Arteriosclerosis, Thrombosis, and Vascular Biology*, 23(8), pp. 1352-1357
- VIRMANI, R. et al., 2000. Lessons From Sudden Coronary Death : A Comprehensive Morphological Classification Scheme for Atherosclerotic Lesions. *Arteriosclerosis, Thrombosis, and Vascular Biology*, 20(5), pp. 1262-1275
- VON SCHACKY, C. et al., 1999. The Effect of Dietary ω -3 Fatty Acids on Coronary Atherosclerosis. *Annals of Internal Medicine*, 130(7), pp. 554-562
- VOSPER, H. et al., 2001. The Peroxisome Proliferator-activated Receptor δ Promotes Lipid Accumulation in Human Macrophages. *Journal of Biological Chemistry*, 276 (47), pp. 44258-44265

- WAGNER, J.A. et al., 2001. Endogenous cannabinoids mediate hypotension after experimental myocardial infarction. *Journal of the American College of Cardiology*, 38(7), pp. 2048-2054
- WAGNER, J.A. et al., 2001. Endogenous cannabinoids mediate hypotension after experimental myocardial infarction. *Journal of the American College of Cardiology*, 38(7), pp. 2048-2054
- WAGNER, J.A. et al., 1999. Mesenteric Vasodilation Mediated by Endothelial Anandamide Receptors. *Hypertension*, 33(1), pp. 429-434
- WALLDIUS, G. et al., 2001. High apolipoprotein B, low apolipoprotein A-I, and improvement in the prediction of fatal myocardial infarction (AMORIS study): a prospective study. *The Lancet*, 358(9298), pp. 2026-2033
- WAN, J. et al., 2010. Endogenously Decreasing Tissue n-6/n-3 Fatty Acid Ratio Reduces Atherosclerotic Lesions in Apolipoprotein E-Deficient Mice by Inhibiting Systemic and Vascular Inflammation. *Arteriosclerosis, Thrombosis, and Vascular Biology*, 30(12), pp. 2487-2494
- WANG, S. et al., 2009. Reduction in dietary omega-6 polyunsaturated fatty acids: Eicosapentaenoic acid plus docosahexaenoic acid ratio minimizes atherosclerotic lesion formation and inflammatory response in the LDL receptor null mouse. *Atherosclerosis*, 204(1), pp. 147-155
- WANG, T. et al., 2011. Docosahexaenoic acid attenuates VCAM-1 expression and NF- κ B activation in TNF- α -treated human aortic endothelial cells. *The Journal of nutritional biochemistry*, 22(2), pp. 187-194
- WARNER, G.J. et al., 1995. Cell Toxicity Induced by Inhibition of Acyl Coenzyme A:Cholesterol Acyltransferase and Accumulation of Unesterified Cholesterol. *Journal of Biological Chemistry*, 270(11), pp. 5772-5778
- WATERMAN, I.J. and ZAMMIT, V.A., 2002. Differential Effects of Fenofibrate or Simvastatin Treatment of Rats on Hepatic Microsomal Overt and Latent Diacylglycerol Acyltransferase Activities. *Diabetes*, 51(6), pp. 1708-1713
- WEIS, F. et al., 2010. Substantially altered expression pattern of cannabinoid receptor 2 and activated endocannabinoid system in patients with severe heart failure. *Journal of Molecular and Cellular Cardiology*, 48(6), pp. 1187-1193
- WEITKAMP, B. et al., 1999. Human macrophages synthesize type VIII collagen in vitro and in the atherosclerotic plaque. *The FASEB Journal*, 13(11), pp. 1445-1457
- WELDON, S.M. et al., 2007. Docosahexaenoic acid induces an anti-inflammatory profile in lipopolysaccharide-stimulated human THP-1 macrophages more effectively than eicosapentaenoic acid. *The Journal of nutritional biochemistry*, 18(4), pp. 250-258
- WILLECKE, F. et al., 2011. Cannabinoid Receptor 2 Signaling Does Not Modulate Atherogenesis in Mice. *PLoS ONE*, 6(4),

- WILLIAMS, K.J. and TABAS, I., 1995. The Response-to-Retention Hypothesis of Early Atherogenesis. *Arteriosclerosis, Thrombosis, and Vascular Biology*, 15(5), pp. 551-561
- WILLIAMSON, P.R. and KAGAN, H.M., 1986. Reaction pathway of bovine aortic lysyl oxidase. *Journal of Biological Chemistry*, 261(20), pp. 9477-9482
- WOOD, J.T. et al., 2010. Dietary docosahexaenoic acid supplementation alters select physiological endocannabinoid-system metabolites in brain and plasma. *Journal of lipid research*, 51(6), pp. 1416-1423
- WOODIWISS, A.J. et al., 2001. Reduction in Myocardial Collagen Cross-Linking Parallels Left Ventricular Dilatation in Rat Models of Systolic Chamber Dysfunction. *Circulation*, 103(1), pp. 155-160
- WORGALL, T.S. et al., 2002. Unsaturated Fatty Acid-mediated Decreases in Sterol Regulatory Element-mediated Gene Transcription Are Linked to Cellular Sphingolipid Metabolism. *Journal of Biological Chemistry*, 277(6), pp. 3878-3885
- WORGALL, T.S. et al., 1998. Polyunsaturated Fatty Acids Decrease Expression of Promoters with Sterol Regulatory Elements by Decreasing Levels of Mature Sterol Regulatory Element-binding Protein. *Journal of Biological Chemistry*, 273(40), pp. 25537-25540
- XU, Z. et al., 2007. Fish oil significantly alters fatty acid profiles in various lipid fractions but not atherogenesis in apo E-KO mice. *European Journal of Nutrition*, 46(2), pp. 103-110
- XU, H.E. et al., 1999. Molecular Recognition of Fatty Acids by Peroxisome Proliferator-Activated Receptors. *Molecular cell*, 3(3), pp. 397-403
- XU, H. et al., 2007. Anti-inflammatory property of the cannabinoid receptor-2-selective agonist JWH-133 in a rodent model of autoimmune uveoretinitis. *Journal of leukocyte biology*, 82(3), pp. 532-541
- XU, X. et al., 2007. Anti-LOX-1 Rescues Endothelial Function in Coronary Arterioles in Atherosclerotic ApoE Knockout Mice. *Arteriosclerosis, Thrombosis, and Vascular Biology*, 27(4), pp. 871-877
- YAMADA, H. et al., 2008. In Vivo and In Vitro Inhibition of Monocyte Adhesion to Endothelial Cells and Endothelial Adhesion Molecules by Eicosapentaenoic Acid. *Arteriosclerosis, Thrombosis, and Vascular Biology*, 28(12), pp. 2173-2179
- YAMAUCHI, M. et al., 1987. Structure and formation of a stable histidine-based trifunctional cross-link in skin collagen. *Journal of Biological Chemistry*, 262(24), pp. 11428-11434
- YANG, B. et al., 1993. Dietary Fish Oil Supplementation Attenuates Myocardial Dysfunction and Injury Caused by Global Ischemia and Reperfusion in Isolated Rat Hearts. *The Journal of nutrition*, 123(12), pp. 2067-2074
- YAO, W., LI, K. and LIAO, K., 2009. Macropinocytosis contributes to the macrophage foam cell formation in RAW264.7 cells. *Acta Biochimica et Biophysica Sinica*, 41(9), pp. 773-780

- YAQOOB, P. and CALDER, P., 1995. Effects of Dietary Lipid Manipulation upon Inflammatory Mediator Production by Murine Macrophages. *Cellular immunology*, 163(1), pp. 120-128
- YOKOYAMA, M. et al., 2007. Effects of eicosapentaenoic acid on major coronary events in hypercholesterolaemic patients (JELIS): a randomised open-label, blinded endpoint analysis. *The Lancet*, 369(9567), pp. 1090-1098
- YURI V., B., 2006. Monocyte recruitment and foam cell formation in atherosclerosis. *Micron*, 37(3), pp. 208-222
- ZAIMA, N. et al., 2006. Trans geometric isomers of EPA decrease LXR α -induced cellular triacylglycerol via suppression of SREBP-1c and PGC-1 β . *Journal of lipid research*, 47(12), pp. 2712-2717
- ZARAGOZA, C. et al., 2011. Animal Models of Cardiovascular Diseases. *Journal of Biomedicine and Biotechnology*, 2011
- ZHANG, S.H. et al., 1994. Diet-induced atherosclerosis in mice heterozygous and homozygous for apolipoprotein E gene disruption. *The Journal of Clinical Investigation*, 94(3), pp. 937-945
- ZHAO, B. et al., 2006. Constitutive Receptor-independent Low Density Lipoprotein Uptake and Cholesterol Accumulation by Macrophages Differentiated from Human Monocytes with Macrophage-Colony-stimulating Factor (M-CSF). *Journal of Biological Chemistry*, 281(23), pp. 15757-15762
- ZHAO, B. et al., 2007. Stable overexpression of human macrophage cholesteryl ester hydrolase results in enhanced free cholesterol efflux from human THP1 macrophages. *American Journal of Physiology - Cell Physiology*, 292(1), pp. C405-C412
- ZHAO, Y. et al., 2004. Eicosapentaenoic Acid Prevents LPS-Induced TNF- α Expression by Preventing NF- κ B Activation. *Journal of the American College of Nutrition*, 23(1), pp. 71-78
- ZHU, X. et al., 2007. Redox-sensitive myocardial remodeling and dysfunction in swine diet-induced experimental hypercholesterolemia. *Atherosclerosis*, 193(1), pp. 62-69
- ZIBADI, S. et al., September 2009. Myocardial lysyl oxidase regulation of cardiac remodeling in a murine model of diet-induced metabolic syndrome. *American Journal of Physiology - Heart and Circulatory Physiology*, 297(3), pp. H976-H982
- ZINGG, J. et al., 2002. Novel 5' Exon of Scavenger Receptor CD36 Is Expressed in Cultured Human Vascular Smooth Muscle Cells and Atherosclerotic Plaques. *Arteriosclerosis, Thrombosis, and Vascular Biology*, 22(3), pp. 412-417
- ZYGMUNT, P.M. et al., 1999. Vanilloid receptors on sensory nerves mediate the vasodilator action of anandamide. *Nature*, 400(6743), pp. 452-457